

Advances in Polymer Science 240

H.G. Börner  
J.-F. Lutz *Editors*

# Bioactive Surfaces

 Springer

**Editorial Board:**

**A. Abe · A.-C. Albertsson · K. Dušek · J. Genzer  
W.H. de Jeu · S. Kobayashi · K.-S. Lee · L. Leibler  
T.E. Long · I. Manners · M. Möller · E.M. Terentjev  
M. Vicent · B. Voit · G. Wegner · U. Wiesner**

# Advances in Polymer Science

Recently Published and Forthcoming Volumes

## **Bioactive Surfaces**

Volume Editors: Börner, H.G., Lutz, J.-F.  
Vol. 240, 2011

## **Advanced Rubber Composites**

Volume Editor: Heinrich, G.  
Vol. 239, 2011

## **Polymer Thermodynamics**

Volume Editors: Enders, S., Wolf, B.A.  
Vol. 238, 2011

## **Enzymatic Polymerisation**

Volume Editors: Palmans, A.R.A., Heise, A.  
Vol. 237, 2010

## **High Solid Dispersion**

Volume Editor: Cloitre, M.  
Vol. 236, 2010

## **Silicon Polymers**

Volume Editor: Muzafarov, A.  
Vol. 235, 2011

## **Chemical Design of Responsive Microgels**

Volume Editors: Pich, A., Richtering, W.  
Vol. 234, 2010

## **Hybrid Latex Particles – Preparation with Emulsion**

Volume Editors: van Herk, A.M., Landfester, K.  
Vol. 233, 2010

## **Biopolymers**

Volume Editors: Abe, A., Dušek, K., Kobayashi, S.  
Vol. 232, 2010

## **Polymer Materials**

Volume Editors: Lee, K.-S., Kobayashi, S.  
Vol. 231, 2010

## **Polymer Characterization**

Volume Editors: Dušek, K., Joanny, J.-F.  
Vol. 230, 2010

## **Modern Techniques for Nano- and Microreactors/-reactions**

Volume Editor: Caruso, F.  
Vol. 229, 2010

## **Complex Macromolecular Systems II**

Volume Editors: Müller, A.H.E., Schmidt, H.-W.  
Vol. 228, 2010

## **Complex Macromolecular Systems I**

Volume Editors: Müller, A.H.E., Schmidt, H.-W.  
Vol. 227, 2010

## **Shape-Memory Polymers**

Volume Editor: Lendlein, A.  
Vol. 226, 2010

## **Polymer Libraries**

Volume Editors: Meier, M.A.R., Webster, D.C.  
Vol. 225, 2010

## **Polymer Membranes/Biomembranes**

Volume Editors: Meier, W.P., Knoll, W.  
Vol. 224, 2010

## **Organic Electronics**

Volume Editors: Meller, G., Grasser, T.  
Vol. 223, 2010

## **Inclusion Polymers**

Volume Editor: Wenz, G.  
Vol. 222, 2009

## **Advanced Computer Simulation Approaches for Soft Matter Sciences III**

Volume Editors: Holm, C., Kremer, K.  
Vol. 221, 2009

## **Self-Assembled Nanomaterials II**

Nanotubes  
Volume Editor: Shimizu, T.  
Vol. 220, 2008

## **Self-Assembled Nanomaterials I**

Nanofibers  
Volume Editor: Shimizu, T.  
Vol. 219, 2008

## **Interfacial Processes and Molecular Aggregation of Surfactants**

Volume Editor: Narayanan, R.  
Vol. 218, 2008

## **New Frontiers in Polymer Synthesis**

Volume Editor: Kobayashi, S.  
Vol. 217, 2008

# Bioactive Surfaces

Volume Editors: Hans G. Börner  
Jean-François Lutz

With contributions by

N. Badi · M. Biesalski · H.G. Börner · M. Gattermayer  
R. Gentsch · A. Laschewsky · J.-F. Lutz · H. Möhwald  
S. Petersen · J. Polleux · A. Pulsipher · A. Skirtach  
J.C. Tiller · D. Volodkin · E. Wischerhoff · M.N. Yousaf

 Springer

*Editors*

Prof. Dr. Hans G. Börner  
Department of Chemistry  
Laboratory of Organic Synthesis  
of Functional Systems  
Humboldt-Universität zu Berlin  
Brook-Taylor-Strasse 2  
12489 Berlin  
Germany  
[h.boerner@hu-berlin.de](mailto:h.boerner@hu-berlin.de)

Prof. Dr. Jean-François Lutz  
Institut Charles Sadron  
UPR22-CNRS 23  
Precision Macromolecular Chemistry Group  
rue du Loess BP 84047 69  
67034 Strasbourg  
France  
[jflutz@unistra.fr](mailto:jflutz@unistra.fr)

ISSN 0065-3195                      e-ISSN 1436-5030  
ISBN 978-3-642-20154-7            e-ISSN 978-3-642-20155-4  
DOI 10.1007/978-3-642-20155-4  
Springer Heidelberg Dordrecht London New York

Library of Congress Control Number: 2011926528

© Springer-Verlag Berlin Heidelberg 2011

This work is subject to copyright. All rights are reserved, whether the whole or part of the material is concerned, specifically the rights of translation, reprinting, reuse of illustrations, recitation, broadcasting, reproduction on microfilm or in any other way, and storage in data banks. Duplication of this publication or parts thereof is permitted only under the provisions of the German Copyright Law of September 9, 1965, in its current version, and permission for use must always be obtained from Springer. Violations are liable to prosecution under the German Copyright Law.

The use of general descriptive names, registered names, trademarks, etc. in this publication does not imply, even in the absence of a specific statement, that such names are exempt from the relevant protective laws and regulations and therefore free for general use.

*Cover design:* WMXDesign GmbH, Heidelberg

Printed on acid-free paper

Springer is part of Springer Science+Business Media ([www.springer.com](http://www.springer.com))

---

## Volume Editors

Prof. Dr. Hans G. Börner  
Department of Chemistry  
Laboratory of Organic Synthesis  
of Functional Systems  
Humboldt-Universität zu Berlin  
Brook-Taylor-Strasse 2  
12489 Berlin  
Germany  
[h.boerner@hu-berlin.de](mailto:h.boerner@hu-berlin.de)

Prof. Dr. Jean-François Lutz  
Institut Charles Sadron  
UPR22-CNRS 23  
Precision Macromolecular Chemistry Group  
rue du Loess BP 84047 69  
67034 Strasbourg  
France  
[jflutz@unistra.fr](mailto:jflutz@unistra.fr)

## Editorial Board

Prof. Akihiro Abe  
Professor Emeritus  
Tokyo Institute of Technology  
6-27-12 Hiyoshi-Honcho, Kohoku-ku  
Yokohama 223-0062, Japan  
[aabe34@xc4.so-net.ne.jp](mailto:aabe34@xc4.so-net.ne.jp)

Prof. A.-C. Albertsson  
Department of Polymer Technology  
The Royal Institute of Technology  
10044 Stockholm, Sweden  
[aila@polymer.kth.se](mailto:aila@polymer.kth.se)

Prof. Karel Dušek  
Institute of Macromolecular Chemistry  
Czech Academy of Sciences  
of the Czech Republic  
Heyrovský Sq. 2  
16206 Prague 6, Czech Republic  
[dusek@imc.cas.cz](mailto:dusek@imc.cas.cz)

Prof. Jan Genzer  
Department of Chemical &  
Biomolecular Engineering  
North Carolina State University  
911 Partners Way  
27695-7905 Raleigh, North Carolina  
USA

Prof. Dr. Wim H. de Jeu  
DWI an der RWTH Aachen eV  
Pauwelsstraße 8  
D-52056 Aachen, Germany  
[dejeu@dw1.rwth-aachen.de](mailto:dejeu@dw1.rwth-aachen.de)

Prof. Shiro Kobayashi  
R & D Center for Bio-based Materials  
Kyoto Institute of Technology  
Matsugasaki, Sakyo-ku  
Kyoto 606-8585, Japan  
[kobayash@kit.ac.jp](mailto:kobayash@kit.ac.jp)

Prof. Kwang-Sup Lee  
Department of Advanced Materials  
Hannam University  
561-6 Jeonmin-Dong  
Yuseong-Gu 305-811  
Daejeon, South Korea  
[kslee@hnu.kr](mailto:kslee@hnu.kr)

Prof. L. Leibler  
Matière Molle et Chimie  
Ecole Supérieure de Physique  
et Chimie Industrielles (ESPCI)  
10 rue Vauquelin  
75231 Paris Cedex 05, France  
[ludwik.leibler@espci.fr](mailto:ludwik.leibler@espci.fr)

Prof. Timothy E. Long  
Department of Chemistry  
and Research Institute  
Virginia Tech  
2110 Hahn Hall (0344)  
Blacksburg, VA 24061, USA  
[telong@vt.edu](mailto:telong@vt.edu)

Prof. Ian Manners  
School of Chemistry  
University of Bristol  
Cantock's Close  
BS8 1TS Bristol, UK  
[ian.manners@bristol.ac.uk](mailto:ian.manners@bristol.ac.uk)

Prof. Martin Möller  
Deutsches Wollforschungsinstitut  
an der RWTH Aachen e.V.  
Pauwelsstraße 8  
52056 Aachen, Germany  
[moeller@dw.rwth-aachen.de](mailto:moeller@dw.rwth-aachen.de)

Prof. E.M. Terentjev  
Cavendish Laboratory  
Madingley Road  
Cambridge CB 3 OHE, UK  
[emt1000@cam.ac.uk](mailto:emt1000@cam.ac.uk)

Prof. Dr. Maria Jesus Vicent  
Centro de Investigacion Principe Felipe  
Medicinal Chemistry Unit  
Polymer Therapeutics Laboratory  
Av. Autopista del Saler, 16  
46012 Valencia, Spain  
[mjvicent@cipf.es](mailto:mjvicent@cipf.es)

Prof. Brigitte Voit  
Leibniz-Institut für Polymerforschung  
Dresden  
Hohe Straße 6  
01069 Dresden, Germany  
[voit@ipfdd.de](mailto:voit@ipfdd.de)

Prof. Gerhard Wegner  
Max-Planck-Institut  
für Polymerforschung  
Ackermannweg 10  
55128 Mainz, Germany  
[wegner@mpip-mainz.mpg.de](mailto:wegner@mpip-mainz.mpg.de)

Prof. Ulrich Wiesner  
Materials Science & Engineering  
Cornell University  
329 Bard Hall  
Ithaca, NY 14853, USA  
[ubw1@cornell.edu](mailto:ubw1@cornell.edu)

---

## **Advances in Polymer Sciences**

### **Also Available Electronically**

*Advances in Polymer Sciences* is included in Springer's eBook package *Chemistry and Materials Science*. If a library does not opt for the whole package, the book series may be bought on a subscription basis. Also, all back volumes are available electronically.

For all customers who have a standing order to the print version of *Advances in Polymer Sciences*, we offer free access to the electronic volumes of the Series published in the current year via SpringerLink.

If you do not have access, you can still view the table of contents of each volume and the abstract of each article by going to the SpringerLink homepage, clicking on "Browse by Online Libraries", then "Chemical Sciences", and finally choose *Advances in Polymer Science*.

You will find information about the

- Editorial Board
- Aims and Scope
- Instructions for Authors
- Sample Contribution

at [springer.com](http://springer.com) using the search function by typing in *Advances in Polymer Sciences*.

*Color figures* are published in full color in the electronic version on SpringerLink.



## **Aims and Scope**

The series *Advances in Polymer Science* presents critical reviews of the present and future trends in polymer and biopolymer science including chemistry, physical chemistry, physics and material science. It is addressed to all scientists at universities and in industry who wish to keep abreast of advances in the topics covered.

Review articles for the topical volumes are invited by the volume editors. As a rule, single contributions are also specially commissioned. The editors and publishers will, however, always be pleased to receive suggestions and supplementary information. Papers are accepted for *Advances in Polymer Science* in English.

In references *Advances in Polymer Sciences* is abbreviated as *Adv Polym Sci* and is cited as a journal.

Special volumes are edited by well known guest editors who invite reputed authors for the review articles in their volumes.

Impact Factor in 2009: 4.600; Section "Polymer Science": Rank 4 of 73

# Preface

Biosciences and material sciences emerged initially as distinct disciplines. However, recent progresses in polymer and material sciences led to congruent research interests, thus fusing the fields of material and biosciences progressively. To concretize visionary ideas such as adaptive bio-host systems, bio-instructive materials, bio-integrated functional systems, or regenerative tissue engineering, the interfaces between synthetic materials and biological systems have been identified as one key issue. The present volume of *Advances in Polymer Science* covers the most important aspects of the emerging area of “Bioactive Surfaces.” Selected experts in the field of polymer science, soft-matter engineering, and biophysics have been invited to highlight their personal views and perspectives on this crucial field of research.

Even though molecular biologists developed lately precise analytical tools of genomics, regulomics, and proteomics, allowing for progressively accurate insight into systemic functions of cells and tissues, the interfaces between synthetic materials and biological systems are still far from being fundamentally understood. In the last decade, joint multidisciplinary efforts and intense exchange between the biology and materials research communities set the focus on signaling of materials toward biological systems. Cells or cell populations at a bio-material interface experience a broad spectrum of chemo-, mechano- physico-, and topological signals, which are interpreted by the biosystem. This triggers distinct responses, which often occur on all functional bio-hierarchy levels from altering cell metabolism to changing cell status, regulating cell proliferation, differentiation or motility to macroscopic changes of the cell shape, orientation, migration, or adhesion behavior. Fundamental understanding of the events and responses paves the way to actively communicate with biological systems via the material-interface to influence, guide, or direct cells and tissues. This promises enormous progress for life science applications, however, puts challenges on materials design and accurate fabrication, as precisely tailored materials and interfaces are mandatory.

In this exciting context, this volume provides a broad overview on the field of synthetic biologically active surfaces. In particular, three important aspects are emphasized in this volume: (1) surface design, (2) interactions of 2D and 3D surfaces with biosystems, and (3) applications. Regarding surface preparation and modification, the reader will find in this book a practical description of synthetic tools, which constitute the state of the art in the field. For instance, surface functionalization

strategies, using responsive polymer brushes (Chap. 1), peptide arrays (Chap. 2), self-assembled monolayers (Chap. 4), or polyelectrolyte multilayers (Chap. 5), are described in this volume. The middle section of this book (i.e. Chaps. 3–6) describes principally the interactions of 2D and 3D surfaces with biological systems. For instance, important topics such as surface nanostructuring (Chap. 3), the fabrication of micro-reservoirs (Chap. 5), and the preparation and processing of active 3D scaffolds (Chap. 6) are specifically addressed in this volume. Furthermore, practical applications of synthetic bioactive surfaces are described throughout the book. In particular, concrete examples of applications in research fields as diverse as tissue engineering, drug delivery, biochips, biosensors, bioseparation, cell engineering, stem-cell differentiation, and antimicrobial surfaces are discussed in this volume.

The editors express their thanks to the authors and to the Springer editorial team for their help in publishing this book.

Berlin, Potsdam  
April 2011

Hans G. Börner and Jean-François Lutz

# Contents

<b>Smart Polymer Surfaces: Concepts and Applications in Biosciences</b> .....	1
Erik Wischerhoff, Nezha Badi, André Laschewsky, and Jean-François Lutz	
<b>Hold on at the Right Spot: Bioactive Surfaces for the Design of Live-Cell Micropatterns</b> .....	35
S. Petersen, M. Gattermayer, and M. Biesalski	
<b>Interfacing Cell Surface Receptors to Hybrid Nanopatterned Surfaces: A Molecular Approach for Dissecting the Adhesion Machinery</b> .....	79
Julien Polleux	
<b>Self-Assembled Monolayers as Dynamic Model Substrates for Cell Biology</b> .....	103
Abigail Pulsipher and Muhammad N. Yousaf	
<b>LbL Films as Reservoirs for Bioactive Molecules</b> .....	135
D. Volodkin, A. Skirtach, and H. Möhwald	
<b>Designing Three-Dimensional Materials at the Interface to Biology</b> .....	163
R. Gentsch and H.G. Börner	
<b>Antimicrobial Surfaces</b> .....	193
Joerg C. Tiller	
<b>Index</b> .....	219



# Smart Polymer Surfaces: Concepts and Applications in Biosciences

Erik Wischerhoff, Nezha Badi, André Laschewsky, and Jean-François Lutz

**Abstract** Stimuli-responsive macromolecules (i.e., pH-, thermo-, photo-, chemo-, and bioresponsive polymers) have gained exponential importance in materials science, nanotechnology, and biotechnology during the last two decades. This chapter describes the usefulness of this class of polymer for preparing smart surfaces (e.g., modified planar surfaces, particles surfaces, and surfaces of three-dimensional scaffolds). Some efficient pathways for connecting these macromolecules to inorganic, polymer, or biological substrates are described. In addition, some emerging bioapplications of smart polymer surfaces (e.g., antifouling surfaces, cell engineering, protein chromatography, tissue engineering, biochips, and bioassays) are critically discussed.

**Keywords** Antifouling surfaces · Bioactive surfaces · Biocompatible polymers · Bioseparation · Cell engineering · Polymer-modified surfaces · Stimuli-responsive polymers

## Contents

1	Introduction .....	2
2	Types of Smart Polymer Surfaces .....	3
	2.1 Thermoresponsive Polymers.....	3
	2.2 pH-Responsive Polymers .....	4

---

E. Wischerhoff, N. Badi, and J.-F. Lutz (✉)  
Fraunhofer Institute for Applied Polymer Research, Geiselbergstrasse 69, 14476 Potsdam-Golm,  
Germany  
e-mail: lutz@iap.fhg.de; erik.wischerhoff@iap.fraunhofer.de; nezhabadi@yahoo.fr

A. Laschewsky  
Fraunhofer Institute for Applied Polymer Research, Geiselbergstrasse 69, 14476 Potsdam-Golm,  
Germany  
and  
Department of Chemistry, University of Potsdam, Potsdam, Germany  
e-mail: andre.laschewsky@iap.fraunhofer.de

2.3	Photoresponsive Polymers .....	5
2.4	Chemoresponsive and Bioresponsive Polymers .....	8
3	Surfaces Chemistries .....	13
3.1	“Grafting onto” and “Grafting from” Approaches .....	13
3.2	Adsorption of Block Copolymers .....	16
3.3	Surface-Bounded Hydrogels .....	17
4	Bioapplications of Smart Polymer Surfaces .....	19
4.1	Antifouling Surfaces .....	19
4.2	Control of Protein Adhesion .....	21
4.3	Control of Cell Adhesion .....	22
4.4	Bioseparation .....	24
4.5	Bioassays .....	26
5	Conclusion and Outlook .....	29
	References .....	29

## 1 Introduction

The face of applied polymer science has changed drastically over the recent years. Although commodity polymers still dominate the polymer market, specialty polymers have gained an increased importance in the scientific literature as well as in patents. For instance, in recent polymer and materials science the number of studies on so-called smart polymers has increased exponentially. These polymers are synthetic or biological macromolecules that undergo rapid conformational change in response to an external stimulus. For example, polymers reacting to physical (e.g., temperature, light, redox signal, or magnetic field), chemical (e.g., pH, ionic strength, or a specific molecule), or biological (e.g., viruses or bacteria) stimuli have been described in the literature [1, 2]. These types of macromolecules have opened huge technological perspectives in emerging applications such as nanoelectronics, photonics, renewable energies, biomedicine, and biotechnologies [2, 3].

In this context, the present chapter highlights the importance of smart polymers in applied surface science. It should be noted that the term “surface” is employed in this review in a relatively broad sense and is therefore not limited to 2D planar substrates but also refers to colloidal surfaces, scaffolds, and surfaces of bulk materials. Yet, the possible applications of such smart surfaces are almost unlimited and, therefore, the content of the present chapter is intentionally limited to bioapplicable polymer surfaces. This chapter places particular emphasis on the emerging field of smart bioactive surfaces [4–6]. The term “bioactive” refers here to materials that are capable of interacting with biological systems, such as nucleic acids, proteins, polysaccharides, viruses, bacteria, or living cells. This novel area of research undoubtedly goes beyond the traditional field of biocompatible surfaces.

This chapter is composed of three main sections. In Sect. 2, some background information about stimuli-responsive polymers is provided. This section is deliberately not exhaustive because several comprehensive reviews on stimuli-responsive polymers have already been published in recent years [1–3, 7–10]. In Sect. 3, some general strategies for connecting stimuli-responsive macromolecules to various

types of substrates (e.g., inorganic, polymer, or biological substrates) are described. Lastly, the bioapplications of smart polymer surfaces are discussed in Sect. 4. In particular, the utilization of smart polymer surfaces for controlling protein adhesion, cell adhesion, biorecognition, and bioseparation is emphasized.

## 2 Types of Smart Polymer Surfaces

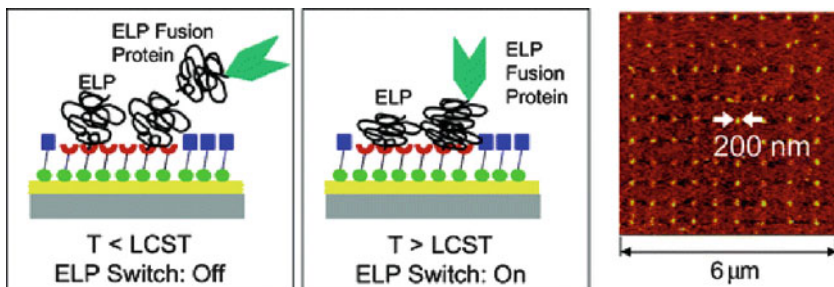
### 2.1 Thermoresponsive Polymers

Stimuli-responsive polymers offer a wealth of opportunities for the design of smart surfaces. Among all the systems studied, thermosensitive polymers have drawn much attention, in particular for biomedical applications because several diseases states are characterized by a change in temperature [11, 12]. Thermoresponsive polymers generally exhibit a lower critical solution temperature (LCST), below which they are soluble, and above which they dehydrate and aggregate. The surfaces made of these stimuli-responsive polymers switch from hydrophilic to hydrophobic states in response to temperature changes. For the design of smart thermosensitive surfaces, poly(*N*-isopropylacrylamide) (PNIPAM) is by far the most studied polymer because of a LCST around 32°C in water, which is close to physiological temperature [13–19]. For instance, this polymer has been used in different fields such as chromatography [20, 21], the control of surface wettability [22], the study of interactions between the surface and biological species, and the control of cell adhesion [14, 16–18, 23]. In addition, PNIPAM-coated surfaces prepared via atom transfer radical polymerization (ATRP) have also been used in drug delivery [24]. Nevertheless, other polymeric systems exhibiting a thermal behavior have been studied [25–28]. Du Prez and coworkers for instance, covered the surface of poly(ethylene terephthalate) track-etched membranes with poly(vinylcaprolactam) (PVCL) in order to control its permeability [29]. Indeed, they obtain a thermosensitive filtration membrane in which the pore diameters increased when the temperature reached the cloud point of the PVCL (around 27°C).

Elastin-like polypeptides (ELP) are also among the most studied thermoresponsive systems [30, 31]. These linear polypeptides are composed of repeating units of the pentapeptide valine-proline-glycine-X-glycine (with X corresponding to any amino acid except proline) and were described in the literature for the reversible immobilization of thiol-redoxin-ELP fusion proteins (Trx-ELP) onto gold surfaces [32]. Furthermore, the biological activity of Trx-ELP nanoarrays was demonstrated by binding an antibody and showing that the resulting complex could be released from the surface above the LCST (Fig. 1).

Several other thermally responsive systems can be cited, such as poly- or oligo(ethylene glycol) methacrylate (OEGMA) derivatives [33–43]. We recently showed that copolymers of 2-(2-methoxyethoxy)ethyl methacrylate (MEO<sub>2</sub>MA) and OEGMA exhibited a LCST in water that can be adjusted to physiological





**Fig. 1** Nanopatterned surface bearing thermoresponsive elastin-like polypeptides (ELP) allowing reversible capture and release of fusion proteins: *left* ELP switch off; *center* ELP switch on; *right* AFM image of a  $10 \times 9$  ELP dot array in PBS at room temperature. Reprinted, with permission, from [32]. Copyright (2004) American Chemical Society

temperature by varying the composition of the two monomers [44–47]. Polymer brushes have been prepared on flat gold surfaces and demonstrated an ability to control cell adhesion [45, 46]. These smart surfaces combined switching ability and biorepellency [48]. Indeed, at  $37^\circ\text{C}$  cells adhered to the surface and when the temperature of the medium was decreased to  $25^\circ\text{C}$ , a cell rounding was observed that allowed their easy detachment from the surface without trypsinization.

## 2.2 pH-Responsive Polymers

pH triggering is another suitable method for creating smart bioactive surfaces. Weak acids and bases display a change in their ionization state when changes in pH occur. This leads to physicochemical changes such as the formation of aggregates or the swelling/deswelling of hydrogels [49]. Several pH-responsive polymers can be used. For instance, poly(methacrylic acid) (PMAA) [50, 51] and poly(*N,N*-dimethylaminoethyl methacrylate) (PDMAEMA) [52] are typical examples of poly(acid) and poly(base). Recently, Argentiere et al. developed novel smart surfaces for in situ cell staining [50]. They covalently immobilized pH-responsive microgels made of PMAA on a glass surface and loaded them with an oligothiophene-conjugated anti-human CD4 monoclonal antibody. They showed that the increase in pH from 5.0 to 8.0 led to the augmentation of microgel height. The pH-sensitivity of the surface was exploited to control the encapsulation and release of antibodies in an on-demand way. Van Camp et al. reported the synthesis of poly(acrylic acid) with disulfide bonds as pH-responsive brush surfaces and demonstrated the collapsing/swelling properties by atomic force microscopy [53].

pH-switchable surfaces were designed for various biological applications. For instance, Barroso et al., prepared porous pH-sensitive membranes for protein filtration [54]. In their synthetic pathway, poly(MMA-*co*-MAA) thin films were prepared

via a radical polymerization process in supercritical CO<sub>2</sub>. Another application was proposed by Wei et al. [55], who used pH-responsive polymers as the stationary phase in column chromatography.

The pH-induced swelling and collapsing behavior of polymers has also been exploited for the tumor-targeted delivery of paclitaxel [56] or the controlled release of doxorubicin [57]. The group of Stoddart has developed several pH-responsive systems for drug delivery [58, 59]. For example, they designed mesoporous silica nanoparticle (MNP)-based drug-delivery systems in which the release was triggered by pH changes. Supramolecular machines comprising cucurbit[6]uril (CB[6]) rings encircling tethered trisammonium stalks were attached to the MNP surfaces (Fig. 2). The guest molecules were entrapped in the MNPs at neutral pH and were released when the pH was lowered.

In this complex system, when the pH was lowered, the anilinium nitrogen atom was protonated and the CB[6] rings lifted to the top of the stalk. The consequence was the opening of the pores, leading to the drug release. When the pH was then raised, the nitrogen atoms were deprotonated and this led to the detachment of the CB[6] rings from the stalk.

Some research groups studied double- or multisensitive surfaces bearing pH-switchable polymers. For instance, Ayres et al., prepared poly(acrylic acid) polymer brushes via the ATRP of *tert*-butyl acrylate followed by the conversion to acrylic acid using a pyrolysis approach. The obtained polymer brushes responded to two stimuli, i.e., pH and ionic strength [51]. Nevertheless, the most developed systems combine temperature and pH stimulations [19, 52, 60, 61]. Zhang et al. investigated temperature and pH-responsive polymeric membranes based on poly(NIPAM-*co*-MAA) nanoparticles and their permeability to proteins and peptides [62]. The nanoparticles functioned as thermo- and pH-responsive nanovalves: when the particles swelled, the valve was in a closed state; when the particles shrank, more space was generated, thus increasing the membrane permeability to solutes. The monomer composition of the particles can be varied to increase either the temperature- or the pH-sensitivity according to the application.

### 2.3 Photoresponsive Polymers

There are numerous functional groups that can render polymers photoresponsive, such as azo groups, merocyanines, fulgides, and groups that can undergo a 2 + 2 cycloaddition, e.g., cinnamoyl groups. While 2 + 2 cycloadditions are not always fully reversible, the other mentioned groups permit a switching from one state to the other and back. Azo dyes are particularly popular as photoresponsive groups and, consequently, many examples of photoresponsive polymer surfaces incorporating azo dyes can be found.

In 1982, an azo-dye-containing copolymer of 2-hydroxymethyl methacrylate was used for modulation of lysozyme adsorption on polymer beads. The amount of the protein adsorbed on a microsphere decreased upon irradiation, but rather long



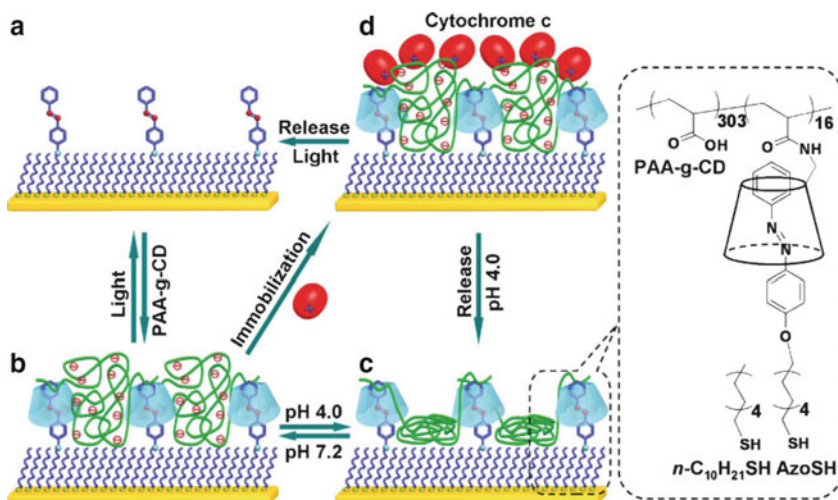
irradiation times (approx. 40 min) were needed to reach the maximum effect [64]. In a subsequent publication, the utilization of the same azo-dye-containing polymer surface for control of adhesion of erythrocytes was reported [64].

Tieke and Saremi demonstrated in 1998 the *cis-trans* switching of azo dyes incorporated into a polyelectrolyte multilayer system [65]. A change in the absorbance at 340 nm served as proof of the change in conformation. In 1999, Seki and coworkers demonstrated that the morphology of an azo-dye-containing polymer film deposited on mica can be switched by irradiation with UV and visible light. According to AFM studies, after irradiation with UV light, the polymer chains adopted a more expanded conformation, and upon exposure to visible light, the polymer structures on the mica surface shrank [66]. Hong and Kumar recently incorporated azo-dye-bearing polycations into a polyelectrolyte multilayer system deposited on a porous membrane. They used *cis-trans* switching for the control of an  $\text{SO}_4^{2-}$  ion flux [67].

Zhang and coworkers [68] used surface-tethered azo dyes for the immobilization of partially cyclodextrin-modified poly(acrylic acid) via photocontrolled host-guest interaction of the azo dye and the cyclodextrin. This surface was then capable of binding and release of cytochrome c. At neutral pH, the majority of the carboxylic acid groups are deprotonated, and cytochrome c is attracted to this surface by electrostatic interactions. In acidic conditions, the acrylic acid units in the copolymer chains are protonated and therefore the positively charged cytochrome c is no longer attracted. Alternatively, the cytochrome c can be released by irradiation with UV light (365 nm). In this case, the surface-tethered azo dyes adopt a *cis* conformation and the host-guest interactions are broken. Consequently, the cyclodextrin-modified poly(acrylic acid) is released from the surface together with cytochrome c (Fig. 3).

Azo dyes were also incorporated into molecularly imprinted polymers (MIPs) to switch the molecular recognition [69]. Photoisomerization of the crosslinked polymer matrix enabled modulation of the substrate affinity by altering the geometry and spatial arrangement of imprinted receptor binding sites. As a result, controlled release and uptake of the template (or analogous ligands) were obtained. Depending on the type of ligand, the affinity varied up to approximately 40% upon irradiation with UV light (Fig. 4).

Another photoresponsive group that is utilized for the generation of photoresponsive polymer coatings is the spiropyran-merocyanine system. Shiyong Liu and coworkers coated silica nanoparticles with the thermoresponsive PNIPAM, incorporating co-units with spiropyran and with benzoxadiazole functionalities [70]. The latter, serving as fluorescence resonance energy transfer (FRET) donors, were arranged in an inner layer, whereas the spiropyrans were located in an outer layer of the coating. UV irradiation of these surfaces was demonstrated to induce the transformation of nonfluorescent spiropyran moieties in the outer layer of the coating into the fluorescent merocyanine form. This resulted in occurrence of FRET between the benzoxadiazole and merocyanine residues, as evidenced by the changes in the fluorescence spectra. Due to the thermoresponsive nature of the coating, switching by heating and cooling was also possible (see Fig. 5).



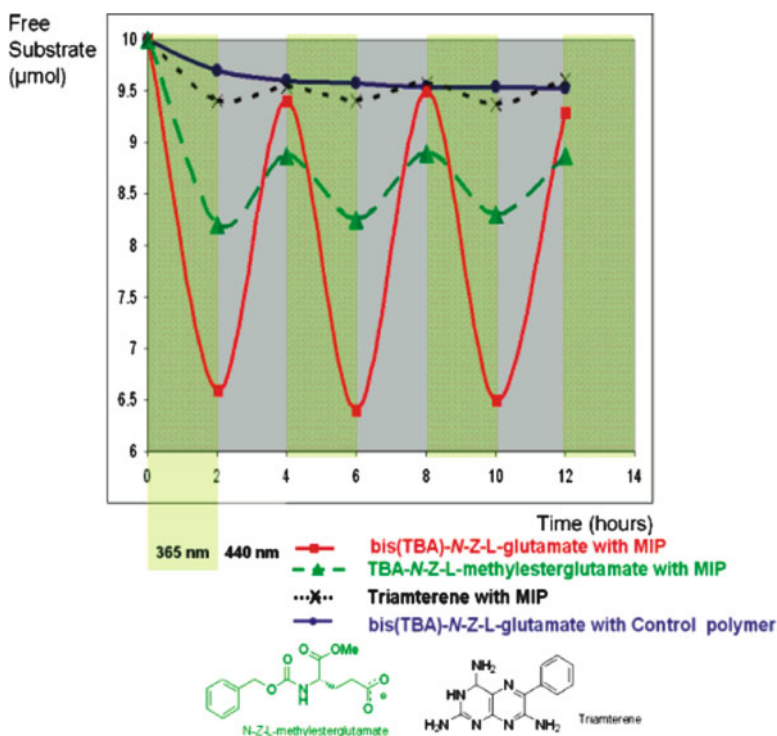
**Fig. 3** Photoresponsive polymer surface sensitive to pH and light. Adsorption and release of cytochrome *c* triggered by pH (**b**, **c**, and **d**); release of the polymer layer and cytochrome *c* by breaking the host–guest interactions between surface-tethered azo dye and cyclodextrin via light irradiation (**a** and **d**). The molecular structure on the right represents the host-guest complexation of the azo dye with the cyclodextrin-modified poly(acrylic acid). Reprinted, with permission, from [68]. Copyright (2009) Wiley Interscience

Not only synthetic photoresponsive groups can be utilized for smart polymer coatings. Tian and Saaem grafted poly(acrylic acid) modified with bacteriorhodopsin to glass surfaces using an electron beam for the introduction of crosslinks [71]. Exposing this hydrogel to green light induced a multistage photocycle involving conformational change in the bacteriorhodopsin from all-*trans* to 13-*cis*. This in turn resulted in an increased flux of protons and a local decrease in pH, causing the polyacrylic acid groups to protonate and the hydrogel to deswell into a shrunken form. Thus, the thickness of this smart hydrogel coating can be switched by light.

## 2.4 Chemoresponsive and Bioresponsive Polymers

There are numerous examples of polymer surfaces that react with a change of their properties when brought into contact with certain species. These trigger species can be low molar mass molecules (chemoresponsive) or complex biomolecules like DNA or proteins (bioresponsive). Both types of responsive surfaces exist in several varieties depending on their mode of action and the parameter that they affect.

One way of obtaining chemically responsive polymer surfaces relies on the concept of structural color. In this case, the color of an object is not generated by selective absorption of light, but by interference and Bragg reflection induced by

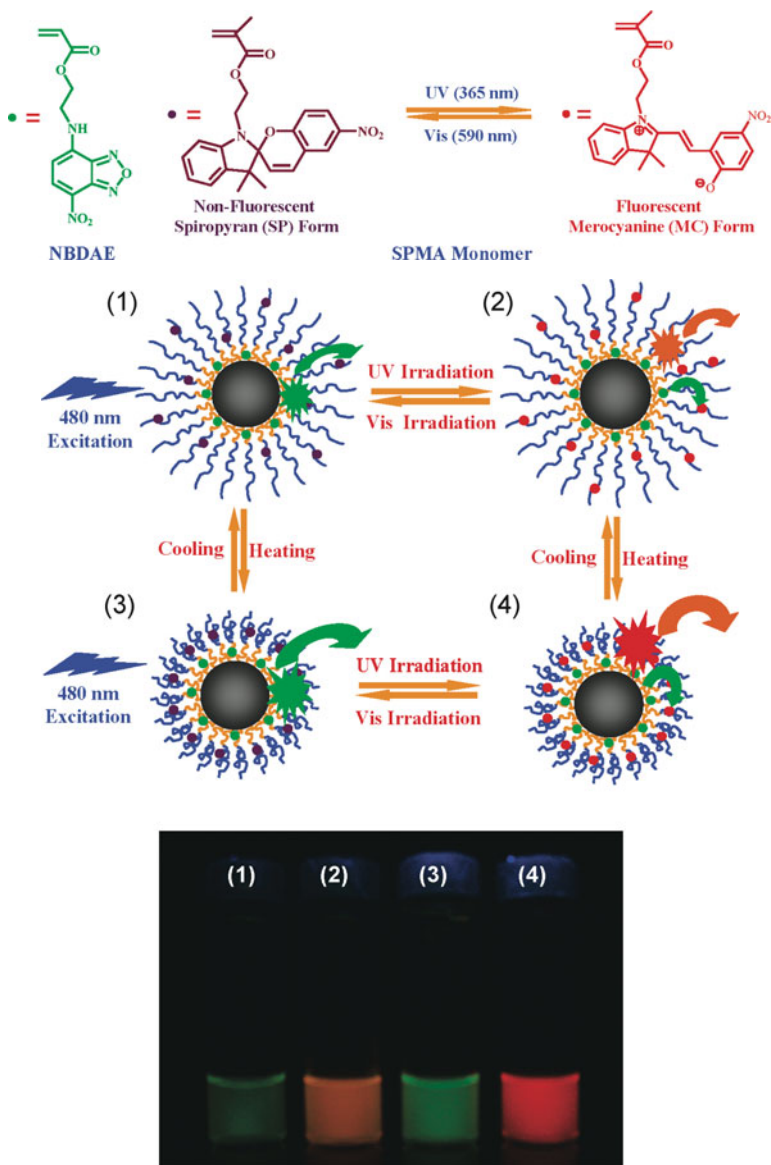


**Fig. 4** Photoswitching in molecularly imprinted polymers incorporating azo dyes. Upon UV irradiation, the affinity of the MIP decreases. The extent of the effect is dependent on the ligand. The most significant effect was observed with bis(TBA)-N-Z-L-glutamate (squares) and N-Z-L-methylesterglutamate (triangles). On the other hand, only a weak effect was observed with triamterene (crosses). Reprinted, with permission, from [69]. Copyright (2009) American Chemical Society

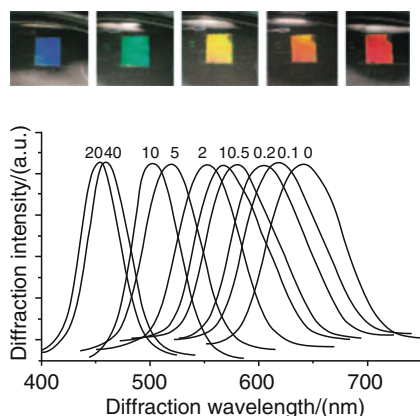
periodic structures with an appropriate repeat distance. The periodic structures can either form lamellar [72] or 3D patterns [73], analogous to the naturally occurring mineral opal. Upon binding of an analyte, the repeat distance is changed, and this change results in shift of the reflected color.

Based on this fundamental principle, Alexeev et al. developed a photonic crystal glucose-sensing material [74], which consisted of a 3D periodic structure embedded in a polyacrylamide–poly(ethylene glycol) (PEG) hydrogel with pendant phenylboronic acid groups. In subsequent work [75], they optimized the system by incorporating boronic acid derivatives such as 4-amino-3-fluorophenylboronic acid and 4-carboxy-3-fluorophenylboronic acid as the molecular recognition elements. This enabled sensing at physiologic pH values (Fig. 6). Similarly, Braun and coworkers [76] reported a polymeric system incorporating boronic acid moieties, in which exposure to glucose induced a color change. However, in this case, a hydrogel inverse opal was created. Although strong diffraction of green light was observed when the





**Fig. 5** Smart UV-responsive coating on silica nanoparticles with PNIPAM brushes functionalized with FRET donors, 4-(2-acryloyloxyethylamino)-7-nitro-2,1,3-benzoxadiazole (NBD-DAE), and photoswitchable acceptors, 1'-(2-methacryloxyethyl)-3',3'-dimethyl-6-nitro-spiro(2*H*-1-benzopyran-2,2'-indoline) (SPMA). The UV radiation induces the change from colorless spiropyran derivatives in the outer part of the coating (1) to the fluorescent merocyanine form (2). Thus, FRET with the benzoxadiazole moieties in the inner part of the coating is enabled and the fluorescence color changes from *green* to *red*. By variation of the temperature and induction of a collapse of the PNIPAM chains (3), the FRET efficiency can be tuned (4). Reprinted, with permission, from [70], Copyright (2009) American Chemical Society



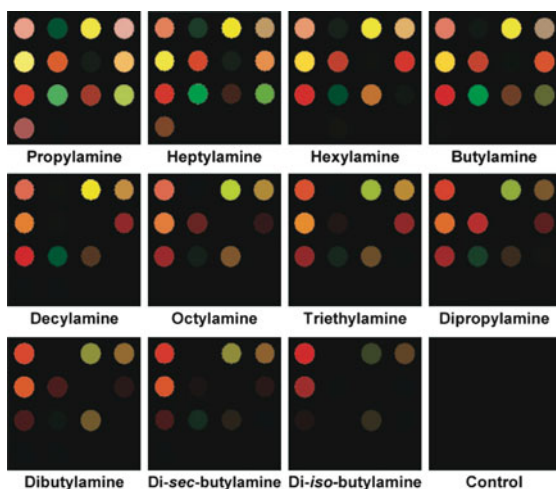
**Fig. 6** Color change of a glucose-responsive colloidal crystal in dependence on the glucose concentration. Adapted from [75] with kind permission of the authors (Prof. Sanford A. Asher)

hydrogel was in contact with deionized water, exposure to  $1 \text{ mmol L}^{-1}$  glucose in pH 9 buffer for 20 min shifted the diffraction to red. In an analogous manner, Asher and coworkers [77] created inverse opals of poly(2-hydroxyethyl methacrylate) that were sensitive to protons and ethanol.

Chemosensors of this type permit the simultaneous detection of chemically similar species, which may be desirable in some situations, but do not allow an unambiguous identification of the analyte. This is different for multispot sensor arrays, such as described by Suslick and coworkers [78]. In this work, various nanoporous pigment microspheres were spotted onto chromatography paper. Sixteen different pigments (14 pH dyes and two solvatochromic dyes) were used and therefore each type of microsphere exhibited a different color change upon exposure to amines. As a consequence, each amine gave a specific response fingerprint, thus permitting the unambiguous identification of a single compound (Fig. 7).

Apart from systems responding to exposure to low molar mass molecules, there are also bioresponsive systems. These often react with a volume change upon exposure to the trigger species. This was put into practice in several ways: Kokufata et al. [79] described a crosslinked PNIPAM gel in which concanavalin A was immobilized. When exposed to a solution of dextran sulfate at a temperature close to the LCST, the gel swelled to a fivefold greater volume, because the hydrophilic polysaccharide binds to the hydrogel and shifts its LCST. Miyata et al. prepared an acrylamide-based gel, to which an antibody [goat anti-rabbit immunoglobulin G (IgG)] and its antigen (rabbit IgG) were immobilized [80]. The specific binding reaction between these two species caused additional crosslinking in the gel, and these crosslinks were broken when it was brought into contact with rabbit IgG. As a result, the gel swelled by about 15% in response to an aqueous solution of rabbit IgG, which was, however, rather concentrated ( $8 \text{ mg mL}^{-1}$ ). Lyon and coworkers observed swelling of a biotinylated microgel upon exposure to antibiotin antibodies or avidin [81]. They exploited the effect for biosensing by observing the effect



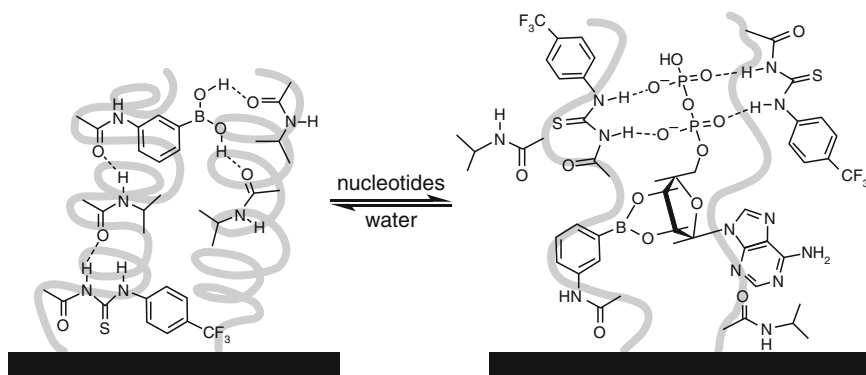


**Fig. 7** Multispot sensor arrays composed of nanoporous pigment microspheres, exhibiting different responses to aliphatic amines. By combination of different pigment particles, fingerprint patterns specific for each amine can be obtained. Reprinted, with permission, from [78]. Copyright (2008) American Chemical Society

through an optical microscope. An example from 2008 based on MIPs demonstrated that the inverse effect is also possible [82]. Using lysozyme or cytochrome c as templates, MIPs were prepared of NIPAM, acrylamide and methacrylic acid. These crosslinked gels shrank upon exposure to solutions of the template protein by up to 15% of their original size.

Volume changes are not the only parameter that can change in response to exposure to biomolecules. A polynucleotide-responsive surface was reported to exhibit variations in contact angle [83]. Copolymers of NIPAM and derivatives of phenylboronic acid and phenylthiourea were immobilized on silicon using surface-initiated ATRP. When in contact with nucleotides, these surfaces showed a decrease in water contact angle. This decrease was demonstrated to be a function of the logarithmic nucleotide concentration. As an explanation, the authors suggest the breaking of intrapolymer hydrogen bonds when nucleotides are available. The copolymer chains are supposed to become stretched, exposing more hydrophilic groups to the environment (Fig. 8).

Bioresponsive surfaces can even exhibit logical functions. Katz and coworkers described membranes with “and” or “or” functions [84]. An example of a membrane with an “and” function involved glucose oxidase immobilized onto an alginate membrane immersed in a solution of urea and  $O_2$  at pH 6. The absence of both invertase and sucrose or either corresponded to “0,0”, “0,1”, and “1,0” input signals, respectively. For these input signals, the membrane remained in its closed status. Adding both invertase and sucrose (“1,1” input signal) caused a decrease of the local pH to 4. This in turn caused a collapse of the alginate gel, which ultimately resulted in opening of the pores of the membrane.



**Fig. 8** Model for the response of polynucleotide-sensitive copolymers of NIPAM and derivatives of phenylboronic acid and phenylthiourea on silicon surfaces. Interaction with the nucleotide is supposed to result in unwinding of the polymer structure, causing decrease in contact angle by exposure of hydrophilic moieties. Reprinted, with permission, from [83]. Copyright (2009) American Chemical Society

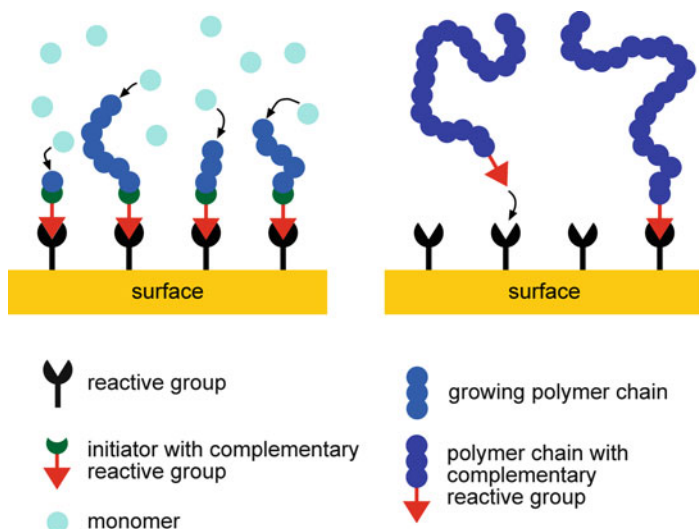
### 3 Surfaces Chemistries

#### 3.1 “Grafting onto” and “Grafting from” Approaches

When polymers are to be tethered to surfaces by covalent bonds, there are two fundamental approaches for achieving this: “grafting from” and “grafting onto.” “Grafting from” means surface-initiated polymerization, whereby the polymer chains are created in situ. “Grafting onto” involves formation of covalent bonds between previously formed polymer chains and reactive groups at a surface (Fig. 9). Both methods have specific pros and cons.

To perform “grafting from” reactions, only relatively small molecules – the monomers – need to reach the reactive sites located in the confined space at the surface. As a consequence, higher grafting densities are possible with this approach, compared to “grafting onto” reactions, in which rather bulky polymer chains need to diffuse to the surface and find sufficient space to reach a reactive site, some of which might already be shielded by previously tethered polymer chains. However, “grafting onto” processes are frequently more convenient and they permit a sufficiently high grafting density for many purposes. Furthermore, the soluble polymers can be characterized more easily in advance before they are immobilized. Therefore, the approach to be chosen will depend on the specific question to be addressed.

For “grafting onto”, a wide variety of surface chemistries is available (Table 1). This makes it a versatile approach that can be applied on many different types of surfaces. Frequently, polymers incorporating thiol [85] or disulfide groups [86] are tethered to noble metal surfaces, but there are many other appropriate reactive pairs, such as carboxy–amine [87], epoxide–hydroxy [88] or epoxide–amine



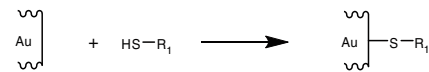
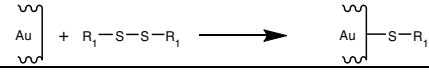
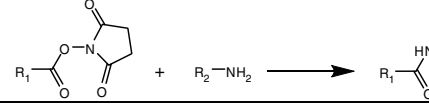
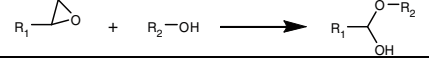
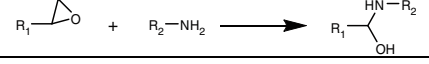
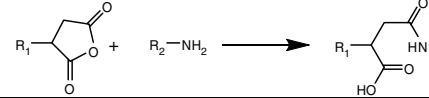
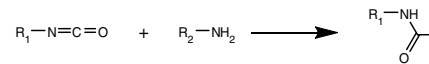
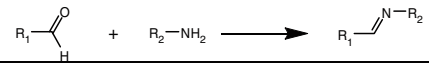
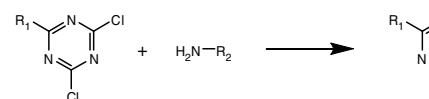
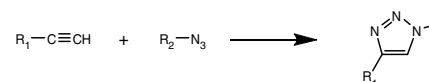
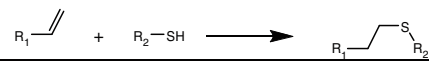
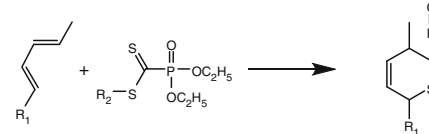
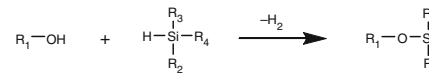
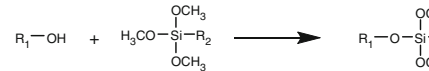
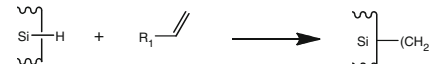
**Fig. 9** Representation of the “grafting from” (*left*) and the “grafting onto” approach (*right*)

[89], amine–anhydride and isocyanate–amine [90], aldehyde–amine [91], cyanuric chloride–amine [92], alkyne–azide [93, 99, 100] thiol–ene [94], dienophile–diene [95], hydroxy–silane [96], hydroxy–silanole [97], or hydrosilylation [98]. Moreover, the option of electrostatic adsorption exists [101].

“Grafting from” relies on the immobilization of initiator species on the surfaces. To accomplish this, fundamentally the same options exist as for the immobilization of polymer chains via the “grafting onto” approach. Furthermore, initiator molecules can be immobilized by binding of phosphonic acid groups to metal oxide surfaces [102]. Alternatively, a UV-assisted tethering of initiating thioxanthone groups on olefin polymer surfaces is possible [103]. Recently, conversion of low density poly(ethylene) surfaces into ATRP initiators by exposure to elementary bromine was reported [104]. “Grafting from” reactions can also be started from immobilized macroinitiators. Even initiating multilayer systems were put into practice [105].

Although some work on the “grafting from” method employing anionic or ring-opening polymerization exists, examples involving cationic polymerization are rare [106, 107]. The vast majority of research was devoted to “grafting from” involving radical polymerization. This concerned conventional free-radical polymerization in many variations [101, 108], but also controlled variants such as ATRP [109, 110], reversible addition-fragmentation chain transfer (RAFT) [111], nitroxide-mediated polymerization (NMP) [112, 113] and the photoiniferter technique [114]. Creation of smart surfaces involving “grafting onto” or “grafting from” approaches has gained considerable attention in recent years. Some practical examples are described in the following sections of this chapter.

**Table 1** Pairs of reactive groups for the immobilization of polymers on surfaces

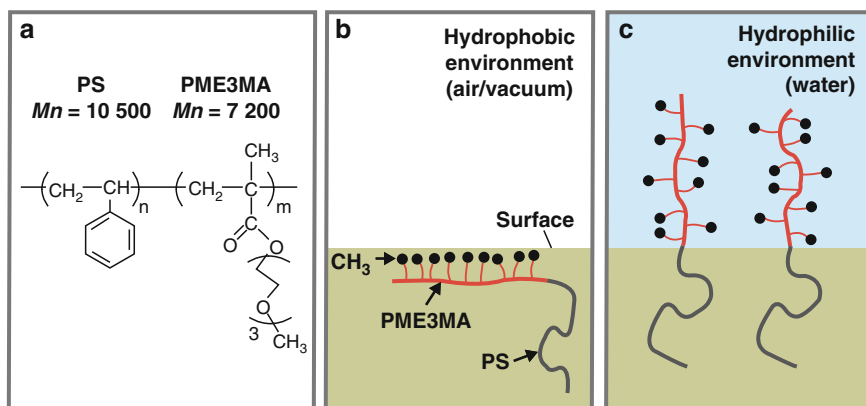
Reaction	Reference
	[85]
	[86]
	[87]
	[88]
	[89]
	[90]
	
	[91]
	[92]
	[93]
	[94]
	[95]
	[96]
	[97]
	[98]

### 3.2 Adsorption of Block Copolymers

Adsorption of block copolymers onto a surface is another pathway for surface functionalization. Block copolymers in solution of selective solvent afford the possibility to both self-assemble and adsorb onto a surface. The adsorption behavior is governed mostly by the interaction between the polymers and the solvent, but also by the size and the conformation of the polymer chains and by the interfacial contact energy of the polymer chains with the substrate [115–119]. Indeed, in a selective solvent, one of the blocks is in a good solvent; it swells and does not adsorb to the surface while the other block, which is in a poor solvent, will adsorb strongly to the surface to minimize its contact with the solvent. There have been a considerable number of studies dedicated to the adsorption of block copolymers to flat or curved surfaces, including adsorption of poly(*tert*-butylstyrene)-*block*-sodium poly(styrenesulfonate) onto silica surfaces [120], polystyrene-*block*-poly(acrylic acid) onto weak polyelectrolyte multilayer surfaces [121], polyethylene-*block*-poly(ethylene oxide) on alkanethiol-patterned gold surfaces [122], or poly(ethylene oxide)-*block*-poly(lactide) onto colloidal polystyrene particles [123].

So far, the most studied systems are polystyrene-based block copolymers or are composed of pluronics [124, 125]. In a recent work, Hershkovits et al. studied the adsorption of asymmetric polystyrene-*block*-poly(methyl methacrylate) (PS-*b*-PMMA) onto alumina particles having variable radii [126]. 2-Methoxyethanol was used as a solvent in this study because it is a good solvent for the PMMA block and a bad solvent for the PS. Nevertheless, in their systems the two polymer blocks interacted competitively with the alumina substrates. The polystyrene block adsorbed to the surface because of the presence of the bad solvent, and the PMMA monomers were attracted to the metallic surface because of the strong interaction of its segments with this kind of surface. Yokoyama et al. studied the coadsorption of polystyrene homopolymers with polystyrene-*block*-poly[tri(ethylene glycol) methyl ether methacrylate] (PS-*b*-PMEO<sub>3</sub>MA) block copolymers on planar substrates [127]. It was demonstrated that the hydrophilic PME<sub>3</sub>MA segments spontaneously cover the air–substrate or water–substrate interfaces (Fig. 10) [127, 128]. Interestingly, these modified surfaces have been studied as blood-compatible materials [128].

The adsorption of block copolymers can be controlled by different stimuli, in particular by the pH since most of the brushes formed by block copolymers adsorption are polyelectrolyte brushes [129, 130]. The group of Armes, for instance, studied the pH-controlled adsorption of a series of block copolymers [131, 132]. In the case of copolymers bearing hydrophobic 2-(diethylamino)ethyl methacrylate groups (DEA) and a water-soluble zwitterionic poly(2-methacryloyl phosphorylcholine) (MPC) block, they showed that at low pH the cationic DEA flattened to the anionic silicon surface while the MPC was in contact with the solution [132]. At around neutral pH, micelles were formed in solution and adsorbed onto the surface because the DEA core was still weakly cationic. The MPC block formed the micelle coronas. Nevertheless, at higher pH the micelles became less cationic and the adsorption rate decreased.



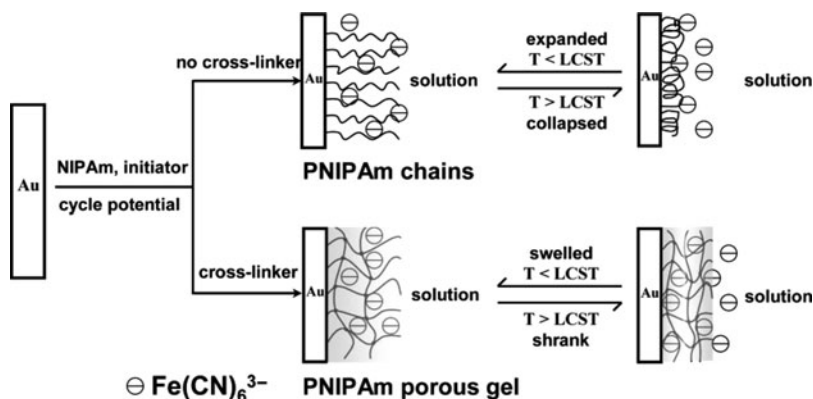
**Fig. 10** (a) Structure of PS-*b*-PME<sub>3</sub>MA. (b) Copolymer-modified surface in a hydrophobic environment and (c) in a hydrophilic environment. Reprinted, with permission, from [128]. Copyright (2005) Wiley Interscience

### 3.3 Surface-Bounded Hydrogels

A hydrogel is a crosslinked polymer network composed of water-swallowable or water-soluble macromolecules. If the macromolecules are tethered to surfaces, the surface as such can act as a crosslinker. Therefore, almost any surface decorated with water-soluble or hydrophilic polymer chains may be regarded as a hydrogel [133]. There are many examples for such structures; some were created with the goal of antifouling properties (see Sect. 4.1) and others served as biocompatible platforms for biosensing purposes (see Sect. 4.5). This section will focus on examples of stimuli-responsive hydrogel coatings. Such stimuli can be pH, light, ionic strength, or temperature. pH-responsive hydrogels were used as valves in microfluidic channels [134]. Moore and Zhao described a similar approach, with the goal of improved response times [135]. Light-responsive hydrogels were prepared by Sumaru and coworkers [136]. They were used for the control of cell adhesion; further details are given in Sect. 4.3.

Temperature as a stimulus has important advantages if biological systems need to be handled. Whereas light is not a suitable stimulus for turbid biological fluids like blood, and changes in ionic strength and/or pH require transport of matter and can provoke sensitive reactions of biological systems, moderate temperature changes can be applied to most specimens without an adverse effect. Although a wide variety of chemical structures can mediate thermoresponsive behavior [137], hydrogels made of PNIPAM account for the vast majority of thermoresponsive examples.

For example, surfaces comprising PNIPAM microgels were utilized for drug delivery [138]. Electrostatic layer-by-layer assembly with poly(NIPAM-*co*-acrylic acid) and poly(allylamine hydrochloride) on an amino-functionalized surface yielded thermoresponsive thin films. These were capable of a thermally regulated uptake and release of the chemotherapeutic drug doxorubicin. The films were loaded



**Fig. 11** Thermoresponsive ion storage behavior of immobilized noncrosslinked (*top*) and crosslinked PNIPAM (*bottom*). Reprinted, with permission, from [139]. Copyright (2007) Wiley Interscience

with doxorubicin by cycling the temperature of the film in an aqueous doxorubicin solution between 25 and 50°C. Release characteristics were then examined using UV–vis spectroscopy, which revealed temperature-dependent release properties. In another recent example [139], surfaces were modified with tethered linear PNIPAM chains or with crosslinked porous PNIPAM hydrogels. With respect to  $[\text{Fe}(\text{CN})_6]^{3-}$  ion permeability and uptake, the tethered chains showed on/off switching behavior, whereas the PNIPAM gel-modified interface exhibited a “breathing in” process (Fig. 11).

This was evidenced by cyclic voltammetric measurements. In both linear and crosslinked systems, there is a temperature-dependent switching of the  $[\text{Fe}(\text{CN})_6]^{3-}$  reduction peak current from high current at 25°C to low current at 45°C. However, while the process is fully reversible in the linear system, the reduction peak current values continuously increase cycle by cycle in the crosslinked system. This indicates that ions becoming entrapped in the collapsed hydrogel at elevated temperature accumulate in the hydrogel.

In spite of the dominance of PNIPAM, there are examples of thermoresponsive hydrogels made of other compounds [140]. Here, tailoring of the LCST was achieved by polymer-analogous acetylation or cinnamoylation of the water-soluble precursor polymers, namely poly(*N*-2-hydroxypropylmethacrylamide), poly[*N,N*-bis(hydroxyethyl)acrylamide] and poly[*N*-[tris(hydroxymethyl)-methyl]acrylamide]. The LCST could be tailored easily by choice of the degree of acylation. By polymerization using a disulfide-functionalized azo-initiator, it was possible to prepare thin hydrogel films composed of the modified copolymers on noble metal surfaces [26, 141]. Alternatively, non-PNIPAM hydrogels exhibiting an LCST can be formed of poly[(diethylene glycol) methyl ether methacrylate]-*co*-oligo(ethylene glycol) methyl ether methacrylate] P(MEO<sub>2</sub>MA-*co*-OEGMA) [142]. The thermoresponsive hydrogels were prepared on planar silicon substrates by the “grafting from” method, using surface-initiated ATRP. As a general tendency, the

collapse temperatures of the surface-bound systems were reported to be higher than those of the polymers in solution; however, with increasing OEGMA content, the difference became increasingly smaller.

## 4 Bioapplications of Smart Polymer Surfaces

### 4.1 Antifouling Surfaces

The term “fouling” has been adapted from the research of Epstein, where this word has been defined as the undesirable deposition of material on surfaces [143]. Non-specific adsorption of proteins, cells, or bacteria on surfaces is known as biofouling and is a major problem that can damage the function of medical devices or diagnostic systems and can lead to many diseases. For instance, keratitis can occur due to bacterial colonization of contact lenses [144, 145], and one of the causes of the failure of *in vivo* biosensors is protein accumulation on their surfaces [146]. In their review, Wisniewski and Reichert reported some methods for minimizing biosensor membrane biofouling, including hydrogel or biomimetic phospholipid coatings and changes in surface topology [146]. Moreover, several other antifouling surfaces have been developed to overcome this phenomenon [147]. The (co)polymers used to create the antifouling surfaces include poly(OEGMA) [148, 149], poly(2-hydroxyethyl methacrylate) [150, 151], poly(acrylonitrile-*co*-maleic acid) [152], poly(acrylamide) [153, 154], PEG-poly(propylene sulfide)-PEG triblock copolymers [155], or poly(glycerol monomethacrylate) [156]. PEG and its derivatives have been the most used antifouling systems. PEG is a nontoxic, nonimmunogenic, and biocompatible polymer that exhibits a good antifouling efficiency [147]. The group of Chilkoti, for instance, prepared surfaces coated with poly(OEGMA) using surface-initiated ATRP from a self-assembled monolayer (SAM) on gold surfaces [148]. With this method, they obtained a high surface density of PEGylated polymers, which conferred to the surface an excellent protein resistance. Indeed, by surface plasmon resonance (SPR) spectroscopy, they showed that the resulting brushes reduced the adsorption of proteins from 100% of serum or fibronectin solution to the detection limit of the technique. Moreover, the protein resistance seemed to be dependent on surface thickness and density.

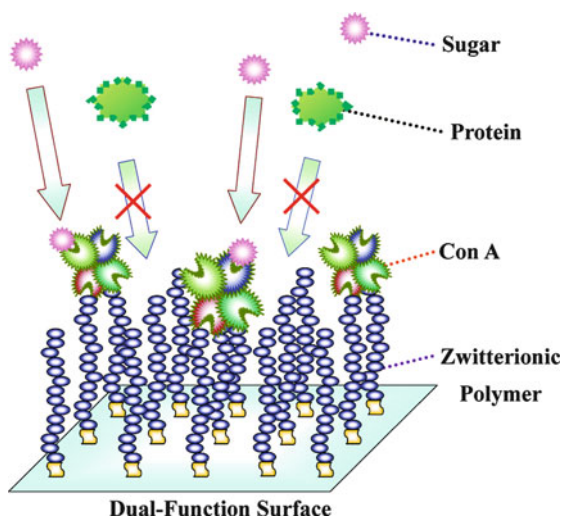
Although the field of antifouling surfaces is dominated by coatings based on PEG [92, 157], polysaccharides [88, 158–160], or combinations [161] thereof even in recent studies [162–168], there are many examples of the utilization of other chemical structures. Recently, polymer surfaces presenting zwitterionic groups have also gained considerable attention. Following some studies on SAMs [169, 170], the effects of surface-tethered zwitterionic polymers were investigated [171–173]. Jiang et al. observed low nonspecific adsorption of fibrinogen and HRP-conjugated anti-fibrinogen antibodies on hydrogels prepared from equimolar mixtures of monomers bearing a positive charge [aminoethyl methacrylate hydrochloride, 2-(dimethylamino)ethyl methacrylate (DMAEMA), 2-(diethylamino)



ethyl methacrylate, 2-(methacryloyloxy) ethyl trimethylammonium chloride] and monomers bearing a negative charge (2-carboxyethyl acrylate, 3-sulfopropyl methacrylate potassium salt) [172]. Following a slightly different approach, Chen and coworkers [173] and, recently, Kitano et al. [171] immobilized polymers bearing sulfobetain groups via ATRP (“grafting from” method) and found very low nonspecific adsorption of proteins such as fibrinogen,  $\gamma$ -globulin, human serum albumin [173] or bovine serum albumin and lysozyme [171]. In addition, Kitano et al. covalently immobilized a sugar-binding protein (concanavalin A) onto the brushes to create a scaffold for sugar sensing (Fig. 12). There are more similar examples from the same and other groups [174], and even polyelectrolyte multilayer systems topped with a phosphorylcholine-modified poly(acrylate) are effective in reduction of nonspecific protein adsorption [175].

Another antifouling system using peptidomimetic polymers was presented by the group of Messersmith [176]. Using solid-phase Rink amide resin, they synthesized a polymer bearing a short peptide domain and an N-substituted glycine oligomer of various lengths (peptoid). This new mimetic compound was found to provide protein resistance, and the antifouling properties could be maintained for several months. This last characteristic can be exploited for the design of long-term antifouling surfaces in physiologic or marine environments.

The mechanisms that prevent nonspecific adsorption are still under debate, and since there is no generally accepted, standardized testing method for nonspecific adsorption, results are often hard to compare. Work from Whitesides and coworkers suggested an important role of hydrogen bond acceptors [159, 177]. Many reports on sufficient suppression of nonspecific adsorption by polysaccharide coatings



**Fig. 12** Representation of the antibiofouling and sugar-specific recognition of a zwitterionic polymer-brush-based surface containing concanavalin A. Reprinted, with permission, from [171]. Copyright (2010) American Chemical Society

incorporating hydrogen bond donors raise doubts about the universal validity of these statements; and more recent work by Unsworth et al. on end-tethered PEG oligomers hints at an important influence of the polymer chain density [178]. According to this work, there is an optimum chain density for methoxy-terminated PEGs and, if a threshold chain density is surpassed, then hydroxy groups as distal PEG chain ends are superior to methoxy groups. However, at least for polymers tethered by the “grafting from” method, there also seems to be a practical upper limit for the grafting density, because otherwise the tendency of the polymer chains to detach from the surface becomes too strong [179]. A publication by Fukuda and coworkers suggests that high brush densities enhance suppression of nonspecific protein adsorption by size-exclusion effects [180].

## 4.2 Control of Protein Adhesion

Fundamentally, surfaces can interact with proteins in a nonspecific or a specific way. Although nonspecific interaction of proteins with surfaces is undesirable in most cases, it can be of interest to switch the capability of adsorption using an external stimulus. Alternatively, it might be advantageous to switch the *specific* interaction of a surface with a distinct protein, while keeping it repellent for all other biological species under all conditions. For either approach, polymers are important building blocks that can mediate the stimuli-responsive properties.

There are several recent examples of the switching of nonspecific protein binding on polymer surfaces by application of an external stimulus. Alexander and coworkers demonstrated that protein adhesion can be controlled on PNIPAM surface brushes [14, 181]. For instance, it was reported that the adsorption of FITC-labeled bovine serum albumin (FITC-BSA) on PNIPAM/hexadecanethiol micropatterned surfaces could be tuned by LCST. However, this effect was found to be less pronounced after prolonged incubation times or repeated heating/cooling cycles. The authors suggested that this behavior could be due to unspecific PNIPAM–protein interactions [14].

Sukhishvili and coworkers prepared hydrogels composed of PMAA using layer-by-layer multilayer assembly of poly(*N*-vinylpyrrolidone) and PMAA, crosslinking the layer by formation of amide bonds with ethylenediamine and subsequently washing out the poly(*N*-vinylpyrrolidone) by exposing the surfaces to a phosphate buffer solution at pH 7.5 [182]. The resulting PMAA hydrogel was capable of reversible loading and release of dyes and proteins. For instance, lysine and heparin were tested as model compounds. Lysine was retained at neutral pH and released in acidic conditions, whereas the opposite was found for heparin. Uhlmann and coworkers applied a polymer coating with combined pH- and thermoresponsiveness to obtain controlled protein binding. They grafted poly(2-vinylpyridine) and PNIPAM to silicon surfaces [183]. With this system, a switching of human serum albumin adsorption by changing the temperature from 23 to 40°C was observed.

In contrast to these approaches based on nonspecific interactions, Zhang and coworkers described a molecularly imprinted hydrogel based on the thermoresponsive PNIPAM [184]. This hydrogel was prepared by copolymerization of a metal chelate monomer *N*-(4-vinyl)-benzyl iminodiacetic acid, which formed a coordination complex with the template protein in the presence of Cu ions, *N*-isopropylacrylamide, acrylamide, and *N,N*-methylenebisacrylamide as crosslinker. The interaction of the imprinted thermoresponsive hydrogel with the protein could be switched between coordination effects and electrostatic attraction by addition or omission of Cu ions. Furthermore, this imprinted hydrogel allowed switching of lysozyme adsorption by changing the temperature.

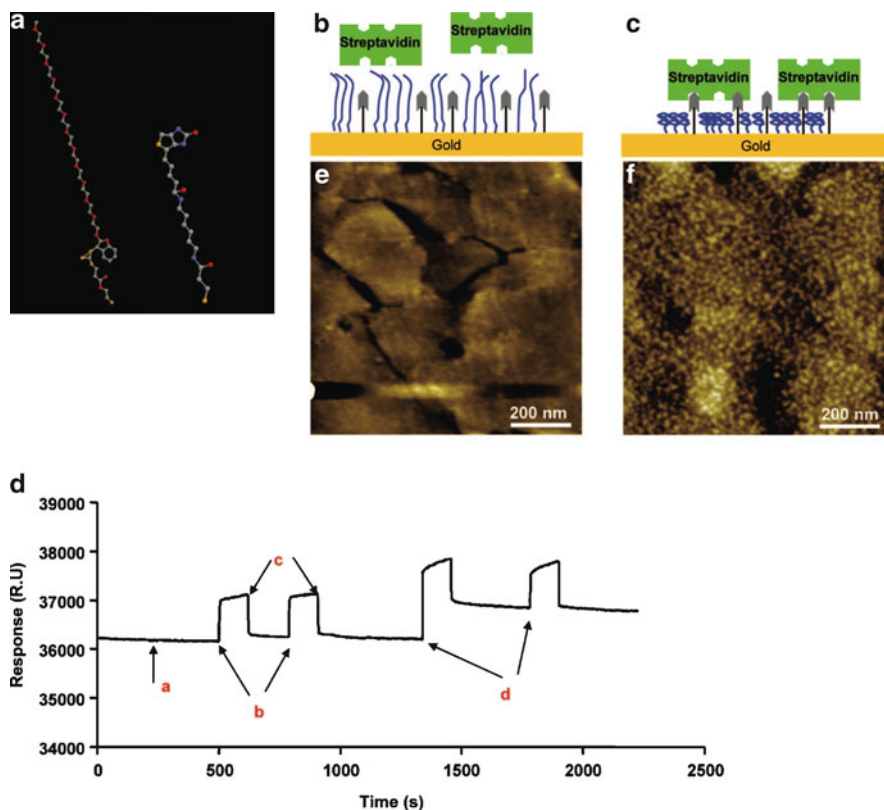
Another example of switching specific biomolecular interactions by a change in temperature was reported by Bulmus and coworkers [185]. Using biotin and streptavidin with a dissociation constant ( $K_D$ ) of approximately  $10^{-15}$  mol L<sup>-1</sup>, they chose one of the strongest interacting biochemical systems known. Gold surfaces were modified by coimmobilization of biotin and oligo(ethylene glycol) (OEG) chains exhibiting a LCST behavior (Fig. 13). The OEG chains were long enough to shield the surface-tethered biotin groups in the expanded state, while in the collapsed state, access to biotin was free. The interaction of this system with streptavidin was monitored by SPR in dependence of the temperature. At 23°C, there was almost no streptavidin binding to the modified surface, whereas at 45°C the change in resonance angle was quite substantial, indicating the binding of streptavidin to the now freely accessible surface-tethered biotin groups. Taking into account the extremely high affinity of the binding partners, the effectiveness of switching in this system is interesting.

### 4.3 Control of Cell Adhesion

Culturing of eukaryotic cells is an important element of modern life science. Although there are cells that can grow in free suspension, most cells derived from solid tissues need to be cultured at surfaces and must subsequently be lifted off for further use. Common protocols require the use of digesting enzymes like trypsin for this step, which will destroy any features outside the cell membrane. Hence, with these methods, harvesting of completely intact cells is impossible. Therefore, it was an attractive idea to apply smart polymer surfaces for the control of cell adhesion.

There have been several approaches, utilizing stimuli such as electrochemistry, light, or temperature. As a consequence of the large size of cells, even mechanical deformation can be employed as switching stimulus.

Yousaf and coworkers used an OEG-based surface bearing hydroquinone groups for electrochemical control of cell adhesion [186]. The hydroquinone groups were electrochemically converted into quinones, to which a cyclopentadienyl-modified RGD motif was then coupled via a Diels–Alder reaction. Although the hydroquinone-bearing surface was cell-repellent, fibroblasts attached to the areas



**Fig. 13** SPR and AFM analyses of controlled streptavidin recognition on mixed oligo(ethylene glycol) layers. **(a)** Chemical structure of the mixed layer components: linear oligo(ethylene glycol) (*left*) and biotinylated moiety (*right*). **(b)** Streptavidin binding at 23°C and **(c)** at 45°C. **(d)** SPR sensogram of streptavidin adsorption at 23 and 45°C. *Arrows* show injections of **(a)** water; **(b)** streptavidin solution and **(c)** subsequent water rinse at 23°C; and **(d)** streptavidin solution and subsequent water rinse at 45°C. **(e)** Tapping mode AFM images in liquid phase after injection of streptavidin solution at 23°C and **(f)** at 45°C. Reprinted, with permission, from [185]. Copyright (2008) American Chemical Society

where RGD sequences were immobilized. The surface modification is electrochemically reversible; therefore cells can ultimately be released by reconstitution of the hydroquinone groups.

Kessler and coworkers immobilized RGD peptides to a PMMA surface via a spacer incorporating an azobenzene unit [187]. The molecules were arranged in such a way that the RGD motifs were accessible to cells approaching the surface when the azo unit was in the E-form, and were hidden from the cells when the azo unit was in the Z-form. This enabled the reversible modulation of mouse osteoblast adhesion by irradiation with visible or UV light. However, the difference between “on” and “off” states is not very pronounced. Possibly, the accessibility of the RGD motif is not

changed substantially when switching from the E- to the Z-form. Yet, this interesting concept was optimized in recent work by Shao, Jiang and coworkers [188]. They tethered the azo dye to the surface utilizing an OEG spacer. When optimizing the molar ratio of azo-motif-bearing RGD sequences to biorepellent unsubstituted OEG chains, very pronounced differences in cell adhesion were achieved when switching from the E- to the Z-form.

An alternative photoresponsive coating was proposed by Sumaru and coworkers [136]. This approach did not employ any specific recognition groups, but was based on change of the surface properties of a cell culture substrate modified with a copolymer of NIPAM and a polymerizable spiropyran derivative, simultaneously exhibiting thermo- and photoresponsive properties. Chinese hamster ovary cells adhered to such a surface at 37°C, but were washed off with cold water. Only when the surface was irradiated with UV light ( $\lambda = 365$  nm), causing the isomerization of the spiropyran to a zwitterionic merocyanine form, did the cells remain at the surface. Subsequent irradiation with visible light ( $\lambda = 400$  nm), reversing the isomerization, and washing with cold water caused the cells to be lifted off. Further experiments demonstrated the viability of cells after UV irradiation.

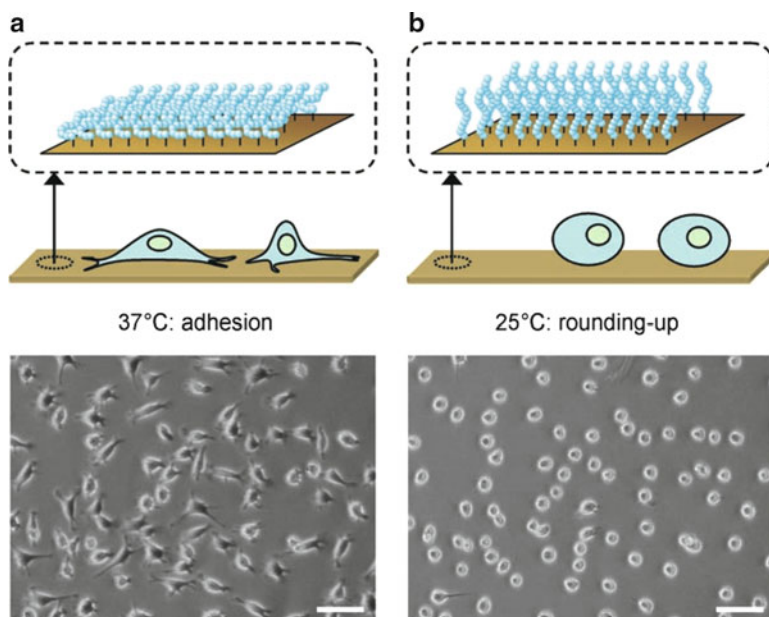
Nonetheless, at present, coatings made of exclusively thermoresponsive polymers are the most frequently investigated and, probably because of their easy handling, are the most promising systems practically. First and foremost, coatings based on PNIPAM were investigated for this purpose. There are, for example, a number of publications by the research groups of Okano [17, 23] and Duschl [18, 189, 190] on this subject. Here, cells adhere to the more hydrophobic surfaces at elevated temperature (37°C, as frequently used for eukaryotic cell culturing), and minimize the contact with the more hydrophilic surfaces at ambient temperature. In this state, cells can be removed from the surface for further use by mild rinsing.

Recently, coatings composed of thermoresponsive side chain OEGs were employed for this purpose (Fig. 14) [44, 45]. They offer the advantage of a better inherent biocompatibility than PNIPAM, show reduction of nonspecific protein adsorption even above the LCST, and exhibit effective control of cell adhesion by reducing the temperature from 37 to 25°C [191].

Interestingly, there is yet another approach for the control of cell adhesion, which relies on mechanical effects [192]. It was demonstrated that micron-sized model particles with multiple recognition groups on their surface, and also yeast cells, were detached from a macroporous hydrogel bearing the corresponding binding groups upon mechanical deformation, whereas no release of an affinity-bound protein occurred when the same conditions were applied.

#### **4.4 Bioseparation**

Several thermoresponsive polymer coatings have been applied in the chromatographic separation of biomolecules. The group of Okano has been active in the field for some time. In recent work, silica beads modified with PNIPAM brushes prepared

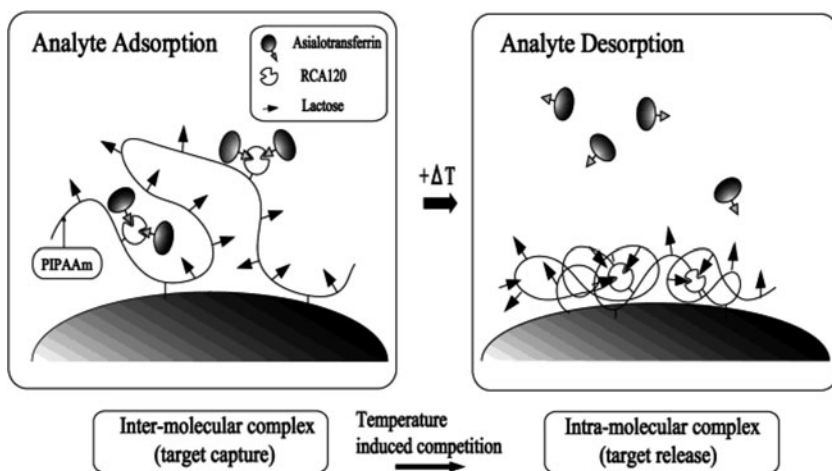


**Fig. 14** *Top*: Representations of a P(OEGMA-*co*-MEO<sub>2</sub>MA) coating at 37°C (**a**) and 25°C (**b**), and the corresponding cell response. *Bottom*: Phase-contrast microscopy images of L929 mouse fibroblasts on P(OEGMA-*co*-MEO<sub>2</sub>MA)-modified gold substrates after 44 h of incubation at 37°C (*left*), and 30 min after cooling the sample to 25°C (*right*). Scale bars: 100 μm. Reprinted, with permission, from [45]. Copyright (2008) Wiley Interscience

via ATRP were used as stationary phase in HPLC for the temperature-modulated separation of steroids and peptides [21]. Using silica beads modified by terpolymer brushes incorporating the monomers NIPAM, DMAEMA and butyl methacrylate, capable of responding to temperature and pH, the separation of bioactive lysozyme was possible in an aqueous mobile phase [20].

PNIPAM and its copolymers are not the only options for thermoresponsive stationary HPLC phases. Poly(acrylates) and poly(methacrylates) bearing OEG groups in the side chains are known as thermoresponsive polymers that offer some advantages over PNIPAM [40]. Such polymers were recently employed for the modification of silica monoliths, which then served as stationary phase in the HPLC separation of steroids [193]. Unsurprisingly, the results were qualitatively similar to those obtained for PNIPAM-based systems, but the separation of relatively hydrophilic steroids was superior.

In the examples mentioned above, there is no specific interaction between the stationary phase and the molecules dissolved in the mobile phase, but Okano's group prepared thermoresponsive polymer coatings for affinity chromatography (Fig. 15) [194]. Using PNIPAM as a scaffold for attachment of a hapten (lactose) and a competing affinity ligand *Ricinus communis agglutinin* (RCA120), binding and release of the glycoprotein target, asialotransferrin, was controlled by changing the



**Fig. 15** Specific protein separation by a smart thermoresponsive polymer coating. *Left*: PNIPAM with immobilized lactose and RCA120 is below the LCST. The moieties are separated and, therefore, proteins from the mobile phase can bind to RCA120. *Right*: PNIPAM below LCST. Polymer-bound lactose and RCA120 come into close contact and lactose displaces the protein. Reprinted, with permission, from [194]. Copyright (2003) American Chemical Society

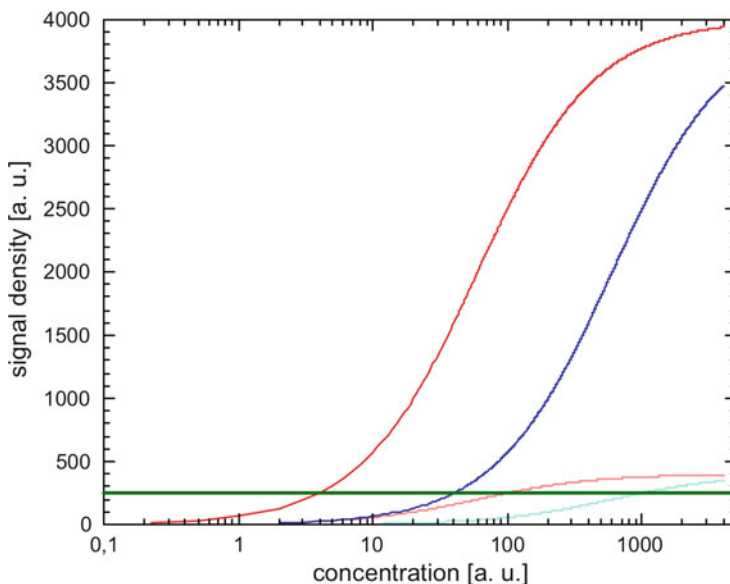
temperature. At 5°C, the column retained the glycoprotein, but 95% of the asialotransferrin were released upon warming to 30°C. The temperature-induced elution was much greater than the temperature dependency of sugar recognition by RCA120 could explain. Most probably, thermally induced dehydration and collapse of the PNIPAM chains brings the coimmobilized RCA120 ligands and lactose haptens into close proximity to each other, enabling immobilized lactose to displace affinity-bound asialotransferrin from the RCA120 lectin.

## 4.5 Bioassays

Smart polymer surfaces consisting of hydrogels with immobilized biorecognition units such as DNA single strands, aptamers, or antibodies are particularly useful for the performance of bioassays. As discussed above, hydrogel-decorated surfaces are capable of suppressing nonspecific adsorption. This is particularly important if the assay is in a label-free format (e.g., real-time biosensors based on quartz crystal microbalances, waveguides, grating couplers, reflectometric interference spectroscopy, or SPR instruments), but is also beneficial for assays involving subsequent binding of a labeled species to the bound analyte.

Aside from the issue of nonspecific adsorption, hydrogels serve as a 3D binding matrix, thus increasing the number of specific binding sites per sensor area unit. For any sensor, there will be a threshold value of bound analyte molecules per area, which must be exceeded to read out a signal distinguishable from noise. Equation (1)





**Fig. 16** Response of a biosensor versus analyte concentration as described by (1). The signal density (in arbitrary units) depends on the  $K_D$  value of the capture probes [*dark curves* (high capture probe density) vs. *light curves* (low capture probe density)], and on the capture probe density [*red curves* (low  $K_D$ ) vs. *blue curves* (high  $K_D$ )]. The *green horizontal line* represents the threshold signal density required to obtain a signal distinguishable from noise. High capture probe density and high  $K_D$  (*dark blue curve*) can result in lower limits of detection than low capture probe density and low  $K_D$  (*light red curve*)

describing the Langmuir adsorption isotherm, gives a good approximation for the loading of a sensor surface in dependence of the analyte concentration (Fig. 16):

$$\theta = \frac{\theta_{\max} \cdot c}{c + K_D} \quad (1)$$

where  $\theta$  is loading of the sensor,  $\theta_{\max}$  the theoretical maximum loading,  $c$  the analyte concentration, and  $K_D$  the dissociation constant of the biochemical interaction.

According to this equation, the loading at given concentration and  $K_D$  values is proportional to the theoretical maximum loading, which is determined by the number of specific binding sites per area unit. Consequently, an increased  $\theta_{\max}$  will lower the limit of detection, at least as long as the analyte binding on the surface does not evoke depletion of the analyte in solution [195]. The beneficial effects depend on a sufficient permeability of the hydrogel. Taking into account that many biologically relevant molecules are rather bulky macromolecules, this cannot be taken for granted. Zacher and Wischerhoff [196] demonstrated by SPR experiments that binding of biotinylated protein A to streptavidin immobilized in a 3D dextran matrix remained restricted to an upper zone of the hydrogel.



To date, many hydrogel systems for bioassays have been proposed and put into practice, many of them based on polysaccharides or PEGs. In 1990, Löfås and Johnsson introduced a method to modify noble metal surfaces for use in biosensors [197]. A hydrogel matrix composed of dextran was utilized to immobilize biomolecules, analogously to procedures in affinity chromatography. In order to create a dense barrier between the original noble metal surface and the hydrogel itself, they used a SAM of long-chain  $\omega$ -functionalized alkyl thiols for primary surface functionalization. Such a layer is much less prone to defects than shorter chain variants due to secondary valence interactions between the alkyl chains. The combination of this dense SAM and the dextran layer on top is rather efficient and became the “standard” sensor surface for the SPR-based biosensor system commercialized by Biacore AB (Sweden). It still enjoys high popularity among the users of such biosensors today.

In 1996, Gauglitz and coworkers coated surfaces with various amino- and carboxy-substituted polymers [198]. The polymers tested were branched poly(ethyleneimine),  $\alpha,\omega$ -amino-functionalized PEG, chitosan, poly(acrylamide-*co*-acrylic acid) and an amino-modified dextran. The amino-substituted polymers were immobilized on glass by first immobilizing an aminosilane, followed by succinic anhydride/*N*-hydroxysuccinimide linker chemistry. Poly(acrylamide-*co*-acrylic acid) was directly coupled to an aminosilanized surface. When probed with 1 mg mL<sup>-1</sup> ovalbumin solution, nonspecific adsorption was lowest for the dextran derivative. Notably, nonspecific adsorption increased in most cases when a hydrophobic hapten (atrazine) was coupled to the polymer-modified surface.

Arenkov et al. prepared poly(acrylamide) gel pads for use in protein microarrays [199]. The gels were prepared by photopolymerization of acrylamide and crosslinkers. Capture probes were immobilized, either by use of glutaraldehyde or by converting some of the acrylamide groups into hydrazides and subsequent coupling of aldehyde-modified antibodies to the pending hydrazide groups. Then, immunoassays were performed on the pads, either assays with directly labeled analytes or sandwich assays. Furthermore, the gel pads were used for enzyme activity studies.

With the application of protein microarrays in mind, Spencer and coworkers immobilized poly(lysine) with grafted PEG side chains on various metal or semiconductor oxide surfaces via electrostatic adsorption [200]. Part of the PEG side chain was functionalized with biotin at the distal end. Streptavidin was bound to the surface-tethered biotin in a subsequent step, and the remaining unoccupied binding pockets of streptavidin were then used to immobilize biotinylated capture antibodies. As an example of an immunoassay, biotinylated goat anti-rabbit IgG was immobilized, which then specifically bound rabbit IgG.

Recently, the Klok group also prepared side-chain PEG-coated surfaces for protein immobilization [201]. They employed surface-initiated ATRP for the synthesis. Terminal hydroxyl groups of the PEGs were activated with *p*-nitrophenyl chloroformate, and subsequently O<sub>6</sub>-benzylguanine was bound. The O<sub>6</sub>-benzylguanine-functionalized PEG brushes were used to chemoselectively immobilize O<sub>6</sub>-alkylguanine-DNA-alkyltransferase fusion proteins with a defined orientation and surface density.

## 5 Conclusion and Outlook

As demonstrated in this chapter, stimuli-responsive polymer surfaces have gained a central role in applied biosciences. Indeed, polymer-based dynamic surfaces allow a broad range of interactions with biological objects (e.g., control of protein and cell adhesion, antifouling behavior, or controlled permeation). Thus, this field of research is currently still expanding. Yet, it should be specified that this success is not only academic. Although not specifically discussed in the present chapter, a large number of patents on smart polymer surfaces have been recently issued. Therefore, many of the examples discussed herein have a real industrial relevance. For instance, commercial products based on thermoresponsive polymers are already available on the biotechnology market.

It should be also noted that the field of smart polymer surfaces is not limited to the macromolecular structures presented in the first part of this chapter. Although some “classic” stimuli-responsive polymers such as PNIPAM or poly(acrylic acid) have been studied for several years, new exciting options are reported every week in the polymer literature. For instance, the synthesis of chemo- and bioresponsive polymers is a topic in full expansion [9]. Thus, new developments in the fields of bioassays and biosensors may be expected in the near future. For instance, more advanced surface concepts (e.g., multiresponsive behaviors, signal cascades) can be anticipated with reasonable certainty.

## References

1. Gil ES, Hudson SM (2004) *Prog Polym Sci* 29:1173–1222
2. Cohen Stuart MA et al. (2010) *Nat Mater* 9:101–113
3. de las Heras Alarcón C, Pennadam S, Alexander C (2005) *Chem Soc Rev*:276–285
4. Wischerhoff E et al (2009) *Soft Matter* 6:705–713
5. Mendes PM (2008) *Chem Soc Rev* 37:2512–2529
6. Sun A, Lahann J (2009) *Soft Matter* 5:1555–1561
7. Motornov M et al (2010) *Prog Polym Sci* 35:174–211
8. Shanmuganathan K et al (2010) *Prog Polym Sci* 35:212–222
9. Roy D, Cambre JN, Sumerlin BS (2010) *Prog Polym Sci* 35:278–301
10. Lutz J-F (2006) *Polym Int* 55:979–993
11. Martin GR, Jain RK (1994) *Cancer Res* 54:5670–5674
12. Willerson JT, Ridker PM (2004) *Circulation* 109:II-2–II-10
13. Berndt E, Ulbricht M (2009) *Polymer* 50:5181–5191
14. de las Heras Alarcón C et al (2005) *J Mater Chem* 15:2089–2094
15. Kaholek M et al (2004) *Nano Lett* 4:373–376
16. Matsuda N et al (2007) *Adv Mater* 19:3089–3099
17. Mizutani A et al (2008) *Biomaterials* 29:2073–2081
18. Ernst O et al (2008) *Langmuir* 24:10259–10264
19. Zhou F, Huck WTS (2006) *Phys Chem Chem Phys* 8:3815–3823
20. Kanazawa H et al (2008) *J Chromatogr A* 1191:157–161
21. Nagase K et al (2007) *Langmuir* 23:9409–9415
22. Sun T et al (2004) *Angew Chem Int Ed* 43:357–360
23. Okano T et al (1993) *J Biomed Mater Res* 27:1243–1251

24. Wei Q, Ji J, Shen J (2008) *Macromol Rapid Commun* 29:645–650
25. Wischerhoff E et al (2000) *Angew Chem Int Ed* 39:4602–4604
26. Heinz BS et al (2001) Grafting of functionalized water soluble polymers on gold surfaces. In: McCormick CL (ed) *Stimuli-responsive water soluble and amphiphilic polymers*. ACS symposium series, vol 780. ACS, Washington DC, p 162
27. Jeong B, Kim SW, Bae YH (2002) *Adv Drug Deliv Rev* 54:37–51
28. Xu C et al (2006) *Nano Lett* 6:282–287
29. Lequeieu W, Shtanko NI, Du Prez FE (2005) *J Membr Sci* 256:64–71
30. Meyer DE, Chilkoti A (2004) *Biomacromolecules* 5:846–851
31. Fernández-Trillo F et al (2009) *Adv Mater* 21:55–59
32. Hyun J et al (2004) *J Am Chem Soc* 126:7330–7335
33. Han S, Hagiwara M, Ishizone T (2003) *Macromolecules* 26:8312–8319
34. Ali MM, Stöver HDH (2004) *Macromolecules* 37:5219–5227
35. Yamamoto S-I, Pietrasik J, Matyjaszewski K (2007) *Macromolecules* 40:9348–9353
36. Lutz J-F, Akdemir Ö, Hoth A (2006) *J Am Chem Soc* 128:13046–13047
37. Lutz J-F, Hoth A (2006) *Macromolecules* 39:893–896
38. Lutz J-F et al (2007) *Macromolecules* 40:8540–8543
39. Lutz J-F et al (2007) *Macromolecules* 40:2503–2508
40. Lutz J-F (2008) *J Polym Sci A Polym Chem* 46:3459–3470
41. Lutz J-F, Hoth A, Schade K (2009) *Des Monomers Polym* 12:343–353
42. Becer CR et al (2008) *J Polym Sci A Polym Chem* 46:7138–7147
43. Holder SJ et al (2008) *J Polym Sci A Polym Chem* 46:7739–7756
44. Wischerhoff E et al (2009) *Langmuir* 25:5949–5956
45. Wischerhoff E et al (2008) *Angew Chem Int Ed* 47:5666–5668
46. Fechner N et al (2009) *Macromolecules* 42:33–36
47. Badi N, Lutz J-F (2009) *J Control Release* 140:224–229
48. Kessel S et al (2010) *Langmuir* 26:3462–3467
49. Dai S, Ravi P, Tam KC (2008) *Soft Matter* 4:435–449
50. Argenti S et al (2009) *Soft Matter* 5:4101–4103
51. Ayres N, Boyes SG, Brittain WJ (2007) *Langmuir* 23:182–189
52. Yamamoto S-I, Pietrasik J, Matyjaszewski K (2008) *Macromolecules* 41:7013–7020
53. Van Camp W et al (2010) *Eur Polym J* 46:195–201
54. Barroso T et al (2009) *J Supercrit Fluids* 51:57–66
55. Wei X et al (2009) *Talanta* 79:739–745
56. Devalapally H et al (2007) *Cancer Chemother Pharmacol* 59:477–484
57. Gillies ER, Fréchet JMJ (2005) *Bioconjug Chem* 16:361–368
58. Angelos S et al (2009) *J Am Chem Soc* 131:12912–12914
59. Angelos S et al (2008) *Angew Chem Int Ed* 47:2222–2226
60. Dong L et al (2006) *Nature* 442:551–554
61. Reinicke S et al (2009) *Soft Matter* 5:2648–2657
62. Zhang K, Wu XY (2004) *Biomaterials* 25:5281–5291
63. Ishihara K, Negishi N, Shinohara I (1982) *J Appl Polym Sci* 27:1897–1902
64. Ishihara K et al (1983) *J Appl Polym Sci* 28:1321–1329
65. Saremi F, Tieke B (1998) *Adv Mater* 10:388–391
66. Seki T, Kojima J-Y, Ichimura K (1999) *J Phys Chem B* 103:10338–10340
67. Kumar SK, Hong J-D (2008) *Langmuir* 24:4190–4193
68. Wan P et al (2009) *Adv Mater* 21:4362–4365
69. Gomy C, Schmitzer AR (2007) *Org Lett* 9:3865–3868
70. Wu T et al (2009) *Chem Mater* 21:3788–3798
71. Saaem I, Tian J (2007) *Adv Mater* 19:4268–4271
72. Kang Y et al (2009) *J Am Chem Soc* 131:7538–7539
73. Hu Z et al (2008) *Macromolecules* 41:9508–9512
74. Alexeev VL et al (2003) *Anal Chem* 75:2316–2323
75. Alexeev VL et al (2004) *Clin Chem* 50:2353–2360
76. Lee Y-J, Pruzinsky SA, Braun PV (2004) *Langmuir* 20:3096–3106

77. Xu X, Goponenko AV, Asher SA (2008) *J Am Chem Soc* 130:3113–3119
78. Bang JH et al (2008) *Langmuir* 24:13168–13172
79. Kokufata E, Zhang Y-Q, Tanaka T (1991) *Nature* 351:302–304
80. Miyata T, Asami N, Uragami T (1999) *Nature* 399:766–769
81. Kim J, Nayak S, Lyon LA (2005) *J Am Chem Soc* 127:9588–9592
82. Chen Z et al (2008) *J Mol Recognit* 21:71–77
83. Qing G et al (2009) *J Am Chem Soc* 131:8370–8371
84. Tokarev I et al (2009) *ACS Appl Mater Interfaces* 1:532–536
85. Stouffer JM, McCarthy TJ (1988) *Macromolecules* 21:1204–1208
86. Erdelen C et al (1994) *Langmuir* 10:1246–1250
87. Serizawa T et al (2002) *Macromolecules* 35:2184–2189
88. Elam JH, Nygren H, Stenberg M (1984) *J Biomed Mater Res* 18:953–959
89. Huang H, Fulchiero EC, Penn LS (2005) *Macromolecules* 38:1028–1030
90. Beyer D et al (1998) *Langmuir* 14:3030–3035
91. Wang J et al (2003) *J Biochem Biophys Methods* 55:215–232
92. Gombotz WR et al (1991) *J Biomed Mater Res* 25:1547–1562
93. Ostaci R-V et al (2008) *Langmuir* 24:2732–2739
94. Kim J, Wacker BK, Elbert DL (2007) *Biomacromolecules* 8:3682–3686
95. Barner-Kowollik C et al (2008) *Macromol Rapid Commun* 29:1431–1437
96. Rühle J et al (2008) *Macromolecules* 41:873–878
97. Bouloussa O, Rondelez F, Semetey V (2008) *Chem Commun* 951–953
98. Maas JH et al (2003) *Thin Solid Films* 426:135–139
99. Barnes TJ et al (2008) *Langmuir* 24:7625–7627
100. Lutz J-F (2007) *Angew Chem Int Ed* 46:1018–1025
101. Bertrand P et al (2000) *Macromol Rapid Commun* 21:319–348
102. Menzel H, Griep-Raming N, Karger M (2004) *Langmuir* 20:11811–11814
103. Yang W, Bai H, Huang Z (2009) *J Polym Sci Polym Chem* 47:6852–6862
104. Lavanant L et al (2010) *Macromol Biosci* 10:101–108
105. Edmondson S, Armes SP (2009) *Polym Int* 58:307–316
106. Zhao B, Brittain WJ (2000) *Macromolecules* 33:342–348
107. Binder WH et al (2009) *Macromolecules* 42:7379–7387
108. Prucker O, Rühle J (1998) *Langmuir* 14:6893–6898
109. Matyjaszewski K et al (1999) *Macromolecules* 32:8716–8724
110. Pyun J, Kowalewski T, Matyjaszewski K (2003) *Macromol Rapid Commun* 24:1043–1059
111. Baum M, Brittain WJ (2002) *Macromolecules* 35:610–615
112. Husseman M et al (1999) *Macromolecules* 32:1424–1431
113. Brinks MK, Studer A (2009) *Macromol Rapid Commun* 30:1043–1057
114. de Boer B et al (2000) *Macromolecules* 33:349–356
115. Marques C, Joanny JF, Leibler L (1988) *Macromolecules* 21:1051–1059
116. Witmore MD, Noelandi J (1990) *Macromolecules* 23:3321–3339
117. Johner A, Joanny JF, Marques C (1991) *Physica A* 172:285–289
118. Tirrell M et al (1991) *Polym J* 23:641–649
119. Rubner MF (2003) pH-controlled fabrication of polyelectrolyte-multilayers: assembly and applications. In: Decher G, Schlenoff JB (eds) *Multilayer thin-films*. Wiley-VCH, Weinheim, p 133–154
120. Amiel C et al (1995) *Macromolecules* 28:3125–3134
121. Choi J, Rubner MF (2001) *J Macromol Sci A* 38:1191–1206
122. Chandekar A et al (2006) *Langmuir* 22:8071–8077
123. Murphy KA, Eisenhauer JM, Savin DA (2007) *J Polym Sci B Polym Phys* 46:244–252
124. Costa AC et al (2005) *Eur Phys J E* 18:159–166
125. Kiss É et al (2004) *J Adhes* 80:815–829
126. Hershkovits E, Tannenbaum A, Tannenbaum R (2008) *Macromolecules* 41:3190–3198
127. Yokoyama H et al (2005) *Macromolecules* 38:5180–5189
128. Oyane A et al (2005) *Adv Mater* 17:2329–2332
129. Andelman D, Joanny JF (2000) *C R Acad Sci IV Phys*:1153–1162

130. Balastre M et al (2002) *Macromolecules* 35:9480–9486
131. Styrkas DA et al (2000) *Langmuir* 16:5980–5986
132. Zhao X et al (2005) *Langmuir* 21:9597–9603
133. Laschewsky A et al (2001) *Macromol Symp* 164:323–340
134. Beebe DJ et al (2000) *Proc Natl Acad Sci USA* 97:13488–13493
135. Zhao B, Moore JS (2001) *Langmuir* 17:4758–4763
136. Edahiro J-I et al (2005) *Biomacromolecules* 6:970–974
137. Saunders BR, Liu R, Fraylich M (2009) *Colloid Polym Sci* 287:627–643
138. Serpe MJ et al (2005) *Biomacromolecules* 6:408–413
139. Li J et al (2007) *Adv Funct Mater* 17:3377–3382
140. Laschewsky A, Rekaï ED, Wischerhoff E (2001) *Macromol Chem Phys* 202:276–286
141. Mangeney C et al (2002) *J Am Chem Soc* 124:5811–5821
142. Jonas AM et al (2007) *Macromolecules* 40:4403–4405
143. Epstein N (1981) Fouling: technical aspects and fouling in heat exchangers. In: Somerscales E, Knudsen J (eds) *Fouling of heat transfer equipment*. Hemisphere, Washington, DC pp 31–53
144. Bryers JD (1994) *Colloids Surf B* 2:9–23
145. Schultz CL, Kunert KS, White R (2000) *J Ind Microbiol Biotechnol* 24:113–115
146. Wisniewski N, Richert M (2000) *Colloids Surf B* 18:197–219
147. Xu FJ, Neoh KG, Kang ET (2009) *Prog Polym Sci* 34:719–761
148. Ma H et al (2006) *Adv Funct Mater* 16:640–648
149. Tugulu S, Klok HA (2008) *Biomacromolecules* 9:906–912
150. Bozukova D et al (2008) *Langmuir* 24:6649–6658
151. Fukuda T et al (2007) *J Polym Sci A Polym Chem* 45:4795–4803
152. Nie F-Q et al (2004) *Polymer* 45:399–407
153. Cringus-Fundeanu I et al (2007) *Langmuir* 23:5120–5126
154. Petersen P et al (2009) *Phys Status Solidi A* 206:468–473
155. Bearer JP et al (2003) *Nat Mater* 2:259–24
156. Patrucco E et al (2009) *Biomacromolecules* 10:3130–3140
157. Snellings GMBF et al (2000) *Adv Mater* 12:1959–1962
158. Gregorius K, Mouritsen S, Elsner HI (1995) *J Immunol Methods* 181:65–73
159. Chapman RG et al (2000) *J Am Chem Soc* 122:8303–8304
160. Lee Y-S et al (2003) *Biosens Bioelectron* 19:485–494
161. De Sousa Delgado A, Léonard M, Dellacherie E (2001) *Langmuir* 17:4386–4391
162. Martwiset S, Koh AE, Chen W (2006) *Langmuir* 22:8192–8196
163. Monchaux E, Vermette P (2007) *Biomacromolecules* 8:3668–3673
164. Perrino C et al (2008) *Langmuir* 24:8850–8856
165. Ekblad T et al (2008) *Biomacromolecules* 9:2775–2783
166. Kizhakkedathu JN et al (2009) *Langmuir* 25:3794–3801
167. Hucknall A, Rangarajan S, Chilkoti A (2009) *Adv Mater* 21:2441–2446
168. Trmcic-Cvitas J et al (2009) *Biomacromolecules* 10:2885–2894
169. Holmlin RE et al (2001) *Langmuir* 17:2841–2850
170. Ostuni E et al (2001) *Langmuir* 17:6336–6343
171. Kitano H et al (2010) *Langmuir* 26:6767–6774
172. Jiang S, Chen S (2008) *Adv Mater* 20:335–338
173. Chang Y et al (2008) *Langmuir* 24:5453–5458
174. Liu P-S et al (2009) *Biomacromolecules* 10:2809–2816
175. Reisch A et al (2008) *J Mater Chem* 18:4242–4245
176. Statz AR et al (2005) *J Am Chem Soc* 127:7972–7973
177. Ostuni E et al (2001) *Langmuir* 17:5605–5620
178. Hucknall LD, Sheardown H, Brash JL (2008) *Langmuir* 24:1924–1929
179. Klok H-A, Tugulu S (2008) *Biomacromolecules* 9:906–912
180. Yoshikawa C et al (2006) *Macromolecules* 39:2284–2290
181. Cunliffe D et al (2003) *Langmuir* 19:2888–2899
182. Kharlampieva E, Erel-Unal I, Sukhishvili S (2007) *Langmuir* 23:175–181

183. Burkert S et al (2010) *Langmuir* 26:1786–1795
184. Qin L et al (2009) *Anal Chem* 81:7206–7216
185. Zareie HM et al (2008) *ACS Nano* 2:757–765
186. Chan EWL, Park S, Yousaf MN (2008) *Angew Chem Int Ed* 47:6267–6271
187. Auernheimer J et al (2005) *J Am Chem Soc* 127:16107–16110
188. Liu D et al (2009) *Angew Chem Int Ed* 48: 4406–4408
189. Ernst O et al (2007) *Lab Chip* 7:1322–1329
190. Hentschel J et al (2008) *Macromolecules* 41:1073–1075
191. Zhu S et al (2009) *Langmuir* 25:10271–10278
192. Galaev IY et al (2006) *Langmuir* 23:35–40
193. Tan I et al (2009) *ACS Appl Mater Interfaces* 1:1869–1872
194. Yamanaka H et al (2003) *Anal Chem* 75:1658–1663
195. Ekins R, Chu F (1992) *Ann Biol Clin* 50:337–353
196. Zacher T, Wischerhoff E (2002) *Langmuir* 18:1748–1759
197. Löfås S, Johnsson B (1990) *J Chem Soc Chem Commun* 1526–1528
198. Piehler J et al (1996) *Biosens Bioelectron* 11:579–590
199. Arenkov P et al (2000) *Anal Biochem* 278:123–131
200. Huang N-P et al (2002) *Langmuir* 18:220–230
201. Klok H-A et al (2005) *Biomacromolecules* 6:1602–1607

# Hold on at the Right Spot: Bioactive Surfaces for the Design of Live-Cell Micropatterns

S. Petersen, M. Gattermayer, and M. Biesalski

**Abstract** The merger of biology and modern microsystem technology bears challenges literally at the interface. Precise control of the interaction between an artificial surface and a biological environment is a prerequisite for a successful interplay of the “living world” with man-made technology. Any design of a chip for a spatially controlled attachment and outgrowth of living cells has to meet two fundamental yet apparently opposing requirements: it has to divide the surface into areas that favor cell adhesion and those that resist it. In the first part of this article, we provide a basis for an understanding of how to achieve both tasks by discussing basic considerations concerning cell adhesion to matrices in vivo and ways to control the interactions between biomacromolecules and surfaces. We also include an overview of current strategies for the integration of living cells on planar devices that aims to provide a starting point for the exploration of the emerging field of cell-chip technology.

**Keywords** Assay · Bioactive surface · Cell adhesion · Cell chip · Hydrogel · Microengineering · Micropattern · Peptide · Polymer brush · Protein adsorption

## Contents

1	Surface-Microengineering and Biology: A Challenge at the Interface .....	36
2	Lessons for Surface Design: Cell Adhesion in Nature .....	38
3	Surfaces that Resist the Adsorption of Proteins and Cells .....	40
3.1	Thermodynamics .....	40
3.2	Examples of Protein-Resistant Surface Coatings .....	43

---

S. Petersen, M. Gattermayer, and M. Biesalski (✉)  
Department of Chemistry, Technical University of Darmstadt, Petersenstraße 22,  
64287 Darmstadt, Germany  
e-mail: [petersen@cellulose.tu-darmstadt.de](mailto:petersen@cellulose.tu-darmstadt.de); [gattermayer@cellulose.tu-darmstadt.de](mailto:gattermayer@cellulose.tu-darmstadt.de);  
[biesalski@tu-darmstadt.de](mailto:biesalski@tu-darmstadt.de)

4	Directed Cell Adhesion to Engineered Surfaces .....	46
4.1	Protein-Decorated Surfaces for Spatially Guided Cell Adhesion .....	47
4.2	Peptide-Decorated Surfaces for Spatially Guided Cell Adhesion .....	56
5	Conclusions and Outlook .....	71
	References .....	71

## 1 Surface-Microengineering and Biology: A Challenge at the Interface

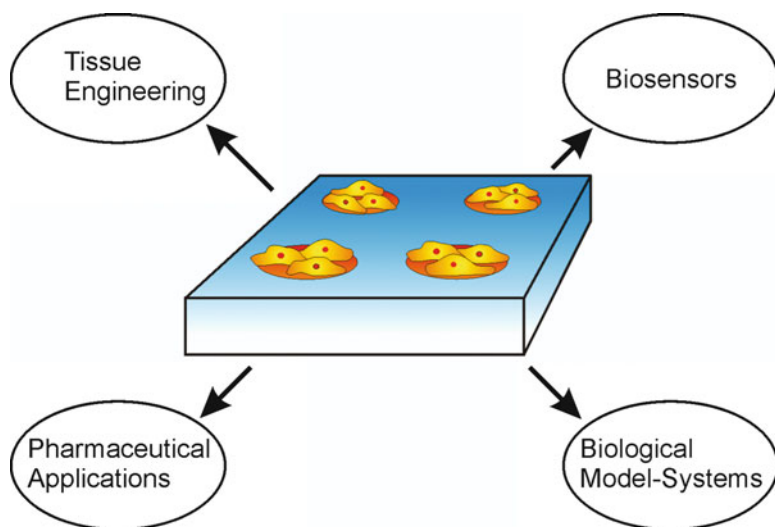
The progress over the past decades in the field of surface science and the development of several microengineering techniques for the precise deposition, manipulation, and characterization of ultrathin films will open new avenues for the design of novel types of medical devices [1–6]. The new devices will, for example, monitor the health-status of a person for extended time-periods, detect critical metabolic situations such as unusually elevated or strongly reduced levels of blood sugar, or recognize an unexpected, serious immune reaction. Although the two research areas (biomedicine and surface-microengineering) involved in these developments, particularly in the tailoring of functional surfaces for specific needs, are both at present highly advanced, the merger of both brings great challenges literally at the interface.

In the field of medical diagnostics, surfaces are required that allow a specific interaction with a particular environment (e.g., an analyte) and meanwhile suppress unspecific reactions. A well-established implementation of this kind of a “smart” biomaterial is the development of DNA-analyzing chips (also known as DNA-chips) [7, 8]. This successful application of a biomedical microengineered system also involves an important concept in microengineering in general – miniaturization. The reduction of dimensions together with an increased sensitivity of the sensorial sites, mainly achieved through a tailor-made bioactive surface, leads to a parallelization of the analytic process that allows tremendous reductions in cost, time, and amount of analyte necessary. In a next step, biochips for the analysis of proteins are of utmost interest in medical diagnostics and therapy. In contrast to DNA analysis, where the “sensors” are single-stranded DNA fragments, the detection of proteins (e.g., disease markers) requires the immobilization of specific proteins (or parts of such proteins), such as antibodies, on the artificial surface [9, 10]. With respect to successful surface-immobilization, however, one has to deal with a number of hurdles when using proteins: they have a complex structure and, hence are highly sensitive to conformational changes (i.e., denaturation) that might be induced upon interaction with a surface. Denaturation (i.e., any change of the natural protein structure) can lead to a reduction or even loss of the functionality and, consequently, to an altered, often poor and nonreproducible performance of the device. Looking at the family of biofunctional analysis chips, one can state that DNA-chips are already well established on the market, with protein-chips starting to follow in their footprints. However, for biomedical diagnostics and research, it would be of great interest to



use even more complex systems as sensorial devices, i.e., living cells. The ability of living organisms (i.e., cells) to react to various environmental changes with a high specificity and sensitivity is as impressive as it is difficult to predict. Therefore, the search for substances that induce a certain (desired) cellular response either for medicinal purposes (drug-screening) or as coatings for medical implants (biocompatibility tests) is mainly done to date in extensive *in vitro* studies using cell culture assays. These assays require comparatively large volumes of the often very expensive substances to be tested. Here, the manipulation of living cells in microscale devices offers distinct advantages over conventional macroscale systems. Microscale devices have the ability to process small sample volumes rapidly and inexpensively, and thereby provide valuable information about important cell parameters such as gene expression and metabolic activity. Figure 1 hints at the vast potential a cell chip could offer to a number of biomedical research areas. Thus, an increasing amount of fundamental research in current bioengineering science is dedicated to the development of such cell chips.

Any successful attempt to create a cell chip has to meet important requirements with respect to the precise surface chemistry and physics that govern the interaction of the substrate with the living cells. Therefore, the quest for the development of a device for guided cell adhesion has to be preceded by a study of the environment of living cells *in vivo* in order to understand the mechanisms and surrounding circumstances of “normal” cell behavior. The key challenge in the development of such cell chips lies in the specific attachment of living cells in a spatially controlled manner. For this, a surface has to be designed that, on the one hand, prevents unspecific protein adsorption that can mediate cell adhesion and, on the other hand, simultaneously promotes specific cell attachment in a spatially resolved way.

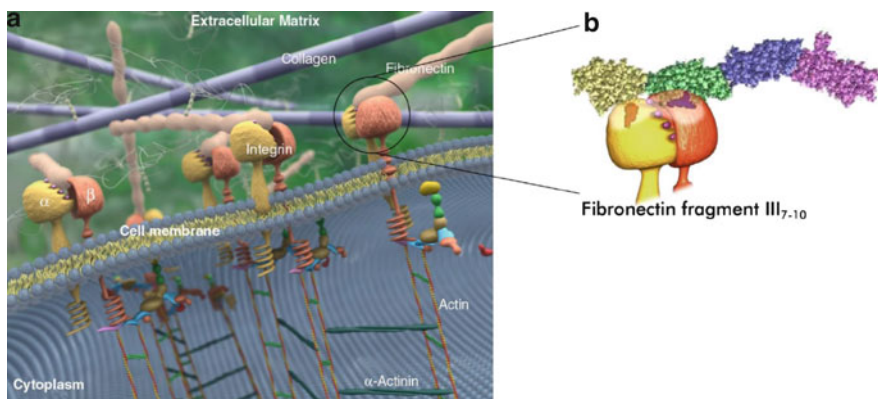


**Fig. 1** Biochip for locally controlled cell adhesion, and possible examples of application of such cell chips

In this review, we focus on novel developments in the design of surfaces that guide a locally controlled adhesion of living cells at desired surface areas. In order to present related work in the context of modern bioengineering, we first review how cells adhere to their neighboring environment in nature (Sect. 2). Then, we briefly discuss strategies for design of surfaces that resist nonspecific interactions with proteins (Sect. 3). In Sect. 4, we then review the current state-of-the-art in confining cells to distinct lateral spots on various artificial surfaces, including those surfaces where surface-adsorbed proteins are used to mediate cell-adhesion, as well as surfaces that have been designed to expose bioactive ligand-modules that promote the adhesion of living cells.

## 2 Lessons for Surface Design: Cell Adhesion in Nature

Our understanding of the molecular mechanisms that underlie the adhesion of living cells in nature has improved tremendously over the past decades. Cell–cell adhesion, as well as the adhesion of living cells to an extracellular matrix (ECM), is governed by specific interactions between distinct “cell adhesion molecules” (CAMs) localized in the plasma membrane as transmembrane proteins (i.e., receptors) and their specific ligands in the ECM. Different major classes of such receptors have been identified [9, 11, 12]. Immunoglobulins and cadherins interact with their counterparts located in a neighboring cell membrane, and thus form cell–cell contacts. Selectins bind to glycosylated mucins, and vice versa, as well as to distinct growth factors. Finally, integrins comprise an important class of CAMs that mainly bind to ECM proteins and also interact with immunoglobulins (Fig. 2).



**Fig. 2** (a) The cell-membrane–ECM interface. Transmembrane integrins are composed of two subunits,  $\alpha$  and  $\beta$ , which anchor the cell to ECM molecules, e.g., fibronectin. The extracellular binding of the integrins triggers the intercellular formation of the cytoskeleton through a highly organized aggregate of proteins, such as actin filaments and others. (b) Specific binding of integrins to recognition sites in the ECM proteins, here to fibronectin. (Figure reproduced in part with permission from [132])

Integrins consist of two noncovalently linked subunits ( $\alpha$ - and  $\beta$ -subunits), i.e., they comprise a heterodimeric structure [13–15]. There are more than 20 different integrins known to date [12]. Most integrins are expressed on a variety of cells, and most cells express several different integrins, enabling them to bind to various matrix molecules. The most important of these matrix molecules are ECM proteins such as fibronectin, collagens, laminin, and vitronectin. The cell–ECM adhesion comprises a cascade of different, mainly consecutively occurring events, and is initiated by the interaction of the integrin receptors with small ligands (peptides) present in ECM proteins [12]. Once the ligand interacts with its specific receptor, the cell begins to flatten (i.e., it “spreads”) on the interface. The chemical information is “transmitted” into the cell by conformational rearrangements of the receptor at the cytosolic side, where it triggers the further organization of actin filaments, which are often called “stress fibers.” Finally, integrin molecules that are attached to both the peptide ligand outside of the cell and to the cytoskeleton inside (stress fibers and a number of other cell proteins, such as focal adhesion kinase, vinculin, talin, and tensin) cluster together in the plasma membrane, thereby forming “focal adhesion contacts” [16–19]. At first view, this scenario seems to be simple; however, it is important to note that from a molecular view, many different steps of the above-described cascade are not yet understood in detail. In addition, it is important to recognize that the interaction of the peptide ligands with integrins not only ensures the structural integrity of living cells, but also triggers a number of different events inside the cell that finally influence the metabolism, differentiation, and proliferation of the cell. The interaction also impacts the systemic responses of the immune system, and is involved in wound-healing cascades [20, 21].

A biomedical device that aims to provoke a normal cell behavior *in vitro* needs to “mimic” the ECM in a way that allows the initiation of the cell adhesion process. In principle, one can either modify a surface with ECM proteins that mediate the attachment of living cells, or one can engineer cell-adhesion-mediating small ligands into/onto appropriate surfaces. A well-known ligand is the minimal cell-recognition peptide sequence RGD (R = arginine, G = glycine, and D = aspartic acid) [22–27], which is found in many different ECM proteins. Although the RGD motif is by far not the only recognition sequence known today, it is of special interest due to its broad distribution and variability. The affinity to different integrins is mainly governed by its flanking amino acids, and a number of oligopeptides that include the RGD sequence have been identified as binding to specific members of the integrin family. For a more detailed overview on different bioactive peptide sequences that interact with various CAMs, the reader is referred to two excellent review articles [28, 29].

Note that the above-mentioned, rather simplified set of characteristics for a biomimetic strategy of “guided cell adhesion” were first developed for planar surfaces. For many cell-types, this accounts for an interesting model system with a sufficient relevance to the biological situation; however, there also exist a number of cell types that might behave differently with respect to surface attachment, growth,

and differentiation if cultured in 2D (as opposed to the 3D biological environment) [30]. However, 3D artificial model systems are much more sophisticated with respect to matrix preparation, as well as peptide–ligand (or protein–ligand) presentation, and therefore studies using such systems are so far very rare. Thus, we restrict further discussions exclusively to planar surfaces.

### 3 Surfaces that Resist the Adsorption of Proteins and Cells

Throughout the last few decades, a number of interesting strategies have evolved that address the construction of both surfaces that resist the adsorption of proteins as well as surfaces that promote protein adsorption, and hence are either capable of suppressing or supporting protein-mediated cell adhesion. Protein adsorption is a crucial issue in the design and performance of materials in contact with living cells. And, perhaps, it is the surface chemistry and physics that govern any successful attempt to design a material that directs the controlled attachment and growth of cells, rather than the bulk properties of the material itself. Both, surfaces that allow the adsorption of proteins and surfaces that repel proteins are of the utmost interest for guiding cells, particularly if a spatially controlled attachment of cells is targeted, where these two properties have to be implemented onto the same substrate.

We will briefly outline the principle thermodynamic considerations that comprise the underlying key issues of protein adsorption on surfaces. Subsequently, we will describe strategies that have been followed for the design of protein-repellent surface coatings. For details on protein adsorption, as well as further discussion on this particular topic, the reader is referred to more comprehensive reviews [31, 32].

#### 3.1 Thermodynamics

From a thermodynamic point of view, protein adsorption at a surface depends on the Gibb's free energy of adsorption ( $\Delta G_{\text{ads}}$ ):

$$\Delta G_{\text{ads}} = \Delta H_{\text{ads}} - T\Delta S_{\text{ads}}.$$

Here  $\Delta H_{\text{ads}}$  is the enthalpy of adsorption,  $T$  is the temperature, and  $\Delta S_{\text{ads}}$  is the entropy change associated with the adsorption of the protein onto the surface. Protein adsorption will take place if  $\Delta G_{\text{ads}} < 0$ . Considering a complex system, where proteins are dissolved in an aqueous environment, and are brought into contact with an artificial interface, there are a vast number of parameters that impact  $\Delta G_{\text{ads}}$ : due to their small size (i.e., large diffusion coefficient), water molecules are the first to reach the surface when a solid substrate is placed in an aqueous biological environment. Hence, a hydrate layer is formed. With some delay, proteins diffuse to the interface and competition for a suitable spot for adsorption starts. This competition

**Table 1** Phenomena occurring during protein adsorption and their influence on Gibb's free energy of adsorption

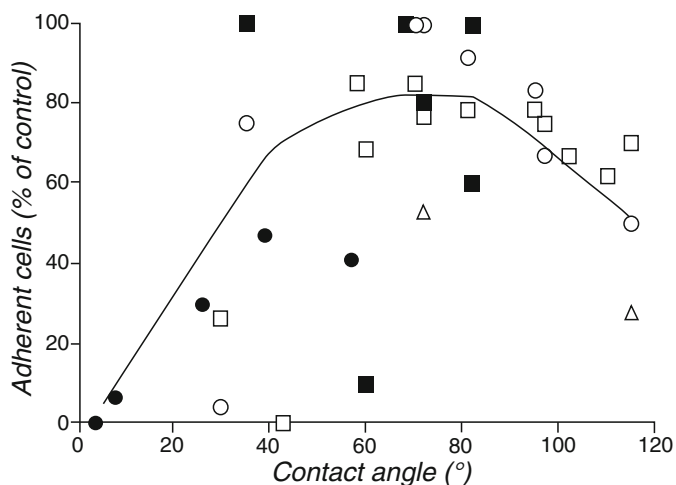
Interaction	Influence on $\Delta H_{\text{ads}}$	Influence on $\Delta S_{\text{ads}}$	Influence on $\Delta G_{\text{ads}}$
Ionic	$\Delta H_{\text{ads}} < 0$		$\Delta G_{\text{ads}} < 0$
surfacedehydration	$\Delta H_{\text{ads}} > 0$	$\Delta S_{\text{ads}} > 0$	$\Delta G_{\text{ads}}$ depends
Protein denaturation	$\Delta H_{\text{ads}} > 0$	$\Delta S_{\text{ads}} < 0$	$\Delta G_{\text{ads}} > 0$
Surface-layer compression	$\Delta H_{\text{ads}} > 0$	$\Delta S_{\text{ads}} < 0$	$\Delta G_{\text{ads}} > 0$
Osmotic repulsion		$\Delta S_{\text{ads}} < 0$	$\Delta G_{\text{ads}} > 0$

$\Delta H_{\text{ads}}$  enthalpy of adsorption,  $\Delta S_{\text{ads}}$  entropy change associated with the adsorption of the protein onto the surface,  $\Delta G_{\text{ads}}$  Gibbs free energy of adsorption

is mainly governed by the surface properties of the material that influence the rate, amount, and conformation of the adsorbed molecules. The surface charge, the degree of swelling in water (if a water-swellaible surface coating is considered), as well as the surface energy of the material are thus important parameters, which influence the kind and strength of interaction of proteins with the substrate. Table 1 summarizes phenomena accompanying protein absorption as well as their influence on the Gibb's free energy.

Considering the polarity of a surface, water molecules will arrange themselves on hydrophobic surfaces in a highly ordered fashion, which decreases the overall entropy of the system (i.e.,  $\Delta S > 0$ ). Adsorption of a protein replaces parts of the ordered water layer at the surface and thus can increase the entropy of the system. Because proteins carry both, hydrophobic as well as hydrophilic chemical groups, adsorption itself relies on the free energy change of the protein molecule during the surface attachment. If the loss in conformational entropy of the protein molecule due to fixation of some parts of it at the surface is compensated by the gain in enthalpy due to the interaction of distinct chemical groups with the hydrophobic surface, adsorption will occur. Proteins will thus mainly attach to hydrophobic interfaces via interactions between hydrophobic residues present in a number of different amino acids and the respective surface chemical groups. The complex structure of soluble proteins can be taken in a very simplified fashion as a "core-shell"-like object, i.e., hydrophobic parts are arranged "inside" the protein, and are covered by more hydrophilic modules that form a soft shell surrounding the hydrophobic core. If such proteins adsorb to a hydrophobic surface, the core of the protein has to turn towards the substrate. Simultaneously, the hydrophilic parts of proteins turn towards the aqueous environment upon adsorption. By this mechanism, the surface energy of the substrate may be significantly decreased. The process is often accompanied by a restructuring of the protein molecule. This "denaturation," which is entropically unfavorable for the protein, is compensated by the gain of entropy of the system due to the release of the water molecules from the surface, as well as the gain in enthalpy of the protein molecule.

In contrast, protein adsorption to hydrophilic surfaces might be even more complex, and is still not completely understood. As will be shown, there exist a number of examples in which hydrophilic surfaces indeed successfully repel proteins; however, there also exist interesting examples in which attractive interactions between



**Fig. 3** Relationship between cell adhesion and water–air contact angle for a variety of polymer surfaces. The data have been collected and plotted by Saltzman, and are summarized in a book by Lanza et al. (Figure reproduced, with permission, from [33])

a strongly hydrophilic surface and proteins in solution can lead to an attachment of the protein to the substrate. In a textbook by Lanza et al. [33], cell adhesion on various polymeric substrates is discussed in the context of surface polarity, as measured by the water–air contact angle. Figure 3 shows the amount of adherent cells as a function of the water contact angle for various polymeric surfaces. The data were collected by Saltzman, and the reader is referred to the literature for details of the polymeric substrates studied [33]. Saltzman claims that surfaces with more hydrophobic properties (i.e., water contact angles greater than  $60^\circ$ ) will probably promote protein adsorption, and thus support protein-mediated cell adhesion. However, the guide to the eye, present as a solid line in the figure, is still questionable because the data scattering is tremendous. In our opinion, water contact angle measurements should not be taken as a measure for protein-repellent surface properties. Despite the surface polarity, protein adsorption will also be largely affected by further parameters such as surface charge, surface elasticity, and the morphological composition of the surface.

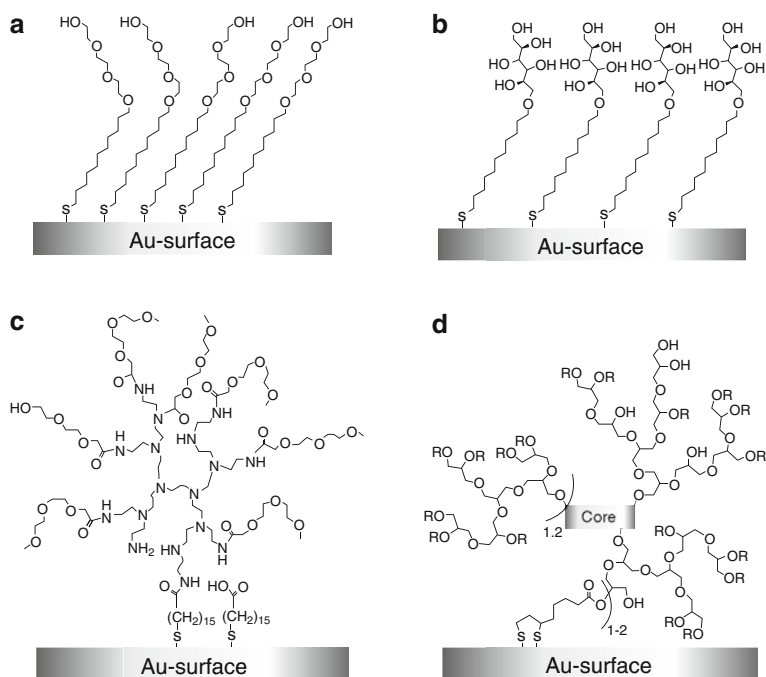
Surface charge has been observed to impact protein adsorption significantly. The net charge of most proteins is negative and adsorption to positively charged surfaces can take place, e.g., by electrostatic, attractive interactions [34]. Negatively charged surfaces can still be subject to protein adsorption when a layer of counterions reverses the effective surface charge. The attraction for protein adsorption is furthermore influenced significantly by the degree of swelling of the surface-confined layers or bulk material in water. Considering a surface layer such as surface-confined hydrophilic polymer films, which are capable of swelling in an aqueous environment, any adsorption of protein molecules leads to a compression

of the surface layer. The latter is always accompanied by a reduction of the conformational entropy of the surface-attached molecules due to the loss in the degree of conformational freedom and, as a result, elastic forces (i.e., excluded volume effects) will act against this compression. As a result, proteins will be pushed away from the surface, rendering water-swellaible surface layers interesting candidates for the implementation of protein-repellent properties.

Following the above-outlined phenomenological considerations, scientists have studied various surfaces with respect to protein adsorption, and a number of different surface chemistries have been successfully applied to the design of surfaces that resist the adsorption of proteins.

### *3.2 Examples of Protein-Resistant Surface Coatings*

Materials that have been used as surface-coatings for the design of protein-resistant surfaces include natural polymers such as heparin [35] or dextran [36] as well as synthetic polymers such as poly(ethylloxazoline) (PEtOx) [37, 38], poly(dimethylacrylamide) (PDMAA) [39, 40], poly(glycerols) [41], and poly(ethylene glycol) (PEG) [42]. Due to its availability, as well as biocompatible properties, PEG is perhaps the most common example of a polymeric material used to produce surfaces that are inert to nonspecific protein adsorption [43–45]. Despite PEG polymers, self-assembled monolayers (SAMs) presenting similar chemical surface-functionalities [i.e., oligo(ethylene glycol) groups] have been successfully used as protein-resistant surface-coating materials [46, 47]. Although PEG-based surface coatings are widely used, these materials also exhibit some severe limitations with respect to chemical and thermal stability. For example, Whitesides and coworkers have shown that PEG-based films can undergo autooxidative degradation in the presence of transition metals, or enzymatically *in vivo* [48]. In addition, from a mechanistic point of view, the protein resistance of PEG coatings is still controversially discussed in the literature. Nagaoka et al. proposed that the underlying mechanism governing the protein resistance of PEG coatings is the restriction of the mobility of PEG chains if protein molecules adhere to the surface. This accounts for the loss in conformational entropy of the surface-confined chains [49]. Other groups proposed the helical conformation of short PEG chains, as well as tightly bound water molecules, to be crucial for protein-resistant properties [50–52]. Based on extensive studies using short PEG segments anchored to a solid substrate via self-assembled monolayers (SAMs), Whitesides and coworkers concluded that hydrophilic surface chemistries with hydrogen-bond accepting rather than donating functionalities (i.e., acidic protons) exhibit protein-resistant properties [53]. However, to date it is not clear whether this finding holds for all kind of hydrophilic surface coatings. Mrksich and coworkers, for example, showed that surface-adsorbed monolayers exposing mannitol-groups, which offer a moiety with acidic protons, are inert to protein adsorption [54]. The latter finding is even

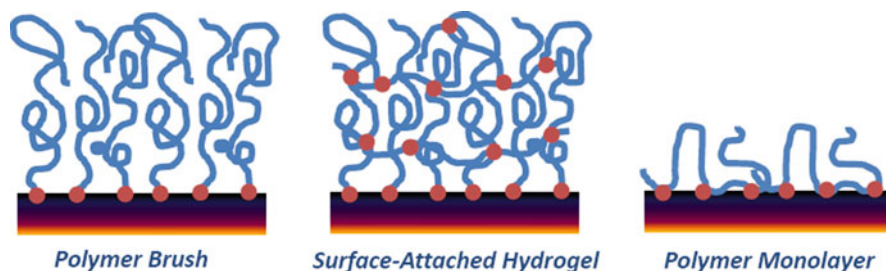


**Fig. 4** Examples (a) PEGylated monolayer; (b) Glucose-modified monolayer; (c) Surface-attached hyper-branched polyethylene imine; and (d) Surface-attached hyperbranched polyglycerols of surface-coatings that resist the nonspecific adsorption of proteins. (Figure reproduced in part with permission from [41])

more interesting because films consisting of different sugar derivatives do not resist the adsorption of proteins [48]. In addition to surface coatings consisting of linear PEG polymers and oligomers, branched polymeric systems, such as surface-attached PEG-derivatized poly(ethyleneimine) (PEI) [55], or dendritic polyglycerol layers [41] have also been shown to resist the nonspecific adsorption of proteins. Figure 4 schematically summarizes some of the hydrophilic surface coatings that have been shown to prevent nonspecific protein adsorption.

An interesting class of surface coatings consists of so-called polymer brushes. These are polymer monolayers that are end-attached to a surface with a high grafting density, which leads to a stretching of the molecules normal to the surface (Fig. 5) due to strong excluded volume interactions. Polymer brushes can be prepared by either growing macromolecules in situ using surface-immobilized initiator groups (“grafting from”) or by grafting end-functional macromolecules onto a reactive surface-site (“grafting to”). Note that polymer brushes can also be prepared by physisorption of block copolymers onto solid substrates from selective solvents, or by using surface-immobilized monomers and a “grafting through” process, respectively. The preparation of polymer brushes, characterization of the physicochemical





**Fig. 5** Surface-attached polymer brush (*left*); surface-attached hydrogel (*center*); and surface-attached polymer monolayer (*right*)

properties (e.g., swelling in solvents), and initial studies on interesting applications of such layers, including bioactive surfaces, are described in a comprehensive book by Advincula et al. [56], as well as in a recent review by Klok and coworkers that includes an impressive list of almost 1000 references [57].

Hydrophilic polymer brushes have been shown to resist the nonspecific adsorption of proteins. The underlying mechanism has been ascribed to a strong loss in entropy of the surface-attached chains if a protein attaches to a polymer brush; hence, protein attachment to a highly swollen polymer brush in an aqueous environment is thermodynamically unfavorable [57–59]. These brushes differ from the oligo-PEG SAM coatings described above in the sense that protein-resistancy might not be influenced by the chemistry of the surface-linked macromolecules as long as neutral, water-swallowable chains of sufficient molar masses and high grafting densities are considered. Interestingly, attractive forces between a brush, swollen in water, and a protein can lead to strong protein-adsorption. This was shown in studies by Ballauff and coworkers in which charged polymer brushes (i.e., polyelectrolyte brushes) were used to confine protein molecules into/onto the brush via electrostatic interactions [34].

Similar to hydrophilic polymer brushes, surface-confined, cross-linked polymer films (i.e., surface-attached hydrogels) (Fig. 5), can prevent a nonspecific adsorption of proteins to the underlying substrate [60, 61]. The driving forces resisting protein-adsorption are again of thermodynamic nature, provided that attractive forces (e.g., electrostatic interactions or hydrogen bonding) can be neglected. Protein attachment onto the hydrogel leads to a decrease in the conformational entropy, and strong osmotic forces retain water molecules inside the gel, thus repelling proteins from the interface. Finally, hydrophilic polymer monolayers of just a few nanometers in thickness have been proven to be suitable for implementation of protein-repellent properties onto glass-substrates (Fig. 5 and Sect. 4.2) [40]. The underlying driving forces for resisting the nonspecific adsorption of proteins are probably of thermodynamic (i.e., entropic) nature, as for polymer brushes, and hydrogels.

## 4 Directed Cell Adhesion to Engineered Surfaces

Several routes have been followed to create a local environment suitable for the attachment of living cells on an artificial surface. On the basis of the insight that cell adhesion *in vivo* is based on the interaction of CAMs and proteins found in the ECM, an approach that utilizes locally deposited proteins from the ECM represents a suitable starting point for “successful” cell attachment. A close control over the local surface chemistry, on the other hand, is the decisive factor for a controlled placement of proteins on a surface, because of its influence on the whole adsorption process of the biomolecule. Although denaturation of the adsorbed proteins can significantly alter the biological functions of the protein, the degree of biomimicry of the ECM can be – in the best case – high, simply by employing the main building blocks (i.e., proteins) that constitute the extracellular space *in vivo* for applications *in vitro*. However, some restrictions apply for certain applications. The nonspecific adsorption of proteins is based on physisorption and can be altered or reversed by thermodynamic processes. For example, the cell-adhesion-mediating film can bleed off or can be replaced over time by other molecules with a higher enthalpy of adsorption. Consequently, the properties of the surface can be subject to a dynamic change in a biological environment unless the bioactive film is covalently immobilized on the surface. Furthermore, proteins are subject to proteolytic degradation and need to be replaced continuously to ensure a sufficient longevity.

Despite the problems mentioned, the passive control of protein adsorption is excellently suited for short-term applications and many situations in a controlled environment *ex vivo*.

As described in Sect. 2, the binding of CAMs is highly specific to certain peptide sequences present in the proteins of the ECM. The last few decades have seen a number of interesting approaches that employ the mere minimum binding sites for guided cell adhesion through surface modification, either by directly (e.g., through short linker molecules) placing the peptides on the substrate or by incorporation of the biomolecules into polymeric backgrounds. Although this strategy compromises on the degree of biomimicry as compared to the protein-based approach, it is able to offer unique advantages in terms of controllability of cell–substrate interactions.

In combination with the techniques for rendering a surface nonfouling (as discussed in Sect. 3), a powerful “box of building blocks” arose for the design of live-cell chips. The choice of cell- or protein-repellent components, in combination with a cell-adhesion-mediating entity, of course depends on the application. Important parameters that have to be taken into account are:

- Degree of biomimicry
- Control over the specific cell–surface interaction
- Stability and longevity of the surface coating under cell culture conditions
- Ease of synthesis and availability of components
- Microstructuring method (which also depends on the application)
- Instruments required for production and experiment

## ***4.1 Protein-Decorated Surfaces for Spatially Guided Cell Adhesion***

The deposition of proteins onto surfaces for the purpose of a guided cell adhesion requires two major prerequisites: first, the immobilized proteins have to exert their native biofunctionality towards cell binding, i.e., the specific recognition sites have to remain active and accessible for the cell. Second, the deposited protein layer has to be sufficiently stable under cell culture conditions in order to provide a controlled experimental setup. Both criteria have been the focus of extensive studies in the last two decades. As discussed, the driving forces for protein adsorption onto surfaces can be categorized into enthalpic (e.g., electrostatic interactions due to redistributions of charged groups at the interface, and hydrogen bonding, to name the most prominent kind of interactions) and entropic contributions. The latter include (partial) dehydration of the protein and/or the sorbent surface or a structural reorganization of the protein molecule [62].

For the preservation of a protein's cell-binding ability (also termed "molecular potency"), unfolding (denaturation) can be a prohibiting factor and leads to a loss of the natural adhesion-mediating ability of the protein. Results by Norde and Giacomelli, who investigated a number of proteins and surfaces, suggest that at least some conformational changes occur with most protein adsorption processes [63–65]. Although these studies indicate that adsorbed proteins retain a major part of their secondary structure, other reports propose changes in protein folding as likely causes for enhanced or impaired protein activity towards cell adhesion [66–71]. In fact, the actual role a biomolecule plays in the cell–surface interaction can be dramatically altered by the adsorption process and the resulting conformational changes in the protein. Human albumin, the most abundant protein in blood, might serve as a good example. Although it is conventionally considered nonadhesive to platelets and therefore widely used as a surface-passivation against nonspecific platelet–surface interactions in platelet adhesion studies, Sivaraman and Latour reported that platelet adhesion can be substantially mediated by specific interactions with denatured albumin, if the protein is adsorbed from low concentrations and/or onto hydrophobic surfaces [72]. Other examples for the close dependency of the biological function of a protein and its conformation include the enhanced adhesion of pre-osteoblastic cells on partially denatured collagen type I as compared to its native form [70]; and the activation of low levels of adhesion proteins (too low to promote cell adhesion when deposited by themselves) for cell adhesion by co-adsorption with high concentrations of nonadhesion proteins (likely causes for enhanced or impaired protein activity towards cell adhesion) [70]. For a more detailed discussion on the unfolding of proteins on surfaces, the reader is referred to reviews by Horbett [73, 74].

Since the build-up of multilayers of proteins on a surface is thermodynamically unfavorable (parts of the protein layer exposed towards the ambient solution may act as a kind of a swollen hydrophilic layer, rendering the adsorption of other proteins to the surface thermodynamically unfavorable), competitive adsorption becomes a decisive factor in the cell's response once the protein-coated surface is placed into

contact with cell culture media, which is often enriched with a mixture of more than 400 different proteins from the serum supplement [12]. The surface concentration of adsorbed proteins from plasma or model protein mixtures depends on their relative abundance and affinity towards the surface [75–79]. Over time, the composition of the adsorbed protein layer is subject to a dynamic change. Initial coverage is dominated by smaller proteins with a faster diffusion (e.g., albumin), which are subsequently replaced by molecules with a higher affinity towards the surface (also known as Vroman effect [80–84]). On the other hand, cells actively remodel their extracellular environment by expression of proteins or their removal by proteolysis [85–88]. Although chemisorption of the proteins (e.g., through crosslinking the biomolecules to the matrix [89, 90]), might stabilize the adsorbed layer against competitive replacement in cell culture medium, proteolysis and a consequent degradation of the biofunctional surface coating remains an issue in the control of the cell–surface interaction.

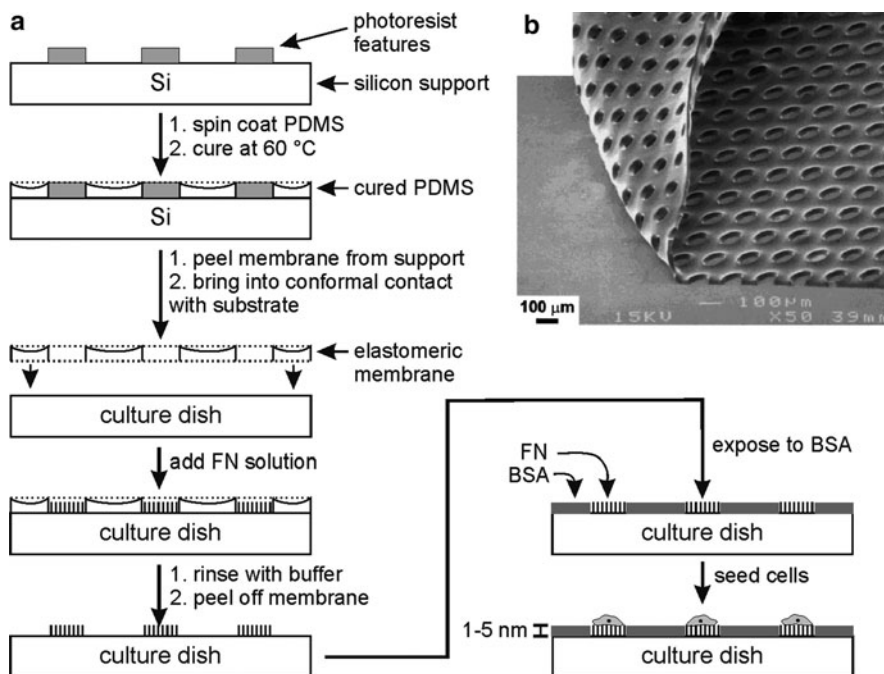
For a more comprehensive treatment of the concepts discussed here, the reader is referred to an excellent review by Wilson et al. [91]. In summary, one has to keep in mind that the composition of a protein film interacting with cells *in vitro* (and more so *in vivo*) generally differs from the initially deposited physisorbed proteins, especially if long-term experiments are conducted. Nevertheless, protein-based surface films have often been shown to provide an excellent platform for cell adhesion experiments in which the precise control of the cell–surface interactions does not play a key role.

Most reports on protein-mediated cell adhesion can be categorized into one of two basic concepts for structuring the cell-adhesive islands:

1. *Indirect patterning*: A protein repellent background is locally “opened,” rendering areas of the surface prone to protein adsorption. The patterning of cell-attractive areas is indirectly achieved by a subsequent deposition of proteins either by preincubation with a solution of proteins (most prominent are fibronectin, vitronectin, and laminin) or by adsorption from serum-supplemented cell culture media during cell seeding.
2. *Direct patterning*: Cell-adhesion-mediating proteins are directly placed on a surface that is already protein-resistant or is later backfilled with a passivating film.

#### 4.1.1 Indirect Patterning of Proteins

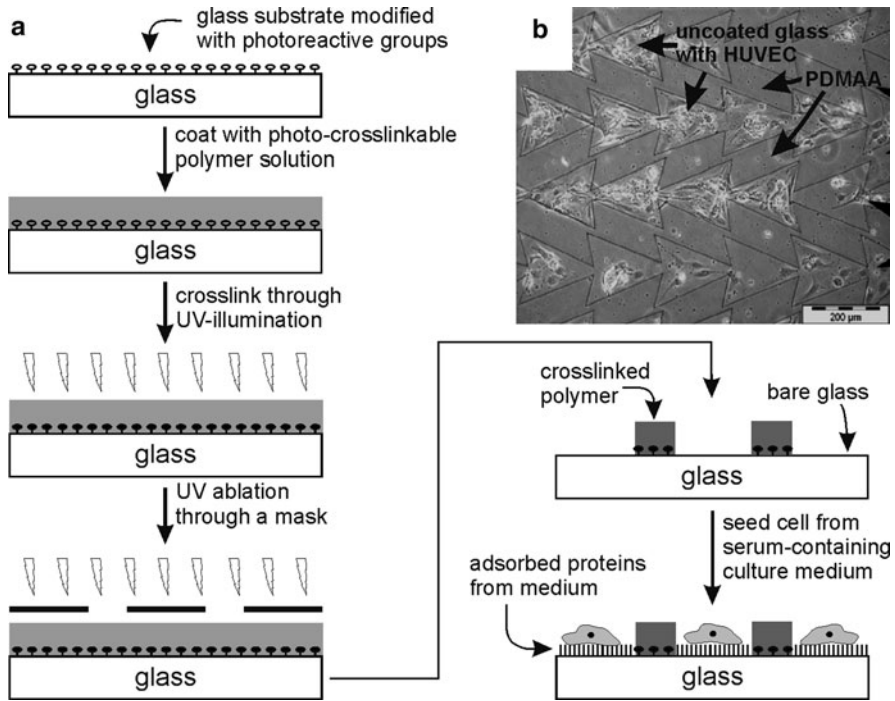
Whitesides and coworkers describe the use of an elastomeric membrane to pattern proteins and cells on bacteriological polystyrene (PS), glass, and poly(dimethylsiloxane) (PDMS) substrates [92]. A patterned PDMS membrane was casted from lithographically structured photoresists and brought into close contact with the substrates (Fig. 6). When incubated with a solution of fibronectin (FN), adsorption of the cell-adhesion-mediating protein to the surface was restricted to the exposed areas. The membrane was peeled off and cells were seeded from a serum-free medium. Passivation to cell attachment of the untreated portions of the surface was achieved by adding 1% bovine serum albumin (BSA) to the cell-seeding medium, which



**Fig. 6** (a) Micropatterning through the use of a “lift-off membrane”: PDMS prepolymer is poured on a silicon master featuring microstructures of photoresist, and then spin coated to produce a silicone film thinner than the photoresist structures. Following a thermal curing process, the PDMS membrane can be peeled off the silicon wafer and brought into conformal contact with a standard culture plate. In the next step, the protected surface is exposed to a protein solution to allow proteins to adsorb to the uncovered culture dish. After removal of the elastomeric membrane, the remaining areas are rendered protein-repellent by a treatment with a BSA-containing solution. Cells can be subsequently seeded on the chemically micropatterned surface. (b) Scanning electron micrograph of a PDMS membrane used as a stencil for protein patterning. (Figure adapted from [92])

can adsorb to areas not coated with FN. This easy-to-use strategy for passivating the surface against cell adhesion proved to be sufficient to limit the attachment of bovine adrenal capillary endothelial (BCE) cells selectively to the FN patterned areas. However, this approach is limited to short-term experiments or the use of serum-free medium because passivation with BSA is not stable in the presence of other proteins (e.g., those present in serum supplements in cell culture medium). In an interesting variation of this approach, the group seeded cells directly onto the membrane–substrate assembly. When the PDMS membrane was passivated by adsorption of BSA before cell seeding, BCE cell adhesion could be physically constrained to the patterned areas. Following the removal of the membrane after 7–24 h in culture, spreading of the cells to the unprotected areas could be analyzed.

Protein adsorption onto intrinsically repellent materials is enhanced by a brief plasma treatment that chemically and physically alters the surface properties. Stencil-assisted plasma oxidation of inherently hydrophobic polymers (e.g., PDMS



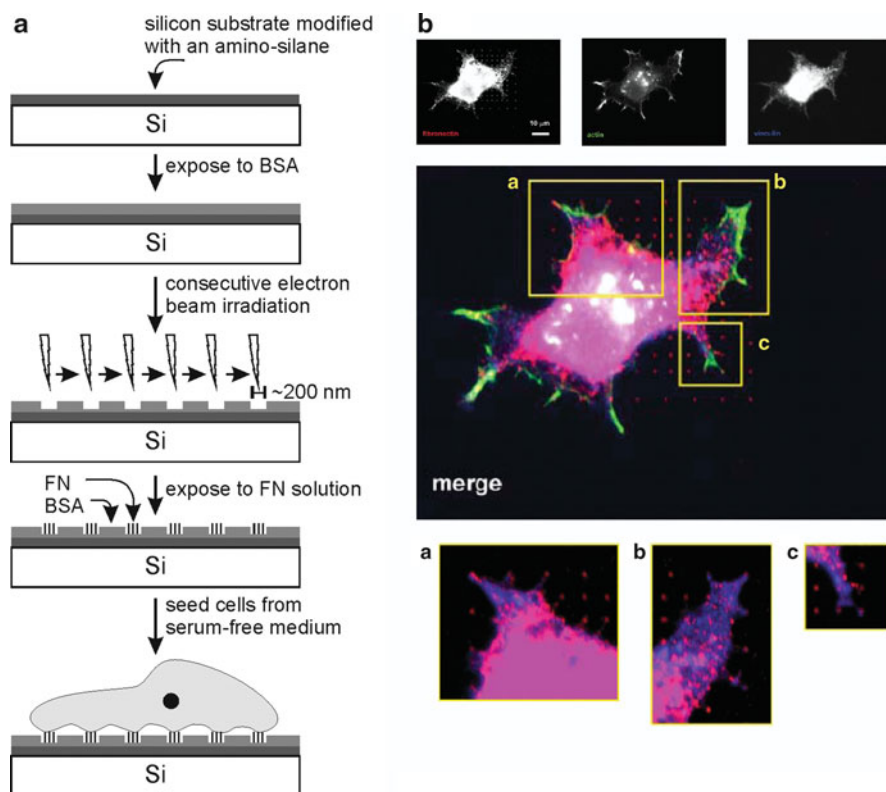
**Fig. 7** (a) Micropatterning by local photo-ablation of protein-repellent polymer hydrogel: A photo-crosslinkable prepolymer is coated onto a glass substrate bearing photoreactive groups. Simultaneous crosslinking and binding of the polymer film is achieved by illumination with UV light. The surface coating is subsequently micropatterned by UV ablation through a mask. Uncoated areas of the substrate mediate cell adhesion through unspecific adsorption of serum proteins from cell culture medium. (b) HUVEC growing on a glass surface coated with a cell-repellent PDMAA film. Microstructuring was achieved by local ablation of the protein-resistant PDMAA hydrogel. (Figure in part (b) Courtesy of Jürgen Rühle, University of Freiburg, Germany)

or PS) increases the hydrophilicity of the surface and, more importantly, introduces charged groups into the substrate and produces a pronounced roughening of PDMS and PS, favoring the adsorption of proteins in their bioactive form [93–95]. As an alternative to modification of the bulk material, a protein-repellent surface coating can be selectively removed by plasma ablation, laying bare the protein-attractive bulk substrate (Fig. 7) [93, 96–98]. Stencils for plasma treatment are commonly prepared by molding of PDMS from photoresist masters using standard photolithography methods.

Microcontact printing ( $\mu$ CP, see Fig. 10 for an example) has been used for the spatially resolved modification of gold, silver, or titanium surfaces with SAMs of methyl-terminated alkanethiolates, which favor protein adsorption [99–101]. Backfilling around the patterned protein-attractive islands was performed by a subsequent self-assembly of an ethylene-glycol-terminated alkanethiol. In a next step, the hydrophobic methyl-terminated SAMs were covered by adsorbed FN or other cell-adhesion-mediating proteins.

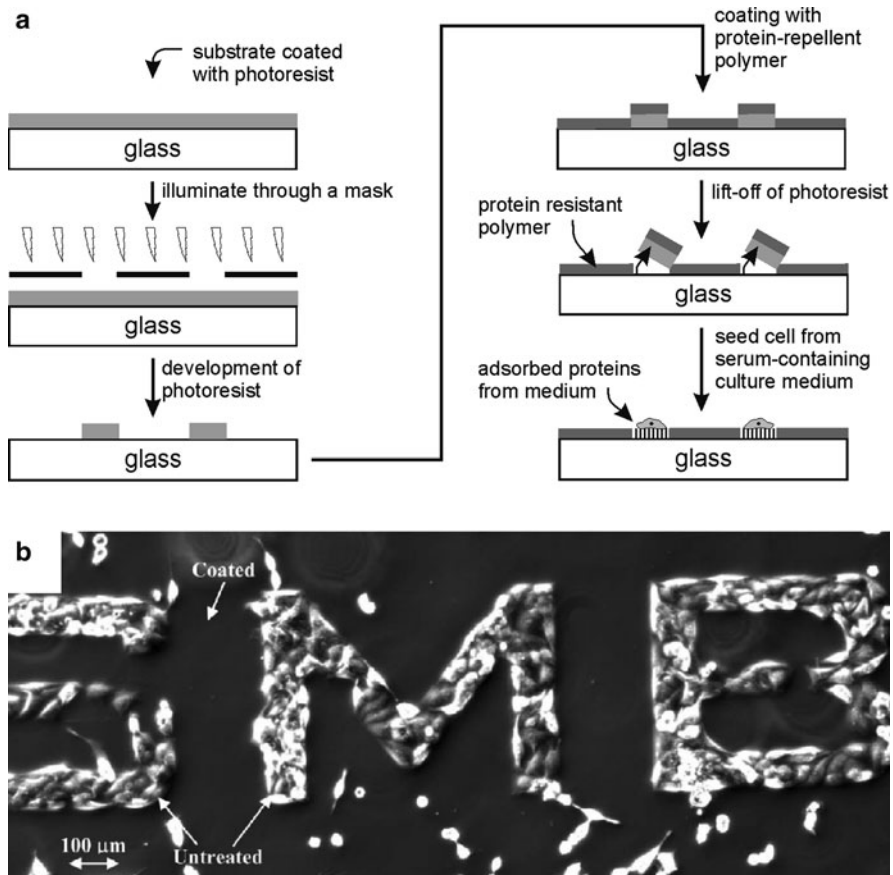


Direct writing methods have also been proposed for the generation of high-resolution cell patterns. In one example, UV laser ablation was used to locally remove polyacrylamide and thus create areas for spatially controlled protein adsorption [102]. Pesen et al. modified a layer of physisorbed BSA through electron beam lithography (EBL), creating nanodots of fragmented BSA with radii as small as 100 nm (Fig. 8) [103]. The dissociated protein acts as a template for a selective adsorption of FN, allowing precise modulation of the cell–surface contacts. Robotically controlled pin-printing of diluted solutions of sodium hypochlorite on poly(vinylalcohol) films or commercially available ultralow attachment dishes (from Corning) has been used to locally oxidize the surface, leaving it open for protein adsorption and cell adhesion [98].



**Fig. 8** (a) Nanopatterning by EBL: A silicon substrate is functionalized with an amino-silane and coated with BSA. A focused electron beam is employed to “write” nanopatterns into the BSA film. Proteins from solution can selectively adsorb into the nanopatterns and guide the formation of cell–surface contacts. (b) Fibroblast on fibronectin  $10 \times 10$  nanodot matrix created by electron beam lithography. Cells spread, and fluorescent staining of intracellular proteins shows that focal contacts are located on the nanodots: actin (green), fibronectin (red), and vinculin (blue). Areas *a*, *b*, and *c* are shown magnified. (Figure in part reproduced with permission from [103])

In a different approach, Bouaidat et al. adapted the lift-off technique to pattern a cell-repellent poly(ethyleneoxide)-like (PEO-like) coating on glass substrates [104]. In brief, a photoresist was microstructured using conventional photolithography, and a plasma polymerized protein-repellent film (plasma-polymerized hexene as adhesion layer and 1,4,7,10-tetraoxacyclododecane (12-crown-4)) was subsequently deposited on the substrate. Lift-off of the photoresist opened the cell-repellent PEO-like coating for a targeted adsorption of proteins (Fig. 9). The group of Chang



**Fig. 9** (a) Micropatterning through the use of the lift-off technique: A photoresist is coated onto a glass substrate and patterned by illumination through a mask. In the case of a negative resist, shaded areas remain soluble in the developer-solution and can be removed. The substrate surface is then completely modified with a protein-repellent polymer. Using a good solvent for the patterned photoresist, the polymer layer is locally removed together with the underlying photoresist (“lift-off”). (b) Optical microscope image of HeLa cells adherent on untreated glass surrounded by a PEG-like film structured through a lift-off process. The surface was not rinsed to remove unadherent (round) cells prior to inspection. (Figure in part reproduced with permission from [104])



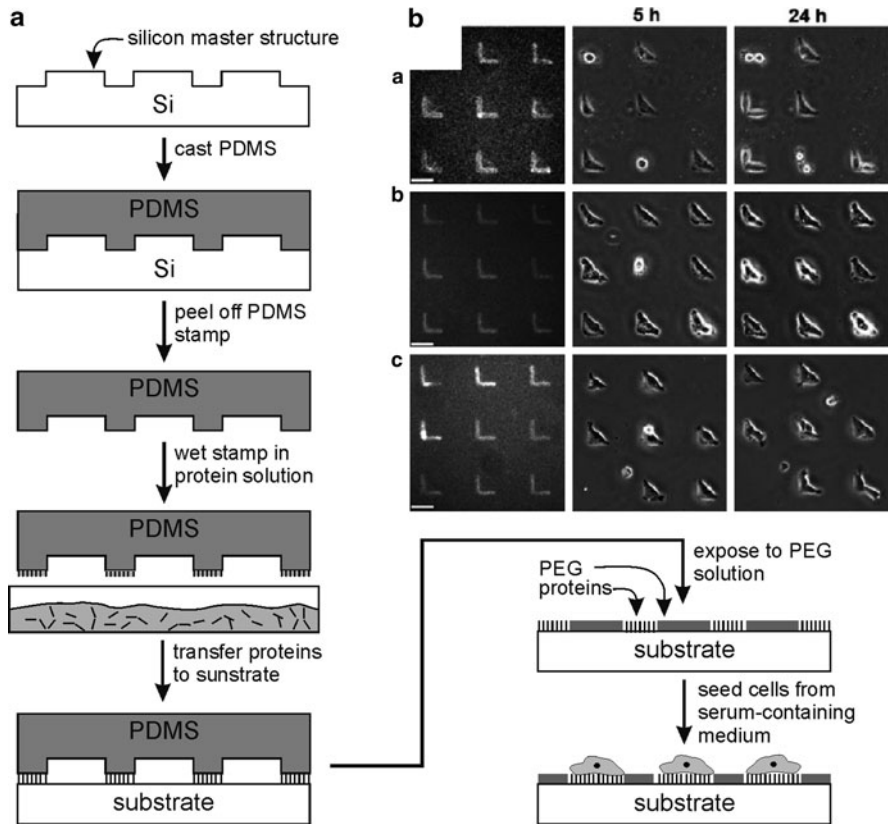
and Sretavan also chose the lift-off technique to pattern the protein-attractive areas rather than the protein-repellent patches [105]. Again, a plasma-polymerized PEO-like film was grafted onto a surface and over-coated with a photoresist. The latter was microstructured using photolithography, and the underlying PEO activated for the adsorption of polylysine by a brief plasma treatment. After the lift-off of the photoresist, the adsorbed polylysine remained on the patterned areas, enabling a successful spatially resolved cultivation of mice embryonic hippocampus neurons. Polylysine (positively charged) adsorbed to plasma-activated PEO-like films can also be used as a template to selectively adsorb other molecules (e.g., laminin or immunoglobulin G) in order to make this approach compatible with other cell types.

A way to pattern the protein-repellent background by lithography without the need for an intermediate overcoat is to incorporate a photoinitiator into the precursor solution of the polymer. For example, Revzin et al. used 1% 2,2'-dimethoxy-2-phenylacetophenone (DMPA) in poly(ethylene glycol) diacrylate (PEG-DA) precursor solution to create microwells for cell culturing that had a glass base and PEG-DA side walls [106]. As an alternative to the widely used PEG as protein-resistant background, Rhe and coworkers copolymerized hydrophilic dimethylacrylamide (DMAA) and a photoreactive comonomer (benzophenone) to produce a directly photo-patternable polymer system that showed excellent protein-repellent properties [39, 107, 108]. In combination with photoreactive benzophenone-silane attached to the underlying glass substrate, polymer coatings that allow protein adsorption (e.g., PMMA) were copatterned with PDMAA hydrogel by standard mask lithography [109]. This approach allowed fine tuning of the surface-bound film to meet the specific requirements imposed by different cell types, e.g., human skin fibroblasts (HSF) and human umbilical vein endothelial cells (HUVEC) attached nicely to PMMA coating, whereas neuronal cells only adhered to PEI surfaces.

Similarly, Chien et al. used a poly(acrylic acid)/poly(acrylamide) (PAA/PAM) multilayer system in which PAA was replaced by PAA conjugated with photoreactive 4-azidoaniline (AZ) after several bilayers [110]. As a result, the polyelectrolyte multilayer could be covalently crosslinked by UV irradiation through a mask. For an enhanced cell repellence, poly(allylamine) was conjugated with poly(ethylene glycol methyl ether) and incorporated into the top layers of the film.

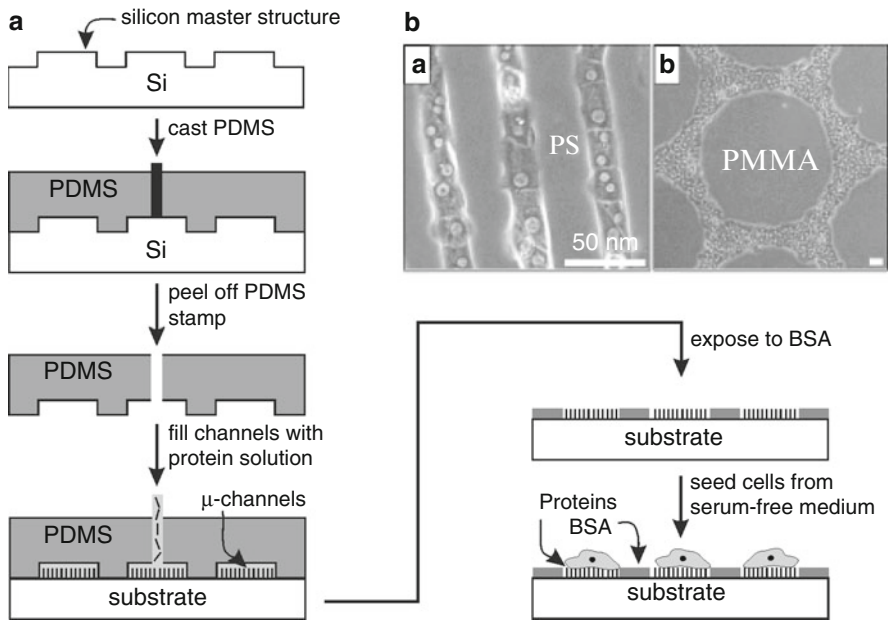
#### 4.1.2 Direct Patterning of Proteins

For the direct placement of adhesion-mediating proteins onto surfaces,  $\mu$ CP is probably one of the most popular methods (Fig. 10). This technique offers great flexibility with respect to the molecules patterned as well as to the choice of substrate. Examples include the modification of glass, PS, BSA and biodegradable polyurethane or hydrogel-coated surfaces with proteins, commonly FN, laminin, or poly-L-lysine (PLL) [89, 111–117]. The transfer of the proteins in  $\mu$ CP is done in the dry state, opening the opportunity to physisorb molecules even to substrates that prevent the adsorption of material in the hydrated state (e.g., hydrogels). In this



**Fig. 10** (a) Microstructuring by  $\mu$ CP: PDMS prepolymer is poured on a silicon master featuring microstructures of photoresist. After thermal curing, the PDMS stamp is peeled off the master structure and stamped into a protein-containing solution. After drying of the “ink solution” on the stamp, the attached proteins are transferred to another surface by placing the PDMS onto the target substrate for a short time (minutes). Uncoated areas can be backfilled with BSA, and cells are seeded onto the substrate. (b) Cell patterns produced by  $\mu$ CP on different surfaces (*top row*: untreated glass, *middle row*: tissue culture polystyrene (TCPS), *bottom row*: ibidi plastic). Printing efficiency was investigated using fibronectin-Cy3 (*left column*). Printing was followed by a back-fill with PLL-g-PEG to prevent unspecific cell attachment. Cell patterns remain intact for 24 h in culture. (Figure reproduced in part with permission from [89])

case,  $\mu$ CP allows single-step patterning of proteins on an otherwise protein-repellent background (i.e., no backfill is needed). The stability of the printed protein films, especially on protein-repellent backgrounds, has been assessed for different surfaces and the results indicate a more persistent protein immobilization with an increasing “softness” of the underlying substrate [89, 111, 113, 114]. Although a sometimes reduced transfer efficiency and denaturation of the stamped (dry) proteins causes a diminished protein activity towards cell binding on the surface,  $\mu$ CP has been reported to be a very robust method for protein patterning and thus cell patterning.



**Fig. 11** (a) Microstructuring by microfluidic printing ( $\mu$ FP): PDMS prepolymer is poured onto a silicon master featuring connected microstructures of photoresist. After thermal curing, the PDMS stencil is peeled off the master structure and brought into firm contact with a substrate (e.g., glass or Petri dish). The recesses in the PDMS stencil form a microfluidic network on the substrate that is subsequently filled with a protein-containing solution. After removal of the stencil, uncoated areas are backfilled with BSA. To enhance selective cell attachment, cell seeding is performed from serum-free medium. (b) Hepatocyte micropatterns on PS (a), and PMMA (b). Surfaces were structured by microfluidic printing of ECM proteins. Substrates were backfilled with BSA, and cells were seeded in serum-free culture medium to prevent unspecific adsorption of serum proteins onto uncoated areas. (Figure in part reproduced with permission from [118])

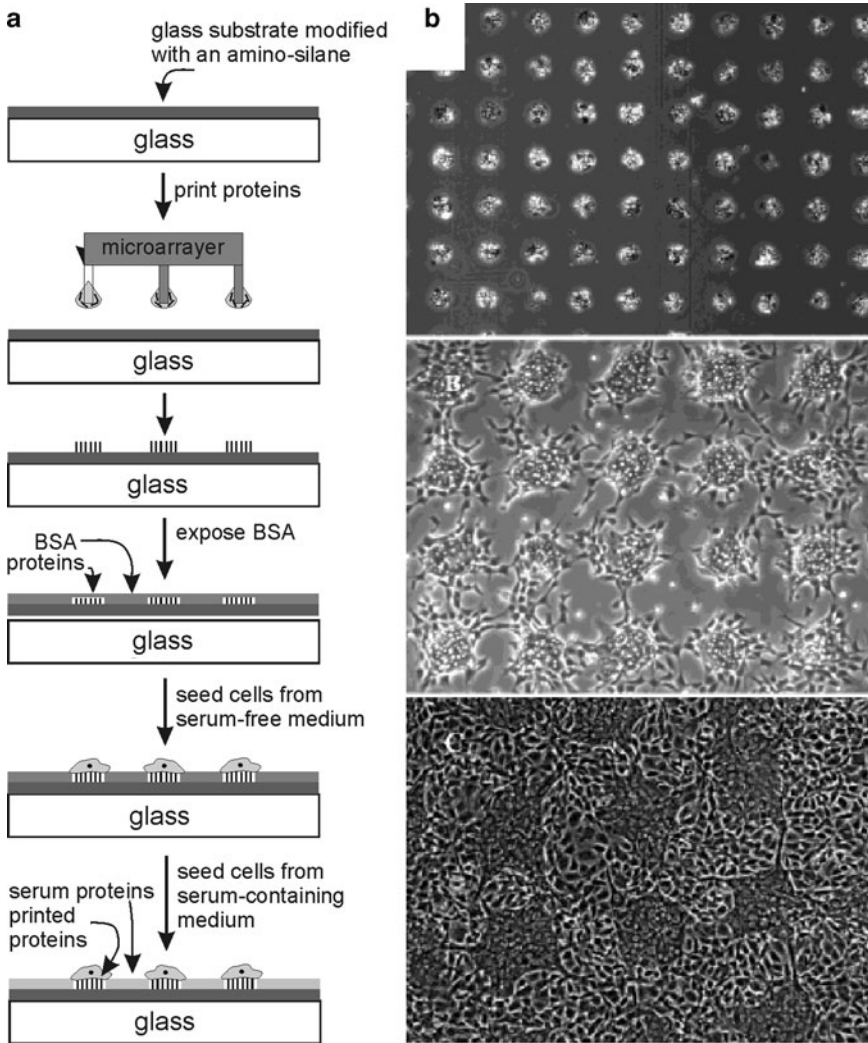
Microfluidic patterning ( $\mu$ FP), a technique closely related to  $\mu$ CP, employs microfluidic channels to selectively deliver molecules on a surface (Fig. 11). Identically flexible as  $\mu$ CP with respect to choice of patterning solution and substrate,  $\mu$ FP is capable of depositing proteins in the wet state, thus reducing problems resulting from denaturation. Depending on the application, a subsequent backfill of uncoated areas after removal of the stamp material is, in most cases, mandatory. Another appealing property of  $\mu$ FP lies in its ability to pattern different binding proteins in a single step using separated microchannels [119]. A drawback of this technique is the geometric limitation to connected protein areas, although Folch and Toner reported the implementation of cell-adhesive islands by filling the microchannels with hot agarose [120]. After solidification of the agarose inside the channels, the PDMS stamp was removed from the support, turned upside-down and used as substrate for cell cultivation, the PDMS representing the protein- and

cell-attractive spots. A combination of  $\mu$ CP and  $\mu$ FP was reported by Cuvelier et al. [121]. The group used a BSA-coated PDMS stamp to create the microchannels, which were filled with a biotin-containing solution, creating protein-repellent and protein-attractive areas simultaneously.

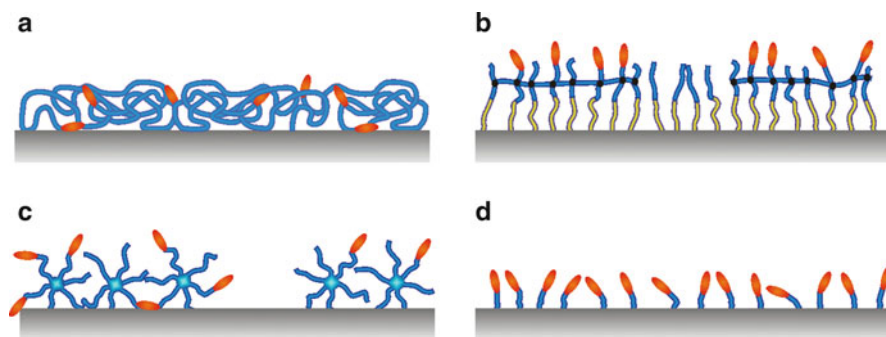
Direct printing techniques have become a standard tool in genomics and proteomics, where large-scale and high-throughput microarrays allow fast and easy detection of thousands of different elements in a single experiment. Among other applicable molecules for printing, protein microarrays have been studied for antibody–antigen, protein–protein, protein–nucleic acid, and protein–small-molecule interactions [122, 123]. Apart from its use in proteomics, printing of proteins has also been employed in cellomics, for example by printing cell-adhesion-mediating proteins onto glass [124], and printing polymers that contain photoreactive groups for subsequent covalent binding of proteins to the surface [90]. Folch and Toner reported the preparation of cocultures of hepatocytes and fibroblasts using printed collagen arrays with a preliminary backfill of BSA during the first seeding step of hepatocytes, which was done from serum-free medium to ensure a sufficient site-selectivity in cell attachment (Fig. 12) [120]. In a second step, BSA-covered areas were populated by fibroblasts, presumably through replacement of BSA by a competitive adsorption of serum proteins contained in the medium of the second seeding.

## ***4.2 Peptide-Decorated Surfaces for Spatially Guided Cell Adhesion***

Another interesting way to guide the adhesion of living cells is to selectively present the recognition sites on the surface instead of whole proteins. It is self-evident that this “breaking-down” of ECM proteins into their functional components will offer only a minimalistic, and therefore limited, reproduction of the natural environment of cells in vivo. Nevertheless, the strategy to use distinct peptide moieties for a direct mediation of cell attachment has the potential to create highly defined model systems for cell adhesion that will, and indeed have already, elevate our understanding of basic mechanisms involved in cell–substrate interaction. Apart from the chemical identity (i.e., the amino acid sequence) of the peptide, the presentation of the binding ligands to the cell is a key parameter for such investigations. In the last three decades, model surfaces have been created that allow for different degrees of control over the presentation and surface density of the functional moieties, progressing from randomly distributed peptides in polymer matrices (e.g., hydrogels or monolayers) to highly ordered systems such as SAMs of peptide–amphiphiles or star-PEG assemblies (Fig. 13). Depending on the application, scientists can nowadays choose a system that meets their requirements in terms of control of interaction, long-term stability of the cell guidance, ease of synthesis, and coating technique.



**Fig. 12** (a) Microstructuring through contact printing: A robotic microarrayer is used to print a protein-containing solution on an amino-silane functionalized substrate (e.g., glass). Surrounding areas can be backfilled with BSA and cells are seeded from serum-free medium to enhance the site-selective attachment. In a variation of this technique, cocultures of different cell types can be achieved through addition of serum proteins to the culture medium and (using a short incubation time for the first cell type) a subsequent seeding of a second cell type on the same surface. Attachment of the first cell type is restricted to the protein-coated areas by the adsorbed BSA. Over time, BSA is replaced by proteins from the culture medium, which provide adhesion sites for cells from a second seeding. (b) Microstructured coculture of hepatocytes and fibroblasts. Hepatocytes adhere to printed spots of collagen surrounded by BSA (*top*). After 24 h of incubation, a second cell type (fibroblasts) was added and cells attached in the formerly BSA-coated areas (*middle*). Co-culture after 5 days of incubation (*bottom*). (Figure in part reproduced with permission from [124])



**Fig. 13** Different strategies for immobilizing peptide moieties on solid surfaces. **(a)** Peptide-polymer hybrid copolymers are attached to the substrate, offering no direct control of the peptide orientation (scheme refers to surfaces introduced by [40, 135]). The peptide moieties are statistically distributed in the polymer film. **(b)** A polymerized monolayer of peptide-amphiphiles is immobilized on a planar substrate, giving control over peptide orientation and concentration on the surface through coattachment of a nonmodified polymerizable amphiphile (scheme refers to surfaces introduced by [134]). **(c)** Minimal integrin adhesion ligands (YGRGD) are attached to surface-immobilized star PEO tethers to allow control over spatial distribution (through the formation of clusters of more than one peptide per star molecule) and the total average concentration (through blending with unmodified star polymers) (scheme refers to surfaces introduced by [146]). **(d)** RGD moieties are attached to substrates using virtually no spacer, giving an excellent control over peptide concentration at the cost of limited flexibility for peptide clustering (scheme refers to surfaces introduced by [145])

Many approaches comprise some attractive features with respect to specific binding to certain integrins and long-term stability of the produced surface coatings. In order to ensure the exclusive interaction of the cells with the recognition sites presented (and not with unspecifically adsorbed proteins), the matrix (i.e., the background) must possess protein-repellent properties.

Moreover, a strong linkage of the adhesion moiety to the polymer matrix is the prerequisite to supply a mechanically and chemically stable support for cell adhesion that withstands the considerable contractile forces exerted by many cell types [125–127]. Furthermore, cells can actively remodel their extracellular environment by redistribution or internalization of small and mobile ligands [68, 125, 127–131]. A number of chemistries are readily available for covalently attaching short peptide sequences to a polymeric background. For an in-depth discussion of this topic, the interested reader is referred to reviews by Tirrell et al. and by Hersel and Kessler [29, 132]. Most commonly, the peptide is grafted to an already protein-repellent surface in a postsynthetic modification step, either via its amine or carboxylic acid end-group, by bioconjugate chemistry means or through photoreactive linkers (e.g., benzophenone or aromatic azide functionalized peptides). The introduction of suitable functional groups into the polymeric background can be achieved by blending of polymers with functional groups with the base polymer, by copolymerization or through a chemical or physical treatment of the protein-repellent background, such as alkaline hydrolysis, reduction or oxidation, track-etching,



or plasma deposition. As an alternative to the postsynthetic modification of a preformed polymeric background, the employment of so-called peptide–polymer hybrid materials was suggested [133–135]. Hereby, solid-phase organic synthesis is used to attach specific peptide moieties to synthetic polymers or amphiphiles, or vice versa. The resulting peptide–polymer hybrids are then self-assembled (in the case of peptide–amphiphiles) or chemically immobilized onto a surface.

The last three decades have seen great advances in the characterization of specific cell–substrate interactions through the use of peptide-containing surfaces [29]. Several parameters have been identified that influence the specificity and binding efficacy of synthetically formed biomimetic films. Among these, the conformation of the presented peptide ligand plays an important role. For example, if the RGD peptide is isolated from the context of the protein, it loses some specificity as well as binding affinity to integrins as compared to its native counterpart [24]. However, if the RGD sequence is presented in a “looped” conformation resembling its natural structure in FN more closely, the adhesion and spreading of cells is enhanced, as compared to the linear peptide, in a concentration-dependent manner [136, 137]. Cell attachment is also influenced by the presence of immediate side groups and short peptide sequences in close proximity (so-called synergy sites) to the integrin-binding motif RGD. Hirano et al. compared the binding affinity of different tetra-peptides comprising the RGD sequence derived from the ECM proteins FN (RGDS), vitronectin (RGDV), and collagen (RGDT) towards five cell types. They found a strong influence of the residue amino acid X in RGDX on the cell-binding activity [138]. The incorporation of the recognition site into its wider context in nature – instead of using the minimal recognition sequences – was also found to improve cell response. For example, in FN the peptide sequence PHSRN is found in the ninth type III module (FNIII9) and therefore in close proximity to the recognition motif RGD (FNIII10). When tested for its influence on cell attachment, the synergy site PHSRN in a defined distance to RGD was found to lead to an overall strengthening of the cell–substrate binding as compared to the minimal recognition motif RGD [139, 140]. However, whether PHSRN acts as a synergy site only, or binds to the integrin receptor in a competitive fashion, is still controversially discussed [141].

Apart from a favorable conformation and context of the peptide, the *accessibility* of the recognition motif for the integrin-binding site must be provided by the artificial synthetic background. A number of studies investigated the optimal spacer length between recognition site and polymeric support. Through systematic introduction of amino acids between the binding motif and the background, a spacer length of 3–4 nm was identified by several groups as optimal with regard to cell adhesion [142–144]. In other experiments by Massia and Hubbell however, although virtually no spacer between GRGDY and the anchoring group to a glass surface was used, satisfying adhesion of human foreskin fibroblasts could be observed (Fig. 13d) [145]. Although the question of whether a spacer is needed or not has not yet been fully resolved, most systems incorporate some form of soft polymeric matrix (e.g., hydrogels, brushes, or SAMs, as outlined in Sect. 3) for protein-repellent purposes as a background for peptide immobilization and thus provide at least some flexibility and mobility to the recognition motifs.

Another parameter that influences the ability of a bioactive surface coating to mediate cell adhesion is the surface concentration of the binding recognition site. Pioneer work on the question of minimal peptide concentrations for cell attachment was reported by Massia and Hubbell in 1991 [145]. Here, a functionalized peptide-ligand was directly immobilized onto glass substrates. The concentration of the peptide was varied by coimmobilizing an inert compound that does not support cell attachment. Using these substrates, a minimum surface concentration of GRGDY ligand of  $1 \text{ fmol/cm}^2$  was sufficient to promote fibroblast cell spreading on an otherwise poorly adhesive glass substrate. However, a tenfold higher surface concentration (i.e.,  $10 \text{ fmol/cm}^2$ ) was needed to induce the formation of focal contacts.

Besides the overall concentration of the recognition motif on the surface, the lateral distribution of the presented peptides can also evoke different cellular responses, e.g., trigger the aggregation of integrins in the cell membrane to form focal adhesions [146–148]. For the investigation of the effects of peptide clustering in a polymeric film, star-like polymers were functionalized with a recognition motif (Fig. 13c) [146]. Nanoscale RGD clustering, for example, was found to result in a significantly higher stress resistance and in the formation of well-formed stress fibers and focal contacts in fibroblasts. Using block copolymer micelle nanolithography, Spatz and coworkers were able to control the lateral spacing of single integrin-receptor binding sites by a highly defined presentation of cyclic RGD peptide on a rather rigid support [149]. Their studies emphasize the importance of nanoscale integrin clustering over the macroscale peptide density for normal cell adhesion and cytoskeleton development.

Although the RGD motif is by far the most studied cell-binding moiety, other peptide sequences have been identified for specific cell binding [150, 151]. The exact peptide sequence presented has a significant influence on the selectivity towards certain integrins and thus different cell types [152–155]. This difference in affinity has been exploited by Plouffe et al. for the design of an adhesion-based cell separating system, embedded in a microfluidic device [154, 155]. Using three successive stages of different peptide coatings (REDV, VAPG, and RGDS) in a microchannel, a heterogeneous cell suspension of endothelial cells, smooth muscle cells, and fibroblasts could be successfully depleted. This could open the door to an automated cell-sorting device that selectively immobilizes cells on the basis of the expression level of certain integrins.

The deciphering of the fundamental mechanisms involved in integrin-mediated cell adhesion has come a long way since the discovery of the minimal recognition motif RGD(S) by Pierschbacher and Ruoslahti in 1984 [24]. Synthetic peptide–polymer model systems presenting biofunctional moieties in a highly defined context contribute an important tool to this quest. Although precise control over parameters such as peptide surface concentration and distribution (i.e., clustering), spacer length, and conformation of the binding motif often requires elaborate synthesis and coating protocols for the biofunctional conjugate, alternative approaches exist that provide for a more simple, versatile and chemically stable surface modification. Although compromising on the degree of control over the



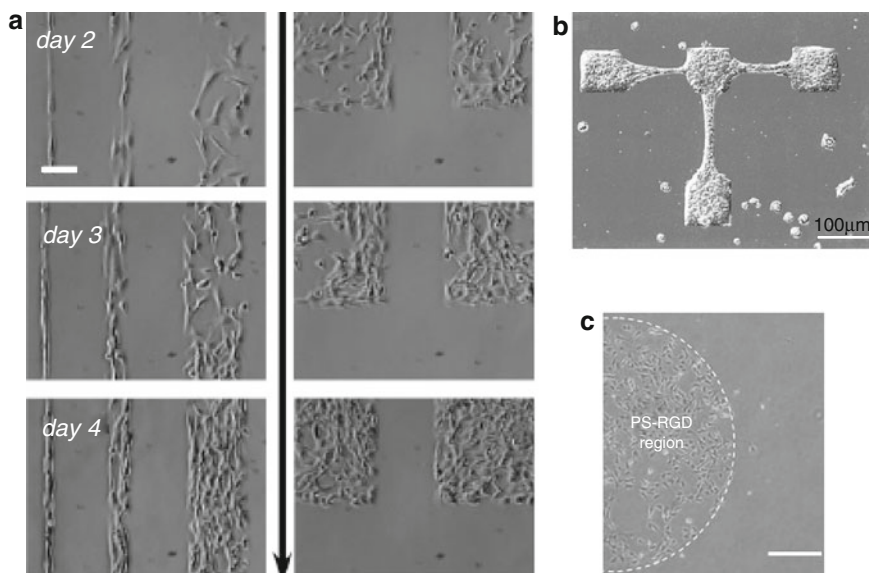
exact presentation of the peptide, these systems constitute an extremely defined environment for cell–matrix interactions. Moreover, well-designed setups (e.g., based on postsynthetically peptide-modified hydrogels or surface-bound peptide–polymer monolayers) often allow for long-term cell studies while preserving their comparatively high inertness towards changes in the experimental conditions (e.g., induced by protein adsorption/desorption, or proteolytic degradation).

Compared to systems that rely on protein adsorption for spatially guided cell adhesion, reports on cell chips based on peptide-mediated adhesion are less frequent, but emerging. In principle, identical methods to those used for the microstructuring of proteins can be employed for peptides, although reports on direct patterning (controlled deposition of peptides) prevail.

As for protein patterning,  $\mu$ CP of thiol-conjugated molecules onto gold surfaces was among the first methods used for locally resolved deposition of peptides. Zhang et al. used a combination of microcontact-printed ethylene glycol thiolate and self-assembled oligopeptides containing the cell adhesion motif (RADS) and a cysteine linker to guide the adhesion of cells onto gold substrates (Fig. 14) [156].

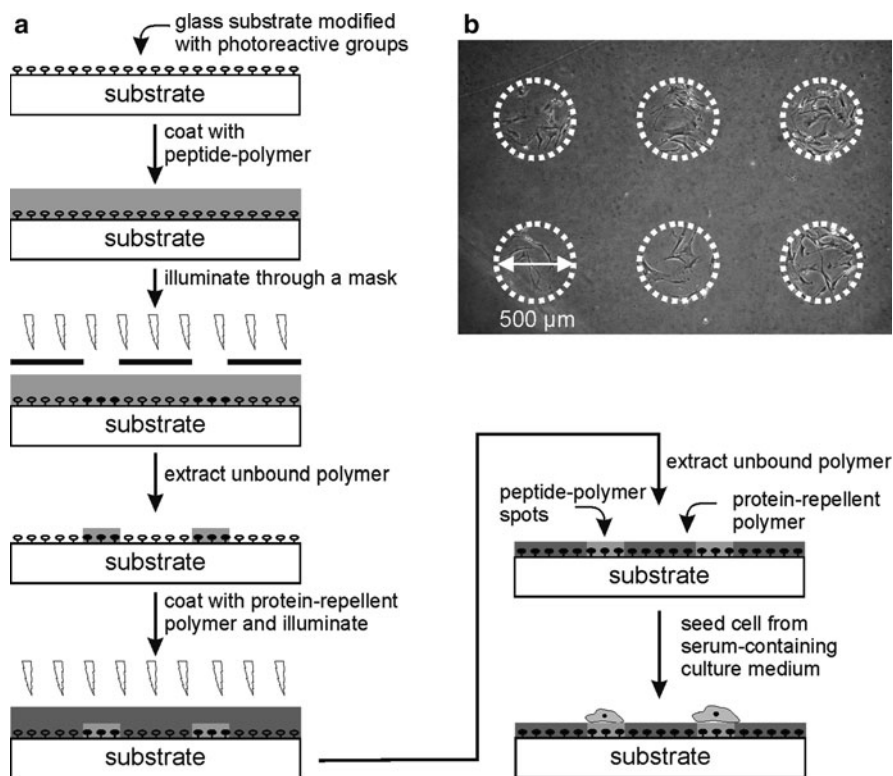
Grainger and coworkers used commercially available telechelic *N*-hydroxy succinimide (NHS)-terminated PEG to create a protein-resistant film containing reactive groups [157]. Microstructuring was achieved through a conventional photolithographic process based on microstructuring of a photoresist film deposited onto the hydrogel, which serves in a second step as a stencil for site-selective methoxylation of exposed areas. Following removal of the photoresist, the remaining NHS-capped regions were treated with a GRGDS peptide, allowing for covalent attachment of the adhesion-mediating ligand. Fibroblasts (NIH-3T3) adhered exclusively to the RGD-patterned areas and showed a “normal” behavior with respect to proliferation and spreading (Fig. 14). Our own group recently reported on the synthesis and spatially resolved surface immobilization of a peptide–polymer hybrid for the controlled adhesion of cells (Fig. 15) [40, 135]. The novel peptide–polymer hybrid was synthesized by a controlled radical polymerization of dimethylacrylamide (DMAA) from an initiator-modified RGD peptide [135]. Monolayers of hydrophilic peptide–PDMAA were shown to resist the unspecific adsorption of proteins and can be covalently bound and microstructured by lithography on surfaces modified with photoreactive benzophenone groups [40]. Peptide–PDMAA areas can be back-filled with (chemically almost identical) PDMAA and shown to be able to locally constrain the adhesion of human fibroblasts under serum conditions for more than 2 weeks.

Printing of peptides, either using a contact pin microarrayer [124, 159] or non-contact printer (using ink-jet technology) [160, 161], was used as a versatile tool for delivery of cell-adhesive ligands onto protein-repellent surfaces (Fig. 14). An attractive property of this technique lies in the ability to simultaneously print different peptides in one step. For example, Monchaux and Vermette used a noncontact automatic dispensing robot to covalently graft three different bioactive peptides in combination with RGD on a protein-repellent carboxy-methyl-dextran (CMD) background [161]. Although RGD was necessary to initiate the adhesion of endothelial and fibroblast cells, the coimmobilization of SVVYGLR or VEGF enhanced



**Fig. 14** (a) Photolithographic lift-off process has been used to selectively deactivate a commercially available amine-reactive polymer coating (OptiChem, Accelr8 Technology, Denver, CO) (please refer to Fig. 8 for a process description). After removal of the photoresist, RGD peptide was immobilized in unreacted areas. NIH-3T3 fibroblasts follow the implemented structures for several days. (Figure in part reproduced with permission from [159]). (b) Human epidermal carcinoma cells on self-assembled monolayer of oligopeptides containing the cell-adhesion motif RADS. Microstructures were transferred onto gold-coated silicon surfaces by microcontact printing of ethylene glycol thiolate and a subsequent backfill with the thiolated oligopeptides (please refer to Fig. 10 for a process description). Note that the unpatterned round cells are not adherent to the surface, but free-floating. (Figure in part reproduced with permission from [156]). (c) PS-binding peptides were printed by an automated pin microarrayer on native PS (please refer to Fig. 12 for a process description). A subsequent backfill with BSA renders the remaining PS surface sufficiently protein repellent to confine HUVEC attachment to the peptide-coated areas. (Figure in part reproduced with permission from [157]). *Scale bars: 100 µm*

endothelial cell adhesion, and coimmobilization of SVVYGLR and REDV caused a reduction of cell spreading. Combination of RGD with any of the three bioactive molecules interfered with the formation of stress fibers and caused a rearrangement of focal adhesions in endothelial cells. Interestingly, fibroblasts were not affected by spot composition. EBL, another direct writing technique, was employed in combination with block copolymer nanolithography of gold nanodots by Spatz and coworkers for the implementation of micro-nanostructured interfaces of cyclic RDGfK-thiols [149]. This approach allows a remarkable degree of control over the integrin–receptor interaction because it combines a defined presentation of the peptide (loop-type conformation), a precise control of the single peptide spacing (through block copolymer nanolithography and short thiol anchors), as well as an arbitrary distribution of the cell-adhesive spots on the surface (by electron beam patterning of the gold nanodots).



**Fig. 15** (a) Microstructuring by photopatterning: A direct photoinduced structuring of surface chemistry has been employed by our own group to guide human skin fibroblasts on peptide-polymer monolayers. Here, we used a surface-bound photoreactive benzophenone-silane to covalently attach monolayers of a cell-attractive, yet protein-repellent RGD-polymer (GRGDSP-PDMAA) on glass using UV illumination through a mask. Polymer in the shaded areas can be extracted, and the peptide-polymer microstructures are backfilled with a protein-repellent polymer (PDMAA). (b) Human skin fibroblasts adhere to peptide-polymer spots implemented in a protein-repellent environment through direct photopatterning. Cells follow the implemented structures for more than 2 weeks in culture [40]

As reviewed in this chapter, surface chemistry plays a key role in the interaction between living cells and artificial substrates. However, reducing this complex interplay solely to the underlying chemistry would draw a too-simplified picture. Cells are also highly sensitive to other environmental cues such as surface topography and elasticity, which can influence almost any aspect of a cell's life, from cell proliferation, contraction, migration, internal cytoskeleton organization, and even cell death [162]. A thorough discussion of these influences lies far beyond the scope of this article and the interested reader is referred to an interesting recent commentary as well as references therein [162]. Tables 2 and 3 summarize recent examples of bioactive, microengineered surfaces for the spatial control of the attachment and outgrowth of living cells, using protein- or peptide-decorated surfaces. We hope that they serve to outline recent trends and strategies in the implementation of cell chips (Tables 2 and 3).

**Table 2** Examples for microengineered surfaces for a spatially controlled cell attachment that use proteins as adhesion-mediating component

Cell-adhesion-mediating compound	Cell-resistant compound	Cell types tested	Patterning technique	Year	Ref.
<i>Indirect protein patterning</i>					
Serum proteins from cell culture medium	PDMS, methylated glass, bacterial grade PS	Human epithelial cells, human keratinocytes, human neuroblastoma cells, human breast cancer cells, human fibroblasts, human embryonic kidney cells, murine macrophages	Stencil guided plasma induced oxidation of hydrophobic surfaces	2009	[93]
Serum proteins from cell culture medium	PDMS	Human liver carcinoma cells	Photocatalytic hydrophilization of PDMS (mask lithography)	2009	[163]
Deposition from serum-free medium; culturing in serum-containing medium	Fluorinated polymer	Spatially separated coculture of human alveolar epithelial cells, human hepatoma cells, and mouse 3T3 fibroblast	Photocatalytic removal of fluorinated polymer (mask lithography)	2009	[164]
Collagen, poly-L-lysine/serum proteins from cell culture medium	Crosslinked polyacrylic acid/polyacrylamide multilayer films, PEG	Coculture of rat adrenal medulla cells and mouse fibroblasts L929	Photopatterning of polyelectrolyte multilayer film	2009	[110]
Serum proteins from cell culture medium	PEG	CHO-K1, MDCK, Balb/3T3, HepG2	UV patterning of photoresponsive polymer in situ to release physisorbed PEG	2009	[165]

First seeding: collagen	First seeding: collagen-specific attachment of hepatocytes	Coculture of primary rat hepatocytes and 3T3-J2 fibroblasts	Membrane-based patterning of protein	2008	[166]
Second seeding: serum proteins from cell culture medium	Second seeding: contact-inhibition in cell cocultures				
Serum proteins from cell culture medium	OEG-thiol	CaSki, HeLa, 3T3 fibroblasts	Release of OEG-thiol SAM from gold electrodes	2008	[167]
Adsorbed polylysine on plasma-activated PEG	PEO	Hippocampal neurons from embryonic mice	Photolithography for local oxidation of PEO (lift-off process), protein backfill	2008	[105]
Fibronectin	PLL- <i>g</i> -PEG-wells	HUVEC	Inverted $\mu$ CP of protein resistant PLL- <i>g</i> -PEG on PDMS microstructures, protein backfill	2007	[168]
Poly-L-lysine/serum proteins from cell culture medium	PEG-DMA	NIH-3T3 fibroblasts	$\mu$ FP of PEG-DMA on PEL	2007	[169]
Serum proteins from cell culture medium	PDMAA network	HUVEC, human skin fibroblasts	UV patterning of photoresponsive protein-resistant polymer	2007	[39]
Fibronectin	BSA	Swiss 3T3 fibroblasts	EBL to open protein-resistant BSA film, protein backfill	2007	[103]
Serum proteins from cell culture medium	None, direct placement of cells	Murine embryonic stem cells	Bio Flip Chip	2007	[170]

(continued)

Table 2 (continued)

Cell-adhesion-mediating compound	Cell-resistant compound	Cell types tested	Patterning technique	Year	Ref.
Serum proteins from cell culture medium	Polyvinyl alcohol (PVA)	Rat skeletal myoblasts, human embryonic kidney cells, colon carcinoma cells	$\mu$ CP of etching solution or UV ablation of PVA	2006	[98]
Fibronectin	BSA	Bovine adrenal capillary endothelial cells	Membrane-based patterning of protein, BSA backfill	2000	[92]
Fibronectin	Polyacrylamide	Bovine carotid artery endothelial cells	UV excimer laser ablation to open polyacrylamide coating, protein backfill	2005	[102]
Serum proteins from cell culture medium	PEO	HeLa	Photolithography and lift-off process/PEO	2004	[104]
Serum proteins from cell culture medium	Poly(AAm-co-EG) network	Murine NIH 3T3 fibroblasts, C2C12 myoblasts, rat aorta smooth muscle cells, and rat aortic endothelial cells	Stencilguided plasmainduced oxidation of proteinresistant polymer network	2003	[96]
Serum proteins from cell culture medium, collagen	PEG	Murine 3T3 fibroblasts, primary rat hepatocytes	Photopatterning of PEG-DA film containing a photoinitiator	2003	[106]
Fibronectin	BSA	Bovine adrenal capillary endothelial cells	Selective wetting of topographical features with BSA, protein backfill	2000	[171]

Serum proteins from cell culture medium, fibronectin, collagen	Native PS, pluronic F68, BSA	Pheochromocytoma (PC12) cells, Schwann (MSC80) cells	Plasma induced oxidation of PS guided by photoresist patterns	1998	[97]
Fibronectin	PEG-terminated alkanthiols	Bovine capillary endothelial cells, human microvascular endothelial cells	$\mu$ CP of alkanthiols on gold surface, protein backfill	1997, 1998	[99, 101]
Laminin	PEG-terminated alkanthiols	Primary rat hepatocytes	$\mu$ CP of alkanthiols on gold surface, protein backfill	1994	[100]
<i>Direct protein patterning</i>					
Laminin	Polyacrylamide-based hydrogel	Murine skeletal muscle cells, rat neonatal cardiomyocytes, primary myocytes	$\mu$ CP of protein on hydrogel background	2009	[111]
Poly-L-lysine/serum proteins from cell culture medium	PEO	Neuronal stem cells	$\mu$ CP of poly-L-lysine on PEO background	2008	[172]
Concanavalin A	Crosslinked star-PEG	Cricket terminal ganglia neurons	$\mu$ CP of protein on partly crosslinked star-PEG background	2008, 2007	[115, 117]
Fibronectin, collagen	PEG	HeLa, embryonic mouse fibroblasts, human epithelial cells	$\mu$ CP of proteins or PEG, photo- patterning through light-induced crosslinking of FN-benzophenone	2007	[89]

(continued)

Table 2 (continued)

Cell-adhesion-mediating compound	Cell-resistant compound	Cell types tested	Patterning technique	Year	Ref.
Fibronectin, collagen	Photoreactive PVA modified with phenylazido groups	Monkey kidney fibroblasts, murine macrophage-like cells, human liver carcinoma cells, mouse embryonic fibroblasts	$\mu$ CP of proteins onto hydrogel background and subsequent photoactivated immobilization	2005	[90]
Streptavidin conjugated to immobilized biotin	BSA, PEG	Red blood cells	$\mu$ CP of protein-linker with PEG backfill simultaneous coating of protein linker via $\mu$ FP	2003	[121]
Laminin	BSA	Primary rat cardiomyocytes	$\mu$ CP of protein onto BSA-coated PS or poly-urethane	2002, 2003	[113, 114]
First seeding: fibronectin, collagen Second seeding: serum proteins from cell culture medium	First seeding: serum depletion of culture medium Second seeding: contact-inhibition in cell cocultures	Coculture of rat hepatocytes and 3T3-J2 fibroblasts	$\mu$ FP of proteins	1998	[120]
Laminin	Contact-inhibition in cell cocultures, additional cell patterning with PEG-DA microwells	Coculture of primary rat hepatocytes and 3T3 fibroblasts	Contact-printing of protein	2004	[124]



**Table 3** Examples of microengineered surfaces for a spatially controlled cell attachment that use peptides as adhesion mediating component

Cell-adhesion-mediating compound	Repellent compound	Cell types tested	Patterning technique	Year	Ref.
<i>Indirect peptide patterning</i>					
GRGSP-PDMAA	PDMAA	Normal human skin fibroblasts	Covalent immobilization of protein resistant PDMAA monolayers to surface-bound photoreactive linkers by lithography through a mask, subsequent backfill and immobilization of peptide-PDMAA (or vice versa)	2008, 2009	[40, 135]
GRGDS	Methoxy-capped PEG	NIH-3T3 fibroblasts	Local modification of NHS-terminated PEG with 2-methoxyethylamine through a micropatterned photoresist (photolithography), backfill with peptide after resist removal	2008	[157]
RGDS	Poly( <i>N</i> -isopropylacrylamide) (PIPAAm)	NIH-3T3 fibroblasts	Electron beam activated polymerization of 2-carboxy- <i>N</i> -isopropylacrylamide through a mask on PIPAAm (or vice versa), subsequent NHS mediated binding of peptide to carboxyl functional groups	2007	[173]

(continued)

Table 3 (continued)

Cell-adhesion-mediating compound	Repellent compound	Cell types tested	Patterning technique	Year	Ref.
(RADS) <sub>2</sub> and <sub>3</sub> with alanine spacer	OEG	Human epidermoid carcinoma cells	μCP of ethylene glycol thiolate on gold, backfill with peptide (with cysteine anchor group)	1999	[156]
Cyclic RGDfK	PEG	Mouse osteoblasts and melanocytes, rat fibroblasts	Electron beam patterning of nanopatterned Au-nanodots on PEGmodified substrates, backfill with peptide (with lysine anchor group)	2004	[149]
<i>Direct peptide patterning</i> PS-binding peptides with RGD, RGE, and biotin end-group	BSA	HUVEC	Pin-microarrayer to print PS-binding peptides, BSA backfill	2009	[159]
RGDS	PEG-DA	HUVEC	Local polymerization of a peptide-PEG precursor solution to a PEG hydrogel by lithography through a mask	2009	[174]
RGDS-PEG	PEG-DA	Human dermal fibroblasts	Two-photon laser scanning photolithography to crosslink peptide-PEG inside a precrosslinked hydrogel to create 3D cell adhesion patterns	2008	[175]
GRGDS, GRGES, GREDVDY, GSVVYGLR	Carboxy-methyl-dextran	HUVEC, human foreskin fibroblasts	Noncontact printing of peptides onto activated hydrogel	2007	[161]

## 5 Conclusions and Outlook

Precise control of the interaction between an artificial surface and the biological environment is the key challenge for any successful interplay of the biological world with man-made technology. Live-cell biochips are increasingly attractive to both academia and industry due to a large number of potentially interesting applications, progressing from pharmaceutical sciences to biosensor development, and to biophysical model systems.

The demands that are posed on the surface coating are challenging. The coating must provide areas that are inert to cell adhesion in the neighborhood of regions that allow, promote, and sustain the adhesion of living cells, all this in the context of a complex, changing and insufficiently defined environment, such as found in modern cell culture. Derived from nature, proteins or even short peptide-ligands, micropatterned on the surface, are used to guide cell adhesion in a spatially resolved manner. Both strategies, protein- and peptide-mediated cell adhesion, offer distinct advantages in terms of a high biomimicry for cell–matrix adhesion (as for proteins) or a precise control over integrin–ligand interactions (as for peptides). Restriction of cell adhesion to defined spots demands equally challenging properties, especially with respect to the longevity of cell- and protein-repellence *in vitro*. Scientists have gathered a toolbox of different surface-coating strategies that allow the engineering of surfaces that resist nonspecific protein-adsorption and thus prevent non-desired protein-mediated cell adhesion. Examples include polymer brushes, surface-attached hydrogels, and hydrophilic, noncharged polymer monolayers.

Eventually, the optimal combination of cell-attractive and cell-repellent surface modification depends on the application and, although we have witnessed a number of very promising design strategies, successful integration into technological microdevices is still to come. With respect to the latter, persistency of the coating *in vitro*, the exact control of the cell–surface interaction, and the ability to induce and understand “normal” cell behavior on-chip, are of utmost importance and need to be covered by extensive (comparative) studies in the future.

## References

1. Goodsell DS (2004) *Bionanotechnology – lessons from nature*. Wiley, Hoboken, NJ
2. Staples M, Daniel K, Cima MJ, Langer R (2006) Application of micro- and nano-electromechanical devices to drug delivery. *Pharmaceut Res* 23:847–863
3. Santini JT, Cima MJ, Langer R (1999) A controlled-release microchip. *Nature* 397:335–338
4. Lee SJ, Lee SY (2004) Micro total analysis system ( $\mu$ -TAS) in biotechnology. *Appl Microbiol Biotechnol* 64:289–299
5. Willner I, Willner B (2001) Biomaterials integrated with electronic elements: en route to bioelectronics. *Trends Biotechnol* 19:222–230
6. Voldman J, Gray ML, Schmidt MA (1999) Microfabrication in biology and medicine. *Annu Rev Biomed Eng* 1:401–425
7. Brown PO, Botstein D (1999) Exploring the new world of the genome with DNA microarrays. *Nat Genet* 21:33–37

8. Panda S, Sato TK, Hampton GM (2003) An arrays of insights: application of DNA chip technology in the study of cell biology. *Trends Cell Biol* 13(3):151–156
9. Norde W, Baszkin A (2000) *Physical chemistry of biological interfaces*. Marcel Dekker, New York
10. Templin MF, Stoll D, Schwenk JM et al (2003) Protein microarrays: promising tools for proteomic research. *Proteomics* 3:2155–2166
11. Lodish H, Berk A, Zipursky SL, Matsudaira P, Baltimore D, Darnell J (2000) *Molecular cell biology*, 4th edn. Freeman, New York
12. Alberts B, Bray D, Lewis J et al (2002) *Molecular biology of the cell*, 4th edn. Taylor & Francis, New York
13. Hynes RO (2002) Integrins: bidirectional, allosteric signaling machines. *Cell* 110:673–687
14. van der Flier A, Sonnenberg A (2001) Function and interactions of integrins. *Cell Tissue Res* 305:285–298
15. Humphries MJ (1990) The molecular basis and specificity of integrin ligand interactions. *J Cell Sci* 97:585
16. Zamir E, Geiger B (2001) Molecular complexity and dynamics of cell-matrix adhesions. *J Cell Sci* 114:3583–3590
17. Geiger B, Bershadsky A (2001) Assembly and mechanosensory function of focal contacts. *Curr Opin Cell Biol* 13:584–592
18. Petit V, Thiery JP (2000) Focal adhesions: structure and dynamics. *Cell* 92:477–494
19. Pande G (2000) The role of membrane lipids in regulation of integrin functions. *Curr Opin Cell Biol* 12:569–574
20. Albeda SM, Buck CA (1990) Integrins and other cell adhesion molecules. *FASEB J* 4: 2868–2880
21. Travis J (1993) *Frontiers in biotechnology – biotech gets a grip on cell adhesion*. *Science* 260:906–908
22. Giancotti FG, Ruoslahti E (1999) Transduction – integrin signalling. *Science* 285:1028–1032
23. Giancotti FG (2000) Complexity and specificity of integrin signalling. *Nat Cell Biol* 2:E13–E14
24. Pierschbacher MD, Ruoslahti E (1984) Cell attachment activity of fibronectin can be duplicated by small synthetic fragments of the molecule. *Nature* 309(5963):30–33
25. Pierschbacher MD, Ruoslahti E (1984) Variants of the cell recognition site of fibronectin that retain attachment-promoting activity. *Proc Natl Acad Sci* 81:5985
26. Ruoslahti E, Pierschbacher MD (1987) New perspectives in cell-adhesion – RGD and integrins. *Science* 238:491–497
27. Ruoslahti E (1996) RGD and other recognition sequences for integrins. *Annu Rev Cell Dev Biol* 12:697–715
28. Wintermantel E, Ha SW (2003) *Medizintechnik mit biokompatiblen Werkstoffen und Verfahren*. Springer, Berlin
29. Hersel U, Kessler H (2003) RGD modified polymers: biomaterials for stimulated cell adhesion and beyond. *Biomaterials* 24:4385–4414
30. Yamada KM, Clark K (2002) Survival in three dimensions. *Science* 419:790–791
31. Andrade JD, Hlady V, Jeon SI (1996) Poly(ethylene oxide) and protein resistance – principles, problems, and possibilities. *Adv Chem Ser* 248:51–59
32. Horbett TA, Brash JL (1995) *Proteins at interfaces II: fundamentals and application*. *Adv Symp Ser* 602. American Chemical Society, Washington
33. Lanza RP, Langer R, Vacanti V (eds) (1997) *Principles of tissue engineering*, 2nd edn. Academic, San Diego
34. Ballauff M (2007) Spherical polyelectrolyte brushes. *Progr Polym Sci* 32:1135–1151
35. Römpp H, Falbe J, Regnitz M (1995) *Römpp Chemie Lexikon*. Thieme, Stuttgart
36. Frazier RA, Matthijs G, Davies MC et al (2000) Characterization of protein-resistant dextran monolayers. *Biomaterials* 21:957–966
37. Rabinow BE, Ding YS, Qin C et al (1994) Biomaterials with permanent hydrophilic surfaces and low-protein adsorption properties. *J Biomater Sci Polym Ed* 6:91–109

38. Lehmann T, Rühle J (1999) Polyethyloxazoline monolayers for polymer supported biomembrane models. *Macromol Symp* 142:1–12
39. Wörz A, Berchthold B, Kandler S et al (2007) Tailormade surfaces for a guided adhesion and outgrowth of cells. *MikroSystemTechnik Kongress 2007 Dresden*
40. Petersen S, Loschonsky S, Prucker O et al (2009) Cell micro-arrays from surface-attached peptide-polymer monolayers. *Physica Status Solidi A* 206(3):468–473
41. Siegers C, Biesalski M, Haag R (2004) Self-assembled monolayers of dendritic polyglycerol derivatives on gold that resist the adsorption of proteins. *Chem Eur J* 10:2831–2838
42. Harris JM, Zalipsky S (1987) *Poly(ethylene glycol): chemistry and biological applications*. American Chemical Society, Washington
43. Jenney CR, Anderson JM (1999) Effects of surface-coupled polyethylene oxide in human macrophage adhesion and foreign body giant cell formation in vitro. *J Biomed Mater Res* 44:206–216
44. Jeon SI, Lee JH, Andrade JD et al (1991) Protein surface interactions in the presence of poly(ethylene oxide). 1. Simplified theory. *J Colloids Interf Sci* 142:149–158
45. Jeon SI, Andrade JD (1991) Protein surface interactions in the presence of poly(ethylene oxide). 2. Effect of protein size. *J Colloids Interf Sci* 142:159–166
46. Yang ZH, Galloway JA, Yu HU (1999) Protein interactions with poly(ethylene glycol) self-assembled monolayers on glass substrates: diffusion and adsorption. *Langmuir* 15: 8405–8411
47. Prime KL, Whitesides GM (1993) Adsorption of proteins onto surfaces containing end-attached oligo (ethylene oxide) – A model system using self-assembled monolayers. *J Am Chem Soc* 115:10714–10721
48. Ostuni E, Chapman RG, Holmlin RE, Takayama S, Whitesides GM et al (2001) A survey of structure-property relationships of surfaces that resist the adsorption of proteins. *Langmuir* 17:5605–5620
49. Nagaoka S, Mori Y, Takiuchi H et al. (1984) In: Shalaby SH, Hoffman AS, Ratner BD, Horbett TA et al (eds) (1984) *Polymers as biomaterials*. Plenum, New York, pp 361–374
50. Harder P, Grunze M, Dahint R et al (1998) Molecular conformation in oligo (ethylene glycol)-terminated self-assembled monolayers on gold and silver surfaces determines their ability to resist protein adsorption. *J Phys Chem B* 102:426–436
51. Matsuura H, Fukuhara K (1985) Conformational-analysis of poly(oxyethylene) chain in aqueous-solution as a hydrophilic moiety of non-ionic surfactants. *J Mol Struct* 126: 251–260
52. Wang RCL, Kreuzer HJ, Grunze M (1997) Molecular conformation and solvation of oligo(ethylen glycol)-terminated self-assembled monolayers and their resistance to protein adsorption. *J Phys Chem* 101:9767–9773
53. Chapman RG, Ostuni E, Takayama S et al (2000) Surveying for surfaces that resist the adsorption of proteins. *J Am Chem Soc* 122:8303–8304
54. Luk Y-Y, Kato M, Mrksich M (2000) Self-assembled monolayers of alkanethiolates presenting mannitol groups are inert to protein adsorption and cell attachment. *Langmuir* 16:9604–9608
55. Chapman RG, Ostuni E, Liang ME et al (2001) Polymeric thin films that resist the adsorption of proteins and the adhesion of bacteria. *Langmuir* 17:1225–1233
56. Advincula RC, Brittain WJ, Caster KC, Rühle J (eds) (2004) *Polymer brushes: synthesis, characterization and applications*. Wiley, UK
57. Barbey R, Lavanant L, Paripovic D et al (2009) Polymer brushes via surface-initiated controlled radical polymerization: synthesis, characterization, properties, and applications. *Chem Rev* 109:5437–5527
58. Szeleifer I, Carignano MA (2000) Tethered polymer layers: phase transitions and reduction of protein adsorption. *Rapid Commun* 21:423–448
59. Fristrup CJ, Jankova K, Hvilsted S (2009) Surface-initiated radical polymerization – a technique to develop biofunctional coatings. *Soft Matter* 23:4623–4634
60. Peppas NA, Huang Y, Torres-Lugo M et al (2000) Physicochemical foundations and structural design of hydrogels in medicine and biology. *Annu Rev Biomed Eng* 2:9–29

61. Park JH, Bae YH (2002) Hydrogels based on poly(ethylene oxide) and poly(tetramethylene oxide) or poly(dimethylsiloxane): synthesis, characterization, in vitro protein adsorption and platelet adhesion. *Biomaterials* 23:1797–1808
62. Haynes CA, Norde W (1995) Structures and stabilities of adsorbed protein of colloid and interface. *Science* 169(2):313–328
63. Giacomelli CE, Norde W (2001) The adsorption-desorption cycle. Reversibility of the BSA-silica system. *J Colloids Interf Sci* 233(2):234–240
64. Norde W, Giacomelli CE (1999) Conformational changes in proteins at interfaces: from solution to the interface, and back. *Macromol Symp* 145:125–136
65. Norde W, Giacomelli CE (2000) BSA structural changes during homomolecular exchange between the adsorbed and the dissolved states. *J Biotechnol* 79(3):259–268
66. Steele JG, Dalton BA, Johnson G et al (1993) Polystyrene chemistry affects vitronectin activity – an explanation for cell attachment to tissue-culture polystyrene but not to unmodified polystyrene. *J Biomed Mater Res* 27(7):927–940
67. Lewandowska K, Balachander N, Sukenik CN et al (1989) Modulation of fibronectin adhesive functions for fibroblasts and neural cells by chemically derivatized substrata. *J Cell Physiol* 141(2):334–345
68. Grinnell F, Feld MK (1981) Adsorption characteristics of plasma fibronectin in relationship to biological-activity. *J Biomed Mater Res* 15:363–381
69. Liu LY, Chen SF, Giachelli CM et al (2005) Controlling osteopontin orientation on surfaces to modulate endothelial cell adhesion. *J Biomed Mater Res A* 74A(1):23–31
70. Taubenberger A, Woodruff MA, Bai H F et al (2010) The effect of unlocking RGD-motifs in collagen I on pre-osteoblast adhesion and differentiation. *Biomaterials* 31:2827–2835
71. Egles C, Shamis Y, Mauney JR et al (2008) Denatured collagen modulates the phenotype of normal and wounded human skin equivalents. *J Invest Dermatol* 128:1830–1837
72. Sivaraman B, Latour RA (2010) The adherence of platelets to adsorbed albumin by receptor-mediated recognition of binding sites exposed by adsorption-induced unfolding. *Biomaterials* 31:1036–1044
73. Horbett TA (2003) Biological activity of adsorbed proteins. In: Malmsten M (ed) *Biopolymers at interfaces*, 2nd edn. Marcel Dekker, New York
74. Horbett TA (1994) The role of adsorbed proteins in animal-cell adhesion. *Colloids Surf B Biointerf* 2(1–3):225–240
75. Fabriziushoman DJ, Cooper SL (1991) Competitive adsorption of vitronectin with albumin, fibrinogen, and fibronectin on polymeric biomaterials. *J Biomed Mater Res* 25(8):953–971
76. Horbett TA (1996) Proteins: structure, properties, and adsorption to surfaces. In: Ratner BD, Hoffman AS, Schoen FJ, Lemons JE et al (eds) *Biomaterials science*. Academic, San Diego
77. Slack SM, Horbett TA (1988) Physicochemical and biochemical aspects of fibrinogen adsorption from plasma and binary protein solutions onto polyethylene and glass. *J Colloids Interf Sci* 124(2):535–551
78. Bale MD, Wohlfahrt LA, Mosher DF et al (1989) Identification of vitronectin as a major plasma-protein adsorbed on polymer surfaces of different copolymer composition. *Blood* 74(8):2698–2706
79. Green RJ, Davies MC, Roberts CJ et al (1999) Competitive protein adsorption as observed by surface plasmon resonance. *Biomaterials* 20(4):385–391
80. Vroman L, Adams AL (1986) Adsorption of proteins out of plasma and solutions in narrow spaces. *J Colloids Interf Sci* 111(2):391–402
81. Wertz CF, Santore MM (1999) Adsorption and relaxation kinetics of albumin and fibrinogen on hydrophobic surfaces: single-species and competitive behavior. *Langmuir* 15(26):8884–8894
82. Slack SM, Horbett TA (1995) The Vroman effect – a critical review. *Proteins Interf Ii* 602:112–128
83. Jung SY, Lim SM, Albertorio F et al (2003) The Vroman effect: a molecular level description of fibrinogen displacement. *J Am Chem Soc* 125(42):12782–12786
84. Krishnan A, Siedlecki CA, Vogler EA (2004) Mixology of protein solutions and the Vroman effect. *Langmuir* 20(12):5071–5078

85. Brown LF, Dubin D, Lavigne L et al (1993) Macrophages and fibroblasts express embryonic fibronectins during cutaneous wound-healing. *Am J Pathol* 142(3):793–801
86. Werb Z (1997) ECM and cell surface proteolysis: regulating cellular ecology. *Cell* 91(4):439–442
87. Grinnell F (1986) Focal adhesion sites and the removal of substratum-bound fibronectin. *J Cell Biol* 103(6):2697–2706
88. Nelson CM, Raghavan S, Tan JL et al (2003) Degradation of micropatterned surfaces by cell-dependent and -independent processes. *Langmuir* 19(5):1493–1499
89. Fink J, Thery M, Azioune A et al (2007) Comparative study and improvement of current cell micro-patterning techniques. *Lab on a Chip* 7(6):672–680
90. Ito Y, Nogawa M, Taheda M et al (2005) Photo-reactive polyvinylalcohol for photo-immobilized microarray. *Biomaterials* 26(2):211–216
91. Wilson CJ, Clegg RE, Leawesley DI et al (2005) Mediation of biomaterial-cell interactions by adsorbed proteins: a review. *Tissue Eng* 11(1–2):1–18
92. Ostuni E, Kane R, Chen CS et al (2000) Patterning mammalian cells using elastomeric membranes. *Langmuir* 16(20):7811–7819
93. Frimat J-P, Menne H, Michels A et al (2009) Plasma stencilling methods for cell patterning. *Anal Bioanal Chem* 395(3):601–609
94. Underwood PA, Steele JG, Dalton BA (1993) Effects of polystyrene surface-chemistry on the biological-activity of solid-phase fibronectin and vitronectin, analyzed with monoclonal-antibodies. *J Cell Sci* 104:793–803
95. Curtis ASG (1984) The competitive effects of serum-proteins on cell-adhesion. *J Cell Sci* 71:17–35
96. Tourovskaia A, Barber T, Wickes BT et al (2003) Micropatterns of chemisorbed cell adhesion-repellent films using oxygen plasma etching and elastomeric masks. *Langmuir* 19(11):4754–4764
97. Detrait E, Lhoest JB, Knoops B et al (1998) Orientation of cell adhesion and growth on patterned heterogeneous polystyrene surface. *J Neurosci Methods* 84(1–2):193–204
98. Peterbauer T, Heitz J, Olbrich M et al (2006) Simple and versatile methods for the fabrication of arrays of live mammalian cells. *Lab on a Chip* 6(7):857–863
99. Chen CS, Mrksich M, Huang S et al (1998) Micropatterned surfaces for control of cell shape, position, and function. *Biotechnol Prog* 14(3):356–363
100. Singhvi R, Kumar A, Lopez GP et al (1994) Engineering cell-shape and function. *Science* 264(5159):696–698
101. Mrksich M, Dike LE, Tien J et al (1997) Using microcontact printing to pattern the attachment of mammalian cells to self-assembled monolayers of alkanethiolates on transparent films of gold and silver. *Exp Cell Res* 235(2):305–313
102. Iwanaga S, Akiyama Y, Kikuchi A et al (2005) Fabrication of a cell array on ultrathin hydrophilic polymer gels utilizing electron beam irradiation and UV excimer laser ablation. *Biomaterials* 26(26):5395–5404
103. Pesen D, Heinz WF, Werbin JL et al (2007) Electron beam patterning of fibronectin nanodots that support focal adhesion formation. *Soft Matter* 3:1280–1284
104. Bouaidat S, Berendsen C, Thomsen P et al (2004) Micro patterning of cell and protein non-adhesive plasma polymerized coatings for biochip applications. *Lab on a Chip* 4(6):632–637
105. Chang WC, Sretavan DW (2008) Novel high-resolution micropatterning for neuron culture using polylysine adsorption on a cell repellent, plasma-polymerized background. *Langmuir* 24(22):13048–13057
106. Revzin A, Tompkins RG, Toner M (2003) Surface engineering with poly(ethylene glycol) photolithography to create high-density cell arrays on glass. *Langmuir* 19(23):9855–9862
107. Berchtold B (2005) Oberflächengebundene Polymernetzwerke zur Re-Endothelialisierung von porcinen Herzklappenbioprothesen. Department of Microsystems Engineering, Albert-Ludwigs-Universität, Freiburg, Germany
108. Prucker O, Naumann CA, Ruhe J et al (1999) Photochemical attachment of polymer films to solid surfaces via monolayers of benzophenone derivatives. *J Am Chem Soc* 121(38):8766–8770

109. Worz A, Berchtold B, Kandler S (2007) Tailor-made surfaces for the guidance of neuronal cells. *Tissue Eng* 13:908–909
110. Chien HW, Chang ZY, Tsai WB (2009) Spatial control of cellular adhesion using photo-crosslinked micropatterned polyelectrolyte multilayer films. *Biomaterials* 30(12):2209–2218
111. Cimetta E, Pizzato S, Bollini S et al (2009) Production of arrays of cardiac and skeletal muscle myofibers by micropatterning techniques on a soft substrate. *Biomed Microdevices* 11(2):389–400
112. Ruiz A, Valsesia A, Bretagnol F et al (2007) Large-area protein nano-arrays patterned by soft lithography. *Nanotechnology* 18:1–6
113. McDevitt TC, Angello JC, Whitney ML et al (2002) In vitro generation of differentiated cardiac myofibers on micropatterned laminin surfaces. *J Biomed Mater Res* 60(3):472–479
114. McDevitt TC, Woodhouse KA, Hauschka SD et al (2003) Spatially organized layers of cardiomyocytes on biodegradable polyurethane films for myocardial repair. *J Biomed Mater Res A* 66A(3):586–595
115. Gasteier P, Reska A, Schulte P et al (2007) Surface grafting of PEO-based star-shaped molecules for bioanalytical and biomedical applications. *Macromol Biosci* 7:1010–1023
116. Ahmed WW, Wolfram T, Goldyn AM et al (2010) Myoblast morphology and organization on biochemically micro-patterned hydrogel coatings under cyclic mechanical strain. *Biomaterials* 31:250–258
117. Reska A, Gasteier P, Schulte P et al (2008) Ultrathin coatings with change in reactivity over time enable functional in vitro networks of insect neurons. *Adv Mater* 20:2751–2755
118. Folch A, Toner M (2000) Microengineering of cellular interactions. *Annu Rev Biomed Eng* 2:227–256
119. Delamarche E, Bernard A, Schmid H et al (1997) Patterned delivery of immunoglobulins to surfaces using microfluidic networks. *Science* 276(5313):779–781
120. Folch A, Toner M (1998) Cellular micropatterns on biocompatible materials. *Biotechnol Prog* 14(3):388–392
121. Cuvelier D, Rossier O, Bassereau P et al (2003) Micropatterned “adherent/repellent” glass surfaces for studying the spreading kinetics of individual red blood cells onto protein-decorated substrates. *Eur Biophys J Biophys Lett* 32(4):342–354
122. Zhu H, Snyder M (2003) Protein chip technology. *Curr Opin Chem Biol* 7(1):55–63
123. MacBeath G, Schreiber SL (2000) Printing proteins as microarrays for high-throughput function determination. *Science* 289(5485):1760–1763
124. Revzin A, Rajagopalan P, Tilles AW et al (2004) Designing a hepatocellular microenvironment with protein microarraying and poly(ethylene glycol) photolithography. *Langmuir* 20(8):2999–3005
125. Katz BZ, Zamir E, Bershadsky A et al (2000) Physical state of the extracellular matrix regulates the structure and molecular composition of cell-matrix adhesions. *Mol Biol Cell* 11(3):1047–1060
126. Pelham RJ, Wang YL (1998) Cell locomotion and focal adhesions are regulated by the mechanical properties of the substrate. *Biol Bull* 194(3):348–349
127. Choquet D, Felsenfeld P, Sheetz MP (1997) Extracellular matrix rigidity causes strengthening of integrin-cytoskeleton linkages. *Cell* 88(1):39–48
128. Castel S, Pagan R, Mitjans F et al (2001) RGD peptides and monoclonal antibodies, antagonists of  $\alpha(v)$ -integrin, enter the cells by independent endocytic pathways. *Lab Invest* 81(12):1615–1626
129. Zamir E, Geiger B (2001) Molecular complexity and dynamics of cell-matrix adhesions. *J Cell Sci* 114(20):3583–3590
130. Memmo LM, McKeown-Longo P (1998) The  $\alpha v \beta 5$  integrin functions as an endocytic receptor for vitronectin. *J Cell Sci* 111:425–433
131. Gaebel K, Feuerstein IA (1991) Platelets process adsorbed protein – a morphological-study. *Biomaterials* 12(6):597–602
132. Tirrell M, Kikkoli E, Biesalski M (2002) The role of surface science in bioengineered materials. *Surf Sci* 500(1–3):61–83



133. Biesalski M, Tu R, Tirrell M (2005) Polymerized vesicles carrying molecular recognition sites. *Langmuir* 21:5663–5666
134. Biesalski M, Knaebel A, Tu R et al (2006) Cell adhesion on a polymerized peptide-amphiphile monolayer. *Biomaterials* 27(8):1259–1269
135. Loschonsky S, Shroff K, Wörz A et al (2008) Surface-attached PDMAA-GRGDSP hybrid polymer monolayers that promote the adhesion of living cells. *Biomacromolecules* 9: 543–552
136. Zhu J, Tang C, Kottke-Marchant K et al (2009) Design and synthesis of biomimetic hydrogel scaffolds with controlled organization of cyclic RGD peptides. *Bioconjug Chem* 20(2):333–339
137. Pakalns T, Haverstick KL, Fields GB et al (1999) Cellular recognition of synthetic peptide amphiphiles in self-assembled monolayer films. *Biomaterials* 20(23–24):2265–2279
138. Hirano Y, Okuno M, Hayashi T et al (1993) Cell-attachment activities of surface immobilized oligopeptides RGD, RGDS, RGDV, RGDT, and YIGSRIGrs toward five cell-lines. *J Biomater Sci Polym Ed* 4(3):235–243
139. Mardilovich A, Craig JA, McCammon MQ et al (2006) Design of a novel fibronectin-mimetic peptide-amphiphile for functionalized biomaterials. *Langmuir* 22(7):3259–3264
140. Li FY, Redick SD, Erickson HP et al (2003) Force measurements of the alpha(5)beta(1) integrin-fibronectin interaction. *Biophys J* 84(2):1252–1262
141. Eisenberg JL, Piper JL, Mrksich M (2009) Using self-assembled monolayers to model cell adhesion to the 9th and 10th type III domains of fibronectin. *Langmuir* 25(24):13942–13951
142. Craig WS, Cheng S, Mullen DG et al (1995) Concept and progress in the development of RGD-containing peptide pharmaceuticals. *Biopolymer* 37(2):157–175
143. Beer JH, Springer KT, Collier BS (1992) Immobilized Arg-Gly-Asp (RGD) peptides of varying lengths as structural probes of the platelet glycoprotein-IIb/IIIa receptor. *Blood* 79(1):117–128
144. Kantlehner M, Schaffner P, Finsinger D et al (2000) Surface coating with cyclic RGD peptides stimulates osteoblast adhesion and proliferation as well as bone formation. *Chembiochem* 1(2):107–114
145. Massia SP, Hubbell JA (1991) An RGD spacing of 440 nm is sufficient for integrin alpha-V-beta-3-mediated fibroblast spreading and 140 nm for focal contact and stress fiber formation. *J Cell Biol* 114(5):1089–1100
146. Maheshwari G, Brown G, Lauffenburger DA et al (2000) Cell adhesion and motility depend on nanoscale RGD clustering. *J Cell Sci* 113(10):1677–1686
147. Arnold M, Schwieder M, Blummel J et al (2009) Cell interactions with hierarchically structured nano-patterned adhesive surfaces. *Soft Matter* 5(1):72–77
148. Wolfram T, Spatz JP, Burgess RW (2008) Cell adhesion to agrin presented as a nanopatterned substrate is consistent with an interaction with the extracellular matrix and not transmembrane adhesion molecules. *BMC Cell Biol* 9:64
149. Arnold M, Cavalcanti-Adam EA, Glass R et al (2004) Activation of integrin function by nanopatterned adhesive interfaces. *Chemphyschem* 5:383–388
150. Ruoslahti E (1996) RGD and other recognition sequences for integrins. *Annu Rev Cell Dev Biol* 12:697–715
151. Kato R, Kaga C, Kunimatsu M et al (2006) Peptide array-based interaction assay of solid-bound peptides and anchorage-dependant cells and its effectiveness in cell-adhesive peptide design. *J Biosci Bioeng* 101(6):485–495
152. Gobin AS, West JL (2003) Val-ala-pro-gly, an elastin-derived non-integrin ligand: smooth muscle cell adhesion and specificity. *J Biomed Mat Res A* 67A(1):255–259
153. Hubbell JA, Massia SP, Desai NP et al (1991) Endothelial cell-selective materials for tissue engineering in the vascular graft via a new receptor. *Biotechnology* 9(6):568–572
154. Plouffe BD, Njoka DN, Harris J et al (2007) Peptide-mediated selective adhesion of smooth muscle and endothelial cells in microfluidic shear flow. *Langmuir* 23(9):5050–5055
155. Plouffe BD, Radisic M, Murthy SK (2008) Microfluidic depletion of endothelial cells, smooth muscle cells, and fibroblasts from heterogeneous suspensions. *Lab on a Chip* 8(3):462–472

156. Zhang SG, Yan L, Altman M et al (1999) Biological surface engineering: a simple system for cell pattern formation. *Biomaterials* 20(13):1213–1220
157. Takahashi H, Emoto K, Dubey M et al (2008) Imaging surface immobilization chemistry: correlation with cell patterning on non-adhesive hydrogel thin films. *Adv Funct Mater* 18(14):2079–2088
158. Dubey M, Emoto K, Cheng F et al (2009) Surface analysis of photolithographic patterns using ToF-SIMS and PCA. *Surf and Interface Anal* 41:645–652
159. Meyers SR, Khoo XJ, Huang X et al (2009) The development of peptide-based interfacial biomaterials for generating biological functionality on the surface of bioinert materials. *Biomaterials* 30(3):277–286
160. Gauvreau V, Laroche G (2005) Micropattern printing of adhesion, spreading, and migration peptides on poly(tetrafluoroethylene) films to promote endothelialization. *Bioconj Chem* 16(5):1088–1097
161. Monchaux E, Vermette P (2007) Bioactive microarrays immobilized on low-fouling surfaces to study specific endothelial cell adhesion. *Biomacromolecules* 8:3668–3673
162. Buxboim A, Ivanovska IL, Discher D (2010) Matrix elasticity, cytoskeletal forces and physics of the nucleus: how deeply do cells ‘feel’ outside and in? *J Cell Sci* 123:297–308
163. Montagne K, Komori K, Yang F et al (2009) A micropatterned cell array with an integrated oxygen-sensitive fluorescent membrane. *Photochem Photobiol Sci* 8(11):1529–1533
164. Komori K, Nada J, Nishikawa M et al (2009) Simultaneous evaluation of toxicities using a mammalian cell array chip prepared by photocatalytic lithography. *Anal Chim Acta* 653(2):222–227
165. Kikuchi K, Sumaru K, Edahiro JI et al (2009) Stepwise assembly of micropatterned cocultures using photoresponsive culture surfaces and its application to hepatic tissue arrays. *Biotechnol Bioeng* 103(3):552–561
166. Khetani SR, Bhatia SN (2008) Microscale culture of human liver cells for drug development. *Nat Biotechnol* 26(1):120–126
167. Wang L, Zhu J, Deng C et al (2008) An automatic and quantitative on-chip cell migration assay using self-assembled monolayers combined with real-time cellular impedance sensing. *Lab on a Chip* 8(6):872–878
168. Ochsner M, Dusseiller MR, Grandin HM et al (2007) Micro-well arrays for 3D shape control and high resolution analysis of single cells. *Lab on a Chip* 7(8):1074–1077
169. Shim HW, Lee JH, Hwang TS et al (2007) Patterning of proteins and cells on functionalized surfaces prepared by polyelectrolyte multilayers and micromolding in capillaries. *Biosens Bioelectron* 22(12):3188–3195
170. Rosenthal A, Macdonald A, Voldman J (2007) Cell patterning chip for controlling the stem cell microenvironment. *Biomaterials* 28(21):3208–3216
171. Ostuni E, chen CS, Ingber DE et al (2001) Selective deposition of proteins and cells in arrays of microwells. *Langmuir* 17(9):2828–2834
172. Ruiz A, Buzanska L, Gilliland D et al (2008) Micro-stamped surfaces for the patterned growth of neural stem cells. *Biomaterials* 29(36):4766–4774
173. Hatakeyama H, Kikuchi A, Yamato M et al (2007) Patterned biofunctional designs of thermally responsive surfaces for spatiotemporally controlled cell adhesion, growth, and thermally induced detachment. *Biomaterials* 28(25):3632–3643
174. Moon JJ, Hahn MS, Kim I et al (2009) Micropatterning of poly(ethylene glycol) diacrylate hydrogels with biomolecules to regulate and guide endothelial morphogenesis. *Tissue Eng Part A* 15(3):579–585
175. Lee SH, Moon JJ, West JL (2008) Three-dimensional micropatterning of bioactive hydrogels via two-photon laser scanning photolithography for guided 3D cell migration. *Biomaterials* 29(20):2962–2968

# Interfacing Cell Surface Receptors to Hybrid Nanopatterned Surfaces: A Molecular Approach for Dissecting the Adhesion Machinery

**Julien Polleux**

**Abstract** Over the last 20 years, integrins have proven to be key players in connecting the internal cell machinery to the extracellular environment. Because the properties of the extracellular milieu strongly influence developmental programs triggered by integrin-mediated adhesion, the development of culture platforms with tunable chemical and physical properties is important for further understanding of the complexity of integrin functions. This chapter introduces biochemically modified gold surface models that have been designed to investigate cell adhesion. Specific emphasis is placed on micellar nanolithography, a technique enabling the preparation of gold nanopatterns. Such substrates are used as an analytical tool to control the activation of single-cell surface receptors for the study of integrin-mediated adhesion and signalling in a quantitative manner.

**Keywords** Biofunctionalisation · Cell adhesion · Extracellular matrix · Gold nanopatterns · Integrins

## Contents

1	General Principles of Integrin-Mediated Cell–Matrix Interactions.....	80
2	Toward the Emergence of Surface Models After a Century of Tissue Culture .....	82

---

J. Polleux (✉)

Max Planck Institute of Metals Research, Department of New Materials and Biosystems,  
Heisenbergstraße 3, 70569 Stuttgart, Germany  
and

Max Planck Institute of Biochemistry, Department of Molecular Medicine, Am Klopferspitz 18,  
82152 Martinsried, Germany

e-mail: [polleux@mf.mpg.de](mailto:polleux@mf.mpg.de); [www.mf.mpg.de/spatz/polleux](http://www.mf.mpg.de/spatz/polleux)

3	At All Length Scales, Gold Remains “The Standard” for Studying Cell Adhesion .....	83
3.1	Self-Assembled Monolayers on Gold Thin Film: A Surface Model for Protein Adsorption and Immobilisation .....	83
3.2	Micro patterning: A Revolution for Cell-Adhesion-Based Assays .....	85
3.3	Nanogold: An “All-in-One” Model System .....	86
4	Micellar Nanolithography: A Versatile Technique for Designing Nanopatterned Surfaces .....	88
5	Biofunctionalised Gold Nanopatterns: A Quantitative Tool for Dissecting the Adhesion Machinery of Cells .....	90
5.1	Nanopatterning Biocues .....	90
5.2	Integrin Nanoclustering Mediates Cell Adhesion and Signalling .....	91
5.3	Micro-nanopatterned Surfaces: A Deeper Structural Insight into Integrin-Mediated Adhesion .....	93
5.4	Nanoscale Gradient-Induced Cell Polarisation and Migration .....	95
6	Outlook: Towards More ECM-Mimetic Systems and Cell Manipulation .....	97
6.1	Designing Extracellular Environments with Nanostructured Soft Interfaces .....	97
6.2	Thermoplasmonic Nanoarray for Manipulating Cell Adhesion .....	98
	References .....	100

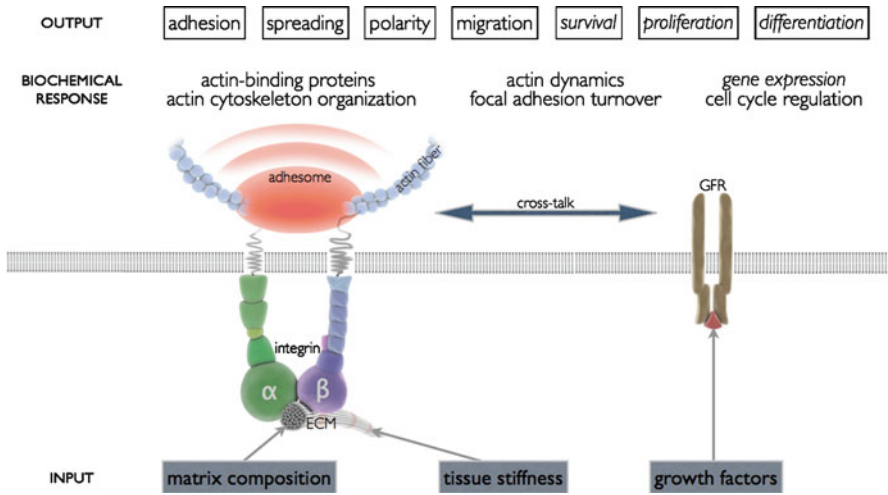
## 1 General Principles of Integrin-Mediated Cell–Matrix Interactions

The cell, as the smallest structural and functional unit of all living organisms, is a fascinating system in view of its highly complex and hierarchical machinery.

Cells build their own microenvironment by secreting and organising matrix proteins into a supramolecular assembly, termed the extracellular matrix (ECM). By shaping the molecular composition of ECM, cells tailor its properties through the exposure of adhesion sites, the establishment of a structural mesh with a defined elasticity, and the presentation of growth factors. Through a complex set of physical and chemical interactions between the cells and the matrix, cells guide the generation of tissues and organs exhibiting specific architectures and functions.

Over the last 20 years, integrins have proven to be key players in mediating cell–ECM interactions and thereby directing tissue morphogenesis. Integrins are cell surface receptors that physically connect the internal cell machinery to the extracellular environment. Integrins not only function as cell anchorage points, but also manipulate and respond to a functional ECM. In doing so, these proteins regulate cell migration, survival, cell cycle progression and differentiation pathways (Fig. 1) [1].

The integrin family in mammalian cells consists of 18  $\alpha$ - and eight  $\beta$ -subunits, which associate into 24 distinct heterodimeric receptors with distinct ligand-binding and signalling specificities. The heterodimers are characterised by a molecular mass of 210–290 kDa, a length of approximately 28 nm, and a lateral diameter between 8 and 12 nm [2]. As displayed in Fig. 1, integrin heterodimers are composed of an extracellular domain consisting of a ligand-binding head domain standing on two long legs, a transmembrane domain, and short cytoplasmic tails forming a flexible V-shaped structure (Fig. 1).



**Fig. 1** Downstream effects of integrin activation during outside-in signalling. The ECM properties and the growth factor environment regulate assembly of the ECM–integrin–adhesome–F-actin system, which controls cell activity. The long-term effects of the outside-in signalling (10–60 min) are indicated in *italics*

Integrins can be classified according to their extracellular ligands, which are partly overlapping among distinct heterodimers [3–5]. For instance, arginine-glycine-aspartate (RGD)-containing proteins, such as fibronectin, fibrinogen, vitronectin, von Willenbrand factor and many other glycoproteins, exhibit a high binding affinity for eight of the 24 integrins [4–6]. The specific binding of RGD motifs by integrins involves salt-bridge formation to the aspartic acid residue (D) and hydrogen bonding with the arginine residue (R) [7].

To bind their extracellular ligands, integrins undergo a conformational change triggered by non-integrin signals. This leads to the recruitment of cytoplasmic proteins such as talin to the cytoplasmic tail of the β-subunits, resulting in the exposure of the ligand-binding head domain [8]. Upon binding to the ECM, integrins subsequently cluster to increase their binding avidity, giving rise to unstable structures called nascent adhesions [9]. Nascent adhesions recruit additional cytoplasmic adaptor proteins and develop into dot-like focal complexes, which eventually mature into larger focal adhesions (FAs). FAs function as signalling platforms that are directly connected to the actin cytoskeleton. A subset of FAs can also elongate into specific matrix assembly sites, termed fibrillar adhesions [10].

Integrins are able to relay both chemical and physical stimuli from the external milieu into the intracellular space and translate this stimulus into biochemical signals [11]. On the one hand, the molecular composition of the ECM determines the set of integrin heterodimers engaged, leading to specific signalling outputs. On the other hand, integrins, through their ability to directly couple to the actin cytoskeleton, sense the physical properties of the matrix, such as elasticity, and respond with specific signals through a process referred to as mechanotransduction [12].

However, unlike other cell surface receptors, integrin tails lack intrinsic catalytic activity. Instead, the tails of integrins recruit a plethora of signalling and adaptor molecules that assemble into FAs to relay intracellular signals, and to engage and remodel the actin cytoskeleton. To date, more than 150 proteins have been identified as being recruited to integrin adhesions and to constitute the “adhesome” [13–15].

A large proportion of the intracellular signals propagated by integrins occur in co-operation with growth factor receptor (GFR) signalling. The cross-talk between integrins and GFRs, which occurs both on the extracellular and intracellular level, results in a cooperative stimulation or suppression of multiple signal transduction pathways regulating fundamental cellular activities such as spreading, motility, differentiation and survival [16, 17] (Fig. 1).

The dynamic connection between integrins and the actin cytoskeleton is a central aspect of integrin signalling. The engagement and remodelling of the actin cytoskeleton upon integrin adhesion orchestrate the regulation of the 3D architecture of the cell as well as cell migration. In a migrating cell, actin polymerisation takes place at the periphery of the cell in a structure called the lamellipodium, generating mechanical forces that push the membrane forward. Simultaneously, the actin network moves backward and undergoes a retrograde flow. Fibrillar (F-) actin couples to integrins, allowing force transmission in respect to the substrate and facilitating forward movement of the cell body as well as maturation of FAs. This structure is called the lamella. Disassembly of adhesion sites at the cell rear then allows net forward movement of the cell [15, 18, 19].

It is important to note that our understanding of events related to cell adhesion and migration is mainly based on observations made on 2D substrates *in vitro*. However, cell adhesion occurring *in vivo* and in 3D matrices was shown to be profoundly different from 2D adhesion [20]. When cells are plated on rigid substrates like polystyrene dishes, cell adhesion is stronger and leads to the formation of larger FAs and thicker stress fibres in comparison to 3D matrices. Interestingly, the rigidity of the extracellular milieu was shown to strongly influence developmental programs triggered by integrin-mediated adhesion [12, 20–23], implying that it is crucial to develop culture platforms with tunable chemical and physical properties. This requires a multidisciplinary approach to merge knowledge and skills from materials to biological sciences.

## **2 Toward the Emergence of Surface Models After a Century of Tissue Culture**

In 1907, Ross Granville Harrison introduced tissue culture as a new technique for the study of nerve fibre outgrowth [24]. At that time, it was hardly envisioned that cell culture would become the most widespread research tool in life sciences and an important method for preparing antibodies, vaccines and drugs. During the development of tissue culture, parameters such as sterility, temperature, gas mixture, medium composition and substrate features were found to be critical for

optimal culture conditions. Today, cell culture methods are widely based on the use of serum-supplemented culture medium and on cultivating cell cultures at 37°C in a humidified atmosphere containing 5% CO<sub>2</sub>. For several decades, cells were typically seeded onto sterile, heat-resistant Pyrex glass, despite its poor efficacy for cell growth. In 1956, George Gey overcame this limitation and reported the use of rat-tail collagen for coating glass substrates, serving to mimic an in vivo environment [25]. This method is still used today.

Following this trend in optimisation, cell culture opened a great opportunity for chemists and materials scientists to design substrates that would efficiently support cell adhesion and growth. On the one hand, industry began with various shapes of glassware, to finally manufacture a large number of polystyrene-based consumables. On the other hand, academic scientists have developed various types of biocompatible substrate models to systematically study how the composition of surfaces influences the behaviour of cells in vitro. However, tissue-engineering research has not reached its full potential in providing deeper insights into the biology of cellular interactions. A particular challenge is the molecular understanding of the cellular machinery that orchestrates tissue regeneration in vivo. Therefore, further development of tissue culture is essential in order to provide more tools for dissecting the functions of the extracellular environment by integrating knowledge from chemistry, physics and biology.

The next sections of this chapter introduce biochemically modified surface models that have been designed to study integrin-mediated adhesion and signalling. Specific emphasis will be placed on micellar nanolithography, a technique enabling controlled activation of single-cell surface receptors such as integrins, for the study of adhesion-mediated signalling.

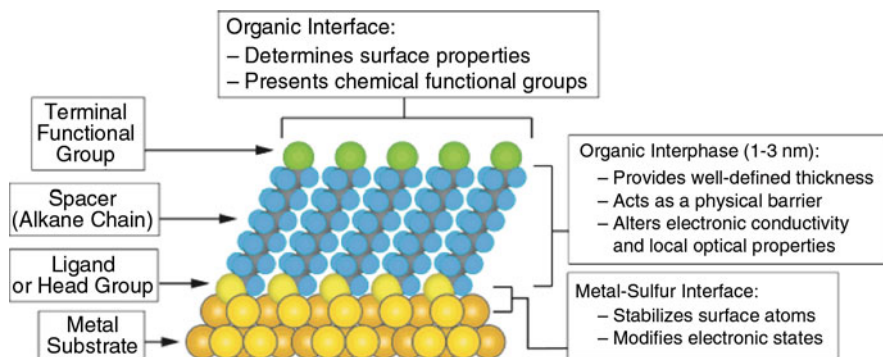
### **3 At All Length Scales, Gold Remains “The Standard” for Studying Cell Adhesion**

#### ***3.1 Self-Assembled Monolayers on Gold Thin Film: A Surface Model for Protein Adsorption and Immobilisation***

Bare surfaces of metals and metal oxides tend to spontaneously adsorb organic molecules by lowering the free energy of the interface. This changes the surface properties of the final system. However, the adsorption of organics and the presentation of specific chemical groups are inhomogeneous, resulting in irreproducible physical properties of the interface between the host surface and its environment.

Self-assembled monolayers (SAMs) provide a versatile system for control of the interfacial properties of inorganic compounds. SAMs result from the spontaneous adsorption and assembly of molecular compounds into crystalline structures. Commonly used molecules consist of a head group with a specific affinity for a particular material, and a terminal group containing a chemical function that becomes exposed





**Fig. 2** An ideal, single crystalline self-assembled monolayer (SAM) of alkanethiolates supported on a gold surface with a (111) texture. The anatomy and characteristics of the SAM are indicated. From Love et al. [26], Copyright © 2005 American Chemical Society

at the interface (Fig. 2). SAMs derived from the adsorption of thiolates to gold is one of the most studied systems in surface chemistry. There are several reasons for this: (1) gold-based materials are easy to prepare, (2) gold is inert and non-toxic, (3) gold binds thiols with high affinity, (4) gold allows the formation of highly organised and stable SAMs, and (5) surfaces made of gold can be easily characterised [26]. Moreover, it is possible to design mixed SAMs from different thiolates in solution as model surfaces for biochemistry and cell biology.

Control over the surface wettability can be adjusted by exposing one type of thiolated molecule or by mixing thiolates that are differently terminated with alkyl chains and hydrophilic chemical groups. Interestingly, Ratner and co-workers reported that cells seeded onto substrates in serum-containing culture medium interact with an adsorbed layer of serum proteins rather than the surface [27]. The amount, conformation and affinity of adsorbed serum proteins, such as albumin and fibronectin, depend on the properties of the SAM. Recently, Valamehr et al. showed that dodecyl-terminated hydrophobic surfaces, upon soaking in serum-containing medium, could prevent the adhesion of embryonic stem cells and favour their differentiation in suspension [28]. Thus, one can influence cell attachment [28], spreading and growth onto the adsorbed protein layer by adjusting the properties of the SAM [27].

Many receptor-binding ligands act at interfaces *in vivo*. To match this scenario *in vitro*, it is of relevance to study cells cultured on immobilised functional molecules. SAMs can be tailored to meet this experimental setup [29–31]. Mixed SAMs, composed of protein-resistant functionalities like poly(ethylene glycol) (PEG) and reactive chemical groups that are suitable for bioconjugation, offer the possibility to covalently immobilise receptor-binding ligands. Importantly, orientation, stability and density are essential parameters of ligand activity. However, standard protocols related to SAMs still face difficulties in controlling these parameters to study cell responses via a defined “outside-in” signalling.



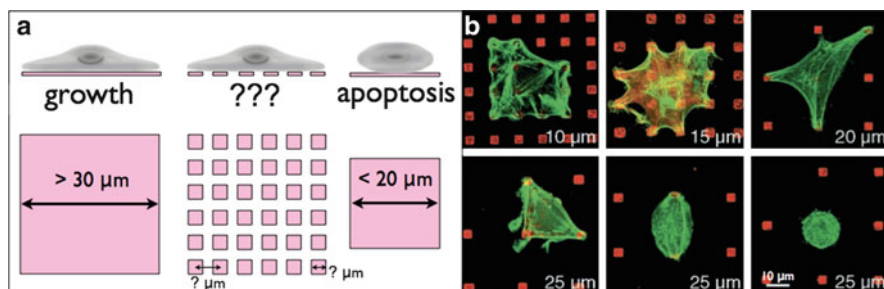
From a more practical standpoint, repairing, replacing or regenerating tissues or organs remain the central goals in tissue engineering research. Modifying surfaces with cell-adhesion proteins, growth factors or cytokines is a promising strategy for the design of implants. This setup has the potential to regulate the cellular response by preventing lateral diffusion or the internalisation of the targeted receptors [30]. For instance, sustained activation of cell receptors has been observed in cells seeded onto immobilised epidermal growth factor (EGF) or insulin, in comparison to the activation obtained with the soluble form of these hormones [32–34]. In another report, immobilised leukaemia inhibitory factor (LIF) was found to conserve the pluripotency of mouse embryonic stem cells for more than 2 weeks in the absence of soluble LIF [35].

With a wide substrate application, SAMs have pioneered the development of new techniques for conjugation of biomolecules. Although the covalent attachment of ligands onto scaffolds appears promising, new conjugation techniques need to be engineered in order to fully mimic the physiological function of signal-transducing ligands. In addition, some substrates could also be designed to spontaneously direct the distribution of single ligands at the nanoscale resolution. This would allow quantitative analysis of the effect of ligand density and clustering of cell surface receptors.

### ***3.2 Micropatterning: A Revolution for Cell-Adhesion-Based Assays***

The precise engineering of cell culture substrates at the microscale (from 100  $\mu\text{m}$  to 100 nm) has undergone extensive development within the last 20 years. The ability to organise living cellular systems and to produce micropatterns of single or co-cultured cells has led to the emergence of bioassays to monitor cellular activity [36–42]. Furthermore, cell patterning remains an important experimental tool for tissue engineering, as well as for cell-based sensing and drug discovery concepts [43].

By combining SAMs on gold with a variety of microlithographic tools such as photolithography [44] and microcontact-printing ( $\mu\text{CP}$ ) [36, 39], it is possible to produce adhesion microassays based on an array of ECM proteins or peptides surrounded by protein-resistant molecules. By culturing single cells on islands of adhesive protein of decreasing size, Chen et al. showed that the restriction in spreading area controls cell fate, independently of the molecular composition of the ECM (Fig. 3). The long-term effect of cell patterning on growth and survival is due to changes in cell tension and architecture, but is not a consequence of the total cell adhesion area [36]. A few years later, Bastmeyer and co-workers used  $\mu\text{CP}$  combined with mixed SAMs to study adhesion of single cells on arrays made of smaller islands ( $<1 \mu\text{m}$ ). Based on these experiments, they could identify three important parameters that affect cell spreading: the density of adhesive molecules per island, a maximal interdistance of 25  $\mu\text{m}$ , and a total surface coverage with ECM proteins above 15% [38].



**Fig. 3** (a) Spreading confinement as a regulator of cell growth and apoptosis. Adapted from Chen et al. [36]. (b) Cell spreading in relation to substratum geometry: cell growth on patterned substrata of  $9 \mu\text{m}^2$  ( $3 \times 3 \mu\text{m}$ ) squares separated by different distances, as indicated in the *bottom right corner*. With distances of 5–20  $\mu\text{m}$  between dots, cells spread and actin cytoskeleton formed stress fibres between adjacent dots. At a distance of 25  $\mu\text{m}$ , spreading was limited and cells became triangular, ellipsoid or round. From Lenhart et al. [38], reproduced with permission of the Company of Biologists

Although micropatterning has revolutionised cell-adhesion-based microassays, it does not allow one to investigate signal transduction of nanolocalised signals. Current preparation methods are also not suitable for immobilising different proteins on the same substrate. Such advances will be crucial to gain more insight into cell surface receptor clustering and cross-talk mechanisms. Alternatively, the design of nanoarrays that direct the immobilisation of biosignals into specific patterns offer a more appropriate tool for studying nanoscale events triggered by cell–ECM interactions.

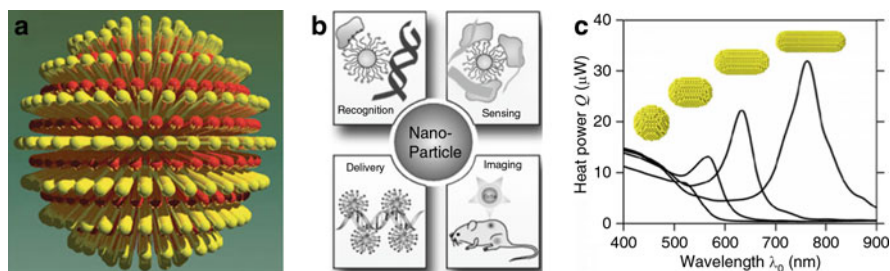
### 3.3 Nanogold: An “All-in-One” Model System

Irrespective of the system, nanoscience always deals with size effects at the nanoscale. What makes nanoscale materials so interesting is the fact that many of their properties are different from bulk properties and that they depend on particle size. Two major effects are responsible for these differences: (1) the number of surface atoms in nanocrystals is a large fraction of the total (a 3 nm spherical iron particle has 50% of its atoms on the surface, whereas a 10 nm particle has just 20%, and a 30 nm particle only 5%); and (2) the quantum size effects, i.e. changes in the density of electronic energy levels depending on the size of the interior. Therefore, a nanocrystal is an intermediary state of matter lying between atoms and molecules, and exhibits discrete density of electronic states and macroscopic crystals with continuous bands [45]. Additionally, nanoparticle properties are sensitive, not only to the size, but also to the composition and shape [46]. Over several decades, the understanding of quantum size effects has led to many applications in most research fields, like electronics [47], optics [48], catalysis [49], ceramics [50], magnetic data storage [51] and biology [52].

Within the last century, gold has become the most studied nanosystem. Because of their surface plasmon resonance (SPR), gold nanoparticles inspire an ever-growing number of scientists and remain in the core of modern technologies [53, 54]. SPR results from the interaction between an electromagnetic wave and conduction electrons in a metal. During illumination, these electrons are influenced by the electric field to collectively oscillate at a resonant frequency, for which the gold nanoparticles absorb the incident light. These photons will be scattered, i.e. released in all directions with the same energy, or absorbed and thus converted into crystal lattice vibrations [55]. More practically, the SPR band of gold nanoparticle dispersion is centred at around 520 nm, responsible for the ruby red colour. SPR properties are dependent on the shape of nanoparticles, and they can be tuned across the light spectrum by adjusting their aspect ratio. For instance, elongated gold particles exhibit two SPR bands, one corresponding to the transverse electron oscillations positioned at 520 nm and the other one due to the longitudinal plasmon resonance localised between 600 nm and infrared wavelengths.

From a surface chemistry standpoint, thiolates also form SAMs onto gold nanoparticles [56] (Fig. 4a). This property makes them an excellent platform for bioconjugation because of their similar size to large biomolecules [57, 58]. Because the SPR band is very sensitive to environmental changes, gold nanoparticles are a suitable tool for a broad range of applications in biology and life sciences. The use of biofunctionalised gold colloids has resulted in the emergence of new methods in delivery, targeting, imaging and sensing [52] (Fig. 4b). Moreover, gold nanoparticles are promising for photothermal cancer therapy because of their ability to efficiently generate heat through crystal lattice vibration under laser irradiation [59] (Fig. 4c).

It is possible to prepare optically active substrates by immobilising nanoparticles. Nanostructured surfaces have proven to be effective in biosensing [61], but are incompatible with other applications like tissue culture. Because the preparation



**Fig. 4** (a) 3D rendering of the scanning tunnelling microscopy height image of a gold nanoparticle functionalised with a mixed SAM made of mercaptopropionic acid and dodecanethiol. From Jackson et al. [56], Copyright © 2004 Nature Publishing Group. (b) The wide range of biological applications involving the use of nanoparticles. From De et al. [52], Copyright © 2008 Wiley-VCH. (c) Calculated spectra of the heat generated in four different colloidal gold nanoparticles of the same volume, where the wavelength of maximal heat power corresponds to the one where the longitudinal plasmon resonance band is centred. From Baffou et al. [60], Copyright © 2009 American Institute of Physics

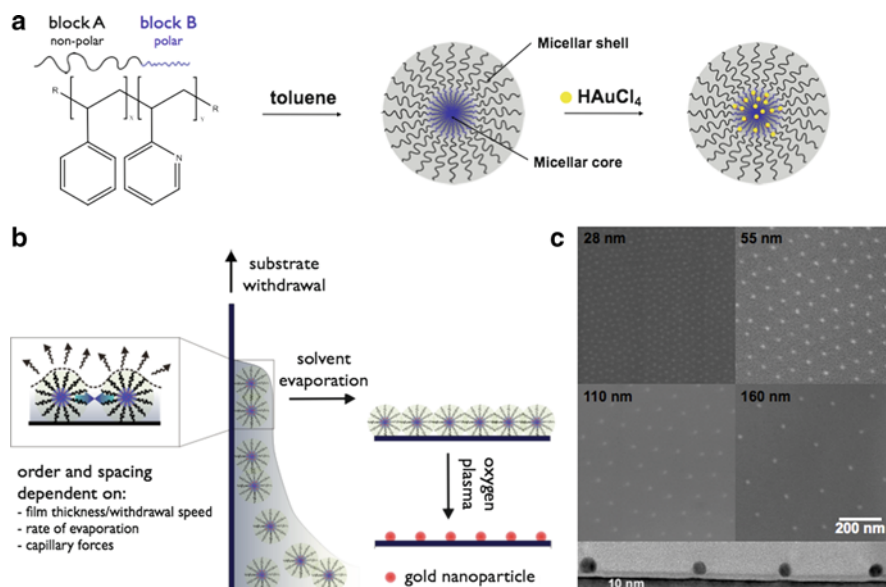
of these substrates is based on the assembly and the attachment of gold colloids onto a chemically modified surface [62], the nanoparticles are weakly bound and easily released by buffered environments or ligand exchange. To overcome this limitation, it is crucial to design a strategy to physically (and not chemically) immobilise nanoparticles onto a substrate that resists various chemical conditions and mechanical forces generated by adherent cells. Moreover, the production of a highly organised monolayer of gold nanoparticles would allow the engineering of surface models to perform experiments in a more quantitative manner.

## 4 Micellar Nanolithography: A Versatile Technique for Designing Nanopatterned Surfaces

In addition to the design of nanoparticles exhibiting specific properties, nanosciences focus more and more on the use of these nanoparticles as building blocks for the fabrication of 1-, 2- and 3D superstructures [63–66]. The ability to guide these nanometre-scale building blocks into complex functional architectures would offer great opportunities for construction of nanodevices and for exploration of their novel collective properties [67]. One of the most promising strategies for the fabrication of such materials is the use of self-assembly processes [66]. The organisation is determined by the interactions between the primary building blocks. The interfaces between organics and inorganics are controlled synthetically at the molecular level to produce composite materials with a structure defined from angström to centimetre length scales [68].

Particularly in 2D systems, control over the self-assembly of colloidal templates has offered a versatile way to produce patterned surfaces or arrays with a precision of few nanometres. Diblock copolymer micellar nanolithography (dBCML) is a versatile method that uses homopolymers or block copolymers for the production of complex surface structures with nanosized features [69]. In contrast to other approaches like electron-beam lithography (EBL) and photolithography, dBCML does not require extensive equipment. In fact, it is commonly used in the fabrication of data storage devices and photonic crystals, in catalyses [70], and for the design of mesoporous films and nanoparticle arrays [71].

Diblock copolymers are large linear molecules composed of two blocks of different repeated units called monomers (A and B). The two blocks (block A and block B) are covalently linked and differ in their chemical composition and the number of monomers. After solubilisation in a solvent that selectively dissolves one of the blocks, and upon exceeding a critical concentration of the polymer [known as the critical micellar concentration, (CMC)], single diblock copolymer molecules tend to minimise their energy by forming micelles [72]. The assembly of the soluble blocks forms a shell around the less soluble ones, preventing energetically unfavourable interactions. The micelle morphology and the overall CMC are usually dependent on the characteristics of the polymer, e.g. the number of repeating units for each block, the molecular interaction strength of the respective blocks, the solvent and the temperature [73].



**Fig. 5** (a) Molecular structure of the amphiphilic block copolymer PS-*b*-P2VP, and loading of the micellar core with an inorganic salt. Upon uptake of hydrochloroauric acid, the P2VP core becomes protonated, which results in an increased hydrophilicity. (b) Different steps for the preparation of gold nanopatterned surfaces. A glass slide is dipped into a micellar solution and withdrawn at a defined speed. Physical forces, such as capillary forces, are responsible for the formation of a hexagonal pattern during the evaporation of the solvent. The obtained micellar monolayer loaded with inorganic precursors is then treated with oxygen plasma. (c) SEM images of gold nanopatterns with four different interparticle distances, as indicated. *Lower panel*: Transmission electron micrograph displaying the profile of embedded particles in the substrate

As depicted in Fig. 5a, the diblock copolymer polystyrene-*block*-poly (2-vinylpyridine) (PS-*b*-P2VP), consisting of a hydrophobic apolar PS block attached to a hydrophilic polar P2VP domain, is widely used to prepare ordered monolayers of inorganic nano-objects. The solubilisation of PS-*b*-P2VP in toluene leads to the formation of homodisperse reverse micelles made of a hydrophilic P2VP core and a hydrophobic PS outer shell interacting with the solvent molecules.

The micellar core is used as a nanocontainer for inorganic precursors like HAuCl4, H2PtCl6 and ZnCl2 because of the high binding affinity of P2VP to metallic cations. These ions interact with P2VP through the formation of complexes, acid–base reactions or hydrogen bridges, which allow the loading of the micellar core. The uptake of an acidic salt, like hydrochloroauric acid, results in the protonation of the P2VP core and the binding of AuCl4- as a counterion. In thermodynamic equilibrium, the metal ions are distributed homogeneously over the micellar core. Moreover, the incorporation of inorganic precursors leads the amphiphilic micelles to be more hydrophilic, which strengthens micelle formation. The loaded micelles are then utilised as nanoreactors to synthesise particles. Metal and metal oxide nanoparticles are obtained chemically by reducing the precursor with reducing agents, or physically by plasma treatment [74]. Interestingly, several

recent studies have shown that not only molecular precursors but also preformed nanoparticles were successfully incorporated into micellar systems to organise a wide range of nano-objects into hexagonal nanopatterns or arrays of nanowires [75].

To transfer and organise loaded micelles onto various types of substrates, dip coating remains a method of choice. This technique is based on immersing and withdrawing a substrate into a micellar solution at a defined speed. The withdrawing step initiates solvent evaporation from the film surface and induces convective transfer of micelles from the bulk of the solution to the thin wetting film. The formation of a close-packed micellar monolayer is driven by attractive capillary forces, which are in equilibrium with repulsive electrostatic and steric forces. The monolayer features mainly depend on the molecular weight of the diblock copolymer, its concentration and the withdrawal speed of the substrate [76, 77] (Fig. 5b). Upon solvent evaporation, the micellar monolayer is treated with oxygen, hydrogen or argon plasma, resulting in the formation of an inorganic nanopattern with geometry similar to that of the assembled micelles. Plasma treatment allows etching the organic part of the micelles to deposit the clustered metal ions onto the substrate and reduces them into atoms to finally form inorganic nanoparticles. Importantly, during plasma treatment, the electric field generated in this process induces heating of the nanoparticles, which consequently causes them to partially diffuse into the underlying substrate. This partial embedding enhances the effective adhesion between the substrate and the nanoparticles. This important effect inhibits the lateral displacement of the particles when exposed to various environments and forces.

In the case of hydrochloroauric acid as a metal precursor to load PS-*b*-P2VP, spherical micelles are usually obtained and self-assemble spontaneously into a hexagonally ordered monolayer upon dip coating. It is then possible to prepare patterns of immobilised spherical gold particles with diameters below 10 nm and variable interparticle distances ranging from 25 to 200 nm. Figure 5 illustrates the theoretical and experimental aspects of preparing gold nanoarrays that exhibit suitable features for cell culture.

## **5 Biofunctionalised Gold Nanopatterns: A Quantitative Tool for Dissecting the Adhesion Machinery of Cells**

### **5.1 Nanopatterning Biocues**

Cell surface receptors collect information by sensing the extracellular environment and coordinating intracellular responses. Many receptors are not functional as single molecules, but rather as oligomeric complexes. Controlled assembly of these signalling complexes is a mechanism by which the cell can achieve spatio-temporal control of its activity. Clustered receptors constitute the main signalling unit in both neural and immune systems, and represent a central activation step of integrin signalling in all cell types [78]. In this context, the nanopatterning of receptor-binding ligands appears to be a promising strategy for studying and quantifying activation and clustering of surface receptors.

As described in the Sect. 3, gold remains the standard over all length scales as a biocompatible platform for the study of cellular systems. Gold nanopatterns utilize the same surface chemistry as extended SAMs and, in addition, allow the control of ligand density at a single protein or macromolecular length scale [79]. Upon functionalising the glass background that surrounds the nanoparticles with silane-modified PEG molecules, it is possible to conjugate nanolocally various types of biomolecules specifically to the gold particles. The orientation of immobilised peptides or proteins at interfaces is crucial to preserve their activity [80]. Cysteine-terminated peptides [81] and histidine-tagged proteins [79] are conventional and compatible ligands for the generation of gold-based bioactive surfaces. Since the nanoparticles are partially embedded in the substrate, the even and immobile distribution of active ligands makes gold nanopatterns an ideal analytical tool for modelling protein–protein interaction at the cell membrane [82].

## 5.2 *Integrin Nanoclustering Mediates Cell Adhesion and Signalling*

As described in Sect. 5.1, integrin-mediated adhesion is essential for bidirectional signalling between the cell and the ECM. ECM proteins are large and complex molecules that, through their multiple ligand-binding motifs, initiate various signalling cascades. However, the RGD motif constitutes one of the most elementary ECM adhesion sites to several central integrin heterodimers such as  $\alpha_v\beta_3$  and  $\alpha_5\beta_1$ , and is thus a useful tool for biofunctionalisation. RGD inhibits cell adhesion in a soluble form, but promotes cell adhesion when properly immobilised onto a surface. In addition, modifications of the RGD peptide can confer additional specificity. For instance, cyclic-RGD molecules bind specifically to the  $\alpha_v\beta_3$  integrin in both soluble and immobilised forms [83].

Surface functionalisation must fulfil several crucial criteria in order to remain effective and stable in cell culture conditions. Immobilised biomolecules must be accessible to the cells and covalently anchored to the substrate to withstand cell contractility and internalisation. In the case of gold substrates, the design of RGD-based ligands is optimal when composed of (1) an N-terminal group with a high affinity for gold, such as thiol or cysteine; (2) a C-terminal binding sequence like RGD; and (3) in between, a spacer made of glycine or PEG to expose the functional motif in an oriented fashion [80].

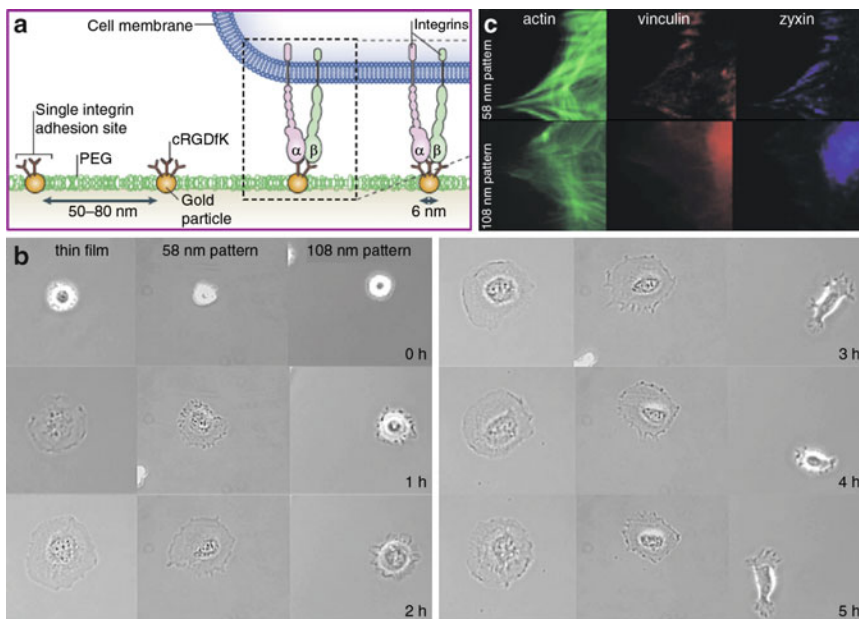
By fulfilling these criteria for surface modification, several groups aimed at developing in vitro strategies to elucidate how ECM components influence cell activity. A body of evidence implies that density and distribution of adhesive molecules affect cell adhesion, morphology and gene expression [38, 84–86]. However, all of these studies were experimentally limited by the random distribution of the immobilised biomolecules or by a low patterning resolution of  $>30$  nm [84]. Since integrins are about 8–12 nm wide, the spatial investigation of integrin clustering could not be conclusively analysed. Therefore, gold templates made



of 6 nm particles functionalised with RGD represent a relevant surface model for investigation of integrin activation functions and to quantify integrin clustering.

Professor Joachim Spatz and his group have developed various technologies, such as micellar nanolithography and glass passivation, in order to prepare such nanopatterned surface models [82]. Nanoarrays with an interparticle distance ranging from 28 to 108 nm and functionalised with thiolated cyclic-RGD were tested with different cell lines. They observed that fibroblasts, osteoblasts and melanocytes remain spread and viable after 24 h on patterns with an interdistance of 58 nm. Surprisingly, cells lose the ability to form stable FAs when interfacing 73-nm arrays. They also tend to minimise their surface area and finally enter apoptosis [82, 83]. This points out the existence of a narrow range of interparticle distance, between 58 and 73 nm, that constitutes a universal length scale for  $\alpha_v\beta_3$  integrins to cluster and activate cell functions.

Further studies were done on rat embryonic fibroblasts (REFs) to identify how cell morphology and molecular composition of FAs are regulated by nanostructured surfaces. In comparison to a gold thin film and a 58-nm-spaced pattern, cells cultured on 108-nm arrays display a delayed spreading followed by repeated protrusion–retraction cycles over several hours (Fig. 6b). The data suggest that cell



**Fig. 6** (a) Biofunctionalised gold nanopattern in contact with a cell membrane. From Geiger et al. [15], Copyright © 2009 Macmillan. (b) Phase contrast images of a cell spreading on surfaces homogeneously presenting RGD peptides, and 58-nm- or 108-nm-spaced RGD patterns. Adapted from Cavalcanti-Adam et al. [87], Copyright © 2007 by the Biophysical Society. (c) Immunofluorescence of the periphery of REF cells adhered on 58-nm- and 108-nm-spaced RGD patterns, and stained for actin, vinculin and zyxin. Vinculin and zyxin are proteins involved in FA formation. Adapted from Cavalcanti-Adam et al. [83], Copyright © 2005 Elsevier



attachment and early spreading are not sensitive to RGD density, whereas the formation of stable FAs necessary for long term spreading is. Moreover, the size and density of FAs decrease when the density of RGD is reduced. It is obvious that cellular contacts do not remain stable above a certain threshold in spacing RGD peptides, which induces major changes in cell shape and polarity controlled by distinct signalling pathways. Indeed, the molecular composition of FAs was found to be different on both nanopatterns. Zyxin and vinculin, two proteins involved in FA formation and their association with actin stress fibres, were only observed as co-localised clusters on denser RGD nanopatterns [87] (Fig. 6c). Thus, the spacing of integrins at the nanoscale strongly influences the recruitment of adhesion proteins that have central functions in regulating FA assembly and maturation, thereby influencing cell adhesion and migration.

### ***5.3 Micro-nanopatterned Surfaces: A Deeper Structural Insight into Integrin-Mediated Adhesion***

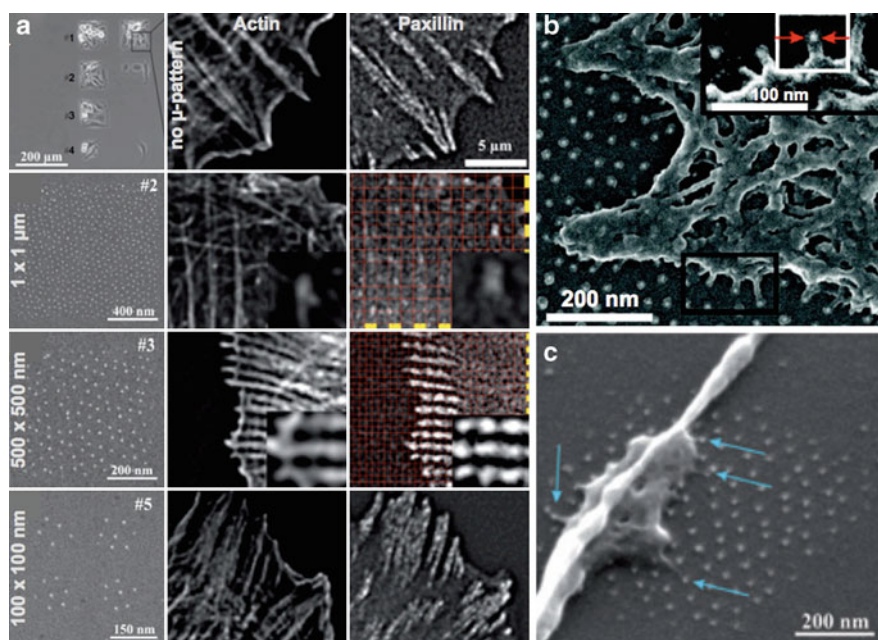
Although micropatterning has revolutionised cell-adhesion-based assays, its length scale does not allow investigation of the activation of single surface receptors. However, the combination of both nanolithography and micropatterning techniques has proven to be an interesting tool for gaining more insight into integrin clustering and FA assembly.

To address these fundamental processes, the group of Professor Joachim Spatz established two strategies for generating micro-nanostructured arrays. Conventional methods such as EBL and photolithography are compatible for generating substrates made of a gold-loaded micellar monolayer [88, 89]. Before plasma treatment, squared islands with sizes ranging from 3 to 0.1  $\mu\text{m}$  and composed of a 58-nm array were routinely produced by EBL for cell experiments. These features provide defined numbers of nanoparticles per micropattern ranging from  $\sim 3000 \pm 200$  to  $6 \pm 1$ . To keep the nanoparticle density constant, each island was separated by its respective size in each pattern field.

In a first experiment with fibroblasts in culture, an extended 73-nm-spaced pattern was compared with a 2- $\mu\text{m}$ -patterned 58-nm array. Although the total nanoparticle density of the micropatterned surface was considerably lower than that of the homogeneously coated one, the cells could only form FAs on 58-nm-spaced RGD motives. It is thus obvious that integrin function critically depends on the spatial confinement of integrins to favour clustering but not on the total number of bound integrins [82].

In an effort to identify the number of integrins required to trigger the formation of a stable FA, Spatz and co-workers studied a REF cell line on smaller nanostructured micropatterns. These experiments revealed that a minimum of six integrins per adhesive micropatterns were necessary to observe persistent cell adhesion. Adhesive islands with a side length larger than 1  $\mu\text{m}$  induce the formation of FAs rich in paxillin, an integrin adaptor protein associated to actin fibres. These

FAs display a comparable size and shape to classical FAs observed in conventional culture dishes. Interestingly, adhesive patches with side lengths of 500 and 100 nm, containing  $83 \pm 11$  and  $6 \pm 1$  gold nanoparticles, respectively, display a significant increase in the length of paxillin-positive adhesions, which bridge across the non-adhesive area on elongated actin bundles. The bridging of actin fibres allows mechanical cross-linking of multiple adhesive sites to stabilise adhesion. In comparison to nanostructured substrates made of 100 nm islands, cells adhering onto extended nanopatterns form interconnected paxillin-positive adhesions of similar length, about 4  $\mu\text{m}$ . However, a larger number of actin bundles associated with paxillin appear more defined and thinner on 100 nm islands, probably because of the homogeneous distribution of intracellular tensions applied to the micropatterned substrate (Fig. 7a). Upon critical-point drying of cells, it is possible to appreciate how a FA or a cell adhesion site binds tightly to both kinds of nanostructured surfaces, where nanoscopic protrusions specifically target the gold particles [90] (Fig. 7b, c).



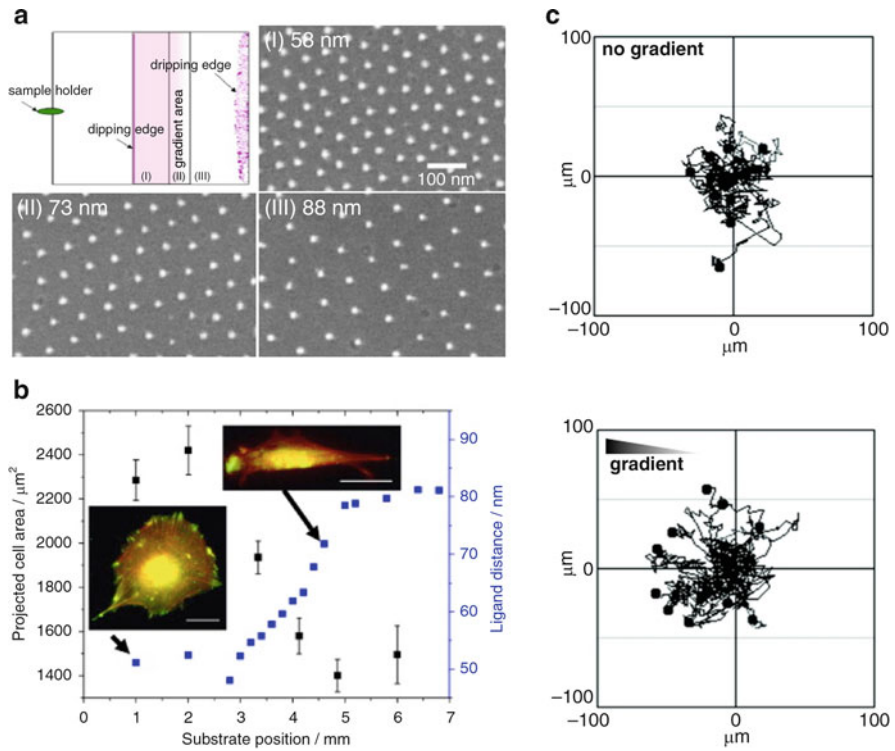
**Fig. 7** (a) Typical design of hierarchically patterned substrates. Phase-contrast micrographs of REF cells plated for 3 h on differently spaced patterns (*left*). SEM images of the different pattern fields: high magnification micrographs of FAs fixed and fluorescently stained against actin (*centre*) and paxillin (*right*). (b) SEM image of a cellular protrusion on an extended patterned surface (indicated in magnified image by *arrows*). (c) Filopodial structure on a micro-nanopattern. *Arrows* point to adhesion sites. Adapted from Arnold et al. [90], reproduced with permission of The Royal Society of Chemistry

## 5.4 Nanoscale Gradient-Induced Cell Polarisation and Migration

Cell polarisation and migration are crucial for embryogenesis, tissue morphogenesis, wound healing and immune responses. Dysregulation of these processes lead to severe developmental disorders, and are frequently associated with pathological conditions such as cancer. Although cell adhesion and migration are usually considered as interdependent phenomena, a recent work demonstrated that adhesive and migratory machineries are uncoupled in leukocytes, which need to migrate rapidly through various different extracellular compartments [18, 91]. In contrast to leukocytes, mesenchymal and epithelial cells migrate through integrin-mediated coupling of the ECM to the cytoskeleton. This migration mode is defined as haptic, and the term “haptotaxis” refers to directed cell motility along gradients of immobilised signals [92].

To mimic in vitro haptotactic gradients of adhesive epitopes, various technologies have been developed to control the presentation of surface-immobilised gradients using techniques such as microfluidics, photolithography or dip-pen lithography [93–97]. Using these approaches, it was observed that ECM protein gradients induce morphological polarisation and haptotaxis towards higher concentrated regions. The net movement (i.e. distance between the start point and the end point) correlates with an increase in the slope of the gradient, whereas the overall migration rate does not [94]. However, control over surface-bound gradients remains difficult to generate. So far, the different methods do not allow positioning receptor-binding ligands with a nanoscale precision and avoiding protein aggregation. In order to investigate the cooperative effects of integrin clustering involved in migration and to gain more insight into the cellular sensitivity to nanoscale variations in lateral spacing, it is important to overcome these preparation limitations.

Since it is possible to trigger cell responses by controlling the precise positioning of biocues, the sensitivity of cells to RGD nanogradients would be interesting to test along such a surface model. Arnold et al. developed a different approach based on dBCML. They slightly modified the dipping step in gold-loaded micellar dispersions by gradually decreasing the withdrawal speed of the substrate [98]. This simple method leads to the formation of a linear decrease of 30 nm between RGD-functionalised nanoparticles over a 2-mm thick band [99] (Fig. 8a,b). Cells respond to this linear variation with a tendency to elongate (or polarise) and migrate along the gradient direction (Fig. 8b,c). The weakest gradient guiding the cells was about 15 nm over 1 mm on the surface, offering interdistances ranging from 58 to 73 nm, critical for integrin signalling. Considering an average cell size of 60  $\mu\text{m}$ , this experiment demonstrates the ability of a cell to sense a spacing variation of 1 nm. The migration mediated through the integration of different integrin-clustering states localised at the front and the rear of the cell appears quite striking, and its mechanism remains unclear. One possible explanation involves contraction of stress fibres coupling opposite FAs. These contractions might allow integrating the mechanical stability on both cell extremities to finally migrate towards the denser RGD area of stronger tension.



**Fig. 8** (a) Schematic and SEM images describing the structure of a glass coverslip coated with a nanoscale gradient of gold particles. (b) Projected cell area along a 2-mm RGD patch spacing gradient on a sample covering a spacing from 50 to 80 nm after 23 h in culture. *Insets*: Mc3t3 osteoblasts on a homogeneously nanopatterned area with 50 nm patch spacing (*left image*), and along the spacing gradient (*right image*). The latter displays a section of the gradient, which represents approximately 70 nm patch spacing. Cells were immunostained for vinculin (*green*), and actin was visualised using TRITC-phalloidin (*red*). Adapted from Hirschfeld-Warneken et al. [99], Copyright © 2008 Elsevier. (c) REF cell migration paths over 12 h on areas presenting a constant ligand patch spacing of 60 nm and a ligand patch gradient with a strength of 25 nm/mm covering 60–110 nm spacing. From Arnold et al. [98], Copyright ©2008 American Chemical Society

This section has attempted to present dBCML as a versatile method for designing nanopatterned substrates. With such a defined platform, it becomes possible to investigate and quantify, in a molecular approach, the role of integrin clustering in cell adhesion. The advantage of such a system, in comparison to previous methods, is that it demonstrated for the first time (1) the existence of a threshold spacing of about 70 nm between integrins to favour effective clustering and persistent cell adhesion, and (2) the outstanding feature of cells to sense variations in ligand spacing as small as 1 nm, inducing cell polarisation and initiating cell migration.

However, it would be interesting to further develop nanopatterned substrates as an analytical platform, taking into account other essential features of the ECM, and as a manipulating tool for dynamic control of the binding states of cell surface

receptors. The next section discusses attempts to address these issues by development of novel strategies based on more sophisticated nanostructured surface models.

## **6 Outlook: Towards More ECM-Mimetic Systems and Cell Manipulation**

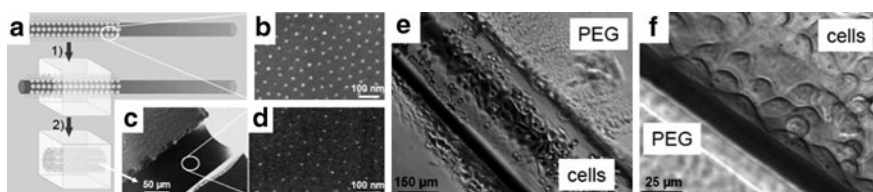
### ***6.1 Designing Extracellular Environments with Nanostructured Soft Interfaces***

Cells generate forces by protruding through actin polymerisation and pulling through integrin-coupled actomyosin contractility. Moreover, cells produce and remodel their own extracellular microenvironment. They secrete and organise ECM proteins to build supramolecular structures exhibiting both chemical and physical properties, which regulate cell activity [100]. When biologists attempt to understand a specific signalling pathway, they investigate genes, proteins and signalling molecules, but they often underestimate the mechanical signals provided by the tissue.

The development of more sophisticated tools (such as atomic force microscopy) and the design of softer interfaces now allow more precise monitoring and manipulation of the extracellular environment. This has facilitated more advanced studies related to the biophysical aspects of cell signalling. For instance, Engler et al. demonstrated that substrate elasticity has a profound effect on stem cell differentiation. This group could induce neurogenic differentiation on soft matrices, myogenic differentiation on stiffer surfaces, and osteogenic differentiation on rigid substrates [21]. Therefore, it has become evident that softer substrates would be a more physiological environment for cell biological studies, and that matrix stiffness plays a central role in regulating cell behaviour.

In an earlier study, Engler et al. demonstrated how matrix rigidity and ligand density influence spreading and cytoskeleton organisation in smooth muscle cells. They observed that these cells, when cultured on soft hydrogels, exhibit a limited spreading that was independent of collagen density. In response to softer interfaces, cells upregulate actin dynamics, enabling spreading and cytoskeleton organisation, whereas integrins play a major role in strengthening and sustaining spreading.

To further understand the cooperation between these two orthogonal biocues and to overcome functionalisation issues, Graeter et al. developed a technique to transfer gold nanopatterns onto soft interfaces such as PEG hydrogels [101]. Taking advantage of the dBCML approach, they designed soft interfaces decorated with ordered nanoparticles, allowing a more reliable control over ligand density [102]. PEG hydrogels remain a system of choice for building 2D and 3D matrices. Their mechanical properties can be controlled within a stiffness range similar to that found *in vivo*, i.e. with an elastic modulus  $E_y$  between 0.6 kPa and 6 MPa. Besides planar



**Fig. 9** Formation of nanostructured hydrogel microtubes. (a) Transfer lithography technique applied to curved surfaces. (b) SEM image of a glass fibre decorated with gold nanoparticles by means of dBCML. (c, d) Cryo-SEM images of PEG hydrogel channel decorated with gold nanoparticles. (e, f) HeLa cells cultured in PEG hydrogel, where the inside of the tube is covered with RGD-functionalised gold nanoparticles. From Graeter et al. [101], Copyright © 2007 American Chemical Society

substrates, gold nanopatterns were embedded in curved surfaces to engineer bio-functionalised channels within a PEG block, potentially mimicking blood vessels (Fig. 9). By combining lateral spacing of adhesive ligands, substrate rigidity and surface curvature, this transfer technique represents a promising tool for systematically studying the adhesion of various cell types in a more physiological manner.

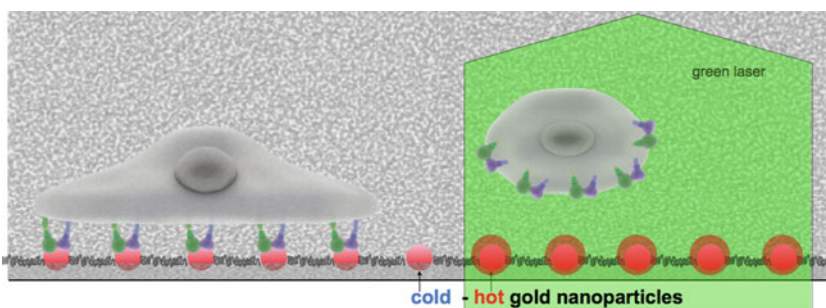
## 6.2 Thermoplasmonic Nanoarray for Manipulating Cell Adhesion

Organising, guiding, releasing and transporting entities of various dimensions over different scales are central goals for further development of lab-on-chip systems and high throughput biological devices. From a material engineering standpoint, patterning approaches have greatly profited from microfabrication technologies and dynamic stimulus-responsive surface chemistries. Stimulus-responsive surfaces, known as smart materials, have attracted the interest of many bioengineers aiming at co-culturing and detaching cells. Temperature-sensitive polymers like poly-*N*-isopropylacrylamide, UV-switchable and cleavable molecules like azo-dyes, and electro-active SAMs remain today the most popular systems in this field [103, 104].

Nanosized gold is also an ideal system for engineering devices with a wide range of potential biological applications. Its ability to strongly absorb laser irradiation allows transforming part of this energy into heat through crystal lattice vibration, the so-called photothermal effect, or thermoplasmonics [60]. Recently, this effect has proven to be a promising tool for the selective destruction of cancerous cells [105] and for the design of nanoparticle-assisted polymerase chain reaction (PCR) [106]. However, thermoplasmonics has been limited to the use of gold nanoparticles typically dispersed in aqueous media, polymer matrices and cellular systems, but never immobilised as a nanoarray to fabricate a light-responsive substrate for bio-applications.

Because integrins bind extracellular ligands like RGD with the help of divalent cations and hydrogen bonds, it would be interesting to develop a laser-based tech-





**Fig. 10** Release of a cell cultured on a thermoplasmonic nanoarray

nique to control spatio-temporal detachment of integrins from RGD-functionalised gold nanopatterns via thermoplasmonics (Fig. 10). In addition to allowing targeted detachment of single cells using a microscope-based setup, it could provide the means to study the kinetics of synchronised cell release and re-spreading as well as reorganisation of the adhesion machinery. This could be achieved by nanoscopic thermal exposure of selected FAs.

For almost 20 years, SAMs on gold have offered concrete opportunities to bridge surface chemistry to cell biology. Biofunctionalised gold nanopatterns have proven to be a superior surface model for dissection of the cell adhesion machinery. Their ability to “hexagonally map” the engagement of individual integrins at the nanoscale have clearly revealed the importance of clustering in the regulation of adhesion-mediated signalling. The nanopatterning of RGD motifs has demonstrated that cells read, process and respond in a stereotypical manner when interfacing a material with defined properties. Together, a spacing threshold of about 70 nm to activate integrin functions, a number of six integrins per adhesive patch to allow stable FA formation, and a sensitivity of 1 nm variation in RGD gradients over the length of a single cell, point out the mechanistic precision of the integrin ligation and signalling. The analysis of genetically modified cell lines that lack key components of the adhesion signalling machinery cultured on biofunctionalised nanopatterns is an important approach for gaining more mechanistic insights into this process. In addition to this, the development of new synthetic substrates offering possibilities for multiparameter modification of the extracellular environment would ultimately be the most appropriate strategy for the study of cellular systems in a more physiological manner. Therefore, it is essential to continue merging knowledge and skills from chemistry, physics and engineering with cell biology to shed new light on the complexity of integrin-mediated cell adhesion.

**Acknowledgments** The author thanks Professors Joachim Pius Spatz and Reinhard Fässler for offering the opportunity and support to work in this pluridisciplinary environment. The author gratefully acknowledges Professor Michael Sixt, Doctor Sara Wickström and Doctor Herbert Schiller for helpful and interesting discussions during the preparation of the manuscript, Josephine Gibson for revising the language of the manuscript, and Max Iglesias for his help with the artwork.

Doctor Julien Polleux is recipient of a Marie Curie fellowship of the European Community 7th Framework Programme.

## References

1. Legate KR, Wickström SA, Fässler R (2009) *Genes Dev* 23:397
2. Xiong JP, Stehle T, Diefenbach B, Zhang R, Dunker R, Scott DL, Joachimiak A, Goodman SL, Arnaout MA (2001) *Science* 294:339
3. Bouvard D, Brakebusch C, Gustafsson E, Aszódi A, Bengtsson T, Berna A, Fässler R (2001) *Circ Res* 89:211
4. Humphries JD, Byron A, Humphries MJ (2006) *J Cell Sci* 119:3901
5. Hynes RO (2002) *Cell* 110:673
6. Takagi J (2004) *Biochem Soc Trans* 32:403
7. Craig D, Gao M, Schulten K, Vogel V (2004) *Structure* 12:2049
8. Luo B-H, Carman CV, Springer TA (2007) *Annu Rev Immunol* 25:619
9. Choi CK, Vicente-Manzanares M, Zareno J, Whitmore LA, Mogilner A, Horwitz AR (2008) *Nat Cell Biol* 10:1039
10. Zaidel-Bar R, Cohen M, Addadi L, Geiger B (2004) *Biochem Soc Trans* 32:416
11. Geiger B, Bershadsky A (2001) *Curr Opin Cell Biol* 13:584
12. Ingber DE (2006) *FASEB J* 20:811
13. Zaidel-Bar R, Itzkovitz S, Ma'ayan A, Iyengar R, Geiger B (2007) *Nat Cell Biol* 9:858
14. Butler B, Gao C, Mersich AT, Blystone SD (2006) *Curr Biol* 16:242
15. Geiger B, Spatz JP, Bershadsky AD (2009) *Nat Rev Mol Cell Biol* 10:21
16. Boeri Erba E, Bergatto E, Cabodi S, Silengo L, Tarone G, Defilippi P, Jensen ON (2005) *Mol Cell Proteomics* 4:1107
17. Miyamoto S, Teramoto H, Gutkind JS, Yamada KM (1996) *J Cell Biol* 135:1633
18. Vicente-Manzanares M, Choi CK, Horwitz AR (2009) *J Cell Sci* 122:1473
19. Vicente-Manzanares M, Webb DJ, Horwitz AR (2005) *J Cell Sci* 118:4917
20. Cukierman E, Pankov R, Stevens DR, Yamada KM (2001) *Science* 294:1708
21. Engler AJ, Sen S, Sweeney HL, Discher DE (2006) *Cell* 126:677
22. Even-Ram S, Artym V, Yamada KM (2006) *Cell* 126:645
23. Pelham RJ, Wang YI (1997) *Proc Natl Acad Sci USA* 94:13661
24. Gähwiler BH (1999) *Brain Res Bull* 50:343
25. Ehrmann RL, Gey GO (1956) *J Natl Cancer Inst* 16:1375
26. Love JC, Estroff LA, Kriebel JK, Nuzzo RG, Whitesides GM (2005) *Chem Rev* 105:1103
27. Tidwell CD, Ertel SI, Ratner BD, Tarasevich BJ, Atre S, Allara DL (1997) *Langmuir* 13:3404
28. Valamehr B, Jonas SJ, Polleux J, Qiao R, Guo S, Gschweng EH, Stiles B, Kam K, Luo T-JM, Witte ON, Liu X, Dunn B, Wu H (2008) *Proc Natl Acad Sci USA* 105:14459
29. Goncalves RM, Martins MCL, Almeida-Porada G, Barbosa MA (2009) *Biomaterials* 30:6879
30. Ito Y (2008) *Soft Matter* 4:46
31. Kato M, Mrksich M (2004) *Biochemistry* 43:2699
32. Ichinose J, Morimatsu M, Yanagida T, Sako Y (2006) *Biomaterials* 27:3343
33. Ito Y, Zheng J, Imanishi Y, Yonezawa K, Kasuga M (1996) *Proc Natl Acad Sci USA* 93:3598
34. Li J, Ito Y, Zheng J, Takahashi T, Imanishi Y (1997) *J Biomed Mater Res* 37:190
35. Alberti K, Davey RE, Onishi K, George S, Salchert K, Seib FP, Bornhäuser M, Pompe T, Nagy A, Werner C, Zandstra PW (2008) *Nat Methods* 5:645
36. Chen CS, Mrksich M, Huang S, Whitesides GM, Ingber DE (1997) *Science* 276:1425
37. Derda R, Li L, Orner BP, Lewis RL, Thomson JA, Kiessling LL (2007) *ACS Chem Biol* 2:347
38. Lehnert D, Wehrle-Haller B, David C, Weiland U, Ballestrem C, Imhof BA, Bastmeyer M (2004) *J Cell Sci* 117:41
39. Singhvi R, Kumar A, Lopez G, Stephanopoulos G, Wang D, Whitesides G, Ingber D (1994) *Science* 264:696



40. Yousaf MN, Houseman BT, Mrksich M (2001) *Proc Natl Acad Sci USA* 98:5992
41. Jiang X, Bruzewicz DA, Wong AP, Piel M, Whitesides GM (2005) *Proc Natl Acad Sci USA* 102:975
42. Slater JH, Frey W (2008) *J Biomed Mater Res* 87:176
43. Falconnet D, Csucs G, Grandin HM, Textor M (2006) *Biomaterials* 27:3044
44. Huang J, Dahlgren D, Hemminger J (1994) *Langmuir* 10:626
45. Alivisatos A (1996) *J Phys Chem* 100:13226
46. El-Sayed M (2004) *Acc Chem Res* 37:326
47. Ashoori R (1996) *Nature* 379:413
48. Shipway A, Katz E, Willner I (2000) *Chemphyschem* 1:18
49. Astruc D, Lu F, Aranzaes J (2005) *Angew Chem Int Ed* 44:7852
50. Cain M, Morrell R (2001) *Appl Organomet Chem* 15:321
51. Awshalom D, Divincenzo D, Smyth J (1992) *Science* 258:414
52. De M, Ghosh PS, Rotello VM (2008) *Adv Mater* 20:4225
53. Daniel M, Astruc D (2004) *Chem Rev* 104:293
54. Hu M, Chen J, Li Z-Y, Au L, Hartland GV, Li X, Marquez M, Xia Y (2006) *Chem Soc Rev* 35:1084
55. Burda C, Chen X, Narayanan R, El-Sayed M (2005) *Chem Rev* 105:1025
56. Jackson A, Myerson J, Stellacci F (2004) *Nat Mater* 3:330
57. Maus L, Spatz JP, Fiammengo R (2009) *Langmuir* 25:7910
58. Michalet X, Pinaud F, Bentolila L, Tsay J, Doose S, Li J, Sundaresan G, Wu A, Gambhir S, Weiss S (2005) *Science* 307:538
59. Sperling RA, Rivera gil P, Zhang F, Zanella M, Parak WJ (2008) *Chem Soc Rev* 37:1896
60. Baffou G, Quidant R, Girard C (2009) *Appl Phys Lett* 94:153109
61. Toderas F, Baia M, Baia L, Astilean S (2007) *Nanotechnology* 18:255702
62. Grabar K, Allison K, Baker B, Bright R, Brown K, Freeman R, Fox A, Keating C, Musick M, Natan M (1996) *Langmuir* 12:2353
63. Davis S, Breulmann M, Rhodes K, Zhang B, Mann S (2001) *Chem Mater* 13:3218
64. Sanchez C, Soler-Illia G, Ribot F, Lalot T, Mayer C, Cabuil V (2001) *Chem Mater* 13:3061
65. Weller H (1996) *Angew Chem Int Ed* 35:1079
66. Whitesides G, Grzybowski B (2002) *Science* 295:2418
67. Antonietti M, Ozin G (2004) *Chem Eur J* 10:29
68. Ozin G (2000) *Chem Commun*:419
69. Forster S (2003) *Top Curr Chem* 226:1
70. Park C, Yoon J, Thomas E (2003) *Polymer* 44:6725
71. Antonietti M, Niederberger M, Smarsly B (2008) *Dalton Trans*:18
72. Forster S, Antonietti M (1998) *Adv Mater* 10:195
73. Gao Z, Eisenberg A (1993) *Macromolecules* 26:7353
74. Kastle G, Boyen H, Weigl F, Lengl G, Herzog T, Ziemann P, Riethmuller S, Mayer O, Hartmann C, Spatz J, Moller M, Ozawa M, Banhart F, Garnier M, Oelhafen P (2003) *Adv Funct Mater* 13:853
75. Nandan B, Gowd EB, Bigall NC, Eychmueller A, Formanek P, Simon P, Stamm M (2009) *Adv Funct Mater* 19:2805
76. Brinker C, Frye G, Hurd A, Ashley C (1991) *Thin Solid Films* 201:97
77. Dimitrov A, Nagayama K (1996) *Langmuir* 12:1303
78. Kiessling L, Gestwicki J, Strong L (2006) *Angew Chem Int Ed* 45:2348
79. Wolfram T, Belz F, Schoen T, Spatz JP (2007) *Biointerphases* 2:44
80. Salinas CN, Anseth KS (2008) *J Tissue Eng Regen Med* 2:296
81. Roberts C, Chen C, Mrksich M, Martichonok V, Ingber D, Whitesides GM (1998) *J Am Chem Soc* 120:6548
82. Arnold M, Cavalcanti-Adam E, Glass R, Blummel J, Eck W, Kantlehner M, Kessler H, Spatz J (2004) *Chemphyschem* 5:383
83. Cavalcanti-Adam E, Micoulet A, Blummel J, Auernheimer J, Kessler H, Spatz J (2006) *Eur J Cell Biol* 85:219
84. Comisar WA, Kazmers NH, Mooney DJ, Linderman JJ (2007) *Biomaterials* 28:4409

85. Koo L, Irvine D, Mayes A, Lauffenburger D, Griffith L (2002) *J Cell Sci* 115:1423
86. Maheshwari G, Brown G, Lauffenburger D, Wells A, Griffith L (2000) *J Cell Sci* 113:1677
87. Cavalcanti-Adam EA, Volberg T, Micoulet A, Kessler H, Geiger B, Spatz JP (2007) *Biophys J* 92:2964
88. Aydin D, Schwieder M, Louban I, Knoppe S, Ulmer J, Haas TL, Walczak H, Spatz JP (2009) *Small* 5:1014
89. Glass R, Arnold M, Blummel J, Kuller A, Moller M, Spatz J (2003) *Adv Funct Mater* 13:569
90. Arnold M, Schwieder M, Bluemmel J, Cavalcanti-Adam EA, Lopez-Garcia M, Kessler H, Geiger B, Spatz JP (2009) *Soft Matter* 5:72
91. Lämmermann T, Bader BL, Monkley SJ, Worbs T, Wedlich-Söldner R, Hirsch K, Keller M, Förster R, Critchley DR, Fässler R, Sixt M (2008) *Nature* 453:51
92. Friedl P, Borgmann S, Bröcker EB (2001) *J Leukoc Biol* 70:491
93. Herbert C, McLernon T, Hypolite C, Adams D, Pikus L, Huang C, Fields G, Letourneau P, Distefano M, Hu W (1997) *Chem Biol* 4:731
94. Rhoads DS, Guan J-L (2007) *Exp Cell Res* 313:3859
95. Smith JT, Elkin JT, Reichert WM (2006) *Exp Cell Res* 312:2424
96. Smith JT, Tomfohr JK, Wells MC, Beebe TP, Kepler TB, Reichert WM (2004) *Langmuir* 20:8279
97. Wang Q, Jakubowski JA, Sweedler JV, Bohn PW (2004) *Anal Chem* 76:1
98. Arnold M, Hirschfeld-Warneken VC, Lohmueller T, Heil P, Bluemmel J, Cavalcanti-Adam EA, Lopez-Garcia M, Walther P, Kessler H, Geiger B, Spatz JP (2008) *Nano Lett* 8:2063
99. Hirschfeld-Warneken VC, Arnold M, Cavalcanti-Adam EA, López-García M, Kessler H, Spatz JP (2008) *Eur J Cell Biol* 87:743
100. Hynes RO (2009) *Science* 326:1216
101. Graeter SV, Huang J, Perschmann N, López-García M, Kessler H, Ding J, Spatz JP (2007) *Nano Lett* 7:1413
102. Segura T, Anderson B, Chung P, Webber R, Shull K, Shea L (2005) *Biomaterials* 26:359
103. Liu Y, Mu L, Liu B, Kong J (2005) *Chem Eur J* 11:2622
104. Mendes PM (2008) *Chem Soc Rev* 37:2512
105. Jain PK, El-Sayed IH, El-Sayed MA (2007) *Nano Today* 2:18
106. Stehr J, Hrelescu C, Sperling RA, Raschke G, Wunderlich M, Nichtl A, Heindl D, Kurzinger K, Parak WJ, Klar TA, Feldmann J (2008) *Nano Lett* 8:619

# Self-Assembled Monolayers as Dynamic Model Substrates for Cell Biology

Abigail Pulsipher and Muhammad N. Yousaf

**Abstract** In recent years, the surface chemistry community has actively pursued the design and generation of stimuli-responsive platforms or dynamic surfaces to control the interface between cells and a solid support. Surface properties can be manipulated through photoactivation, electrochemical potential, pH change, and the addition of a biochemical signal, with the aim of mimicking the extracellular matrix and inducing cellular behavior. This chapter describes recent advances in the development and utility of self-assembled monolayers (SAMs) as dynamic, model substrates for cell biology.

**Keywords** Biological interface · Cell migration · Cellular adhesion · Dynamic substrates · Immobilization · Self-assembled monolayers

## Contents

1	Introduction .....	104
2	Self-Assembled Monolayers .....	105
2.1	SAMs of Alkanethiolates on Gold .....	105
2.2	Immobilization Strategies for Surface Tailoring .....	106
2.3	Patterning Methods.....	108
2.4	Analytical Techniques for SAM Characterization .....	109
3	Modulating Dynamic SAMs for Biological Applications .....	109
3.1	Stimuli-Controlled Dynamic Surfaces .....	110
4	Dynamic Surfaces for Cell Biology .....	116
4.1	Integrins, Signaling, and ECM Interactions.....	117

---

A. Pulsipher and M.N. Yousaf (✉)  
Department of Chemistry, Carolina Center for Genome Science, The University  
of North Carolina at Chapel Hill, Chapel Hill, NC, USA  
e-mail: [mnyousaf@email.unc.edu](mailto:mnyousaf@email.unc.edu)

4.2	SAMs as Dynamic, Model Substrates for Cell Biology .....	119
4.3	Applications of Dynamic Surfaces .....	122
5	Conclusion and Outlook.....	130
	References .....	131

## 1 Introduction

The development and integration of strategies to control the interface between biomolecules and a solid support is crucial to a number of research areas including drug discovery [1], biomedical engineering [2–5], and the design of tissue engineering scaffolds [6, 7]. Such studies require the use of a model substrate in which chemical and physical parameters can be tailored to modulate the desired behavior of biological ligands. Self-assembled monolayers (SAMs) of alkanethiolates on gold have proven to be an ideal class of model substrates [8–10]. In the past few years, the surface chemistry community has actively pursued the design and generation of stimuli-responsive platforms or dynamic surfaces for bioanalysis [11, 12]. The ability to manipulate surface properties through the application of an external stimulus, such as photoactivation, electrochemical potential, pH change, or the addition of a biochemical signal to induce biomolecular behavior, will help provide great insight into a number of fundamental cellular interactions and processes and enable new biotechnologies.

Different materials have been exploited for use as dynamic substrates; however, SAMs of alkanethiolates on gold represents the most studied system due to the synthetic flexibility in tailoring terminal functional groups, large number of patterning and analytical characterization techniques available, and the nonfouling properties of oligo(ethylene glycol)-alkanethiols to create complexly patterned and mixed SAMs [8–10]. There are also a variety of chemoselective ligand immobilization strategies that aim to present a range of specific ligands from the surface for further manipulation. SAMs have been used in many biological studies, including the interrogation of protein–protein, protein–cell, carbohydrate–protein, lipid–carbohydrate, and cell–cell interactions. Of particular interest, dynamic SAMs may be tailored to mimic the natural, *in vivo* dynamic extracellular matrix (ECM) environment [13, 14]. Many cell types adhere to the underlying dynamic matrix and then respond in numerous ways to the various complex physio-mechanical, hydrodynamic, and soluble and insoluble stimuli they receive. Proper cell adhesion and migration are important to tissue repair, inflammation response, wound healing, angiogenesis, and tumor invasion in cancer metastasis [15–26]. Therefore, several reports have explored the integration of SAMs and switchable properties to modulate studies of cell adhesion, polarization, and migration. Technologies to create dynamic SAM gradients with immobilized adhesion molecules and other chemoattractants have also been developed to aid in the elucidation of the mechanism of cell behavior and, in particular, cell migration [27–31].

This chapter describes the design and utility of dynamic surfaces for biological analysis. The structure, physical properties, and advantages of SAMs of alkanethiolates on gold are first summarized. Specific examples demonstrating the use of SAMs to create stimuli-controlled dynamic surfaces are then listed. Finally, other works illustrating SAMs as model substrates for cell biology studies are reported.

## 2 Self-Assembled Monolayers

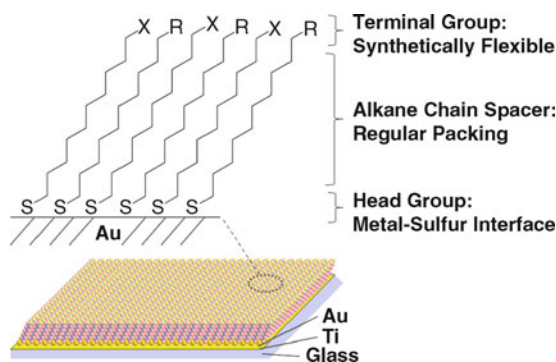
SAMs are highly ordered, monomolecular films formed by the spontaneous adsorption of surfactant molecules on a solid support [8–10]. This phenomenon of self-assembly was first reported in 1983 by Nuzzo and Allara, who described and characterized the organization of bifunctional, dialkyl disulfides on gold substrates [32]. Since then, extensive research has been conducted to elucidate the structure, physical properties, and potential use of SAMs on a number of different materials ranging from planar substrates (glass or silicon, single crystals, metal films or foils) to curved nanostructures (colloids, nanorods, nanospheres) [8–10]. As a result, SAMs have been employed in several basic research areas to serve as a platform for applications ranging from optoelectronics and environmental monitoring technology to the design of tissue engineering scaffolds and mechanistic cell biology studies [2–7]. Possessing many advantages over the other platforms (siloxanes on glass, phosphonates on metal oxides, alkanethiolates on silver, palladium, platinum, or copper), SAMs of alkanethiolates on gold have been widely investigated as a potential model system for biological study. This chapter describes the development, utility, and challenges of dynamic SAMs as a platform to study cell behavior [33].

### 2.1 SAMs of Alkanethiolates on Gold

It has been shown that long-chain alkanethiolates will rapidly and spontaneously form densely packed, well-ordered, and trans-extended monolayers on gold (111) surfaces [8–10, 33]. A scheme representing the structure of an ideal SAM is displayed in Fig. 1. The thiol head-group has a high affinity for transition metals and binds the gold through a Langmuir adsorption process. The sulfur atoms and, in turn, the alkyl chain spacer promote stabilization and regular packing through dipolar and van der Waals intermolecular forces, respectively. Therefore, the alkyl chains adopt the optimum distance between one another to maximize interchain interactions.

In addition to the well-defined physical properties previously listed, SAMs of alkanethiolates on gold offer attractive advantages to serve as model substrates for biological applications. The preparation of the gold films is inexpensive and substrates can be routinely customized according to the appropriate thickness desired. Thiol chemistry is amenable to several different functional groups through standard organic chemistry. Therefore, the synthetically flexible terminal group provides the

**Fig. 1** An ideal self-assembled monolayer of alkanethiolates supported on a gold surface. The terminal groups are amenable to synthesis, providing a means to immobilize and present ligands from the surface; the alkyl chain spacer promotes tight, regular packing, and the gold–sulfur interface stabilizes surface atoms and alkane chains during packing

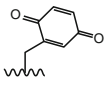
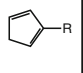
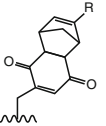
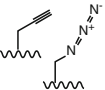
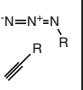
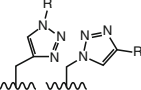
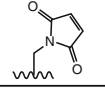
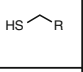
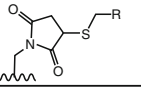
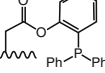
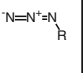
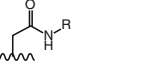
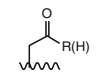
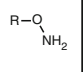
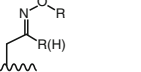

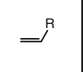

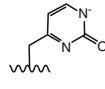
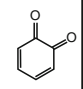
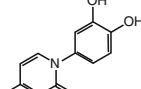


means for specific tailoring with the presentation of a variety of ligands from the surface. Another benefit to using gold is its inherent conductivity and, therefore, gold is compatible with several analytical techniques for characterization (electrochemistry, surface plasmon resonance, scanning electron microscopy, tunneling electron microscopy, etc.), that are unavailable to other SAM systems [8–10, 33]. Similarly, there are many patterning methodologies amenable to SAMs on gold, enabling the opportunity to create complex substrates for the interrogation of biomolecular interactions. For example, microcontact printing ( $\mu$ CP) and dip-pen nanolithography (DPN) have been used to pattern gold, forming micro- and nanostructured SAMs [34–38]. Other techniques, such as photolithography, microfluidics, and electron-beam lithography have been employed to activate a particular terminal group for the subsequent tethering of molecules within a spatial confinement. Finally, planar gold is nontoxic to cells and compatible with cell culture. Furthermore, assembled monolayers of oligo(ethylene glycol)-alkanethiols are known to resist nonspecific adsorption of proteins and cells and, therefore, often serve as the background monolayer for cell biology experiments [39, 40].

## 2.2 Immobilization Strategies for Surface Tailoring

An advantage of using SAMs of alkanethiolates on gold as a model system is that thiol chemistry is compatible with a variety of functional groups. As such, alkanethiols are commercially available or routinely synthesized [41–45]. However, even for simple molecules, synthesis may become laborious and time-consuming endeavors, and obtaining alkanethiols tethered to a peptide, carbohydrate, or desired biomolecule may become a major challenge. To circumvent these difficulties, a number of interfacial coupling strategies that aim to modify preassembled monolayers have been developed. Some of these organic reactions include Diels–Alder conjugation [46, 47], Click chemistry [48, 49], quinone and aldehyde coupling with oxyamines [50–52], Staudinger ligation [53], olefin cross-metathesis [54], Michael addition [55], and maleimide [56] (Table 1). Under the appropriately

**Table 1** Interfacial SAM coupling strategies to immobilize and present ligands from the surface

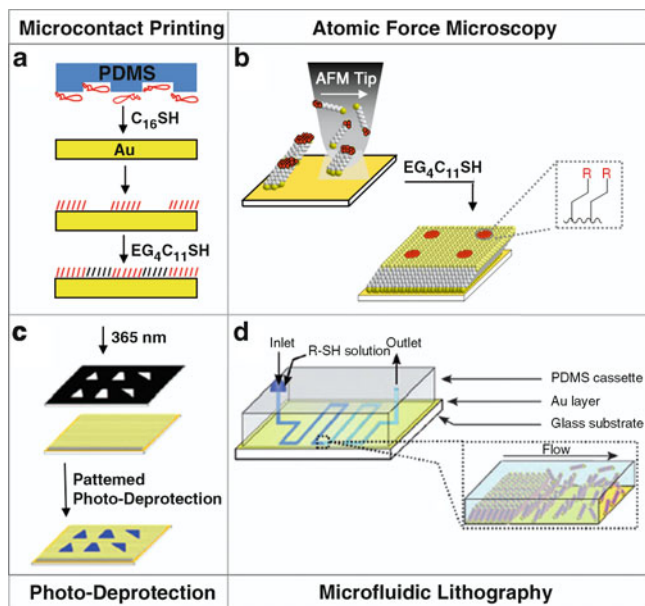
Strategy	Terminal group	Ligand	Coupling
Diels-Alder			
Click			
Maleimide			
Staudinger ligation			
Oxime			
Olefin metathesis			
Michael addition			

designed reaction conditions, these methodologies offer a direct route to generation of a covalent linkage between the terminal SAM group and the functionalized ligand. The Mrksich group has shown the use of maleimide-terminated SAMs for the coupling of thiol-containing peptides and carbohydrates to observe and quantify the effects and products of enzymatic glycosylation [56]. This same group developed the rapid reaction between hydroquinone-presenting SAMs and cyclopentadiene-functionalized peptides to perform cell adhesion studies [57]. To generate quantitative and chemoselective immobilization of ligands to surfaces, Chan and colleagues in the Yousaf group explored the reaction between quinone-terminated SAMs and soluble oxyamine-tethered peptides for protein and cell adhesion studies [58]. It is also possible to alter the terminal group functionality after SAM formation by applying an external stimulus to selectively activate the monolayer for ligand immobilization. For example the quinone-presenting SAMs used by Mrksich and Yousaf assemble, presenting the hydroquinone form, and must be electrochemically oxidized to the quinone before coupling with cyclopentadiene- or

oxyamine-containing ligands. Another report used microfluidics to selectively convert tetra(ethylene glycol)- and hydroxyl-terminated SAMs to aldehyde groups by chemical oxidation for subsequent reaction with oxyamine-containing molecules [59].

### 2.3 Patterning Methods

There has been much interest in developing strategies to spatially control the interface between biomolecules on a solid support for a number of applications ranging from the design of drug-delivery vectors and gene microarray technology to conducting mechanistic studies in cell motility. In combination with the synthetic advantages listed above, several patterning techniques have been adapted with SAMs on gold to enable the selective positioning and manipulation of ligands. The most common method of patterning SAMs, developed by Whitesides, is microcontact printing ( $\mu$ CP) (Fig. 2a) [8–10, 34]. This technique makes use of an elastomeric poly(dimethylsiloxane) (PDMS) stamp (with preformed microfeatures by soft lithography) to ink and transfer hydrophobic alkanethiols onto a gold surface. The surfactant molecules self-assemble instantly upon contact with the substrate, leaving a replica of the features. This method is inexpensive and easily reproducible and, therefore,  $\mu$ CP has been employed in numerous applications, such as patterning SAMs for cell adhesion studies, as well as printing functionalized biomolecules



**Fig. 2** Methods for patterning alkanethiolates on gold: (a) microcontact printing, (b) atomic force microscopy, (c) photo-deprotection, and (d) microfluidic lithography



for ligand immobilization. A similar SAM patterning technique was later developed in which microfluidics was used to form two dimensional SAM features on gold (Fig. 2d). This strategy, microfluidic lithography ( $\mu$ FL), first requires a PDMS microfluidic cassette to be sealed on the surface [29]. A solution of alkanethiol is then flowed through the channels, resulting in the rapid formation of patterned SAMs. Thus far,  $\mu$ FL has been employed to create dynamic SAM gradients for cell polarization, directed migration, and contiguous cell co-cultures studies. Other methods to pattern SAMs include several lithographic techniques such as photo- (Fig. 2c), electron-beam, X-ray, and dip-pen nano- (Fig. 2b) lithography [60–65]. Although most of these surface manipulations require expensive or custom instrumentation, patterns are able to be transferred and formed with high fidelity and resolution (10–30 nm) and only require extremely low sample volumes (nL).

## ***2.4 Analytical Techniques for SAM Characterization***

Planar SAM systems are compatible with a number of surface characterization and spectroscopic techniques. Methods such as ellipsometry, near-edge X-ray absorption fine structure spectroscopy (NEXAFS), reflectance absorption infrared spectroscopy (RAIRS), Raman spectroscopy, X-ray diffraction, and contact angle measurement have all been used to elucidate physical properties about the SAM thickness, tilt angle from the surface, and packing density. Other techniques aim to characterize terminal group transformations including X-ray photoelectron spectroscopy (XPS), infrared spectroscopy (IR), cyclic voltammetry (CV), and mass spectroscopy (MS) [66–73]. Since gold is conductive, electrochemistry has been used to activate SAMs for ligand immobilization, as well as monitor the reaction and calculate ligand density. Similarly, surface plasmon resonance (SPR) has been employed to monitor and calculate binding affinity for the biomolecular interaction between SAM-supported carbohydrates and soluble proteins on gold [58, 74, 75]. There are also several microscopic techniques available to SAMs on gold to aid in imaging and the observation of cell behavior and biomolecular interactions. Atomic force microscopy (AFM) has been employed to pattern SAMs, as well as to image adhered bacteria and cells [37, 38]. Other microscopy methods include total internal reflection fluorescence microscopy (TIRFM) [76], phase contrast and fluorescence microscopy, tunneling electron microscopy (TEM), and scanning electron microscopy (SEM) [77, 78].

## **3 Modulating Dynamic SAMs for Biological Applications**

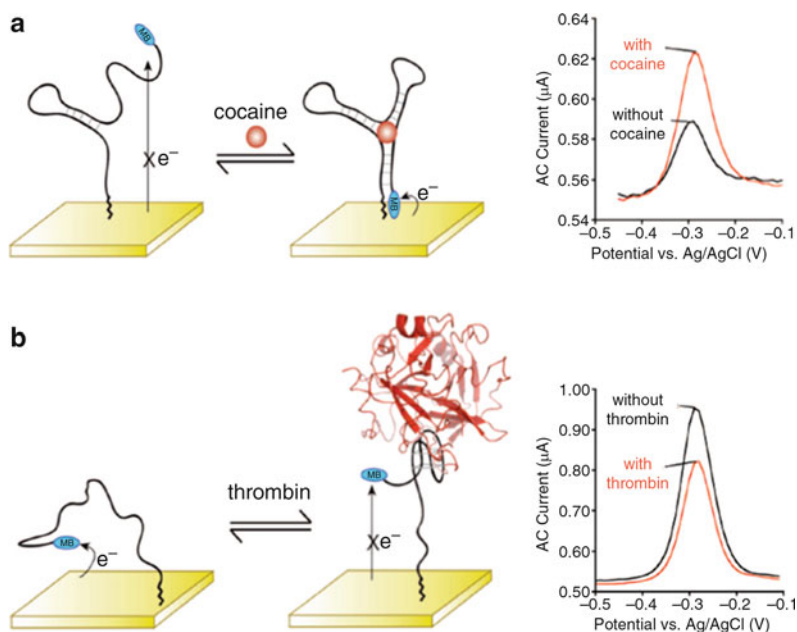
In recent years, there has been tremendous effort to develop materials that are dynamic, offering active control over presented ligands in situ [11–14]. Usually, the chemical and physical properties of the surface or molecules bound are changed by

applying an external stimulus. Some of the earliest studies reported the use of thermally responsive or photoactive hydrogels that were fine-tuned to promote specific cellular interactions while simultaneously discouraging other interactions during cell culture [79]. Other work that has attempted to mimic the dynamic environment of natural biological systems has demonstrated the use of electrochemical, pH, solvent, chemical, and biochemical control to regulate the activity and function of biomolecules. Stimuli-responsive materials are also important for the fabrication of sensitive and reusable biosensors with applications extending to clinical diagnostics, environmental monitoring [80], and DNA analysis [81–87]. SAMs of alkanethiolates on gold have naturally been integrated with this idea of dynamic modulation, due to their extensive characterization and known advantages, to serve as a model substrate for biological investigations. With the number of analytical tools, patterning techniques, and surface-coupling strategies compatible with SAMs on gold, as well as the nonfouling properties of oligo(ethylene glycol)-alkanethiol, SAM substrates provide a strong platform for the simulation and regulation of bioactivity and function. Therefore, SAMs have been implicated in several studies involving the molecular recognition and interactions between antigen–antibody [58], protein–protein, carbohydrate–lectin, cell–peptide, lipid–carbohydrate, and DNA–enzyme. Unlike the highly evolving environment of natural biological surfaces, SAMs are essentially static systems. Therefore, the development of dynamic substrates is crucial for understanding the mechanistic properties of fundamental biological processes and interactions.

### ***3.1 Stimuli-Controlled Dynamic Surfaces***

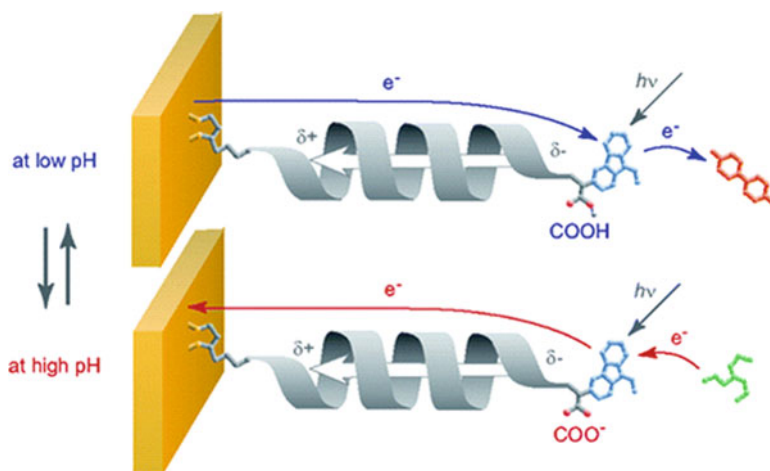
#### **3.1.1 Electrochemical, Biochemical, and pH Control**

Gold is conductive, and therefore serves as a useful platform for the design of sensitive, reusable, and real-time electrochemically-based biosensors for environmental monitoring, forensics analysis, and biochemical signal detection. There are a large number of electroactive molecules available to the SAM surface community that have displayed in situ, on and off switching capability when subject to a particular oxidation or reduction (redox) potential. In a set of experiments conducted by Rant and coworkers, DNA was assembled on gold substrates from an electrolyte solution [81–83]. Upon the application of alternating electrical potentials, the authors were able to induce the switching of the DNA conformation from a “lying” state at the surface of the electrode and a “standing” state perpendicular to the substrate. These reversible conformations were monitored by fluorescence in real-time. Plaxco and colleagues introduced a small biochemical signal to stimulate DNA hybridization and recorded the response by electrochemistry [84, 85]. The group created a specialized biosensor using a redox-tagged DNA aptamer for DNA hybridization experiments (Fig. 3). In developing the sensor, the authors first assembled a stem-loop oligonucleotide, possessing terminal thiol and ferrocene groups



**Fig. 3** Electrochemical aptamer-based sensor of redox-tagged DNA against specific targets. (a) When the aptamer comes in contact with a small molecule, in this case cocaine, it folds, and the redox tag is brought closer to the electrode, increasing the current. (b) When the aptamer comes in contact with thrombin, the tag moves away from the surface, decreasing the electrochemical signal. Reproduced from [85] with permission. Copyright: Langmuir, 2007

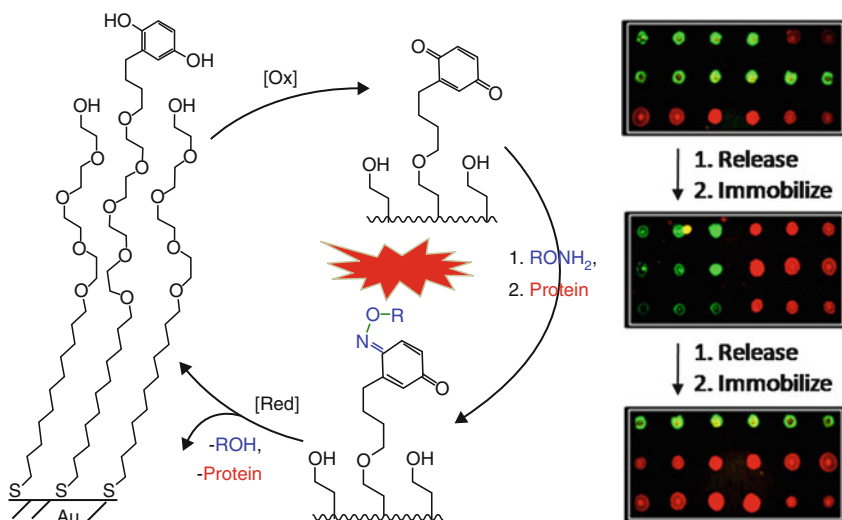
on gold. Without the addition of separate DNA sequence-target, the ferrocene is located close to the gold, resulting in a large current signal and efficient electron transfer upon a redox potential. However, when the target DNA sequence is added, it hybridizes with the stem loop, causing the ferrocene tag to move away from the surface resulting in a decrease in redox current. A similar system was later created to induce DNA folding, detected electrochemically after the addition of a protein, thrombin, and a small molecule, cocaine. A redox tag, methylene blue (MB) was conjugated to the DNA aptamer, which was then assembled on a gold electrode. After the addition of soluble cocaine, the electrochemical current increased, indicating that the interaction between DNA and cocaine caused the redox tag to come in close proximity with the surface. On the other hand, when thrombin was allowed to react with the DNA aptamer, there was a decrease in signal, indicating that MB moved further from the surface. Kong et al. reported fabrication of a similar biosensor design to modulate the adsorption and release of the proteins avidin and streptavidin by electrochemical stimulus [86, 87]. SAM conformations, with a terminal carboxylic acid or amino group, could be controlled by applying electric potential. When the terminal groups were forced to align “straight” from the surface, proteins adsorbed. However, reversing the potential caused SAMs to “bend” toward the electrode, resulting in the detachment of protein.



**Fig. 4** The pH-controlled switching of photocurrent direction in SAMs composed of helical peptides with a carboxylic acid terminal group. Reproduced from [91] with permission. Copyright: The American Chemical Society, 2005

The above-mentioned examples involved the combination of biochemical stimulus and electrochemical output to modulate and detect biomolecular responses. Changing the pH of the electrolyte solution in conjunction with electrochemistry can also be employed to promote and control biological behavior as well [88–90]. Yasutomi and coworkers reported being able to reversibly switch the photocurrent direction of helical peptides from anodic to cathodic by controlling the pH of the solution (Fig. 4) [91, 92]. Peptides were functionalized with a thiol side-chain carboxylic acid terminal group and were assembled on gold. The terminal group exists either as an acid at low pH or as carboxylate anion at high pH. It was found that an anodic photocurrent was generated at low pH, and a cathodic photocurrent was observed in a deprotonating pH, affecting the rates of electron transfer. A recent study by Angelos et al. reported the fabrication of a pH-responsive supramolecular nanovalve, based on a pseudo-rotaxane compound, for the controlled adsorption and release of luminescent molecules [93]. This system was created for testing the healthy and diseased states of cells *in vivo*.

There have also been a number of reports on the use of redox chemistry *in situ*, catalyzed by a chemical oxidant on or by applying electrical potential to the gold electrode, to activate a SAM functional group for the chemoselective coupling of ligands [28–30, 58, 59]. For example, Mendes et al. described the selective electrochemical conversion of NO<sub>2</sub>-terminated SAMs to NH<sub>2</sub> groups for subsequent immobilization of primary antibodies to observe the biospecific binding of proteins [94]. In a different series of experiments, Mrksich and coworkers demonstrated the novel utility of several redox-active SAM terminal groups, including quinone propionic ester [95], catechol orthoformate [96], and hydroquinone [57, 97, 98]. These molecules were turned on through electrochemical oxidation

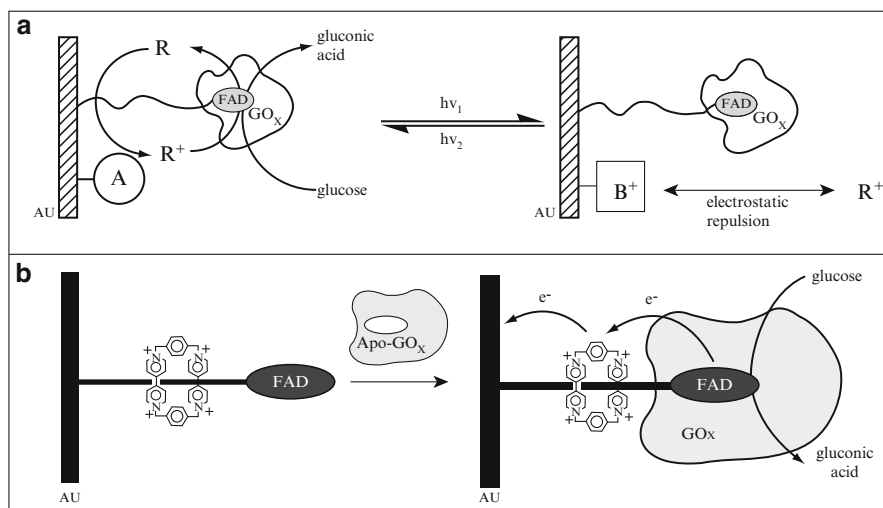


**Fig. 5** Reversible oxidation and reduction of electroactive SAMs to generate renewable microarray surfaces for bioanalysis (*left*). Corresponding fluorescent micrographs (*right*) depicting three cycles of carbohydrate and protein immobilization and release on the same substrate

to react with hydroxyl- and cyclopentadiene-conjugated ligands, and a variety of peptides and carbohydrates were presented from the surface and used for investigation into the mechanisms of cell adhesion, glycosylation, and protein binding. The Yousaf group further adapted the hydroquinone-based platform for reaction with oxyamine-functionalized biomolecules and added a ligand-release component, induced by applying reduction potential under physiological conditions (pH 7) [99]. With the release element, surfaces become reusable for multiple cycles of ligand immobilization, investigation, and release. One study demonstrated the use of hydroquinone-terminated SAMs to create a renewable microarray for the tethering of different carbohydrates and subsequent protein binding assay (Fig. 5). Sugars were released by applying a reductive potential, revealing the original SAM. Other reports have described the same system for generating complex, patterned substrates for studies in cell adhesion, polarization, and migration, which will be discussed in the Sect. 3.1.2 [28].

### 3.1.2 Photochemical Control

Dynamic SAM substrates can be engineered to respond to a light stimulus [27, 28, 31]. For example, photodeprotection strategies to reveal a key functional group in patterns for subsequent ligand coupling have been explored. A photomask of prefabricated features is placed on a surface with assembled mixed monolayers. Illumination with UV light at a particular wavelength catalyzes removal of a protecting group, exposing the desired functional group for bioconjugation [8–10]. This



**Fig. 6** Design of a photoswitchable GOx electrode with electron transfer mediator (a) ferrocenecarboxylic acid and (b) rotaxane-based molecule. (a) Reproduced from [100, 101] with permission. Copyright: The American Chemical Society, 1998. (b) Reproduced from [102] with permission. Copyright: Wiley-VCH, 2009

method is very useful for the generation of complex patterns and gradients for the study of cellular behavior in response to an adhesion molecule or chemoattractant and will be discussed further in the Sect. 3.1.3. Another use of light to modulate or turn on and off certain biointeractions was demonstrated by Blonder and colleagues with the design of a photoswitchable glucose oxidase (GOx) gold electrode for the bioelectrocatalytic oxidation of glucose to gluconic acid (Fig. 6a) [100, 101]. The photoisomerizable enzyme was assembled by reconstituting apo-glucose oxidase with semi-synthetic nitrospiropyran-FAD cofactor. Ferrocenecarboxylic acid acted as an electron-transfer mediator to aid in the biocatalysis of glucose oxidation. This same system was later tuned and made more efficient in carrying out the bioelectrocatalytic oxidation of glucose by threading the carbon-chain linker between the electrode and FAD through a rotaxane-based molecule (RBM) (Fig. 6b) [102]. Ferrocenecarboxylic acid was no longer needed due to the rapid catalyzed electron transfer mediated by the RBM around the reconstituted GOx sensor.

Sortino et al. reported the use of light irradiation on SAMs supporting the anticancer drug flutamide to study its photoreactivity and product release of nitric oxide. The authors were able to conduct studies in the absence of noxious side effects such as singlet-oxygen photosensitization and observed that nitric oxide production halted when the light was turned off [103]. Another photoactive molecule, azobenzene, has recently been exploited in the SAM community to aid in studies on cell adhesion and enzyme inhibition [104]. Pearson and coworkers described the use of photoisomerizable SAMs of azobenzene to conduct a series of serine and cysteine protease inhibition experiments. When light of 340–380 nm is used, the

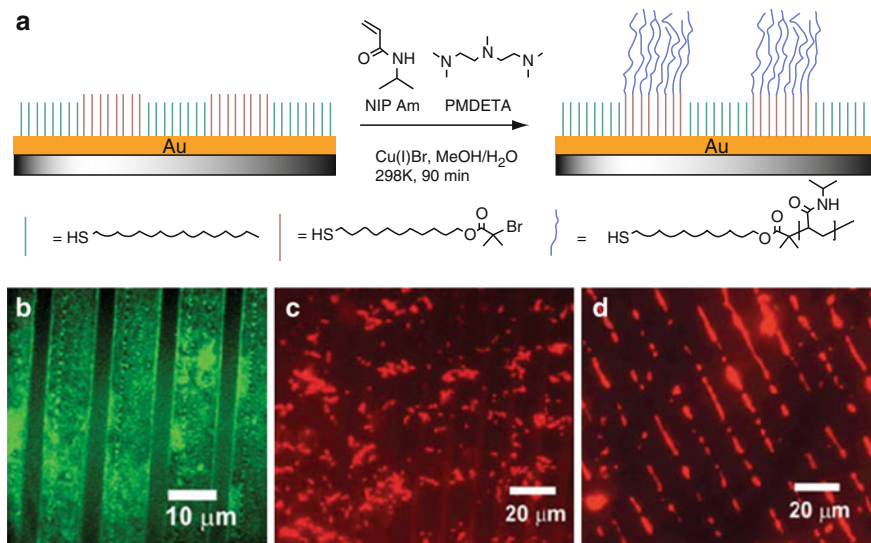
*Z* or *cis* conformation is adopted, burying the tethered-inhibitor within the monolayer and leaving it inaccessible to the serine protease,  $\alpha$ -chymotrypsin. However, when the wavelength is changed to 450–490 nm, the *E* or *trans* configuration is induced, exposing the inhibitor, which then facilitates binding of the protein. This general application can be further extended to small-molecule drug discovery for the synthesis and development of pro- and anti-drugs. Porphyrin monolayer-modified surfaces have potential utility in the development of artificial photosynthetic materials, photocatalysts, and chemical and biochemical sensors [105]. Rather than being activated by light to induce biological interaction or behavior, porphyrins serve as the photoactive molecule, overcoming the efficient photoquenching problem that gold creates when fluorophores come close to the surface, and may be used to fluorescently label proteins and cells.

### 3.1.3 Thermal Control

Applying the external stimulus of temperature is another method for modulating the biological activity on materials [106, 107]. Grunze and Jiang and colleagues conducted numerous studies to explore the physical assembly and nonfouling properties of SAMs of oligo(ethylene glycol) alkanethiol and their resistance to protein adsorption [108, 109]. They characterized the tilt angles and packing density of several differently numbered units of ethylene-glycol-containing compounds and then measured the effects of resistance to fibrinogen and lysozyme. It was concluded that surfaces remained inert, even with only two ethylene glycol units present. A separate study conducted by the Grunze group determined that there was a temperature dependence associated with protein and bacterial adhesion to oligo(ethylene glycol)-terminated SAMs [110]. The authors observed that SAMs no longer resisted pyruvate kinase, lysozyme, fibrinogen, and bacterial attachment when the temperature was increased to 37°C. However, when surfaces were cooled down to room temperature, these biomolecules detached from the substrate. Similarly, Okano and coworkers described that cell adhesion occurred at surfaces presenting the peptide Arg-Gly-Asp (RGD) at culturing conditions (37°C) [111]. However, when substrates were cooled to lower temperatures, cells spontaneously detached. More recent work used the temperature-switchable functionality of oligo(ethylene glycol)-containing SAMs to control the affinity binding of streptavidin to biotin-tethered surfaces. The interaction between streptavidin and biotin was turned on and off by changing the temperature of surface incubation.

Thermally responsive polymers, such as poly(*N*-isopropyl acrylamide) (NIPAm), have also been studied extensively for applications related to those previously discussed [112]. De las Heras et al. described the synthesis and patterning of NIPAm brushes on SAMs and their subsequent performance during temperature-dependent adhesion assays of BSA and *Streptococcus mutans* (Fig. 7). The authors employed  $\mu$ CP to pattern features of hydrophobic hexadecanethiol and backfilled the surface with an initiator-functionalized alkanethiol. Polymer brushes were grown via surface-initiated atom transfer radical polymerization (ATRP). FITC-BSA was then





**Fig. 7** (a) Growth of temperature-dependent, patterned polymer brushes on SAMs on gold surfaces. Images show adhesion of (b) FITC-BSA after incubation at 37°C and rinse at 12°C; (c) *S. mutans* after incubation at 4°C for 1 h; and (d) *S. mutans* after incubation at 37°C for 1 h. Reproduced from [112] with permission. Copyright: The Royal Society of Chemistry, 2005

incubated with the substrates for 1 h at 37°C and rinsed at either 12° or 40°C. Little to no BSA adsorption was observed on the polymer brushes after washing surfaces at 40°C, as opposed substrates washed at 12°C (Fig. 7b). Temperature had a greater effect on *S. mutans* adhesion studies. Bacteria had no preference for attachment (polymer brushes or hydrophobic SAM) when cultured at 4°C for 1 h (Fig. 7c). However, when incubated at 37°C for 1 h, *S. mutans* adhered only to the NIPAm-presenting patterns (Fig. 7d). Ultimately, it was demonstrated that biomolecular adhesion could be thermally switched on and off when the same surface, containing patterned bacteria, was again incubated at 4°C, followed by incubation at 37°C, resulting in detachment from and readsorption to the polymer brushes, respectively.

## 4 Dynamic Surfaces for Cell Biology

Cells exist in a complex, dynamic, and highly evolving environment, a key component of which is the ECM [113–115]. The ECM provides structural support for the cell, and also contains a host of supramolecular assemblies of proteins and glycosaminoglycans, which play a vital role in cell development. In order to undergo a fundamental biological process, cells must adhere to the underlying ECM. Cells then migrate from the various epithelial layers to target locations, where they then

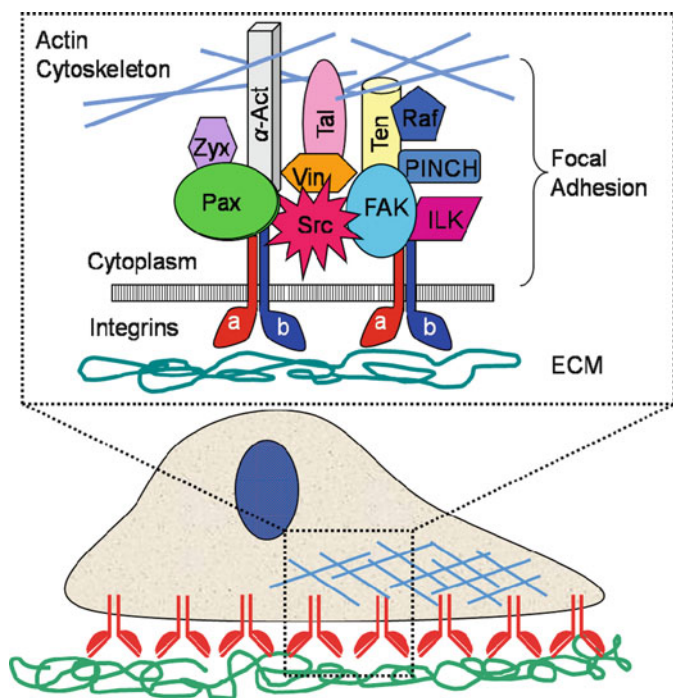


differentiate to form specialized cells that make up different tissues and organs. As a result, cell adhesion and migration are important to processes such as embryogenesis [116], normal tissue repair [15] and the immune response [16, 17], wound healing [18, 19], and angiogenesis [20, 21]. Moreover, improper cell adhesion and migration has been implicated in disease states such as tumor invasion in cancer cell metastasis [22–26]. Depending on the processed signal, the cell will reorient its machinery toward a specific direction and begin migration by forming extensions of the leading edge of the cell membrane while releasing contacts in the rear of the cell body [117, 118]. The complexity and highly evolving nature of biological surfaces make it difficult to study these fundamental processes. Understanding the mechanism of cell adhesion, polarization, and migration will have broad impacts for many research communities, such as medicine and developmental biology. With the ability to model and dynamically modulate the cellular environment and having a well-defined composition, SAMs on gold surfaces represent an ideal platform for conducting detailed mechanistic studies of biomolecular recognition in cell adhesion, polarization, and migration [8–14]. The organic coupling strategies amenable to thiol chemistry permit a vast variety of biomolecules to be tethered to the surface, as well as to be confined to selective regions so that the specific interaction can be observed. In addition to creating protein- and cell-resistant SAMs, gold is compatible with cell culture. Another advantage to this model system is the wide range of analytical techniques available to characterize the cellular behavior.

#### ***4.1 Integrins, Signaling, and ECM Interactions***

In order for cells to migrate *in vivo*, they must first adhere to the ECM through ligand–cell interactions [119]. Although there are many proteins that facilitate this process, integrins represent a family of cell-surface receptors that specifically mediate the attachment of a cell to another cell or to the ECM. Structurally, integrins are heterodimeric, transmembrane glycoproteins that consist of  $\alpha$  and  $\beta$  subunits. There are 18  $\alpha$ - and nine  $\beta$ -subunits and a total of 24 integrin heterodimers known. This chemical diversity gives rise to biological complexity, and thus integrins have been implicated in numerous functions including cell–ECM and cell–cell adhesion, organization of actin filaments, signal transduction, cell survival, cell growth and differentiation, and unique roles in developmental processes [120, 121].

Despite this complexity, most integrins share two, key interrelated functions: first, to promote the assembly and organization of the actin cytoskeleton [122, 123]; and second, to regulate signal transduction cascades [124–126]. Spanning the cell membrane, these subunits serve as a communication pathway, linking the actin cytoskeleton and intracellular cytoplasmic proteins involved in focal adhesion complexes (FACs) with the cell's dynamic extracellular environment (Fig. 8) [127–130]. There are at least 50 distinct proteins known to be involved in FACs. Actin [131], vinculin, talin, tensin,  $\alpha$ -actinin, and filamin provide a structural role, while focal adhesion kinase [132], integrin-linked kinase, Src-family kinase, PINCH, paxillin



**Fig. 8** Simplified schematic of cell adhesion through integrin-mediated communication with the ECM, cytoplasmic proteins, and the actin cytoskeleton in formation of a focal adhesion complex

[132, 133], and G-proteins have been identified as serving regulatory roles in signaling cascades. As mentioned, integrins serve as the link between these internal proteins and enzymes and the outside environment of the cell. Depending on the strength of the ECM interaction, integrins may be loosely connected through a meshwork of filaments at the leading edge or strongly adhered by robust actin fibers or fibrillar adhesions. These interactions affect the rate of cell motility. The short peptide sequence RGD was identified as a binding motif in several ECM components including fibronectin (Fn), fibrinogen, vitronectin, laminin, and some collagens [134–136]. Most of the known integrin receptors recognize the RGD sequence when binding to ECM ligands. With the advent of live-cell imaging, the temporal distribution of integrin complexes could begin to be addressed [137]. It is now clear that the various adhesive structures dynamically mature from nascent structures at the edge of the cell to the larger interior structures, such as FACS. In a migrating cell, there is also loss of adhesion at the trailing edge that involves a combination of regulated proteolysis of integrins and associated proteins, as well as physical tearing. Although previous studies have provided a great deal of information about how cells dynamically control the cytoskeleton–integrin linkages in space and time, new methodologies will be needed to advance our understanding of this process.

### 4.1.1 Cell Polarization and Reorganization

The ability to polarize has been shown to be important in a wide range of cell types, from simple budding yeasts to specialized eukaryotic cells [138–140]. As such, polarization is fundamental to a number of cellular processes and an essential step in directional migration. In vitro wound healing assays demonstrate that after manual disruption of the cell monolayer, the microtubule-organizing center (MTOC), nucleus, and the Golgi apparatus reorient toward the direction of the artificial wound [141]. It has also been shown that when treated with microtubule-depolymerizing drugs, these key organelles are inhibited from reorganization and, subsequently, migration is halted. During most migration processes, the MTOC and Golgi reorient toward the leading edge of the cell, in front of the nucleus, in response to received and integrated intracellular signals [142, 143]. The leading edge of the cell is characterized by the presence of protrusions of the plasma membrane; flattened, wide projections known as lamellipodia, and the smaller, spike-like filopodia. These membrane extensions and leading-edge dynamics are driven primarily by actin polymerization, which in turn is dependent on a variety of signaling pathways.

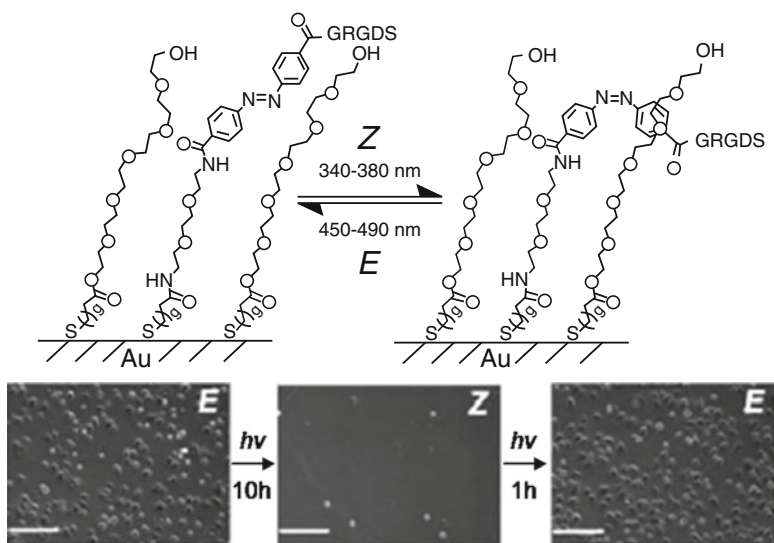
## 4.2 SAMs as Dynamic, Model Substrates for Cell Biology

In order to study the mechanism of cell adhesion, polarization, and migration, we must choose a model platform. For some time, SAMs of alkanethiolates on gold have served as such a model due to a number of factors [8–14]. For one, gold is compatible with cell culture and is nontoxic to cells. The inherent conductivity of gold permits compatibility with a number of characterization and analytical tools (SPR, ellipsometry, electrochemistry, MS), providing a wide range of methods to study cell behavior, as well as the kinetics and thermodynamics of binding events. In addition to the well-defined structure of SAMs, thiol chemistry is synthetically flexible for the specific tailoring of biological ligands through chemoselective conjugation. There are several known patterning techniques to probe the effects of ligand affinity and density on cellular behavior. Also, tetra(ethylene glycol) alkanethiol is known to resist nonspecific adsorption of proteins and cells in order to isolate selective biointeractions on the surface. In fact, early work has shown that mixed monolayers of 1% functionalized alkanethiol and 99% tetra(ethylene glycol) alkanethiol is able to resist protein adsorption until its key biological ligand is tethered from the surface [8–10, 13, 14]. Westcott and coworkers demonstrated that through the controlled oxidation of a tetra(ethylene glycol)-terminated SAM, approximately 1% aldehyde groups were generated and able to resist cell adhesion until cell-adhesive peptide RGD was immobilized to the surface [59]. One limitation to this system is that the gold–thiol bond becomes unstable and can oxidize under cell culture and ambient atmosphere after several days, making it difficult to conduct longer biological studies [144]. Also, the structure of the SAM is essentially static, rather than fluid like the

cell membrane. Addressing this issue, there have been many reports of patterning lipid bilayers to support a more fluid and dynamic surface for cell attachment [145–147].

The term “dynamic surface” refers to the ability to modulate and control biological interaction and cell behavior in response to an applied stimulus that aids in mimicking the dynamic properties of a biological system. For example, a change in pH, temperature, or biochemical signal may affect the cells’ ability to adhere to the surface. Lee and colleagues showed healthily growing cells, confined to microcontact printed regions of Fn (unpublished results from this laboratory). The remaining SAM was backfilled with quinone- and tetra(ethylene glycol)-terminated alkanethiol (1:99) to resist cell adhesion until oxyamine-conjugated RGD peptide was added to the culture. The RGD reacted with quinone molecules on the surface, and within hours of immobilization, cells began to migrate out of the patterns and spread. Similarly, Liu and colleagues demonstrated that cell adhesion can be modulated by photochemical control of azobenzene SAMs on gold (Fig. 9) [148]. When SAMs adopt the *E* configuration at 450–490 nm, RGD is displayed, and cells adhere and grow. Under illumination with light at 340–380 nm, azobenzene converts to the *Z* conformation, masking RGD, and cells are prevented from attaching to the surface.

Extensive work has shown that, through control of electrochemical potential, a monolayer presenting electroactive molecules can undergo reversible oxidation



**Fig. 9** Reversible cell adhesion by photochemical control of azobenzene SAMs on gold. Interconversion of *Z* and *E* configurations (top). Cell adhesive peptide, RGD, is displayed when SAMs adopt the *E* configuration at 450–490 nm, and cells adhere and grow (bottom left and right). At 340–380 nm, azobenzene converts to the *Z* conformation, masking RGD, and cell adhesion is prevented (center bottom). Reproduced from [148] with permission. Copyright: Wiley, 2009

and reduction to modulate their ability to react with other biomolecules, thus dynamically modulating cell adhesion and migration [27–29, 37, 38, 50–52]. It was shown that biotin could be released by an electrochemical reduction of a quinone propionic ester moiety to result in a lactonization reaction [95]. Another study used mixed SAMs of penta(ethylene glycol)- and hydroquinone-terminated SAMs that, when oxidized with an electrochemical potential, converted SAMs to the quinone to permit a Diels–Alder-mediated cycloaddition of cyclopentadiene-conjugated RGD to turn on cell adhesion, spreading, and migration [57]. Other reports have demonstrated the electrochemical release of ligands to turn off cell adhesion [13, 14, 50–52]. Chan and Yousaf also utilized the electroactive behavior of hydroquinone-terminated SAMs to immobilize and pattern oxyamine-containing RGD for the adhesion of fibroblast cells. After the substrate was subject to electrochemical reduction under physiological conditions, the RGD ligand was released, and the cells detached from the surface. Moreover, the ability to create and tailor dynamic surfaces for control of the complex cellular microenvironment has proven important for a range of scientific disciplines, such as biomedical and tissue engineering and cell biology [27, 28, 30, 31, 39]. The multitude of literature devoted to the use of SAMs of alkanethiolates on gold to research key biological problems indicates its broad applicability and proven performance to serve as a model platform for such studies.

#### 4.2.1 Microscopy Techniques to Study Cell Biology

There are several available microscopy techniques to investigate cellular behavior, which have been used to image organelles, protein–cell and protein–protein interactions, as well as cellular and protein dynamics [149–151]. SEM and TEM have been used to observe cellular structure on SAMs; however, in order to image, cells must be cryogenically frozen and fixed [152]. Mirkin had great success in demonstrating that, through the use of an AFM tip, nanofeatures of alkanethiols can be patterned to form a SAM on bare gold for the immobilization of biomolecules and cells [153, 154]. This technique was later employed to provide lateral force images of the newly patterned surface [37, 38]. In addition to imaging cells under culture conditions, phase contrast microscopy has proven to be invaluable for recording movies of cellular behavior [30, 149]. During the 1990s, Yamada, Grant, and Bowditch and colleagues conducted a series of experiments and reported that, along with the known cell-binding site that displays the RGD sequence found in tenth type III domain of Fn, there exists a synergistic site in the ninth type III domain necessary for obtaining maximal cell-binding activity [155–157]. The signal peptide to induce such behavior was isolated and determined to be Phe-His-Ser-Arg-Asn (PHSRN) and, although it is incapable of supporting adhesion on its own, it has been seen to enhance cell attachment and spreading in combination with RGD. Interrogation of this relationship has since been adapted with SAMs of alkanethiolates on gold to study and image the differences in cell protrusions and migration rates

when cultured on surfaces presenting RGD and PHSRN, alone or in different ratios. Phase contrast imaging was able to determine that, on RGD, cells produced focal adhesions at the end and periphery of stress fiber bundles, leading to a rigid body and slower migration rate. On the other hand, cells on PHSRN alone, formed less stress fiber bundles and had longer and thicker adhesion structures at protrusion tips with faster migration rates.

In particular, fluorescence microscopy serves as a major research tool for studying cell biology [137, 150]. However, gold substrates absorb the low-intensity fluorescence within the cells' excitation wavelength used for live-cell fluorescence imaging, causing efficient quenching of the fluorescent molecules [8–10]. Therefore, its integration with SAMs on gold remains difficult, and specific measures must be taken to ensure circumvention of this technical obstacle. It has been reported that a thin layer of gold ( $\leq 10$  nm) produces optically semitransparent substrates compatible with immunofluorescence staining [8–10]. Hahn and Yousaf and coworkers also overcame the fluorescence quenching limitation by applying a substrate-inversion technique to observe protein–cell dynamics and image cellular organelles [158]. By combining surface chemistry with a fluorescence resonance energy transfer (FRET)-based biosensor, the dynamics of RhoA (a small GTPase protein known to regulate the actin cytoskeleton in the formation of stress fibers) activation and inactivation in cell protrusions were observed (Fig. 10a–c). Through measuring the FRET signal intensity, it was found that RhoA activity is much higher at the periphery of the cell relative to within the cell body.

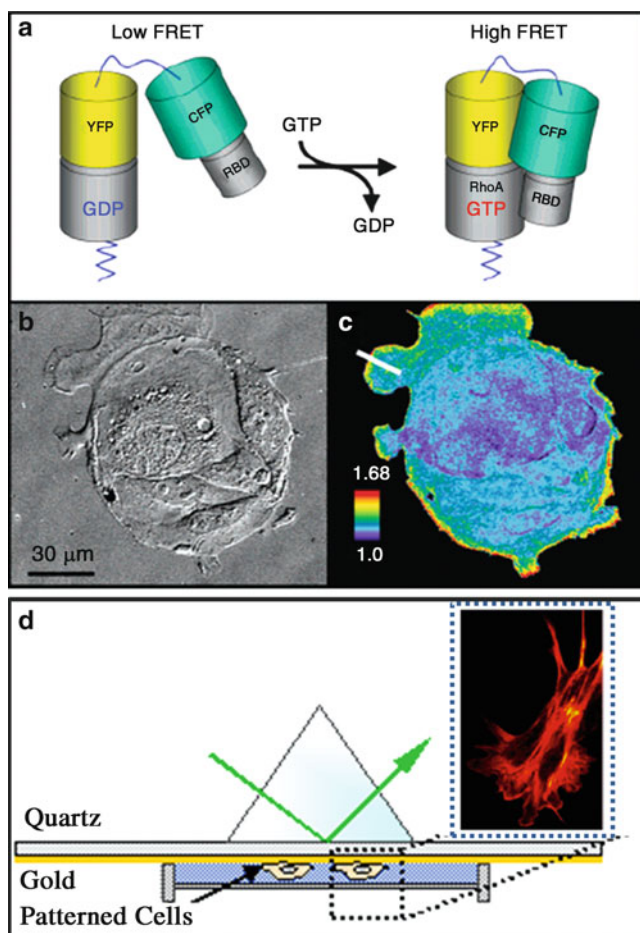
A similar study was performed in which microcontact printed regions supported Fn-mediated cell adhesion, and focal adhesion contacts between the cell and its matrix were imaged by total internal reflection fluorescence microscopy (TIRFM) (Fig. 10d) [159]. This technique is generally employed to study events at the cell plasma membrane on quartz and is based on the principle of total internal reflection; it has also been interfaced with other microscopy methods. It was recently reported, however, that TIRFM can be integrated with SAMs on gold when the surfaces are inverted. A thin layer of gold was evaporated onto a quartz substrate, and fibroblast cells were patterned and allowed to spread, followed by fixing, staining, and imaging for focal adhesions between the cell and its Fn matrix. This initial study may further be explored in order to interface TIRFM with material science for studies in cell signaling and more complex cellular behavior.

### ***4.3 Applications of Dynamic Surfaces***

#### **4.3.1 Cell Adhesion**

In order for cells to receive directional cues for migration, they must first adhere to the underlying matrix through ligand–integrin recognition [119]. Whether the integrins connect loosely through a meshwork of filaments at the leading edge or adhere strongly, forming fibrillar adhesions, is highly influenced by the ligand-binding





**Fig. 10** Examining RhoA activation using a FRET biosensor in cells on patterned hydrophobic SAMs after microcontact printing: (a) FRET biosensor with RhoA-citrine conjugated to yellow and cyan fluorescent protein (*YFP* and *CFP*, respectively) and a small binding domain derived from the RhoA effector protein Rhotekin. (b) Differential interference contrast image of cells expressing the RhoA biosensor. (c) Ratiometric image of FRET emission over CFP emission. Reproduced from [158] with permission. Copyright: The American Chemical Society, 2007. (d) Separate study using TIRFM to examine the nanoarchitecture of cell adhesion on SAMs on a gold-coated quartz surface. Reproduced from [159] with permission. Copyright: Langmuir, 2009

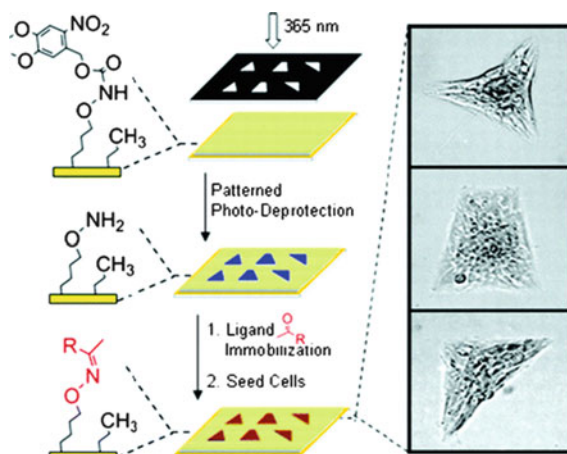
affinity. Much research has been devoted to the elucidation of focal contact structure, strength, and phenotypic response to different ligands and environmental cues [127–130]. Since this is the first step in cellular migration, understanding the mechanism of adhesion is important for a number of fields in biotechnology and developmental biology. In order to study specific biomolecular recognition events between ligands and cells on SAM substrates, a number of organic coupling reactions and

patterning techniques have been developed to immobilize the molecule of interest and observe the cells' biochemical response to that particular stimulus. The use of oligo(ethylene glycol)-containing alkanethiols to serve as an inert background to nonspecific protein and cell adsorption is also of advantage to this platform. The combination of a nonfouling background and the spatial and geometric confinement the cell–ligand interaction influence cell shape and morphology, and thus provide a sound basis for the design of cell structural, differentiation, and motility assays.

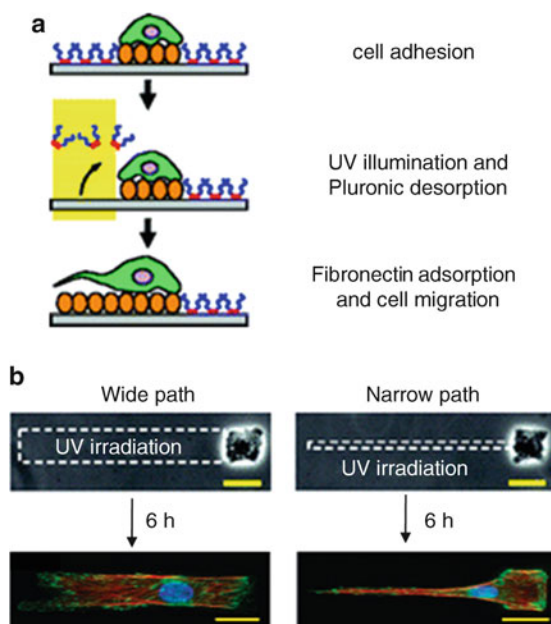
$\mu$ CP is often used to print a SAM on gold that can support protein or ligand-mediated cell adhesion [160]. The substrate is then immersed in a solution containing oligo(ethylene glycol)-terminated alkanethiol to backfill and render the remaining surface biologically inert [161]. Hydrophobic alkanethiols support the adsorption of Fn and other ECM proteins, which induce cell binding through integrin recognition and, therefore, many studies involving  $\mu$ CP as a patterning technique use hexadecane or dodecane alkanethiols. In a recent publication, Xia and colleagues used  $\mu$ CP to create a variety of Fn nanoarrays with differently sized and spaced features to direct NIH cell motility through focal adhesion positioning and spatial control of Rac (a Rho-family GTPase) activation [162]. Immunofluorescence microscopy confirmed that focal adhesion sites were concentrated along the cell periphery and that Rac was activated shortly after peripheral membrane extensions spread to new Fn islands. Mrksich's group employed  $\mu$ CP to survey lamellipodial response and distribution of B16F10 cells to local and global geometric cues, demonstrated by cortactin heat maps from cell populations. They found that local cell curvature influenced directed migration, as well as polarity [163–165].

Photodeprotection strategies have also proven useful for patterning cell-binding areas and gradients in which an alkanethiol is functionalized with a protecting group that is photolabile at a certain wavelength (e.g. *o*-nitroveratryloxycarbonyl, NVOC). Park et al. reported the synthesis and application of a photodeprotection method to reveal oxyamine-terminated groups in different geometric patterns and gradients by UV irradiation at 365 nm (Fig. 11) [31]. RGD-ketone was immobilized, followed by ligand-mediated cell adhesion. Phase contrast images displayed cell spreading within the confines of each shape, as well as the formation of thin appendages of the periphery of the pattern. Similarly, Kaji et al. used a microelectrochemical approach to reveal and pattern binding sites, inducing the local adhesion and growth of HeLa cells [166]. Using substrates coated with bovine serum albumin (BSA), known to resist cell adhesion, a quick oxidation pulse of a scanning microelectrode dosed with HBrO was applied to create a range of microfeatures that turned on cell-binding events [167]. A unique combination of both  $\mu$ CP and photoillumination was demonstrated by Maeda's group to stimulate adhesion and directed migration (Fig. 12) [168, 169]. Single cells were first patterned on  $\mu$ CP islands supporting Fn. The underlying SAM in a narrow and wide path was then desorbed by UV irradiation at 365 nm, and Fn was added to the surface. The Fn adhered only to the specific pattern illuminated by light, and cell polarization and directed migration was observed.





**Fig. 11** Mixed SAMs of NVOC-protected oxyamine- and methyl-terminated alkanethiolates (*left*) are selectively photodeprotected after shining light (365 nm) through a photomask of prepatterned microfeatures (*center*), and the oxyamine terminal groups are reacted with ketone-conjugated peptide (RGD) for cell adhesion studies. Phase contrast images (*right*) show cell spreading within each shape. Reproduced from [31] with permission. Copyright: Langmuir, 2008



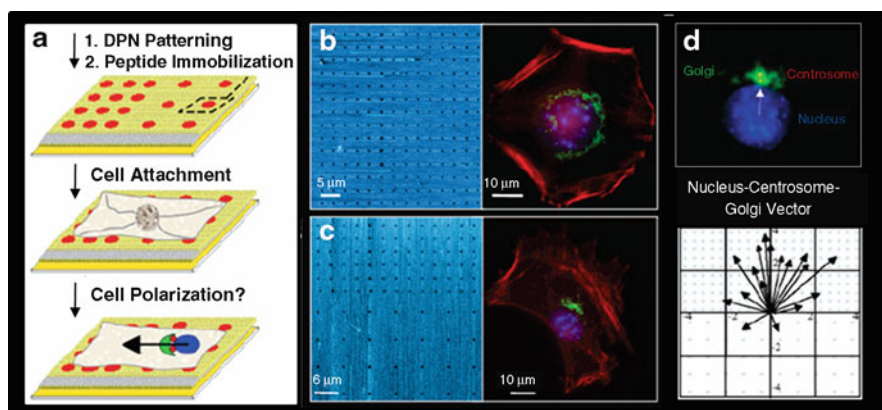
**Fig. 12** Photostimulated cell migration on a SAM substrate: (a) cells adhere, and illumination with light at 365 nm creates either a wide or narrow path. (b) Cells are allowed to migrate along the wide or narrow pathway (for 6 h) and then imaged by fluorescence microscopy. Scale bars represent 25  $\mu\text{m}$ . Reproduced from [168] with permission. Copyright: The American Chemical Society, 2007

### 4.3.2 Cell Polarization and Cell Migration

After a cell adheres to either another cell or the underlying matrix, it communicates with and integrates signals from its surrounding environment before it migrates toward a particular stimulus. After the cell receives a directional cue, it must polarize and reorient its machinery toward the direction of migration [138–143]. The simplest definition of cell polarization is the establishment of morphologically and functionally distinguishable regions of the internal structures of the cell. Several studies have been aimed at creating biospecific gradients of ECM proteins, other cells, or other cell-surface receptor-type molecules on SAMs on gold [27–31]. Thus, polarization is fundamental to a number of cellular processes, yet the mechanism is not fully understood and SAMs have been integrated to address this phenomenon. Until recently, many of the fundamental studies of cell polarization have been performed using wound-healing assays, as previously described. Hoover and colleagues adapted Mirkin's dip-pen nanolithography (DPN) technique to pattern hydroquinone-terminated alkanethiol on bare gold using an AFM tip [37, 38]. Electrochemistry was then used to activate arrays for ligand immobilization. In the first study, the authors patterned cells to symmetric nanoarrays to observe the differences in focal adhesion contacts of adhered cells to linear-RGD and cyclic-RGD. Cells on cyclic-RGD demonstrated more spreading and focal adhesion formation throughout, whereas on linear-RGD, cells made focal contacts only the periphery due to the higher affinity of cells for cyclic-RGD (nM) as opposed to linear-RGD ( $\mu$ M). A diffusive Golgi apparatus for both substrates was also seen. The authors then looked further into the mechanism of polarization by patterning asymmetric nanoarrays of immobilized linear-RGD (Fig. 13). After fluorescently labeling and imaging the MTOC, Golgi apparatus, and actin cytoskeleton, it was concluded that there was a distinct polarization vector formed toward the higher density regions containing the cell-adhesive peptide signal. This was indicated by the reorganization of actin cytoskeleton and positioning of the Golgi apparatus in front of the nucleus toward the higher density ligand, which is hypothesized to occur during polarization.

### 4.3.3 Molecular Surface Gradients and Cell Behavior

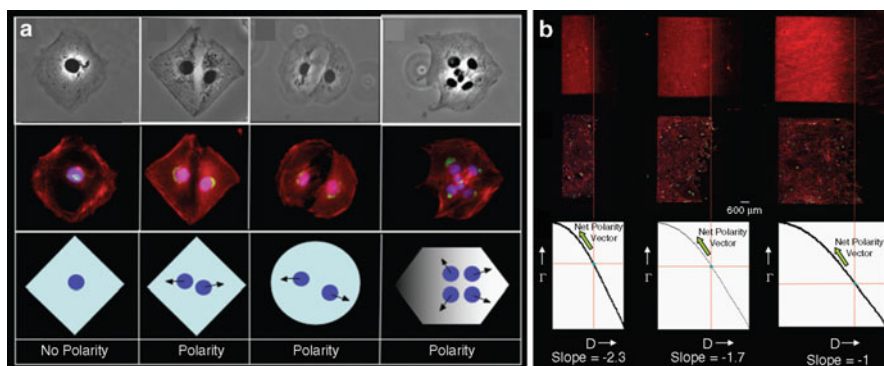
In vivo, cell outgrowth and directional migration usually occur up a concentration gradient of soluble adhesion sites (chemotaxis) or surface-bound chemoattractants (haptotaxis) [170, 171]. These biomolecular gradients are naturally present in the ECM and are critical during early and subsequent developmental stages of a cell's life, as well as during tumor invasion and metastasis. When subject to these gradients of extracellular signals, ligand- and receptor-mediated interactions cause the cell to polarize, resulting in activation and reorganization of organelles and cytoskeletal components. This process then initiates a specific cellular behavioral response. There has been some research toward the creation of artificial gradients



**Fig. 13** Comparative study of symmetric and asymmetric electroactive nanoarrays for the study of cell adhesion and polarization: (a) DPN was used to pattern a SAM nanospot of hydroquinone-terminated alkanethiolates for subsequent RGD immobilization and cell adhesion. (b) Lateral force microscopy image of a symmetric nanoarray (*left*) and fluorescent cell having a diffusive nucleus-centrosome-Golgi vector that indicates no preferential migratory direction (*right*). (c) Cell polarity vectors orient toward the direction of higher RGD density on asymmetric nanoarrays. (d) Higher magnification of the cell polarization vector (*above*) and its schematic (*below*). Reproduced from [37, 38] with permission. Copyright: The American Chemical Society, 2008

on biomaterials. For example, McCarthy and coworkers showed that altering the concentration of substrate-bound laminin, an ECM protein that interacts with integrin receptors and promotes cell adhesion, induced directed RN22F cell migration toward the higher amounts of laminin [170]. They also observed that flowing soluble laminin over attached cells had no effect on the motility rate and that the magnitude of cellular response could be altered by changing the relative density of bound laminin. A similar study using a concentration-dependent gradient of surface-bound proteoglycans (PG) that promote polyvalent interaction of the cell with other ECM components and neighboring cells was conducted by Cattaruzza and Perris [171]. It was found that in contrast to the response to Laminin, cells migrated away from areas of immobilized PG if they sensed a higher density of bound or soluble chemoattractant nearby. Although these studies provided invaluable information into the mechanism of directed-cell mobility, the gradients were not well-defined or quantitatively characterized.

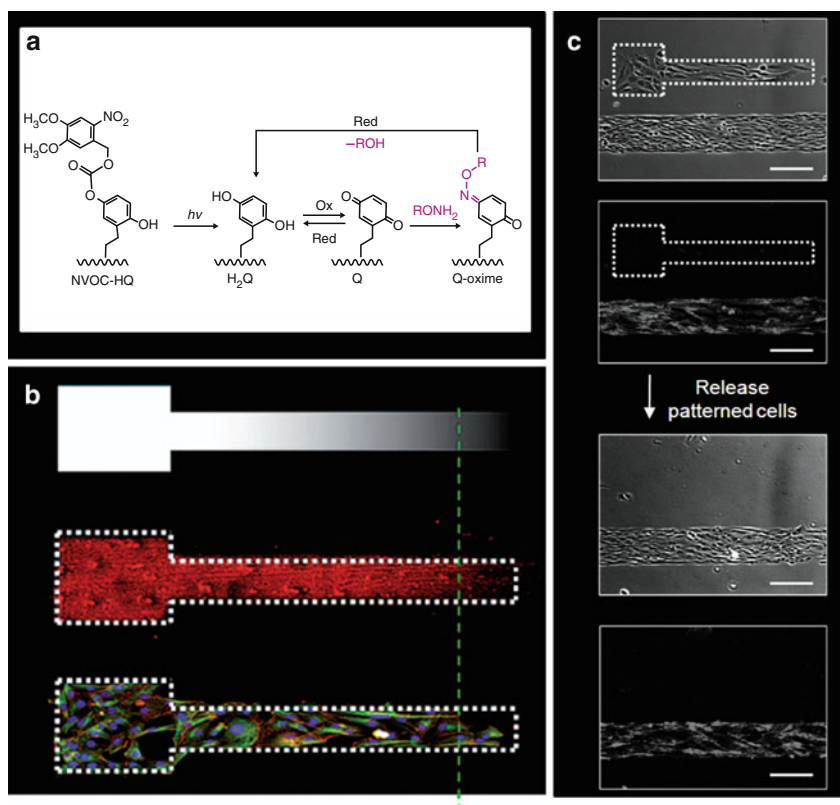
To address this issue, several experiments generating dynamic gradients of SAMs or biomolecules with spatial and temporal control on surfaces supporting SAMs have been reported in studies on cell polarization and migration [27–31]. Chan and coworkers published a series of studies that used a combined photodeprotection and electrochemical methodology to probe the interplay between cell–cell and cell–matrix interactions and the effects on polarization and migration [27]. In the first report, the authors patterned ligands and single and multiple cells on complex geometries, gradients, and overlapping patterns using a number of fabricated



**Fig. 14** Photochemical and electroactive SAM-based strategy to study the polarization of cells on different (a) geometries and (b) spatially controlled gradient patterning. Reproduced from [27] with permission. Copyright: The Royal Society of Chemistry, 2008

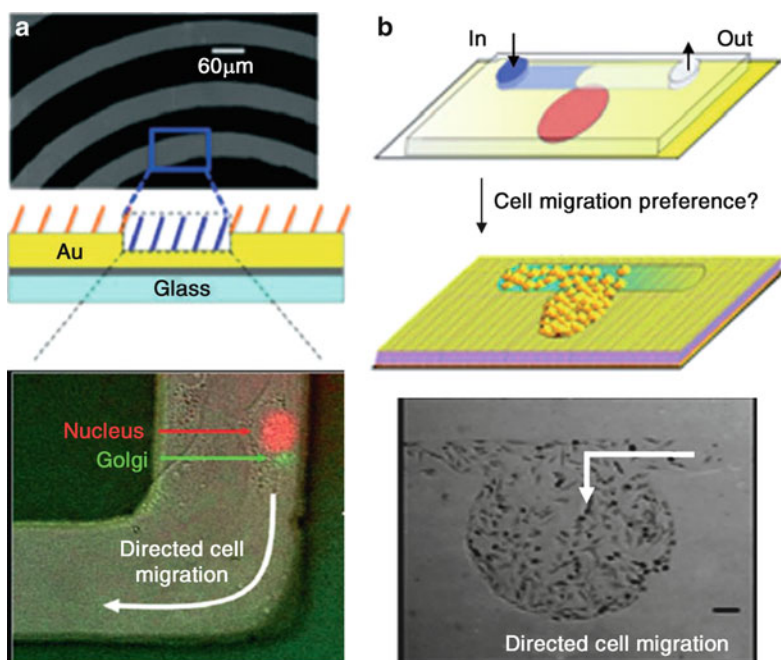
photomasks that reveal hydroquinone-terminated alkanethiols after irradiation at 365 nm (Fig. 14a). It was observed that a single cell adhered to a symmetric pattern has no net polarity, and reorganization of the nucleus, Golgi apparatus, MTOC, and actin cytoskeleton does not occur. However, when a second cell was introduced on the same pattern, cells polarized in opposite directions, away from one another. This was also seen on a different geometric pattern with four cells, displaying four net polarity vectors pointing in opposite corners, away from one another. It was also concluded that with a high cell density on patterned gradients of substrate-bound RGD, the cell–cell contacts override cell–matrix interactions, and directed cell migration was not observed (Fig. 14b). A further study performed by the same authors demonstrated the use of  $\mu$ CP and photodeprotection to pattern and reveal gradients for the investigation of cellular behavior of co-cultures (Fig. 15c) [28]. Transfected mouse fibroblasts expressing Green Fluorescent Protein (GFP)–actin were first patterned on Fn-containing patterns. A photomask was then used to reveal a gradient of hydroquinone-terminated alkanethiol that was subsequently conjugated with RGD-oxamine. A nonfluorescent fibroblast cell line was then cultured on and adhered to the gradient of RGD, most densely populating the higher concentrated areas of the pattern, rather than cohabiting the fluorescent population. Electrochemical-induced release of RGD forced detachment of the cells adhered to the gradient, leaving the population interacting with Fn attachment.

Another strategy that has proven to be powerful in the creation of gradients is microfluidic lithography ( $\mu$ FL), described by Lamb and coworkers [29, 30]. In a series of publications, these authors conveyed the fabrication and use of PDMS elastomeric microfluidic cassettes to generate chemoselective SAM patterns and gradients. In the initial report, a solution of hydroquinone-containing alkanethiol was flowed through the microchannels in a controlled manner, forming a SAM gradient, and RGD was immobilized (Fig. 16b).  $\mu$ CP of circular patterns and



**Fig. 15** Photochemical and electroactive SAM-based strategy to generate a cell co-culture platform with spatially controlled gradient patterning: **(a)** Activation of hydroquinone-terminated SAMs by photodeprotection of NVOC (365 nm) for subsequent tailoring of oxyamine-containing ligands that can be immobilized and released to reuse the surface. **(b)** Photomask used to create hydroquinone-SAM gradients for fluorescent dye conjugation and cell adhesion and migration studies. **(c)** Patterned cells on surfaces that can be released and re-adhered through electrochemical and pH stimuli. Reproduced from [28] with permission. Copyright: Wiley-, 2009

subsequent Fn adsorption was then conducted, followed by cell culture on the surface. Through phase contrast imaging, cells were observed migrating up the Fn gradient, toward the region containing densest Fn (their natural adhesion substrate) and, after some time, were seen to spread out and grow on the pattern. Microfluidics was then employed by the same group to partially etch away the SAM and gold in different patterns and to test the effects of cell-migration in response to the substrate disruption (Fig. 16a). Fluorescence live-cell imaging recorded transfected Rat2 fibroblasts during migration and showed a polarized Golgi and nucleus toward the direction of movement.



**Fig. 16** (a) Strategy for the complete spatial and visual control of directed cell polarity and migration using partially etched SAMs on gold by microfluidic activation (*above*), as shown by live-cell fluorescent image of a polarized Golgi (*below*). (b) Separate study in which microfluidic lithography was used to create gradients of SAMs for studies in cell adhesion and migration. Reproduced from [29, 30] with permission. Copyright: Wiley-VCH, 2008

## 5 Conclusion and Outlook

SAMs offer attractive physical properties that allow fundamental studies of biointerfacial chemistry. The synthetic flexibility in tailoring terminal functional groups and the large number of patterning and analytical characterization techniques compatible with SAMs make them a model platform for a wide range of research disciplines. With the combination of available ligand immobilization strategies and the non-fouling properties of oligo(ethylene glycol)-alkanethiol, complexly patterned and mixed-SAM surfaces can be generated. Due to these advantages, SAMs serve as an ideal substrate in mimicking the natural, dynamic environment of cells. As a result, this system has found great success in conducting cell adhesion, polarization, and migration studies. Attempts to modify planar SAM surfaces for observation of cells sampling their three-dimensional environment have been reported with varying success [172]. Future directions aim to integrate several of the dynamic substrate aspects discussed in this chapter with high-resolution live-cell/tissue imaging to generate platforms that conduct complete analysis and quantization of cell behavior *in vivo* and *in real-time*. This endeavor requires a coordinated multidisciplinary



effort. Overall, there has been much success with the use of SAMs of alkanethiolates on gold in biological investigations; however, a few disadvantages of the system still remain. Limitations include fluorescence quenching and long-term instability of the gold–thiol bond. As a result, alternative model systems (siloxanes on glass, phosphonates on metal oxides) have been explored for use in cell-based assays and biosensors [173, 174]. Thus, extending the surface chemistries and design principles for SAMs on gold to other materials could provide opportunities to conduct novel experiments for cell biology studies and for developing new platform biotechnologies.

## References

1. Manos P, Pancrazio J, Coulombe M, Ma W, Stenger D (1999) *Neurosci Lett* 271:179
2. Zhi Z-L, Laurent N, Turnbull J (2008) *Chembiochem* 9:1568
3. Park T, Shuler M (2003) *Biotechnol Prog* 19:243
4. Panda S, Sata T, Hampton G, Hogenesch J (2003) *Trends Cell Biol* 13:151
5. Laurent N, Voglmeir J, Wright A, Blackburn J, Wong S, Gaskell S, Flitsch S (2008) *Chembiochem* 6:883
6. Lahann J, Balcells M, Rodon T, Lee J, Choi I, Jensen K, Langer R (2002) *Langmuir* 18:3632
7. Yamato M, Konno C, Ustumi M, Kikuchi A, Okano T (2002) *Biomaterials* 23:561
8. Ulman A (1996) *Chem Rev* 96:1533
9. Schwartz D (2001) *Annu Rev Phys Chem* 52:107
10. Love J, Estroff L, Kriebel K, Nuzzo R, Whitesides G (2005) *Chem Rev* 105:1103
11. Mendes P (2008) *Chem Soc Rev* 37:2512
12. Wischerhoff E, Badi N, Lutz J-F, Laschewsky A (2010) *Soft Matter* 6:705
13. Mrksich M (2009) *Acta Biomater* 5:832
14. Yousaf M (2009) *Curr Opin Chem Biol* 13:697
15. Hogg N, Landis R (1993) *Curr Opin Immunol* 5:383
16. Hogg N (1992) *Immunol Today* 13:113
17. Cyster J (2001) *Immunol Rev* 194:48
18. Raghov R (1994) *FASEB J* 8:823
19. Mutsaers S, Bishop J, McGrouther G, Lauret G (1997) *Int J Biochem Cell Biol* 29:5
20. Jacinto A, Martinez-Arias A, Martin P (2001) *Nat Cell Biol* 3:E117
21. Sottile J (2004) *Biochim Biophys Acta* 1654:13
22. Hood J, Cheresch D (2002) *Nat Rev Cancer* 2:91
23. Bogenrieder T, Herlyn M (2003) *Oncogene* 22:6524
24. Liotta L, Kohn E (2001) *Nature* 411:375
25. Keely P, Parise L, Juliano R (1998) *Trends Cell Biol* 8:101
26. Fidler I (2002) *Semin Cancer Biol* 12:89
27. Chan E, Yousaf M (2008) *Mol Biosyst* 4:746
28. Lee E-J, Chan E, Yousaf M (2009) *Chembiochem* 10:1648
29. Lamb B, Westcott N, Yousaf M (2008) *Chembiochem* 9:2628
30. Lamb B, Westcott N, Yousaf M (2008) *Chembiochem* 9:2220
31. Park S, Yousaf M (2008) *Langmuir* 24:6201
32. Nuzzo R, Allara D (1983) *J Am Chem Soc* 105:4481
33. Schreiber F (2004) *J Phys Condens Matter* 16:R881
34. Kane R, Takayama S, Ostuni E, Ingber D, Whitesides G (1999) *Biomaterials* 20:2363
35. Wouters D, Schubert U (2004) *Angew Chem Int Ed* 43:2480
36. Ginger D, Zhang H, Mirkin C (2004) *Angew Chem Int Ed* 43:30
37. Hoover D, Lee E-J, Yousaf M (2007) *Chembiochem* 8:1920

38. Hoover D, Chan E, Yousaf M (2008) *J Am Chem Soc* 130:3280
39. Prime K, Whitesides G (1991) *Science* 252:1164
40. Xia Y, Whitesides G (1997) *Langmuir* 113:2059
41. Hahn M, Taite L, Moon J, Rowland M, Ruffino K, West L (2006) *Biomaterials* 27:2519
42. Carroll G, Wang D, Turro N, Koberstein J (2006) *Langmuir* 22:2899
43. Ryan D, Parviz B, Linder V, Semetey V, Sia S, Su J, Mrksich M, Whitesides G (2004) *Langmuir* 20:9080
44. Pale-Grosdemange C, Simon E, Prime K, Whitesides G (1991) *J Am Chem Soc* 113:12
45. Dillmore S, Yousaf M, Mrksich M (2004) *Langmuir* 20:7223
46. Houseman B, Huh J, Kron S, Mrksich M (2002) *Nat Biotech* 20:270
47. Yousaf M, Chan E, Mrksich M (2000) *Angew Chem Int Ed* 112:2019
48. Kolb H, Finn M, Sharpless K (2002) *Angew Chem Int Ed* 40:2004
49. Zhang Y, Luo S, Tang Y, Yu L, Hu K-Y, Pei J-P, Zeng X, Wang P (2006) *Anal Chem* 78:2001
50. Chan E, Park S, Yousaf M (2008) *Angew Chem Int Ed* 120:6363
51. Lamb B, Barrett D, Westcott N, Yousaf M (2008) *Langmuir* 24:8885
52. Horton R, Herne T, Myles D (1997) *J Am Chem Soc* 119:12980
53. Watzke A, Kohn M, Wacker R, Schroder S, Waldmann H (2006) *Angew Chem Int Ed* 45:1408
54. Lee J, Lee K-B, Kim D, Choi I (2003) *Langmuir* 19:8141
55. Raj C, Behera S (2007) *Langmuir* 3:1600
56. Houseman B, Gawalt E, Mrksich M (2003) *Langmuir* 19:1522
57. Yousaf M, Mrksich M (1999) *J Am Chem Soc* 121:4286
58. Chan E, Yousaf M (2006) *J Am Chem Soc* 128:15542
59. Westcott N, Pulsipher A, Lamb B, Yousaf M (2008) *Langmuir* 24:9237
60. Schilp S, Ballav N, Zharnikov M (2008) *Angew Chem Int Ed* 47:6786
61. Ballav N, Schilp S, Zharnikov M (2008) *Angew Chem Int Ed* 47:1421
62. Schmelmer U, Paul A, Kuller A, Steenackers, M, Ulman A, Grunze M, Golzhauser A, Jordan R (2007) *Small* 3:459
63. Steenackers M, Kuller A, Ballav N, Zharnikov M, Grunze M, Jordan R (2007) *Small* 10:1764
64. Klausner R, Huang M, Wang S, Chen C, Chuang T, Terfort A, Zharnikov M (2004) *Langmuir* 20:2053
65. Brandow, S, Chen M-S, Aggarwal R, Dulcey S, Calvert J, Dressick W (1999) *Langmuir* 15:5429
66. Laurent N, Voglmeir J, Wright A, Blackburn J, Pham N, Wong S, Gaskell S, Flitsch S (2008) *ChemBiochem* 9:883
67. Laurent N, Haddoub R, Voglmeir J, Wong S, Gaskell S, Flitsch S (2008) 9:2592
68. Min D-H, Su J, Mrksich M (2004) *Angew Chem Int Ed* 43:5973
69. Hu Z, Prunici P, Patzner P, Hess P (2006) *J Phys Chem B* 110:14824
70. Bae Y, Park K-W, Oh B-K, Lee W, Choi J-W (2004) *Colloid Surf A* 257:19
71. Michel O, Ravoo B (2008) *Langmuir* 24:12116
72. Kondo M, Nakamura Y, Fujii K, Nagata M, Suemori Y, Dewa T, Iida K, Gardiner A, Cogdell R, Nango M (2007) *Biomacromolecules* 8:2457
73. Kong B, Kim Y, Choi I (2008) *Bull Korean Chem Soc* 29:1843
74. Mrksich M, Sigal G, Whitesides G (1995) *Langmuir* 11:4383
75. Yonzon C, Jeoung E, Zou S, Schatz G, Mrksich M, Van Duyne R (2004) *J Am Chem Soc* 126:12669
76. Hoover D, Yousaf M (2009) *Langmuir* 25:2563
77. Papadantonakis K, Brunschwigg B, Lewis N (2008) *Langmuir* 24:10543
78. Pulsipher A, Yousaf M (2010) *Langmuir* 26:4130
79. Luzinov I, Minko S, Tsukruk V (2004) *Prog Polym Sci* 29:635
80. Uhlmann P, Ionov L, Houbenov N, Nitschke M, Grundke K, Motornov M, Minko S, Stamm M (2006) *Prog Org Coat* 55:168
81. Rant U, Arinaga K, Fujita S, Yokoyama N, Abstreiter G, Tornow M (2004) *Nano Lett* 4:2441
82. Rant U, Arinaga K, Fujita S, Yokoyama N, Abstreiter G, Tornow M (2006) *Org Biomol Chem* 4:3448



83. Rant U, Arinaga K, Scherer S, Pringsheim E, Fujita S, Yokoyama N, Tornow N, Abstreiter G (2007) *Proc Natl Acad Sci USA* 104:17364
84. Fan C, Plaxco K, Heeger A (2003) *Proc Natl Acad Sci USA* 100:9134
85. Ricci F, Lai Y, Heeger A, Plaxco K, Summer J (2007) *Langmuir* 23:6827
86. Mu L, Liu Y, Cai S, Kong J (2007) *Chem Eur J* 13:5113
87. Liu Y, Mu L, Liu B, Zhang S, Yang P, Kong J (2004) *Chem Commun*:1194
88. Sellergreen B, Swietlow A, Arnebrant T, Unger K (1996) *Anal Chem* 68:402
89. Auer F, Schubert D, Stamm M, Arnebrant T, Swietlow A, Zizlsperger M, Sellergreen B (1999) *Chem Eur J* 5:1150
90. Liu N, Dunphy D, Atanassov P, Bunge S, Chen Z, Lopez G, Boyle T, Brinker C (2004) *Nano Lett* 4:551
91. Yasutomi S, Morita T, Kimura S (2005) *J Am Chem Soc* 127:14564
92. Yasutomi S, Morita T, Imanishi Y, Kimura S (2004) *Science* 304:1944
93. Angelos S, Yang Y-W, Patel K, Stoddart J, Zink J (2008) *Angew Chem Int Ed* 47:2222
94. Mendes P, Christman K, Parthasarathy P, Schopf E, Ouyang J, Yang Y, Preece J, Maynard H, Chen Y, Stoddart J (2007) *Bioconjugate Chem* 18:1919
95. Hondeland C, Mrksich (1997) *Langmuir* 13:6001
96. Yeo W-S, Hondeland C, Mrksich M (2001) *ChemBiochem* 7:590
97. Houseman B, Huh J, Kron S, Mrksich M (2002) *Nat Biotech* 20:270–274
98. Houseman B, Mrksich M (2002) *Chem Biol* 9:443
99. Chan E, Park S, Yousaf M (2008) *Angew Chem Int Ed* 47:6267
100. Blonder R, Katz E, Willner I, Wray V, Buckmann A (1997) *J Am Chem Soc* 119:11747
101. Blonder R, Willner I, Buckmann A (1998) *J Am Chem Soc* 120:9335
102. Katz E, Sheeney-Haj-Ichia L, Willner I (2004) *Angew Chem Int Ed* 43:3292
103. Sortino S, Petralia S, Compagnini G, Conoci S, Condorelli G (2002) *Angew Chem Int Ed* 41:1914
104. Imahori H, Fukuzumi S (2001) *Adv Mater* 13:1197
105. Pearson D, Downard A, Muscroft-Taylor A, Abell A (2007) *J Am Chem Soc* 129:14862
106. Ebara M, Yamato M, Aoyagi T, Kikuchi A, Sakai K, Okano T (2004) *Biomacromolecules* 5:505
107. Zareie H, Boyer C, Bulmus V, Nateghi E, Davis T (2008) *ACS Nano* 4:757
108. Herrwerth S, Eck W, Reinhardt S, Grunze M (2003) *J Am Chem Soc* 125:9359
109. Li L, Chen S, Zheng J, Ratner B, Jiang S (2005) *J Phys Chem B* 109:2934
110. Balamurugan S, Ista L, Yan J, Lopez G, Fick J, Himmelhaus M, Grunze M (2005) *J Am Chem Soc* 127:14548
111. Kushida A, Yamato M, Konno C, Kikuchi A, Sakurai Y, Okano T (1999) *J Biomed Mater Res* 45:355
112. de las Herra Alarcon C, Farhan T, Osborne V, Huck W, Alexander C (2005) *J Mater Chem* 15:2089
113. Alberts B, Johnson A, Lewis J, Raff M, Roberts K, Walter P (2002) *Molecular biology of the cell*. Garland Science, New York
114. Rhodes J, Simons M (2007) *J Cell Mol Med* 2:176
115. Danilov Y, Juliano R (1989) *Exp Cell Res* 182:186
116. Halbleib J, Nelso W (2006) *Genes Dev* 20:3199
117. Lauffenburger D, Horwitz A (1996) *Cell* 84:359
118. Ridley A, Schwartz M, Burridge K, Firtel R, Ginsberg M, Borisy G, Parsons J, Horowitz A (2003) *Science* 302:1704
119. Hynes R (1987) *Cell* 48:549
120. Tamkun J, DeSimone D, Fonda D, Patel R, Buck C, Horwitz A, Hynes R (1986) *Cell* 46:271
121. Juliano R, Reddig P, Alahari S, Edin M, Howe A, Aplin A (2004) *Biochem Soc Trans* 32:443
122. Blystone S (2004) *Biochim Biophys Acta* 1692:47
123. Bershadsky A, Balaban N, Geiger B (2003) *Annu Rev Cell Dev Biol* 19:677
124. Juliano R (2002) *Annu Rev Pharmacol Toxicol* 42:283
125. Giancotti F, Tarone G (2003) *Annu Rev Cell Dev Biol* 19:173
126. Forgacs G, Yook S, Janmey P, Jeong H, Burd C (2004) *J Cell Sci* 117:2769

127. Sastry S, Burridge K (2000) *Exp Cell Res* 261:25
128. Zaidel-Bar R (2004) *Biochem Soc Trans* 32:416
129. Zamir E, Geiger B (2001) *J Cell Sci* 114:3577
130. Jockusch B, Bubeck P, Giehl K, Kroemker M, Moschner J, Rothkegel M, Rudiger M, Schluter K, Stanke G, Winkler J (1995) *Annu Rev Cell Dev Biol* 11:379
131. Brakebusch C, Fassler R (2003) *EMBO J* 22:2324
132. Burridge K (1992) *J Cell Biol* 119:893
133. Turner C, Glenney J, Burridge K (1990) *J Cell Biol* 111:1059
134. Danilov Y, Juliano R (1989) *Exp Cell Res* 182:186
135. Maheshwari G, Brown G, Lauffenburger D, Wells A, Griffith L (2000) *J Cell Sci* 113:1677
136. Koo L, Irvine D, Mayes A, Lauffenburger D, Wells A, Griffith L (2002) 115:1423
137. Webb D, Brown C, Horwitz A (2003) *Curr Opin Cell Biol* 15:614
138. Eaton S, Simons K (1995) *Cell* 82:5
139. Drubin D, Nelson W (1996) *Cell* 84:335
140. Dustin M (2002) *Cell* 110:13
141. Euteneuer U, Schliwa M (1992) *J Cell Biol* 116:1157
142. Yvon A, Walker J, Danowski B, Fagerstrom C, Khodjakov A, Wadsworth P (2002) *Mol Biol Cell* 13:1871
143. Manes S, Mira E, Gomez-Mouton C, Lacalle RA, Martinez C (2000) *IUBMB Life* 49:89
144. Schoenfish M, Pemberton J (1998) *J Am Chem Soc* 120:4502
145. Ufheil J, Boldt F, Borsch M, Borgwarth K, Heinze J (2000) *Bioelectrochemistry* 52:103
146. Naumann R, Schiller S, Giess F, Grohe B, Hartman K, Kärcher I, Köper I, Lübben J, Vasilev K, Knoll W (2003) *Langmuir* 19:5435
147. Lahiri J, Kalal P, Frutos A, Jonas S, Schaeffle R (2000) *Langmuir* 16:7805
148. Liu D, Xie Y, Shao H, Jiang X (2009) *Angew Chem Int Ed* 48:4406
149. Steyer J, Almers W (2001) *Nat Rev Mol Cell Biol* 2:268
150. Alerod D (1981) *Cell Biol* 89:141
151. Mathur A, Truskey G, Reichert W (2000) *Biophys J* 78:1725
152. Luo W, Yousaf M (2009) *Chem Commun* 1237:1239
153. Demers L, Ginger D, Park S, Li Z, Chung S, Mirkin C (2002) *Science* 296:1836
154. Wilson D, Martin R, Hong S, Cronin-Golomb M, Mirkin C (2001) *Proc Natl Acad Sci USA* 98:13660
155. Aota S, Nomizu M, Yamada K (1994) *J Biol Chem* 269:24756
156. Bowditch R (1994) *J Biol Chem* 269:10856
157. Mardon H, Grant K (1994) *FEBS Lett* 340:197
158. Hodgson L, Chan E, Hahn K, Yousaf M (2007) *J Am Chem Soc* 129:9264
159. Hoover D, Yousaf M (2009) *Langmuir* 25:2563
160. Whitesides G, Ostuni E, Takayama S, Jiang X, Ingber D (2001) *Annu Rev Biomed Eng* 3:335
161. Pale-Grosdemange C, Simon E, Prime K, Whitesides G (1991) *J Am Chem Soc* 113:12
162. Xia N, Thodeti C, Hunt T, Xu Q, Ho M, Whitesides G (2008) *FASEB J* 22:1649
163. Feng Y, Mrksich (2004) *Biochemistry* 43:15811
164. Mrksich M, Whitesides G (1996) *Annu Rev Biophys Biomol Struct* 25:55
165. James J, Goluch E, Liu C, Mrksich M (2008) *Cell Motil Cytoskeleton* 65:841
166. Kaji H, Kanada M, Oyamatsu D, Matsue T, Mishizawa M (2004) *Langmuir* 20:16
167. Kaji H, Tsukidate K, Hashimoto M, Matsue T, Nishizawa M (2005) *Langmuir* 21:6966
168. Nakanishi J, Kikuchi Y, Inoue S, Yamaguchi K, Takarada T, Maeda M (2007) *J Am Chem Soc* 129:6694
169. Nakanishi J, Kikuchi Y, Yamaguchi K, Takarada T, Nakayama H, Maeda M (2004) *J Am Chem Soc* 126:16314
170. McCarthy J, Palm S, Furcht L (1983) *J Cell Biol* 97:772
171. Cattaruzza S, Perris R (2005) *Matrix Biol* 24:400
172. Hoch H, Staples R, Whitehead B, Comeau J, Wolf E (1987) *Science* 235:1659
173. Pulsipher A, Westcott N, Luo W, Yousaf M (2009) *J Am Chem Soc* 131:7626
174. Pulsipher A, Westcott N, Luo W, Yousaf M (2009) *Adv Mater* 21:3082

# LbL Films as Reservoirs for Bioactive Molecules

D. Volodkin, A. Skirtach, and H. Möhwald

**Abstract** This review presents recent progress in utilizing polymeric films made by the layer-by-layer (LbL) technique (so-called multilayered films) as reservoirs for hosting and releasing bioactive molecules. This relatively new technique is distinguished by its high modularity and structural control at the nanometer level, giving polymeric surface films with tuneable physicochemical properties. A significant increase in research activities regarding the bioapplications of the multilayered films has taken place over the last decade. In this review, we address the bioapplications of LbL films and will focus on the loading and release of the film-embedded bioactive compounds and their bioactivity. Planar and free-standing 3D multilayered polyelectrolyte films (microcapsules) are considered. Special attention is paid to light-stimulated release, interaction of cells with the LbL films, and intracellular light-triggered delivery.

**Keywords** Bioactive · Layer-by-layer · Multilayered films · Polyelectrolyte self-assembly · Remote release

## Contents

1	Introduction .....	136
2	Planar LbL Films .....	137
2.1	Loading of Free and Encapsulated Biomolecules .....	137
2.2	Release Capability .....	141
3	Free-Standing LbL Films (Microcapsules) .....	145
3.1	Cargo Release .....	148
3.2	Intracellular Light-Triggered Delivery .....	150

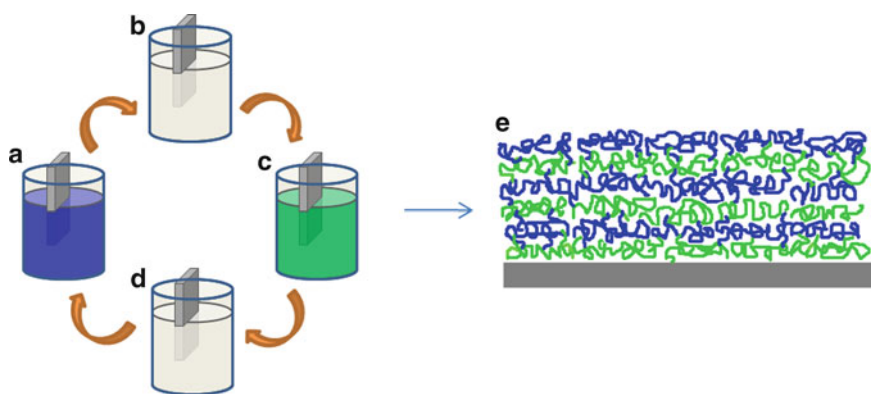
---

D. Volodkin (✉), A. Skirtach, and H. Möhwald  
Max-Planck Institute of Colloids and Interfaces, Research Campus Golm, 14424,  
Potsdam, Germany  
e-mail: [dmitry.volodkin@mpikg.mpg.de](mailto:dmitry.volodkin@mpikg.mpg.de); [andre.skirtach@mpikg.mpg.de](mailto:andre.skirtach@mpikg.mpg.de);  
[helmuth.moehwald@mpikg.mpg.de](mailto:helmuth.moehwald@mpikg.mpg.de)

4	LbL Films Govern Cellular Response .....	152
5	Conclusion .....	153
	References .....	154

## 1 Introduction

Layer-by-layer (LbL) polyelectrolyte self-assembly [1, 2], which is based on consecutive adsorption of polymers that have affinity to each other (Fig. 1), has emerged as a powerful and versatile strategy for engineering surface films aiming bio-functionalization. Not only electrostatic interactions, but also hydrogen bonding [3–5], host–guest interactions [6–11], and hydrophobic interactions [12] can be the main driving forces for assembly of the films. The fundamental physical mechanisms behind the LbL technique have been extensively studied [13–19] but are not fully understood so far. This relatively new technique possesses excellent characteristics such as fine film tuning in terms of thickness (nano- and microscale), stiffness, chemistry, stability, biofunctionality, and dynamics [20–22]. LbL films can be distinguished by the type of film growth: (1) linear with stratified structure interpenetration by each polyelectrolyte only into neighboring layers, or (2) exponential with free diffusion of at least one polyelectrolyte. The poly(styrene sulfonate)/poly(allylamine hydrochloride) (PSS/PAH) film is the most prominent example of the first category, and typical examples of exponentially growing films are films made with polyaminoacids and polysaccharides [23–26]. The nature of the polymer strongly affects the growth regime but is not the dominating factor; linearly growing films can switch their growth regime if interpolymer interaction is weakened by an increase of salt concentration (charge screening) or temperature [17, 27]. LbL films, especially exponentially growing ones, potentially have a high capability



**Fig. 1** LbL film deposition on a planar support. Immersion in polymer solutions of polycation (a) and polyanion (c). (b, d) Washing steps to remove nonadsorbed polymer molecules. (e) Structure of the LbL-assembled film

of loading (during LbL assembly or by postmodification) a variety of biomolecules in a controlled way, as well as controlled release characteristics. The physicochemical characteristics of the films, which are tuneable to a large extent, are the key to modulating the interaction with cells [28, 29].

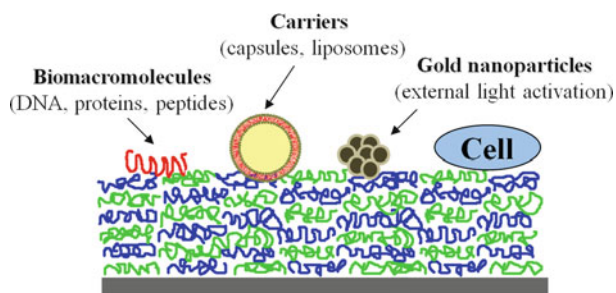
The universal character of the LbL method has catalyzed the introduction of the method for a wide range of bioapplications. Proteins (enzymes) [30–33], polypeptides [34], polysaccharides [35], lipids [36, 37], nucleic acids [38–42], viruses [43], inorganic particles, and crystals [44] have been embedded in the films. Use of these compounds makes the films attractive for biorelated applications such as biosensors, drug delivery, tissue engineering, and biocoatings. Biological [45, 46] and nonbiological [21, 47–49] applications of LbL films are reviewed in the literature.

One of the main challenges in biotechnology and medicine is to develop a system able to provide a controlled release of bioactive compounds. This is attractive in view of the obvious advantages of controlled release, such as high efficiency and lower toxicity. LbL films containing bioactive molecules offer the ability to vary not only the amount of the molecules but also to trigger the release and thus enable control “on demand” with external and noninvasive stimuli such as a light. In this review, we aim to summarize the progress in applications of the polyelectrolyte LbL films as reservoirs and release carriers, highlighting planar and free-standing films and the mechanisms of loading and release, including release stimulated by irradiation with near-IR light.

## 2 Planar LbL Films

### 2.1 Loading of Free and Encapsulated Biomolecules

Bioactive films made by the LbL technique have been extensively studied by many scientific groups worldwide. The films can host not only bioactive molecules introduced as constituents of the film, but also carriers with encapsulated biomolecules, for instance liposomes (Lip) and polymeric capsules (Fig. 2). Stimuli-sensitive



**Fig. 2** LbL-assembled polymeric film, which can host different species and interact with cells

material can be immobilized in the film, giving the option to remotely activate the film to result in the release of active molecules. In this review, we focus on loading of the LbL films with biomolecules, release of the biomolecules (including light-stimulated release), and cell interaction with the film, which is an important issue in biomaterial science.

Bioactive macromolecules like peptides, proteins, and nucleic acids have been successfully embedded in planar LbL films. An important question is the retention of the bioactivity of the film-embedded biomolecules. The structural properties and stability of the LbL films formed from synthesized polypeptides of various amino acid sequences were recently reported [50]. The authors showed that control over the amino acid sequence enables control over non-covalent interpolypeptide interaction in the film, which determines the film properties. Haynie and coworkers showed by circular dichroism spectroscopy that the extent of adsorption of poly(L-glutamic acid) (PGA) and poly(L-lysine) (PLL) in the LbL films scales with the extent of secondary structure of the polypeptides in solution [51]. Boulmedais demonstrated that the secondary structure of the film composed of these polypeptides is the same as the peptide structure in the complex formed in solution [52], as found by Fourier transform IR spectroscopy (FTIR).

The properties of protein- and enzyme-containing films were reported by Ai [45]. The film-incorporated enzymes keep their catalytic activity and, moreover, have high tolerance to harsh conditions [45, 53–55]. Adsorption and embedding of fibrinogen in the multilayers from PSS and PAH preserve the secondary structure of the protein [55]; however, these polyelectrolytes can change the structure of bovine serum albumin and hen egg white lysozyme in the multilayers, and this effect is more pronounced for opposite charges of the last polymer layer and the protein. Proteins can strongly interact with the PSS/PAH film whatever the sign of the charge of both the multilayer and the protein [33], forming a monolayer in the case of the same charge sign and a thick layer for opposite charges, which suggests protein diffusion into the film.

Some controversies on the structural properties of the film-embedded polypeptides are revealed and also highlighted by Tang [46], which reflects the complex nature of the polypeptide interaction in the LbL films and could be also the case for the protein-containing films. An increased number of studies on this topic suggests means of developing polypeptide- and protein-based LbL films, despite the fact that interactions in these films are complex and involve multimode interactions such as electrostatics, hydrogen bonding, and hydrophobic interactions.

DNA has been embedded in LbL films by assembling with polycations like PLL, polyethyleneimine (PEI), and poly(dimethyldiallylammonium chloride) (PDAD) [38–42]. Zhang showed that the DNA released from the film with synthetic degradable polyamine is transcriptionally viable [41]. DNA molecules can keep their structure when incorporated in the film with synthetic polymers [39], making films with DNA suitable candidates for gene delivery.

Small drugs, as are most pharmaceuticals, can be directly loaded in the preformed films [56–58]. Schneider demonstrated that chitosan/hyaluronic acid (CHI/HA)

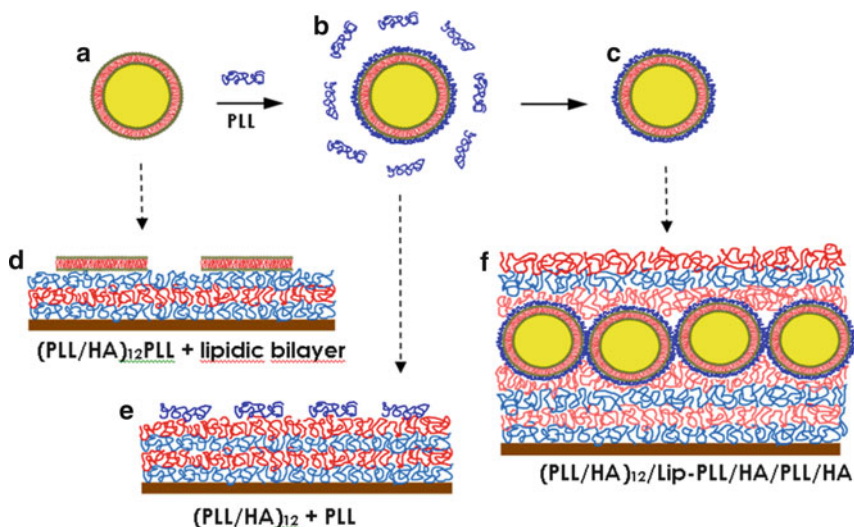
films have high capacity for the drugs diclofenac and paclitaxel. The drug loading can be modulated by varying the number of layers in the film, yielding a diclofenac concentration in the film of the order of 0.1–0.3 mg/mL.

One of the main challenges in the field of biocoating engineering by the LbL method is to increase the load of the films with biomolecules and, at the same time, shield the biomolecules from the surrounding medium. The strategy is the incorporation of reservoirs filled with biomolecules into the film architecture. Recently, phospholipid vesicles were used as such reservoirs due to their low permeability for even small species, biocompatibility, and controlled chemistry and size, which promises liposome utilization in both medical and nonmedical fields [59]. Surface immobilization of liposomes [60] was comprehensively studied, mainly on the basis of biospecific [61–63] and covalent bonding to the surface [64, 65]. However, liposomes are rather unstable and, in general, they undergo collapse or/and fusion when coming into contact with solid surfaces or polyelectrolyte films [36, 66–68]. Many strategies have been proposed in order to overcome liposome instability [69]. They include surface polymerization [70, 71], polymer coating [36, 66–68, 72–75], and LbL coating [76].

Stabilization by polypeptide (PLL) coating has been demonstrated [77–81] and the stabilized vesicles were successfully embedded in the LbL films in an intact state [77, 82–84]. Liposome stabilization by polyelectrolyte coating is attractive due to simplicity, noncovalent surface modification, and because a wide range of polyelectrolytes can provide the vesicles with versatile properties like targeting and stimuli-induced release. Figure 3 shows the vesicle-embedding process. Vesicles, composed of 1,2-dipalmitoyl-*sn*-glycero-3-phosphocholine (DPPC), the sodium salt of 1,2-dipalmitoyl-*sn*-glycero-3-[phospho-*rac*-(1 glycerol)] (DPPG), and cholesterol (CL), with a diameter of around 130 nm were used. Unstabilized vesicles (i.e., without PLL coating) were fused onto HA/PLL films (Fig. 3a, d), but covered vesicles (Fig. 3c) were entrapped in the film by the LbL procedure (Fig. 3c, f) after removal of excess PLL, which adsorbs better than the coated vesicles (Fig. 3b, e). The study was aimed at optimization of liposome coverage with PLL [79, 80] and revealed an influence of many factors (polymer molecular mass, component ratio, mixing rate and order, temperature) on PLL–liposome complexation. Mixing of PLL and liposomes leads to formation of either single PLL-covered vesicles or aggregates. Differential scanning calorimetry experiments suggest that the adsorption of PLL does not induce phase separation in the lipid bilayer, as was previously observed for the polycation poly(*N*-ethyl-4-vinylpyridinium bromide) [72]. Another important finding is that PLL-covered vesicles keep their integrity in the solid state, even in aggregated form, and release carboxyfluorescein (CF) a little faster than native vesicles in the liquid state [80].

Interpolyelectrolyte and lipid–polyelectrolyte interactions play a crucial role in vesicle embedding [84], but the right selection of components can result in a fine structure of liposome-containing films (Fig. 4c, d). The amount of the vesicle-encapsulated material can be varied by a number of vesicle deposition steps (“interlayers”) or by the charge of the liposomes (Fig. 4e). The embedding

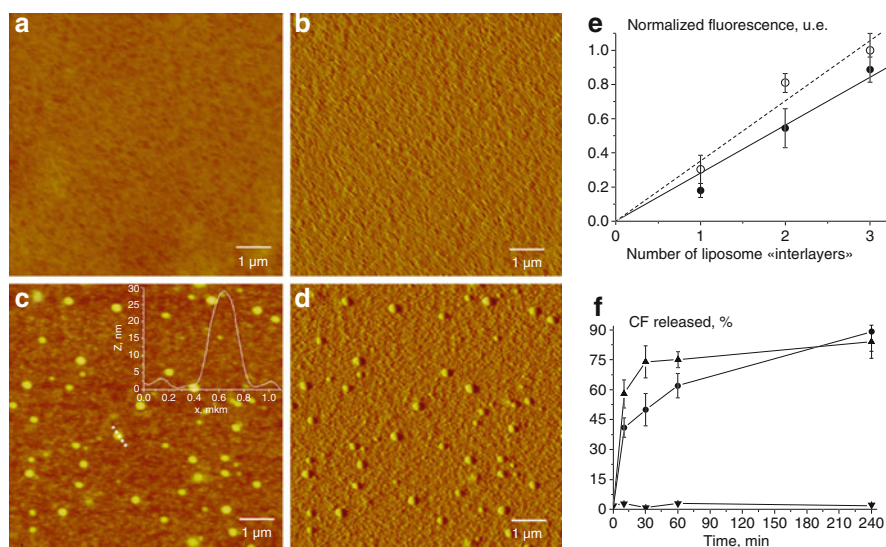




**Fig. 3** Vesicle stabilization by PLL covering (a, b), followed by separation of well-covered single vesicles from excess of nonbound PLL (b, c). Native vesicles are ruptured upon adsorption on a  $(\text{PLL}/\text{HA})_{12}/\text{PLL}$  film, forming a lipidic bilayer (a, d). Free non-bound PLL is preferably adsorbed on a  $(\text{PLL}/\text{HA})_{12}$  film rather than on PLL-covered vesicles (b, e). Liposome-containing film  $(\text{PLL}/\text{HA})_{12}/\text{Lip-PLL}/\text{HA}/\text{PLL}/\text{HA}$  is formed by adsorption of PLL-covered layers (Lip-PLL) on a  $(\text{PLL}/\text{HA})_{12}$  film, followed by additional coating with HA/PLL/HA layers (c, f). Reproduced from [82]

matrix plays an important role, and exponentially growing PGA/PAH [77, 78] and PLL/HA [82–84] films were found to be suitable for embedding by the LbL technique. The main advantage of these exponentially growing films [34, 85] with respect to vesicle incorporation is the high water content, due to a gel-like structure formed by weak interpolymer interactions that make a “friendly environment” for the liposomes. We believe that these features allow successful embedding. To our knowledge, there are no studies aim at liposome embedding in linearly growing LbL films, which are mostly made from synthetic polymers and characterized by a low polymer hydration state. This stresses the unique properties of the exponentially growing films.

The fact that no apparent fusion of the vesicles is revealed by the atomic force microscopy (AFM) does not prove the liposome structural integrity (Fig. 4c, d). Analysis of the profiles of the embedded vesicles show that they are immersed in the film, suggesting the immersion by two different modes of the capping film layers: (1) exponential between the vesicles, and (2) linear on the vesicle top [82]. Evidence of vesicle stability is proved by a direct release study of the vesicle-encapsulated CF marker, as shown in Fig. 4f [82]. Similar results were found for DPPC vesicles filled with ferrocyanide ions [77]. No considerable release of the markers, at least during the first few hours after embedding, points to vesicle integrity.



**Fig. 4** AFM images of (PLL/HA)<sub>12</sub> film (**a** height and **b** deflection images) and liposome-containing film (PLL/HA)<sub>12</sub>/Lip-PLL/HA/PLL/HA (**c** height and **d** deflection images). The *inset* in (**c**) corresponds to the height profile of the vesicle along the dotted line (*x*-axis in  $\mu\text{m}$ , *z*-axis in nm). Reproduced from [82]. (**e**) Fluorescence of solutions obtained by solubilization of liposome-containing films versus the number of vesicle “interlayers” in the films. Liposomes contain 10% (filled circles) and 30% (empty circles) of DDPG. Each value is the average of at least three independent experiments with its standard deviation (error bars). The *straight lines* are a linear fit through zero. Reproduced from [84]. (**f**) Time evolution of the cumulative CF release from vesicles embedded inside a (PLL/HA)<sub>12</sub>/Lip-PLL/HA/PLL/HA film architecture, when the film is maintained at ambient temperature (inverted triangles) or heated and maintained at 45 °C (triangles). These release kinetics are compared to the release kinetics obtained for the same PLL covered vesicles in aqueous solution at 45 °C (circles). Each value is the average of at least three independent experiments. Reproduced from [82]

## 2.2 Release Capability

There are two mechanisms for release of active molecules from planar polyelectrolyte LbL films. The first is based on weakening of the molecule–polymer interaction, resulting in a release. In the second mechanism, the LbL film plays the role of a matrix housing a reservoir with encapsulated biomolecules. In this case, the drug release is determined not by interaction with polymer(s) but by the reservoir capacity. An example of the latter is liposome-containing films in which the release is affected by the lipid membrane permeability. Both mechanisms can take place. For instance, Burke showed that release as well as loading of small hydrophilic dye molecules from PAH/HA films depends not only on the dye–polymer interaction but on the dye aggregation ability and film swelling state [86].

The first mechanism is more widely reported in the literature and is based on various kinds of stimuli. The main principle of this release approach is that the

drug molecules interact with the polyelectrolyte more strongly at loading conditions than at conditions when the drug should be released. pH and ionic strength can affect the ionization of the polyelectrolyte side groups and thus change the interaction of probe molecules with the polyelectrolyte film network [86–88]. Large molecules like proteins were also shown to exhibit pH-dependent release behavior. Müller demonstrated that, for PEI/poly(acrylic acid) films, an adsorption and release of lysozyme and human serum albumin could be switched by changing the pH setting, thanks to electrostatics [88].

A switching to different physicochemical conditions results in both changes in the drug–polyelectrolyte interaction and changes in the interpolyelectrolyte interactions. The latter leads to film decomposition or erosion, which is the second release mechanism. The polymers in the LbL films form a diffusion barrier for the releasing molecules. Sukhishvili and Granick have studied the stability of the multilayered films with variation of pH and ionic strength. The films were formed by hydrogen bonding, and critical values for the film disintegration have been found by FTIR [5]. Decomposition of the polyelectrolyte film structure has been also achieved utilizing hydrolytically degradable polymers [41, 42, 89, 90]. Thin degradable films and coatings that sustain the release of DNA from surfaces under physiological conditions could play an important role in the development of localized approaches to gene therapy [41, 42]. Chuang and co-authors have designed active antibiotic-releasing films with heterostructure by alternating deposition of hydrolytically degradable poly(*beta*-amino ester), HA, and the antibiotic gentamicin [90]. The design allows for direct loading of gentamicin without having to premodify it.

Release of liposome-encapsulated CF from HA/PLL films has been observed at temperatures above the lipid transition temperature (Fig. 4f). Below this temperature, the vesicles were stable at least for a few hours. The polyelectrolyte network destabilizes the embedded vesicles, which show higher lipidic bilayer permeability upon heating than do vesicles in solution [84]. No change in film properties upon heating has been reported as proof of the polyelectrolyte destabilization effect.

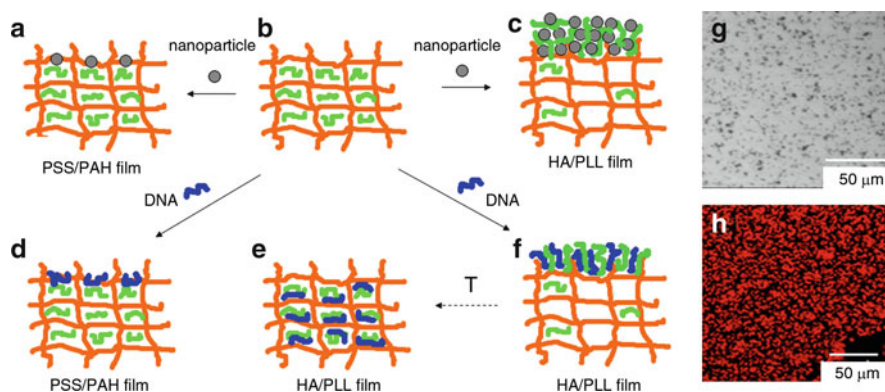
If the LbL film has relatively high thickness, the release rate can be driven by molecule diffusion through the film. Schneider demonstrated that drug diffusion through the film proceeds for several hours, as achieved by placement of the CHI/HA film loaded with diclofenac and paclitaxel in 0.15 M NaCl (pH 7.4) into phosphate-buffered saline solution. Vodouhe showed that the PLL/HA films passively loaded with taxol can regulate cell adhesion and viability by deposition of capping layers of PAH/PSS, which effects both drug release and cell adhesion [57].

Alternative stimuli to induce the release of film-embedded biomolecules have been introduced. Disintegration of a DNA/Zr<sup>4+</sup> film, triggered by an electric field, has been shown by Wang [91]. PLL/heparin films were built on an indium tin oxide semiconductor substrate and electrochemically dissolved [92]. Enzymes can work as agents to decompose polymers in the LbL films, yielding so-called enzymatic degradation [93]. Pepsin erosion of alginate (ALG)/CHI films has been recently reported [94]. Serizawa demonstrated very effective degradation of DNA/PDAD films by DNase I [95]. The use of stimuli-sensitive polymers, or modification of the

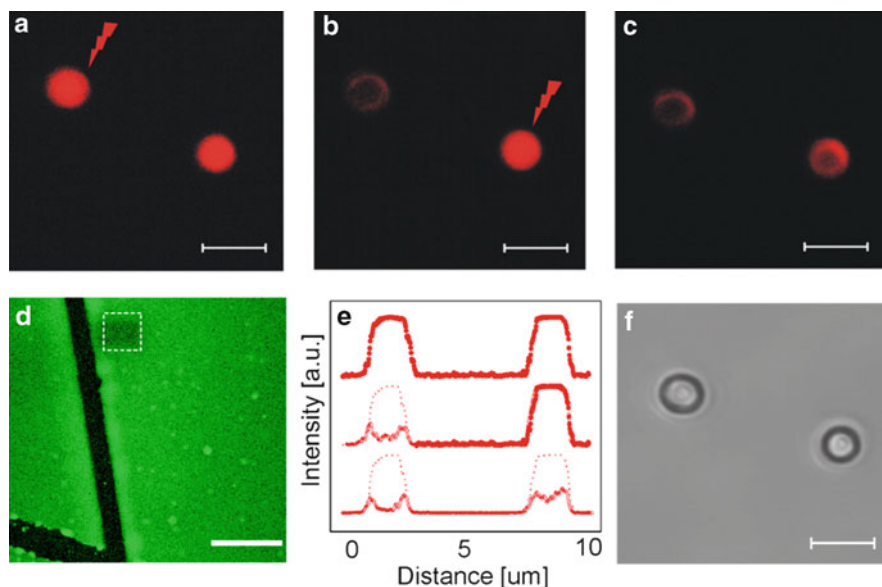
polymers used to form the LbL films with stimuli-responsive moieties, opens ways to establish surface coatings that are sensitive to light irradiation [96] or temperature change [97].

Special attention should be paid to noninvasive release of bioactive molecules from the films because it gives an option of delivery of bioactive molecules to a cell without changes in surrounding medium. Cells are generally very sensitive to changes such as variation in pH, ionic strength, etc. Our recent studies with the LbL films made from biopolymers HA and PLL demonstrate film reservoir properties, i.e., nano- and microcarriers such as liposomes or polymeric capsules as well as biomolecules (DNA, proteins, peptides, etc) can be incorporated in the film [82, 84, 98, 99]. The HA/PLL film has high loading capacity due to the polymer doping at the film surface (Fig. 5), which results in accumulation of a large amount of adsorbing material. This is many times less for PSS/PAH film, which has low polymer mobility [98, 100]. Microcapsules, gold nanoparticles, and DNA can be embedded in the HA/PLL film and located on the film surface [98, 100] (Figs. 5 and 6). Diffusion of embedded molecules (DNA) into the film can be triggered by heating [98, 100]. The amount of material incorporated into HA/PLL films can be larger than the mass of the polymers (HA and PLL) in the film, which is attributed to polymer transport.

Microcapsules can be adsorbed on the hydrogel HA/PLL film by direct contact of the film and the capsules [98, 100] (Fig. 6a). The opposite charges in polyelectrolyte multilayers of microcapsules are almost compensated for overall, but the strong attachment of microcapsules to the film (no capsule removal observed upon intensive film washing) can be attributed to some uncompensated negative charges on the last



**Fig. 5** Principal scheme of interactions of LbL films (**b**), namely, PSS/PAH and HA/PLL, with gold nanoparticles (**a**, **c**) and DNA (**d**, **f**). The nanoparticles and DNA interact only with the surface PAH groups of the PSS/PAH film (**a**, **d**). However, they can accumulate in large quantities as a result of the interaction with PLL “doping” from the whole interior of the HA/PLL film (**c**, **f**). Diffusion of DNA into the HA/PLL film can be triggered by heating to 70 °C (**e**). Optical and confocal fluorescent microscopy images of gold nanoparticles (**g**) and DNA-EtBr (**h**) adsorbed onto the (PLL/HA)<sub>24</sub>/PLL film, respectively. Reproduced from [98]



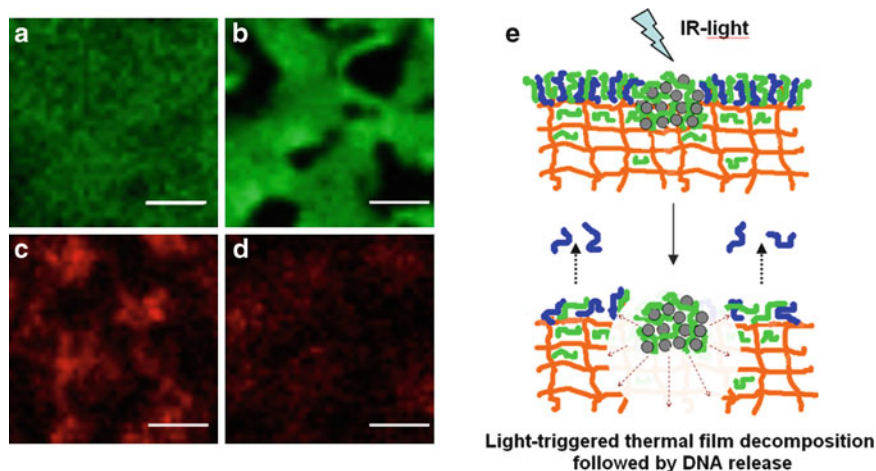
**Fig. 6** Adsorption of microcapsules onto the  $(\text{PLL}/\text{HA})_{24}/\text{PLL}$  films. (a–c) Confocal fluorescent microscopy images of the capsules exposed to the near-IR light irradiation. (d) CLSM image of the film surface (the film is prepared with PLL-FITC; black lines are scratches made by a needle for easier film imaging). (e) Cross-sectional profile of the capsules after step-by-step laser exposure (the sections from top to bottom correspond to the images a–c, respectively). (f) Optical microscopy images of the capsules after light irradiation. Scale bars: (a–c, f) 4  $\mu\text{m}$ , (d) 25  $\mu\text{m}$ . Reproduced from [100]

layer. It seems to be that the immersed capsules adapt to the “best” position in terms of interaction with the doped PLL molecules; the capsules can be immersed into the film as liposomes [82].

An important feature is film activation with micrometer precision by external stimulation with “biofriendly” near-IR light, which results in controlled release of film-embedded material [98, 100]. Laser activation of film-supported microcapsules shows remote release of encapsulated dextran by selective stimulation of the capsules with near-IR light (Fig. 6). Destruction of the HA/PLL film functionalized with gold nanoparticles occurs at irradiation with a light power of over 20 mW. Microcapsules modified with nanoparticles keep their integrity under the same conditions but become more permeable.

The HA/PLL film with adsorbed gold nanoparticles and DNA possesses remote-release features by stimulation with near-IR light of over 20–30 mW (Fig. 7). DNA release from the film modified with gold nanoparticles is thought to be caused by local destruction of the polymer network in the film, followed by blocking of PLL–DNA bonding and, as a result, release of DNA molecules from the film [98, 100]. Laser activation of the films can be used for affecting, releasing, or removing the upper coatings of the films, depending on the power of the laser.



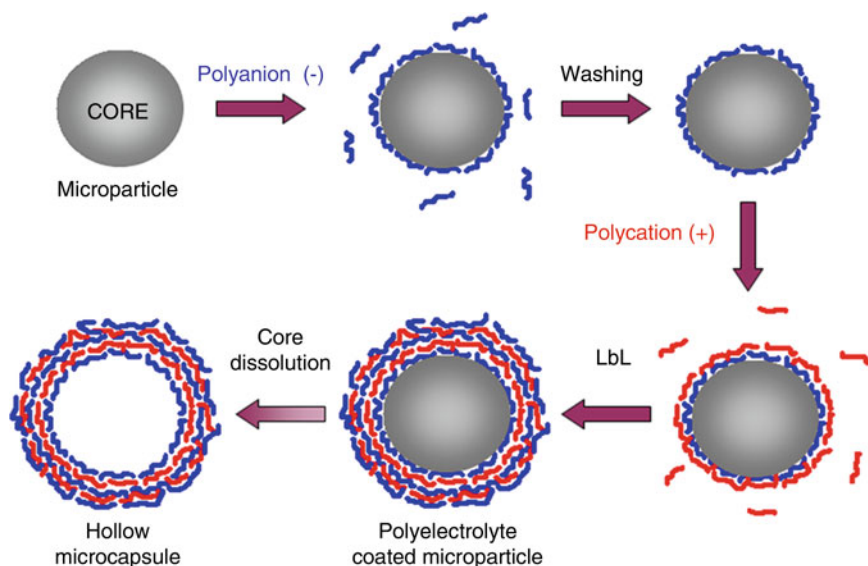


**Fig. 7** (PLL/HA)<sub>24</sub>/PLL film with embedded DNA before (a, c) and after (b, d) irradiation with IR light. PLL in the film is labeled with FITC (a, b), and DNA is labeled with EtBr (c, d). Scale bars: 5  $\mu\text{m}$ . (e) Suggested mechanism of DNA release induced by the distortion of the DNA-doping PLL interaction as a result of partial thermal film decomposition in vicinity of nanoparticle aggregates. Reproduced from [98]

### 3 Free-Standing LbL Films (Microcapsules)

Up to now, several techniques have been applied to encapsulate material of interest into various types of micro- and nanoparticles to achieve different drug administration routes and release characteristics. Some of these techniques are based on liposomes (vesicle-based) and some on polymeric particles (matrix systems, microgel beads or particles prepared by interfacial polymerization) [101]. The LbL technology as alternative method has attracted high interest for the production of microparticulate structures for delivery applications. This concerns first of all the colloidal particles made and/or modified by the LbL technique. The main principles of LbL deposition on colloidal particles [102, 103] are similar to those of film formation on planar surfaces. A very attractive and extremely fast-developing area using colloidal templating is the construction of multilayered polyelectrolyte capsules. The concept of capsule formation by the LbL technique involves alternating polyelectrolyte adsorption on a colloidal template, followed by decomposition of the sacrificial core [102]. This leads to the formation of hollow structures that replicate the templating particles in terms of size and shape. Figure 8 shows the principle scheme of capsule formation by the LbL approach. Fabrication and properties of the multilayer capsules are reviewed elsewhere [47, 104].

A broad variety of sacrificial colloidal cores have been used for hollow capsule fabrication. They are inorganic or organic particles from tens of nanometers and up to tens of micrometers, like melamine formaldehyde (MF), polystyrene spheres,  $\text{CaCO}_3$  and  $\text{MgCO}_3$  particles, protein and DNA aggregates, small dye

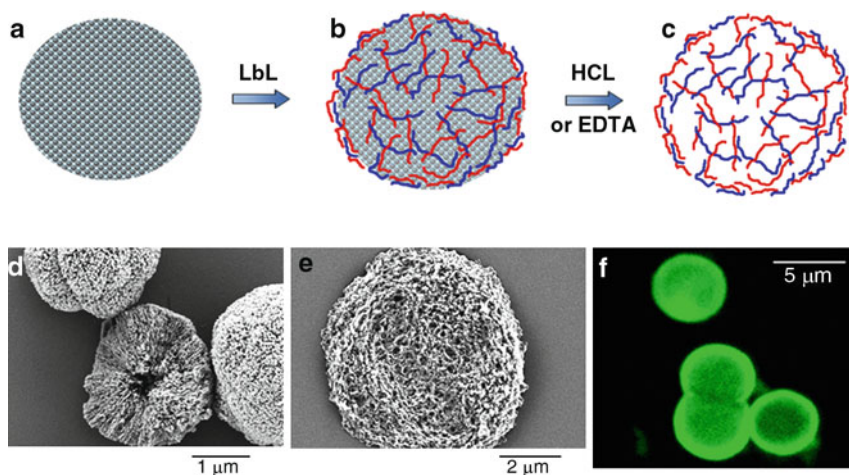


**Fig. 8** Hollow capsule fabrication by the polyelectrolyte LbL self-assembly. The core is alternately coated with polycation and polyanion, followed by core dissolution and capsule formation

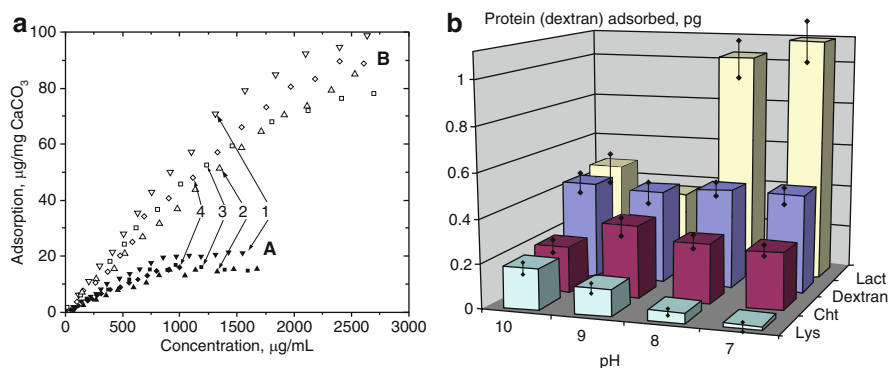
(drug) crystals, and even biological cells [45, 104–113]. MF particles were firstly employed and further intensively studied for capsule templating. However, the incomplete elimination of MF-oligomers during core dissolution strongly limits utilization of the MF cores for biological applications [114]. The oligomers are biologically incompatible. Silica oxide particles could be completely eliminated by dissolution of hazardous HF, which also limits the use of this kind of template. The cores composed of polylactic acid are biodegradable; however, the formed capsules are very polydisperse and possess a high tendency to aggregate [115].

Finally, inorganic particles from  $\text{CaCO}_3$  were found to be the most suitable sacrificial cores for polyelectrolyte capsule templating [111–113, 116, 117] due to their fine structure, biocompatibility, low cost, and simple and mild decomposition (HCl or EDTA). Monodisperse porous spherical particles composed of  $\text{CaCO}_3$  (Fig. 9d) were prepared and used to form polyelectrolyte capsules of a matrix type by the LbL technique [111, 112]. The polymer adsorption takes place not only on the particle surface but also within the porous interior. Dissolution of the  $\text{CaCO}_3$  core leads to formation of polymer gel particles with dimensions equal to the size of the initially employed  $\text{CaCO}_3$  cores (Fig. 9a–c). The capsule image obtained by scanning electron microscopy (Fig. 9e) demonstrates the sponge-like structure of the matrix capsules. Two different ways to encapsulate biological substances (proteins) in the matrix capsules were elaborated: [113] active loading (entrapment is achieved during fabrication of the microcapsules), and passive loading (encapsulation is achieved in the preformed capsules; the material of interest is taken into or generated in situ within the capsules). Protein molecules are distributed within the whole particle





**Fig. 9** (a–c) Preparation of matrix-type polyelectrolyte capsules templated on  $\text{CaCO}_3$  microparticles. (d, e) Scanning microscopy images of the  $\text{CaCO}_3$  microparticles and the matrix-type capsules, respectively. (f) Confocal laser scanning microscopy image of the capsules loaded with fluorescently labeled bovine serum albumin. Adapted from [111, 112]



**Fig. 10** (a) Adsorption isotherms of BSA (1), chymotrypsin (2), lysozyme (3), and PAH (4) adsorbing within  $\text{CaCO}_3$  microparticles. The curves of group A describe the adsorption onto pre-formed  $\text{CaCO}_3$  microparticles, and those of group B the adsorption and capture during the growth of spherical  $\text{CaCO}_3$  microparticles (coprecipitation). (b) Amount of proteins and dextran adsorbed per  $\text{CaCO}_3$  microparticle as a function of pH. Incubation time 1 h. Reproduced from [111]

interior according to the polymer distribution in the capsules because the loading of the protein is driven by the interaction with free polyelectrolyte chains (Fig. 9f). The  $\text{CaCO}_3$  particles and matrix polyelectrolyte capsules have high protein capacity (up to 100 mg of embedded protein per 1 g of  $\text{CaCO}_3$ ) [111, 116, 117], and the protein uptake in the particles was shown to be regulated by electrostatic interactions [111]. Figure 10 presents the protein adsorption isotherms (Fig. 10a) and protein uptake

(Fig. 10b) for the  $\text{CaCO}_3$  cores. About a half of the protein (lactalbumin) molecules initially adsorbed in the  $\text{CaCO}_3$  particles are kept in the formed capsules [111]. Peptidase  $\alpha$ -chymotrypsin encapsulated into the matrix-type capsules keeps 85% of the initial enzymatic activity [116]. The capsules fabricated with biocompatible polymers like ALG and templated on biocompatible  $\text{CaCO}_3$  cores are promising species for controlled delivery [113].

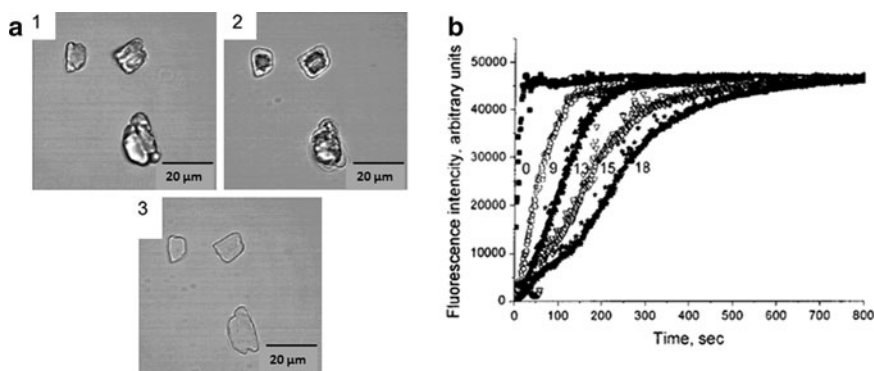
The capsules with a defined shell (so-called hollow multilayered polyelectrolyte capsules) are free-standing LbL films with a peculiar advantage – the ability to uptake the material inside the capsule, in other words to encapsulate it and to control its release by changing the LbL film permeability properties. Macromolecules like proteins have been successfully loaded into polyelectrolyte LbL capsules through pH-controlled and water/ethanol mixture-controlled methods [118, 119]. Alternative stimuli could be applied, e.g., a magnetic field [120]. This approach consists of destabilization of the LbL membrane, which then becomes more permeable. The capsule is loaded with molecules of interest under destabilized conditions and then the conditions are changed back to the initial ones (under which the LbL shell is stable).

Protein aggregates [107, 109, 121] or dye crystals [122–126] can serve as templates for LbL polyelectrolyte adsorption. Chymotrypsin aggregates encapsulated by PSS and PAH deposition contain a high protein amount and the enzyme keeps its bioactivity [107]. The aggregates prepared in this manner have high incorporation efficiency and a protein content of 50–70% [109]. An encapsulated catalase has been shown to be stable against protease degradation [121].

### 3.1 Cargo Release

The mechanism of drug release from multilayered capsules is totally different to that from planar drug-containing surface films. For the capsules filled with encapsulated drug, the release rate depends on capsule membrane permeability, which can be manipulated by stimuli that affect the structure and stability of the interpolyelectrolyte interactions (pH, ionic strength, temperature, etc.). The same stimuli could be applied for flat films and capsules; however, the leakage of the capsule contents is more sensitive to stimuli due to osmotic pressure created by the encapsulated material. DNA/spermidine or ALG/PLL capsules were shown to be decomposable at increased NaCl concentration, thus allowing the release of cargo [127]. The reversible character of the membrane destabilization in shell-like polyelectrolyte microcapsules allows keeping the material in capsules and then releasing it by changing the shell permeability through modifying external factors [128]. The remote activation properties and capsule targeting have been reviewed by Sukhorukov [129].

The matrix polyelectrolyte capsules have high protein-loading capacity, and both the loading and, in principle, the release are driven by electrostatic interaction with polyelectrolytes [111]. Moreover, the loading and release can be controlled by the number of polyelectrolyte adsorption steps [112] as well as by the pore size of the  $\text{CaCO}_3$  cores [116].



**Fig. 11** (a) Optical microscopy images of the release from ibuprofen crystals covered with a  $(\text{CHI}/\text{dextran sulfate})_{15}$  shell: 1 before dissolution; 2 during dissolution; and 3 after removal of the crystal cores. The mean size of the encapsulated ibuprofen microcrystals is  $15.3 \mu\text{m}$ . Reproduced from [112]. (b) Fluorescence increases with time, obtained by dissolving fluorescein crystals covered with shells of different thicknesses (9, 13, 15, and 18 polyelectrolyte-deposited PSS/PAH layers). The release from the native (uncovered) fluorescein crystals is shown as 0. Reproduced from [122]

The LbL film forms a barrier that prolongs the release of dye from crystals coated with the LbL films (Fig. 11). Crystals such as small drug microcrystals [122–126] and protein/enzyme crystals or aggregates [107, 121] can be encapsulated by polyelectrolyte LbL assembly and the release rate adjusted by changing the number of alternating polymer deposition steps or the polyelectrolyte nature. Antipov showed that nine bilayers of PSS and PAH can decrease the release time of the coated fluorescein crystals from seconds to minutes at conditions under which the crystals become soluble [122]. A decrease in the release rate was shown for furosemide crystals coated with a combination of PSS, PDAD, and gelatine [123]. Significantly longer release kinetics were reported by Qiu for ibuprofen encapsulated by coating with biopolymers (polysaccharides dextran sulfate and CHI) [125]. Enzymatic degradation of indomethacin crystals covered by the ALG/CHI shell led to drug release [94], again showing that disintegration of the LbL film formed on the drug crystal surface is the main mechanism for drug release.

Although the polyelectrolyte LbL membrane works as a barrier to prolong drug release, in some applications the release time is already long. Annealing of capsules upon heating can dramatically reduce the film permeability [130, 131]. Thus, polyelectrolyte microcapsules made by the LbL technique are drug delivery carriers with a wide range of release rates. Together with the advantage of being able to control the capsule size within a range of less than  $1 \mu\text{m}$  and up to tens of micrometers, this makes the capsules very promising delivery carriers.

The remote release of encapsulated materials is desired for bioapplications in order to minimize drug toxicity, to control the properties of biosurfaces and interfaces, and to study intracellular processes [132]. Remote release can be more convenient for a patient because external stimuli like a magnetic field, light, and ultrasound are

not harmful. Light-stimulated remote release is of special interest because of the possibility for external control of the light intensity and modulation, and because of its noninvasive character. Numerous examples demonstrate promising applications of this concept using liposomes as carriers [133–137]. For example, liposomes decorated with gold nanoparticles by electrostatic complexation are prospective vehicles for pulsed-light-stimulated release [133]. Irradiation by “biofriendly” near-IR light can induce fast release of vesicle contents within a few seconds of light treatment [133]. Remote release from polyelectrolyte LbL microcapsules functionalized with metal nanoparticles has been demonstrated using laser light to burst open or deform the capsules [138]. Both the magnetic and optical responses of microcapsules modified by iron oxide and gold nanoparticles, respectively, were demonstrated by Gorin and co-authors [139].

The engineering of stable liposome-containing LbL films to allow release of active content in response to external stimuli opens a new route to the preparation of biocoatings for delivery on demand. This is possible thanks to the versatility of the LbL films as an instrument for making functional surfaces sensitive to biorelated stimuli [140].

### ***3.2 Intracellular Light-Triggered Delivery***

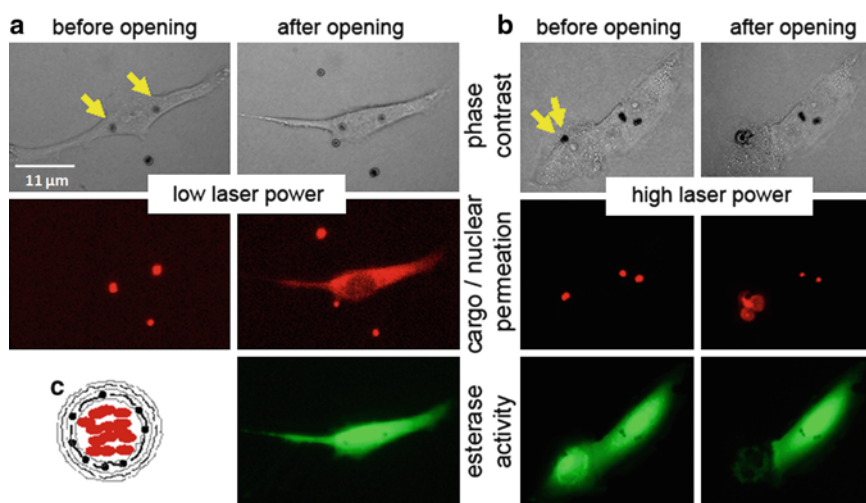
Intracellular trafficking of small peptides and the behavior of various biomolecules can be studied using remote-controlled release from microcapsules by laser irradiation. Polyelectrolyte multilayer microcapsules can be used for encapsulation of these biomolecules. Thermally shrunk microcapsules were shown capable of intracellular delivery of various biomolecules [132]. Intracellular release can be conducted using a laser source that is biologically friendly by using a near-IR laser source; the mechanism of interaction is the localized heating of nanoparticles by laser. One requirement of these experiments is to have minimum absorption by cells and tissue, and maximum absorption by nanoparticles. In regard to lasers, one can choose the wavelength of the laser to be in a desired region in the biologically friendly window (the near-IR part of the spectrum). Absorption by nanoparticles can be tuned to the near-IR region by making aggregates. Aggregation leads to an increased absorption in the near-IR region [141] due to dipole and higher order multipolar contributions, as well as to interaction between the nanoparticles. Also, the concentration of metal nanoparticles is important because (1) when the distance between the two adjacent nanoparticles is of the order of their size, the thermal effects produced by adjacent nanoparticles add up; and (2) the interaction of nanoparticles situated close to each other leads to an increase of absorption at the lower energies or higher wavelengths compared to the surface plasmon resonance band of stand-alone nanoparticles. To reduce the total amount of heat generated in the vicinity of nanoparticles, it is desirable to control the spatial distribution of nanoparticles [142].

Both remote activation and release of encapsulated materials inside living cells have been recently reported [143, 144]. Experiments on remote activation were

conducted using microcapsules containing silver nanoparticles in their walls. Remote release experiments have also been reported for capsules containing gold–gold sulfide nanoparticles in their walls.

Conditions for remote release experiments are extremely important. It was recently reported that at a low incident intensity of laser light, the release can be carried out nondestructively for cells [145]. This case is suitable for intracellular delivery, which is targeted for studying intracellular functions. Another extreme case is that at a high incident intensity of laser light (close to 100 mW), cells can be killed. This approach is suitable for cancer therapy. Figure 12 presents both of these cases: release from microcapsules was carried out into the cytosol of cells and the effects of both low and high intensity light were studied in detail [145].

The methods of remote release described here can be used for studying numerous processes relevant for biology, e.g., the cell-surface presentation of small peptides, transport of biomolecules, and cell functions in general. Also, such methods can be used to study the properties and release from other systems, e.g., liposomes [133, 146, 147].



**Fig. 12** Cargo release and viability/cytotoxicity experiments with capsules filled with red Alexa Fluor 594 dextran as cargo and AuS<sub>2</sub> particles embedded in their walls. Capsules were illuminated with (a) low laser power (2.3 mW), the minimum power needed to open the capsules, and (b) high laser power (31 mW), the maximum power output reachable with the laser diode used in these experiments. Phase contrast images (*top row*) show cells that have incorporated capsules (*arrows*) before and after laser illumination. Fluorescence images in the *middle row* show the cargo release and the nuclear permeation in cases where capsules trapped in cells were excited with low laser power and high laser power, respectively. In the case of high power illumination, permeation of the cell membrane leads to loss of fluorescent cargo by diffusion out of the cell. Fluorescence images on the *bottom row* indicate decrease of esterase activity in cells where capsules were excited with high and low laser power, respectively. (c) Geometry of capsules with Alexa Fluor 594 dextran (*ellipsoids*) in their cavity and AuS<sub>2</sub> particles (*black circles*) embedded in their walls. Reproduced from [145]

## 4 LbL Films Govern Cellular Response

The interaction between the substrate to which cells are attached and the various components of a cell is a major factor in deciding the fate of the cell upon that particular substrate. This is especially true for anchorage-dependent cells, which show specific responses (chemical signals, mechanical alterations, or biological factors) to the substrate on which they are grown. Such adherent cells must attach to and spread on the surface in order to function. In tissue, this surface is the extracellular matrix (ECM), a scaffold formed by the assembly of charged macromolecules – several large proteins (e.g., fibronectin, laminins, collagens) and glucosaminoglycans [148]. The ECM provides a microenvironment that organizes cells into a tissue. The ECM is not only a physical support of cells but a dynamic system with a high traffic of bioactive molecules that inducing certain cellular events. LbL deposition provides unique control over polymer architecture with nanometer precision and is a tool that can be used to emulate the properties of natural ECM. Protein interaction with polyelectrolyte multilayers has been evaluated and quantified [33, 45, 55, 88, 149]. The interaction strongly depends on the sign of the charge of both the film and the protein, as well as on the hydrophilicity of both. Understanding of the interaction between protein molecules and multilayers is the key to engineering an artificial ECM with tailored cellular response.

The interaction of LbL films with cells has been intensively studied [42, 150–156]. The first work devoted to cell interaction with the LbL films was performed at the beginning of this decade [157]. LbL films made from synthetic polyelectrolytes, biopolymers, components of the ECM, and polymers grafted with specific ligands have all been used to study cellular behavior. Picart and Boudou summarized LbL film functionality with respect to the behavior of cells in contact with the films [28, 29]. The physicochemical characteristics of the film can be tuned to a large extent, which gives the option to modulate cell interaction with the film [29, 158, 159]. Cell interactions with multilayered films can be tuned by the number of layers [155], the type of the outermost polymer layer, and the presence of proteins [155, 159, 160]. No adherence of chondrosarcoma cells was found on PGA-terminating films, whereas adhesion to PLL-ending films was significant [155]. This is related to the fact that PGA-ending films prevent the adsorption of serum proteins. Interestingly, the adhesion force decreased when the film thickness increased. Additionally, the films can offer delivery of incorporated active substances, for instance DNA [42, 150].

Surface coating by LbL films can alter the mechanical surface properties, thus opening a way to control cell adhesion. Coating with the film can lead to weakening of cell interactions with the underlying surface making it relatively bioinert [154]. The mechanical properties of LbL films play an important role in various cellular processes including cell attachment, proliferation, and differentiation. Ren studied the effect of PLL/HA film crosslinking on the film stiffness and on skeletal muscle cell adhesion and proliferation [153]. It has been demonstrated that crosslinked films (Young's modulus,  $E_o > 320\text{kPa}$ ) promote cell adhesion and proliferation, but soft films ( $E_o \sim 3\text{kPa}$ ) do not. It is reported that the crosslinking does not



significantly affect the thickness and morphology of the films. Similar findings have been demonstrated for chondrosarcoma cells [156]. LbL films enable control over mechanical properties in a wide range (kPa to GPa) by tuning the film thickness, polymer nature, environmental conditions like pH and salt, introduction of chemical crosslinking, rigidification with stiff material, etc. [158, 159, 161, 162]. Kocgozlu has recently shown the importance of film elasticity for the regulation of replication and transcription activities in a wide range of elastic moduli from 0 to 500 kPa [163]. Mechanical properties of the surface are crucial for cellular response and the wide range of stiffness of the LbL films covers typical values found in natural tissue [164].

LbL films possess multifold properties and very important characteristics that enable their use in bioapplications such as implant biocoatings and functionalization. Drug delivery from permanent or long-term implanted biodevices remains a challenging area in medicine. Direct drug delivery from an implant surface could be, in principle, the main task but the surface-located drugs have another function. They are required to trigger a desired cell response around the implanted material (wound healing, bone growth) and to minimize or prevent biomaterial-associated complications accompanying implantation (e.g., bacterial colonization). Immobilization of bioactive molecules on the implant surface by the LbL approach provides very effective local delivery of often very expensive and toxic pharmaceuticals. Nonspecific protein adsorption could be minimized by surface modification with LbL films and, at the same time, beneficial molecules like proteins could become selectively adsorbed on the biointerfaces by the LbL technique [45, 46]. Minimization of thrombogenicity is a main challenge for biomedical devices that are in contact with blood. Thierry showed that coverage of metal endovascular stents with HA/(CHI/HA)<sub>4</sub> multilayers reduces platelet adhesion by 38% [165].

Potential applications of the LbL films as antibacterial coatings have also been reported. Multilayers of albumin/heparin can significantly reduce bacterial adhesion [166]. In our recent study, we have shown that a PLL/HA multilayer film loaded with liposome aggregates as reservoirs containing silver ions has strong bactericidal activity [167]. A contact of 120 min with an AgNO<sub>3</sub> coating (with 120 ng/cm<sup>2</sup> AgNO<sub>3</sub> concentration) induces a 4-log reduction of the *Escherichia coli* population [167]. Chuang has demonstrated that degradable LbL films can effectively release gentamicine [90].

## 5 Conclusion

The LbL technique is now becoming one of the central tools in biomedical engineering, i.e., for biomaterial modification and drug delivery. The advantages of being able to control material deposition, immobilize almost any molecule from large polymers to small substances, and modify almost any surface, including sophisticated shapes or miniaturized supports, make the technique one of the most dominant in the field of surface nanotechnology. This review demonstrates that polyelectrolyte



LbL films are capable not only of immobilizing bioactive substances but also of opening various routes to control their release, e.g., by remote release with noninvasive stimulus, which is a challenge in medicine. Remote light activation of LbL films can serve future bioapplications in which high loading capacity together with remote-release functionalities are demanded. Additionally, LbL films provide a surface of biomaterials with physical and chemical properties that are desirable for controlling the interaction with living cells. 3D structures (free-standing LbL films or capsules) have been developed and open new perspectives for the formulation of microparticulate material with defined size and surface chemistry, enabling different administration routes and release capabilities.

## References

1. Decher G (1997) Fuzzy nanoassemblies: toward layered polymeric multicomposites. *Science* 277:1232–1237
2. Decher G, Hong J-D (1991) Buildup of ultrathin multilayer films by a self-assembly process: I. Consecutive adsorption of anionic and cationic bipolar amphiphiles. *Makromol Chem* 46:321
3. Cho J, Caruso F (2003) Polymeric multilayer films comprising deconstructible hydrogen-bonded stacks confined between electrostatically assembled layers. *Macromolecules* 36:2845–2851
4. Sukhishvili SA, Granick S (2000) Layered, erasable, ultrathin polymer films. *J Am Chem Soc* 122:9550–9551
5. Sukhishvili SA, Granick S (2002) Layered, erasable polymer multilayers formed by hydrogen-bonded sequential self-assembly. *Macromolecules* 35:301–310
6. Inoue H, Sato K, Anzai J (2005) Disintegration of layer-by-layer assemblies composed of 2-iminobiotin-labeled poly(ethyleneimine) and avidin. *Biomacromolecules* 6:27–29
7. Ling XY, Malaquin L, Reinhoudt DN et al (2007) An in situ study of the adsorption behavior of functionalized particles on self-assembled monolayers via different chemical interactions. *Langmuir* 23:9990–9999
8. Suzuki I, Egawa Y, Mizukawa Y et al (2002) Construction of positively-charged layered assemblies assisted by cyclodextrin complexation. *Chem Commun*:164–165
9. Ling XY, Phang IY, Reinhoudt DN et al (2008) Supramolecular layer-by-layer assembly of 3D multicomponent nanostructures via multivalent molecular recognition. *Int J Mol Sci* 9:486–497
10. Van der Heyden A, Wilczewski M, Labbe P et al (2006) Multilayer films based on host–guest interactions between biocompatible polymers. *Chem Commun*:3220–3222
11. Wang ZP, Feng ZQ, Gao CY (2008) Stepwise assembly of the same polyelectrolytes using host–guest interaction to obtain microcapsules with multiresponsive properties. *Chem Mater* 20:4194–4199
12. Stockton WB, Rubner MF (1997) Molecular-level processing of conjugated polymers. 4. Layer-by-layer manipulation of polyaniline via hydrogen-bonding interactions. *Macromolecules* 30:2717–2725
13. Shiratori SS, Rubner MF (2000) pH-Dependent thickness behavior of sequentially adsorbed layers of weak polyelectrolytes. *Macromolecules* 33:4213–4219
14. Schlenoff JB, Ly H, Li M (1998) Charge and mass balance in polyelectrolyte multilayers. *J Am Chem Soc* 120:7626–7634
15. Schlenoff JB, Dubas ST (2001) Mechanism of polyelectrolyte multilayer growth: charge overcompensation and distribution. *Macromolecules* 34:592–598

16. Sui Z, Salloum D, Schlenoff JB (2003) Effect of molecular weight on the construction of polyelectrolyte multilayers: stripping versus sticking. *Langmuir* 19:2491–2495
17. Salomäki M, Vinokurov IA, Kankare J (2005) Effect of temperature on the buildup of polyelectrolyte multilayers. *Langmuir* 21:11232–11240
18. Laugel N, Betscha C, Winterhalter M et al (2006) Relationship between the growth regime of polyelectrolyte multilayers and the polyanion/polycation complexation enthalpy. *J Phys Chem B* 110:19443–19449
19. Schonhoff M (2003) Layered polyelectrolyte complexes: physics of formation and molecular properties. *J Phys Condens Matter* 15:1781–1808
20. Ariga K, Hill JP, Li Q (2007) Layer-by-layer assembly as a versatile bottom-up nanofabrication technique for exploratory research and realistic application. *Phys Chem Chem Phys* 9:2319–2340
21. Hammond PT (2004) Form and function in multilayer assembly: new applications at the nanoscale. *Adv Mater* 16:1271–1293
22. Wang Y, Angelatos AS, Caruso F (2008) Template synthesis of nanostructured materials via layer-by-layer assembly. *Chem Mater* 20:848–858
23. Picart C, Mutterer J, Richert L et al (2002) Molecular basis for the explanation of the exponential growth of polyelectrolyte multilayers. *Proc Natl Acad Sci USA* 99:12531–12535
24. Jourdainne L, Lecuyer S, Arntz Y et al (2008) Dynamics of poly(L-lysine) in hyaluronic acid/poly(L-lysine) multilayer films studied by fluorescence recovery after pattern photobleaching. *Langmuir* 24:7842–7847
25. Picart C, Lavalle P, Hubert P et al (2001) Buildup mechanism for poly(L-lysine)/hyaluronic acid films onto a solid surface. *Langmuir* 17:7414–7424
26. Boulmedais F, Ball V, Schwinte P et al (2003) Buildup of exponentially growing multilayer polypeptide films with internal secondary structure. *Langmuir* 19:440–445
27. Liu GM, Zhao JP, Sun QY et al (2008) Role of chain interpenetration in layer-by-layer deposition of polyelectrolytes. *J Phys Chem B* 112:3333–3338
28. Picart C (2008) Polyelectrolyte multilayer films: from physico-chemical properties to the control of cellular processes. *Curr Med Chem* 17:685–697
29. Thomas B, Thomas C, Kefeng R et al (2009) Multiple functionalities of polyelectrolyte multilayer films: new biomedical applications. *Adv Mater* 21:1–27
30. Lvov Y, Ariga K, Ichinose I et al (1995) Assembly of multicomponent protein films by means of electrostatic layer-by-layer adsorption. *J Am Chem Soc* 117:6117–6123
31. Anzai JI, Hoshi T, Nakamura N (2000) Construction of multilayer thin films containing avidin by a layer-by-layer deposition of avidin and poly(anions). *Langmuir* 16:6306–6311
32. Jessel N, Atalar F, Lavalle P et al (2003) Bioactive coating based on a polyelectrolyte multilayer architecture functionalized by embedded proteins. *Adv Mater* 15:692–695
33. Ladam G, Schaaf P, Cuisinier FJ et al (2001) Protein adsorption onto auto-assembled polyelectrolyte films. *Langmuir* 17:878–882
34. Boulmedais F, Ball V, Schwinte P et al (2003) Buildup of exponentially growing multilayer polypeptide films with internal secondary structure. *Langmuir* 19:440–445
35. Richert L, Lavalle P, Payan E et al (2004) Layer by layer buildup of polysaccharide films: physical chemistry and cellular adhesion aspects. *Langmuir* 20:448–458
36. Cassier T, Sinner A, Offenhauser A et al (1999) Homogeneity, electrical resistivity and lateral diffusion of lipid bilayers coupled to polyelectrolyte multilayers. *Colloids Surf B* 15:215–225
37. Moya S, Donath E, Sukhorukov GB et al (2000) Lipid coating on polyelectrolyte surface modified colloidal particles and polyelectrolyte capsules. *Macromolecules* 33:4538–4544
38. Lvov Y, Decher G, Sukhorukov GB (1993) Assembly of thin films by means of successive deposition of alternate layers of DNA and poly(allylamine). *Macromolecules* 26:5396–5399
39. Sukhorukov GB, Montrel MM, Petrov AI et al (1996) Multilayer films containing immobilized nucleic acids. Their structure and possibilities in biosensor applications. *Biosens Bioelectron* 11:913–922
40. Pei R, Cui X, Yang X et al (2001) Assembly of alternating polycation and DNA multilayer films by electrostatic layer-by-layer adsorption. *Biomacromolecules* 2:463–468

41. Zhang J, Chua LS, Lynn DM (2004) Multilayered thin films that sustain the release of functional DNA under physiological conditions. *Langmuir* 20:8015–8021
42. Jewell CM, Zhang J, Fredin NJ et al (2005) Multilayered polyelectrolyte films promote the direct and localized delivery of DNA to cells. *J Control Release* 106:214–223
43. Dimitrova M, Arntz Y, Lavalle P et al (2007) Adenoviral gene delivery from multilayered polyelectrolyte architectures. *Adv Funct Mater* 17:233–245
44. Ariga K, Hill JP, Li Q (2007) Layer-by-layer assembly as a versatile bottom-up nanofabrication technique for exploratory research and realistic application. *Phys Chem Chem Phys* 9:2319–2340
45. Ai H, Jones SA, Lvov YM (2003) Biomedical applications of electrostatic layer-by-layer nano-assembly of polymers, enzymes, and nanoparticles. *Cell Biochem Biophys* 39:23–43
46. Tang Z, Wang Y, Podsiadlo P et al (2006) Biomedical applications of layer-by-layer assembly: from biomimetics to tissue engineering. *Adv Mater* 18:3203–3224
47. Peyratout CS, Dahne L (2004) Tailor-made polyelectrolyte microcapsules: from multilayers to smart containers. *Angew Chem Int Ed* 43:3762–3783
48. Bertrand P, Jonas A, Laschewsky A et al (2000) Ultrathin polymer coatings by complexation of polyelectrolytes at interfaces: suitable materials, structure and properties. *Macromol Rapid Commun* 21:319–348
49. Hammond PT (2000) Recent explorations in electrostatic multilayer thin film assembly. *Curr Opin Colloid Interface Sci* 4:430–442
50. Zhang L, Zhao WH, Rudra JS et al (2007) Context dependence of the assembly, structure, and stability of polypeptide multilayer nonofilms. *ACS Nano* 1:476–486
51. Haynie DT, Balkundi S, Palath N et al (2004) Polypeptide multilayer films: role of molecular structure and charge. *Langmuir* 20:4540–4547
52. Boulmedais F, Schwinte P, Gergely C et al (2002) Secondary structure of polypeptide multilayer films: an example of locally ordered polyelectrolyte multilayers. *Langmuir* 18:4523–4525
53. Onda M, Ariga K, Kunitake T (1999) Activity and stability of glucose oxidase in molecular films assembled alternately with polyions. *J Biosci Bioeng* 87:69–75
54. Disawal S, Qiu J, Elmore BB et al (2003) Two-step sequential reaction catalyzed by layer-by-layer assembled urease and arginase multilayers. *Colloids Surf B* 32:145–156
55. Schwinte P, Voegel J-C, Picart C et al (2001) Stabilizing effects of various polyelectrolyte multilayer films on the structure of adsorbed/embedded fibrinogen molecules: an ATR-FTIR study. *J Phys Chem B* 15:11906–11916
56. Schneider A, Vodouhê C, Richert L et al (2007) Multifunctional polyelectrolyte multilayer films: combining mechanical resistance, biodegradability, and bioactivity. *Biomacromolecules* 8:139–145
57. Vodouhê C, Le Guen E, Mendez Garza J et al (2006) Control of drug accessibility on functional polyelectrolyte multilayer films. *Biomaterials* 27:4149–4156
58. Wang XF, Ji J (2009) Postdiffusion of oligo-peptide within exponential growth multilayer films for localized peptide delivery. *Langmuir* 25:11664–11671
59. Barenholz Y (2001) Liposome application: problems and prospects. *Curr Opin Colloid Interface Sci* 6:66–77
60. Christensen SM, Stamou D (2007) Surface-based lipid vesicle reactor systems: fabrication and applications. *Soft Matter* 3:828–836
61. Patolsky F, Lichtenstein A, Willner I (2001) Electronic transduction of DNA sensing processes on surfaces: amplification of DNA detection and analysis of single-base mismatches by tagged liposomes. *J Am Chem Soc* 123:5194–5205
62. Vermette P, Meagher L, Gagnon E et al (2002) Immobilized liposome layers for drug delivery applications: inhibition of angiogenesis. *J Control Release* 80:179–195
63. Yoshina-Ishii C, Miller GP, Kraft ML et al (2005) General method for modification of liposomes for encoded assembly on supported bilayers. *J Am Chem Soc* 127:1356–1357
64. Xu D, Cheng Q (2002) Surface-bound lipid vesicles encapsulating redox species for amperometric biosensing of pore-forming bacterial toxins. *J Am Chem Soc* 124:14314–14315

65. Chifen AN, Forch R, Knoll W et al (2007) Attachment and phospholipase A2-induced lysis of phospholipid bilayer vesicles to plasmopolymerized maleic anhydride/SiO<sub>2</sub> multilayers. *Langmuir* 23:6294–6298
66. Reviakine I, Brisson A (2000) Formation of supported phospholipid bilayers from unilamellar vesicles investigated by atomic force microscopy. *Langmuir* 16:1806–1815
67. Richter RP, Berat R, Brisson AR (2006) Formation of solid-supported lipid bilayers: an integrated view. *Langmuir* 22:3497–3505
68. Seantier B, Breffa C, Félix O et al (2004) In situ investigations of the formation of mixed supported lipid bilayers close to the phase transition temperature. *Nano Lett* 4:5–10
69. Ruyschaert T, Germain M, Pereira da Silva Gomes JF et al (2004) Liposome-based nanocapsules. *IEEE Trans Nanobiosci* 3:49–55
70. Katagiri K, Hamasaki R, Ariga K et al (2002) Layer-by-layer self-assembling of liposomal nanohybrid “cerasome” on substrates. *Langmuir* 18:6709–6711
71. Katagiri K, Hamasaki R, Ariga K et al (2002) Layered paving of vesicular nanoparticles formed with cerasome as a bioinspired organic–inorganic hybrid. *J Am Chem Soc* 124: 7892–7893
72. Kabanov VA, Yaroslavov AA (2002) What happens to negatively charged lipid vesicles upon interacting with polycation species? *J Control Release* 78:267–271
73. Ge L, Mohwald H, Li J (2003) Phospholipid liposomes stabilized by the coverage of polyelectrolyte. *Colloids Surf A Physicochem Eng Aspects* 221:49–53
74. Quemeneur F, Rammal A, Rinaudo M et al (2007) Large and giant vesicles “decorated” with chitosan: effects of pH, salt or glucose stress, and surface adhesion. *Biomacromolecules* 8:2512–2519
75. Ciobanu M, Heurtault B, Schultz P et al (2007) Layersome: development and optimization of stable liposomes as drug delivery system. *Int J Pharm* 344:154–157
76. Germain M, Grube S, Carriere V et al (2006) Composite nanocapsules: lipid vesicles covered with several layers of crosslinked polyelectrolytes. *Adv Mater* 18:2868–2871
77. Michel M, Izquierdo A, Decher G et al (2005) Layer-by-layer self-assembled polyelectrolyte multilayers with embedded phospholipid vesicles obtained by spraying: integrity of the vesicles. *Langmuir* 21:7854–7859
78. Michel M, Vautier D, Voegel J-C et al (2004) Layer-by-layer self-assembled polyelectrolyte multilayers with embedded phospholipid vesicles. *Langmuir* 20:4835–4839
79. Volodkin D, Ball V, Schaaf P et al (2007) Complexation of phosphocholine liposomes with polylysine. Stabilization by surface coverage versus aggregation. *Biochim Biophys Acta* 1768:280–290
80. Volodkin D, Mohwald H, Voegel J-C et al (2007) Stabilization of negatively charged liposomes by polylysine surface coating. Drug release study. *J Control Release* 117:111–120
81. Volodkin DV, Ball V, Voegel J-C et al (2007) Control of the interaction between membranes and vesicles: adhesion, fusion and release of dyes. *Colloids Surf A* 303:89–96
82. Volodkin DV, Arntz Y, Schaaf P et al (2008) Composite multilayered biocompatible polyelectrolyte films with intact liposomes: stability and triggered dye release. *Soft Matter* 4:122–130
83. Volodkin DV, Michel M, Schaaf P et al (2008) Liposome embedding into polyelectrolyte multilayers: a new way to create drug reservoirs at solid–liquid interfaces. In: Liu AL (ed) *Advances in planar lipid bilayers and liposomes*. Elsevier, Amsterdam
84. Volodkin D, Schaaf P, Mohwald H et al (2009) Effective embedding of liposomes into polyelectrolyte multilayered films. The relative importance of lipid–polyelectrolyte and interpolyelectrolyte interactions. *Soft Matter* 5:1394–1405
85. Picart C, Lavalle P, Hubert P et al (2001) Buildup mechanism for poly(L-lysine)/hyaluronic acid films onto a solid surface. *Langmuir* 17:7414–7424
86. Burke SE, Barrett CJ (2004) pH-Dependent loading and release behavior of small hydrophilic molecules in weak polyelectrolyte multilayer films. *Macromolecules* 37:5375–5384
87. Dubas ST, Farhat TR, Schlenoff JB (2001) Multiple membranes from “true” polyelectrolyte multilayers. *J Am Chem Soc* 123:5368–5369

88. Müller M, Kessler B, Adler H-J et al (2004) Reversible switching of protein uptake and release at polyelectrolyte multilayers detected by ATR-FTIR spectroscopy. *Macromol Symp* 210:157–164
89. Wood KC, Boedicker JQ, Lynn DM et al (2005) Tunable drug release from hydrolytically degradable layer-by-layer thin films. *Langmuir* 21:1603–1609
90. Chuang HF, Smith RC, Hammond PT (2008) Polyelectrolyte multilayers for tunable release of antibiotics. *Biomacromolecules* 9:1660–1668
91. Wang F, Li D, Li G et al (2008) Electrodissolution of inorganic ions/DNA multilayer film for tunable DNA release. *Biomacromolecules* 9:2645–2652
92. Boulmedais F, Tang CS, Keller B et al (2006) Controlled electrodissolution of polyelectrolyte multilayers: a platform technology towards the surface-initiated delivery of drugs. *Adv Funct Mater* 16:63–70
93. Ren KF, Ji J, Shen JC (2006) Construction and enzymatic degradation of multilayered poly-L-lysine/DNA films. *Biomaterials* 27:1152–1159
94. Wang CY, Ye SQ, Dai L et al (2007) Enhanced resistance of polyelectrolyte multilayer microcapsules to pepsin erosion and release properties of encapsulated indomethacin. *Biomacromolecules* 8:1739–1744
95. Serizawa T, Yamaguchi M, Akashi M (2003) Time-controlled desorption of ultrathin polymer films triggered by enzymatic degradation. *Angew Chem Int Ed* 42:1115–1118
96. Jensen AW, Desai NK, Maru BS et al (2004) Photohydrolysis of substituted benzyl esters in multilayered polyelectrolyte films. *Macromolecules* 37:4196–4200
97. Serpe MJ, Yarmey KA, Nolan CM et al (2005) Doxorubicin uptake and release from microgel thin films. *Biomacromolecules* 6:408–413
98. Volodkin DV, Madaboosi N, Blacklock J et al (2009) Surface-supported multilayers decorated with bio-active material aimed at light-triggered drug delivery. *Langmuir* 25:14037–14043
99. Volodkin DV, Mohwald H (2009) Polyelectrolyte multilayers for drug delivery. In: Somasundaran P (ed) *Encyclopedia of surface and colloid science*. Taylor & Francis, New York
100. Volodkin DV, Delcea M, Mohwald H et al (2009) Remote near-IR light activation of a hyaluronic acid/poly(L-lysine) multilayered film and film-entrapped microcapsules. *ACS Appl Mater Interfaces* 1:1705–1710
101. Thies C (1999) *Microspheres, microcapsules and liposomes*. Citus Books, London
102. Donath E, Sukhorukov GB, Caruso F et al (1998) Novel hollow polymer shells by colloid-templated assembly of polyelectrolytes. *Angew Chem Int Ed* 37:2201–2205
103. Caruso F (2001) Nanoengineering of particle surfaces. *Adv Mater* 13:11–22
104. Sukhorukov GB (2001) In: Mobius D, Miller R (ed) *Studies in interface science*. Elsevier, Amsterdam
105. Antipov AA, Sukhorukov GB, Donath E et al (2001) *J Phys Chem B* 105:2281–2284
106. Trubetsky VS, Loomis A, Hagstrom JE et al (1999) Layer-by-layer deposition of oppositely charged polyelectrolytes on the surface of condensed DNA particles *Nucleic Acids Res* 27:3090–3095
107. Balabushevitch NG, Sukhorukov GB, Moroz NA et al (2001) Encapsulation of proteins by layer-by-layer adsorption of polyelectrolytes onto protein aggregates. *Biotechnol Bioeng* 76:207–213
108. Larionova NI, Volodkin DV, Balabushevitch NG et al (2001) Microcapsules responsive to physiological pH fabricated by layer-by-layer adsorption of polyelectrolytes on protein aggregates. *Sci Pharm* 69:175–176
109. Volodkin DV, Balabushevitch NG, Sukhorukov GB et al (2003) Model system for controlled protein release: pH-sensitive polyelectrolyte microparticles. *STP Pharma Sci* 13:163–170
110. Volodkin DV, Balabushevitch NG, Sukhorukov GB et al (2003) Inclusion of proteins in polyelectrolyte microparticles by alternative polyelectrolyte adsorption on protein aggregates. *Biochemistry (Moscow)* 68:283–289
111. Volodkin DV, Larionova NI, Sukhorukov GB (2004) Protein encapsulation via porous CaCO<sub>3</sub> microparticles templating. *Biomacromolecules* 5:1962–1972
112. Volodkin DV, Petrov AI, Prevot M et al (2004) Matrix polyelectrolyte microcapsules: new system for macromolecule encapsulation. *Langmuir* 20:3398–3406

113. Sukhorukov GB, Volodkin DV, Günther AM et al (2004) Porous calcium carbonate microparticles as templates for encapsulation of bioactive compounds. *J Mater Chem* 14:2073–2081
114. Gao CY, Moya S, Lichtenfeld H et al (2001) The decomposition process of melamine formaldehyde cores: the key step in the fabrication of ultrathin polyelectrolyte multilayer capsules. *Macromol Mater Eng* 286:355–361
115. Shenoy DB, Antipov AA, Sukhorukov GB et al (2003) Layer-by-layer engineering of bio-compatible, decomposable core–shell. *Biomacromolecules* 4:265–272
116. Petrov AI, Volodkin DV, Sukhorukov GB (2005) Protein–calcium carbonate co-precipitation. A tool for protein encapsulation. *Biotechnol Prog* 21:918–925
117. Stein EW, Volodkin DV, McShane MJ et al (2006) Real-time assessment of spatial and temporal coupled catalysis within polyelectrolyte microcapsules containing co-immobilized glucose oxidase and peroxidase. *Biomacromolecules* 7:710–719
118. Lvov Y, Antipov AA, Mamedov A et al (2001) Urease encapsulation in nanoorganized microshells. *Nano Lett* 1:125–128
119. Antipov AA, Sukhorukov GB, Loporatti S et al (2002) Polyelectrolyte multilayer capsule permeability control. *Colloids Surf A* 198:535–541
120. Lu Z, Prouty MD, Guo Z et al (2005) Magnetic switch of permeability for polyelectrolyte microcapsules embedded with Co@Au nanoparticles. *Langmuir* 21:2042–2050
121. Caruso F, Trau D, Mohwald H et al (2000) Enzyme encapsulation in layer-by-layer engineered polymer multilayer capsules. *Langmuir* 16:1485–1488
122. Antipov AA, Sukhorukov GB, Donath E et al (2001) Sustained release properties of polyelectrolyte multilayer capsules. *J Phys Chem B* 105:2281–2284
123. Ai H, Jones SA, Villiers MM et al (2003) Nano-encapsulation of furosemide microcrystals for controlled drug release. *J Control Release* 86:59–68
124. Caruso F, Yang W, Trau D et al (2000) Microencapsulation of uncharged low molecular weight organic materials by polyelectrolyte multilayer self-assembly. *Langmuir* 16: 8932–8936
125. Qiu X, Loporatti S, Donath E et al (2001) Studies on the drug release properties of polysaccharide multilayers encapsulated ibuprofen microparticles. *Langmuir* 17:5375–5380
126. Shi X, Caruso F (2001) Release behavior of thin-walled microcapsules composed of polyelectrolyte multilayers. *Langmuir* 17:2036–2042
127. Schuler C, Caruso F (2001) Decomposable hollow biopolymer-based capsules. *Biomacromolecules* 2:921–926
128. Hu S-H, Tsai C-H, Liao C-F et al (2008) Controlled rupture of magnetic polyelectrolyte microcapsules for drug delivery. *Langmuir* 24:11811–11818
129. Sukhorukov GB, Mohwald H (2007) Multifunctional cargo systems for biotechnology. *Trends Biotechnol* 25:93–98
130. Kohler K, Biesheuvel PM, Weinkamer R et al (2006) Salt-induced swelling-to-shrinking transition in polyelectrolyte multilayer capsules. *Phys Rev Lett* 97:188301
131. Kohler K, Shchukin DG, Mohwald H et al (2005) Thermal behavior of polyelectrolyte multilayer microcapsules. 1. The effect of odd and even layer number. *J Phys Chem B* 109:18250–18259
132. Skirtach AG, Javier AM, Kreft O et al (2006) Laser-induced release of encapsulated materials inside living cells. *Angew Chem Int Ed* 45:4612–4617
133. Volodkin DV, Skirtach AG, Mohwald H (2009) Near-IR remote release from assemblies of liposomes and nanoparticles. *Angew Chem Int Ed* 48:1807–1809
134. Faure C, Derre A, Neri W (2003) Spontaneous formation of silver nanoparticles in multilamellar vesicles. *J Phys Chem B* 107:4738–4746
135. Mueller A, Bondurant B, O'Brien DF (2000) Visible-light-stimulated destabilization of PEG-liposomes. *Macromolecules* 33:4799–4804
136. Regev O, Backov R, Faure C (2004) Gold nanoparticles spontaneously generated in onion-type multilamellar vesicles. Bilayers-particle coupling imaged by cryo-TEM. *Chem Mater* 16:5280–5285
137. Shum P, Kim J-M, Thompson DH (2001) Phototriggering of liposomal drug delivery systems. *Adv Drug Deliv Rev* 53:273–284



138. Skirtach AG, Antipov AA, Shchukin DG et al (2004) Remote activation of capsules containing Ag nanoparticles and IR dye by laser light. *Langmuir* 20:6988–6992
139. Gorin DA, Portnov SA, Inozemtseva OA et al (2008) Magnetic/gold nanoparticle functionalized biocompatible microcapsules with sensitivity to laser irradiation. *Phys Chem Chem Phys* 10:6899–6905
140. Skirtach AG, Kreft O (2008) In: de Villiers MM, Aramwit P, Kwon GS (eds) *Nanotechnology in drug delivery*. Springer, Berlin. doi:10.1007/978-0-387-77667-5
141. Skirtach AG, Karageorgiev P, Bedard MF et al (2008) Reversibly permeable nanomembranes of polymeric microcapsules. *J Am Chem Soc* 130:11572–11573
142. Skirtach AG, Dejunctat C, Braun D et al (2007) Nanoparticles distribution control by polymers: aggregates versus nonaggregates. *J Phys Chem C* 111:555–564
143. Skirtach AG, Antipov AA, Shchukin DG et al (2004) Remote activation of capsules containing Ag nanoparticles and IR dye by laser light. *Langmuir* 20:6988–6992
144. Radt B, Smith TA, Caruso F (2004) Optically addressable nanostructured capsules. *Adv Mater* 16:2184–2189
145. Muñoz JA, del Pino P, Bedard MF et al (2008) Photoactivated release of cargo from the cavity of polyelectrolyte capsules to the cytosol of cells. *Langmuir* 24:12517–12520
146. Wu G, Mikhailovsky A, Khant HA et al (2008) Remotely triggered liposome release by near-infrared light absorption via hollow gold nanoshells. *J Am Chem Soc* 130:8175–8177
147. Timothy ST, Sarah JL, Marek R (2009) Light-induced content release from plasmon-resonant liposomes. *Adv Mater* 21:2334–2338
148. Lutolf MP, Hubbell JA (2005) Synthetic biomaterials as instructive extracellular microenvironments for morphogenesis in tissue engineering. *Nat Biotechnol* 23:47–55
149. Salloum DS, Schlenoff JB (2004) Protein adsorption modalities on polyelectrolyte multilayers. *Biomacromolecules* 5:1089–1096
150. Jessel N, Oulad-Abdelghani M, Meyer F et al (2006) Multiple and time-scheduled in situ DNA delivery mediated by  $\beta$ -cyclodextrin embedded in a polyelectrolyte multilayer. *Proc Natl Acad Sci USA* 103:8618–8621
151. Benkirane-Jessel N, Lavallo P, Meyer F et al (2004) Control of monocyte morphology on and response to model surfaces for implants equipped with anti-inflammatory agent. *Adv Mater* 16:1507–1511
152. Benkirane-Jessel N, Lavallo P, Hubsch E et al (2005) Short-time tuning of the biological activity of functionalized polyelectrolyte multilayers. *Adv Funct Mater* 15:648–654
153. Ren K, Crouzier T, Roy C et al (2008) Polyelectrolyte multilayer films of controlled stiffness modulate myoblast cell differentiation. *Adv Funct Mater* 18:1–12
154. Elbert DL, Herbert CB, Hubbell JA (1999) Thin polymer layers formed by polyelectrolyte multilayer techniques on biological surfaces. *Langmuir* 15:5355–5362
155. Richter L, Lavallo P, Vautier D et al (2002) Cell interactions with polyelectrolyte multilayer films. *Biomacromolecules* 3:1170–1178
156. Schneider A, Richert L, Francius G et al (2007) Elasticity, biodegradability and cell adhesive properties of chitosan/hyaluronan multilayer films. *Biomed Mater* 2:S45–S51
157. Chluba J, Voegel J-C, Decher G et al (2001) Peptide hormone covalently bound to polyelectrolytes and embedded into multilayer architectures conserving full biological activity. *Biomacromolecules* 2:800–805
158. Picart C (2008) Polyelectrolyte multilayer films: from physico-chemical properties to the control of cellular processes. *Curr Med Chem* 17:685–697
159. Thompson MT, Berg MC, Tobias IS et al (2005) Tuning compliance of nanoscale polyelectrolyte multilayers to modulate cell adhesion. *Biomaterials* 26:6836–6845
160. Tryoen-Toth P, Vautier D, Haikel Y et al (2002) Viability, adhesion, and bone phenotype of osteoblast-like cells on polyelectrolyte multilayer films. *J Biomed Mater Res* 60:657–667
161. Picart C, Schneider A, Etienne O et al (2005) Controlled degradability of polysaccharide multilayer films in vitro and in vivo. *Adv Funct Mater* 15:1771–1780
162. Podsiadlo P, Tang Z, Shim BS et al (2007) Counterintuitive effect of molecular strength and role of molecular rigidity on mechanical properties of layer-by-layer assembled nanocomposites. *Nano Lett* 7:1224–1231



163. Kocgozlu L, Lavalle P, Koenig G et al (2010) Selective and uncoupled role of substrate elasticity in the regulation of replication and transcription in epithelial cells. *J Cell Sci* 123:29–39
164. Discher DE, Janmey P, Wang Y (2005) Tissue cells feel and respond to the stiffness of their substrate. *Science* 310:1139–1143
165. Thierry B, Winnik FM, Merhi Y et al (2003) Bioactive coatings of endovascular stents based on polyelectrolyte multilayers. *Biomacromolecules* 4:1564–1571
166. Brynda E, Houska M (2000) Ordered multilayer assemblies: albumin/heparin for biocompatible coating and monoclonal antibodies for optical immunosensors. In: Lvov Y, Möhwald H (ed) *Protein architecture: interfacial molecular assembly and immobilization biotechnology*. Dekker, New York
167. Malcher M, Volodkin D, Heurtault B et al (2008) Embedded silver ions-containing liposomes in polyelectrolyte multilayers: cargos films for antibacterial agents. *Langmuir* 24: 10209–10215

# Designing Three-Dimensional Materials at the Interface to Biology

R. Gentsch and H.G. Börner

**Abstract** Modern approaches to the production of 3D materials with bioactive interfaces for tissue engineering, biointegrated materials, and biomimetic materials are reviewed. Recent advances in the understanding of how materials passively interact or actively communicate with biological systems via designed material–biology interfaces demand precise means to fabricate macroscopic nanostructured materials. We review modern materials and technology that are available for the production of bioactive scaffolds having spatial control of mechanical, chemical, and biochemical signals at the interface, as well as tailored pore architecture and surface topology.

**Keywords** Bioactive · Biomaterials · Biomimetic · Cellular infiltration · Electrospinning · Extracellular matrix · Hydrogels · Nanofibers · Polymer scaffolds · Tissue engineering

## Contents

1	Introduction .....	164
1.1	Effect of Nanostructures on Biological Systems .....	166
1.2	Biological Activity of 3D Surfaces .....	168
2	Generation of 3D Structured Surfaces .....	171
2.1	Bottom-Up Approaches .....	171
2.2	Top-Down Processing .....	177
3	Biological Aspects .....	185
4	Summary and Outlook .....	187
	References .....	188

---

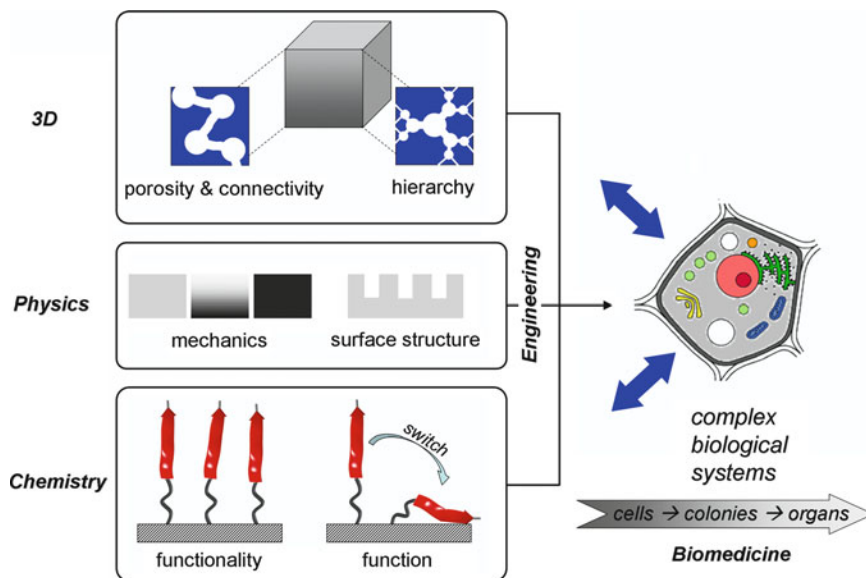
R. Gentsch  
Max Planck Institute of Colloids and Interfaces, Am Mühlenberg 1, 14476 Potsdam, Germany  
e-mail: [rafael.gentsch@mpikg.mpg.de](mailto:rafael.gentsch@mpikg.mpg.de)

H.G. Börner (✉)  
Department of Chemistry, Laboratory of Organic Synthesis of Functional Systems,  
Humboldt-Universität zu Berlin, Brook-Taylor-Strasse 2, 12489 Berlin, Germany  
and  
Max Planck Institute of Colloids and Interfaces, Am Mühlenberg 1, 14476 Potsdam, Germany  
e-mail: [h.boerner@hu-berlin.de](mailto:h.boerner@hu-berlin.de)

## 1 Introduction

Precisely controlling the interface between synthetic materials and biological systems might be one of the most important, but also most demanding, tasks of modern materials science. The resulting opportunities will, however, assure progress in several research areas, ranging from medical technology (e.g., implantation medicine), tissue engineering, regenerative cell biology, and stem cell research to biointegrated materials design as well as bioassisted compound synthesis [1–6]. The rational design of materials that actively interact with biological systems, to guide or even dynamically communicate with biological entities such as cells or tissues, requires a high level of structural and functional control.

Fundamental research that focused on planar interfaces revealed the applicability of basic concepts of bioadhesion and functional signaling in two dimensions (Fig. 1) [7–9]. Despite this progress, biological systems are three-dimensional (3D) in nature and moreover often exhibit hierarchical organization levels [10, 11]. This makes the spatial control of surface structure, pore architecture, mechanical properties, functionality, and complex functions mandatory (Fig. 1) [5]. Cells are roughly 10–100  $\mu\text{m}$  in size, cell sensing takes place with about 5–10 nm precision, and signaling (cell communication) can follow multidimensional concentration gradients with nanometer accuracy [7]. Hence, cells are sensitive to chemistry and topography on the meso-, micro-, and nanoscales [12]. It is exactly this range of length scales that makes materials design at the interface to biology an exciting, but also highly complex task.



**Fig. 1** Constructing scaffolds to mimic the microenvironment of cells in biological systems is a complex task because engineering of chemistry (bioactivity), physics (mechanics, roughness), and 3D control over the pore system (pore size, connectivity, hierarchy) is required

Initial approaches were focused on the design of macroscopic material scaffolds to provide cell support and therefore matched the dimensions of organs. However, the importance of the nanoscale structure has been underestimated for a long time. The significance of the nanoscopic dimension has been brought into focus by progressively understanding the structure, functionality, and function of the extracellular matrix (ECM) [10, 13]. Cells in complex biological systems exist in a highly fibrous structured environment. The ECM provides not only mechanical support, but also directional orientation to the cells and thus presents an instructive grid. The fiber structures of the ECM are mainly composed of proteins of the collagen type [14, 15]. For instance, type II collagen accounts for about 90–95% of the matrix collagen. Its high ratio of carbohydrate groups leads to rather polar fibrillar nanostructures. Other collagen types are also present in the ECM. Sometimes they are enriched at specific regions, but their function is often not fully understood [16].

The fibrils are embedded into an elastin network to modulate mechanical properties of the ECM. The interfibrillar spaces within the matrix are filled to a large extent with proteoglycans, which are macromolecules composed of about 5% proteins and 95% polysaccharides [17]. Moreover, functional polysaccharides are found as well. For instance, hyaluronic acid is one important component and is nowadays used as the base for many biomaterials. In the biological environment of the ECM, no chemical bonds between the collagen fibers and either proteoglycans or hyaluronic acids are found. However, ECM viscoelasticity is adjusted by these molecules because proteoglycans regulate water balance and osmotic pressure within the ECM. Besides these main constituents, the ECM consists of a multitude of other functional proteins, e.g., adhesion proteins such as fibronectins [18] or laminins [19], growth factors [20], and low molecular weight compounds that are exchanged with adjacent cells to realize cell communication [21, 22]. Thus, a highly defined and very specific 3D microenvironment is created. This is considered to be essential to ensure the function of cells, cell colonies, tissues, and complete organs from early embryogenesis to adult repair of damaged tissues [23]. The ECM supports and directs the adhesion and migration of cells. Moreover, ECM contacts influence cells deeply in their regulatory processes on the metabolic level.

To mimic the complex environment of the ECM, the production of macroscopic nanostructured materials is mandatory. In these synthetic systems, the mechanical properties, porosity, pore connectivity, and functionality should be spatially controlled. Ideally, those parameters should be locally adaptable with high precision to meet the requirements of cells, tissues, and full organs. The 3D control of functionality in nanostructured materials still poses difficulties in materials design and synthesis. However, research addressing planar biointerfaces is progressively elucidating the mechanisms of ligand positioning, ligand surface densities, synergistic ligand clustering, and the precise biological responses of cells to those positional functionalities [24–27]. Taking into account that the microenvironment of the ECM *in vivo* controls cell function, it seems to be achievable that synthetic materials can provide precise handles to control cells so that custom-made tissues can be generated on demand [8, 28–30].

Biomimetic ECM systems can be engineered, on the one hand, from naturally derived materials such as polypeptides, polysaccharides, hydroxyapatite or their composites. These biomaterials have excellent physicochemical activities, mechanical properties close to those of natural tissues, biological degradability and, most importantly, they mediate cell adhesion by borrowing natural motifs, e.g., from collagen or fibrin. On the other hand, fully synthetic polymers can be manufactured in a highly reproducible manner. Frequently, they do not impose an inherent risk of antigenicity or complex degradation to immunogenic side products. However, difficulties with synthetic polymers arise from contaminations such as remaining catalysts, solvents, or residual monomers. These clearly impose toxicity issues. Moreover, to mediate specific bioactive contact, cell adhesion peptides/proteins and signaling molecules (growth factors) that might be already present in biological materials have to be incorporated. Ultimately, a hybrid material might combine the favorable properties of synthetic materials and those of biological macromolecules in a synergistic manner. In those hybrids, the synthetic materials introduce tailored mechanical and degradative properties as well as ease of processing. The biomacromolecule components of the hybrids could bring specific bioactivity via precisely positioned functional labels.

## ***1.1 Effect of Nanostructures on Biological Systems***

Nanostructured materials have been brought into focus with the trend towards nanotechnology, and as tools have become available to design, manipulate, and characterize such dimensions. This is reflected in various developments in the field of biomedicine and biotechnology. For example, microarrays of DNA [31], proteins [32], or carbohydrates [33] are used for high-throughput screening. This includes studying the cellular responses to nanostructure, material properties, and chemical functionality (Fig. 1) [34, 35]. Cells, as basic components of tissues, interact with their surrounding either via soluble factors (e.g., growth factors) or via direct cell–cell and cell–ECM contacts. Whether a cell proliferates, differentiates, or dies is thought to depend not only on intrinsic cell factors but also on the extrinsic signals from its microenvironment.

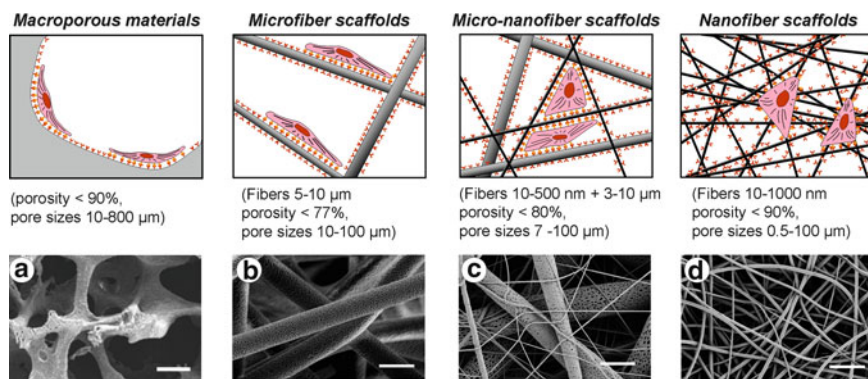
### **1.1.1 Nanometer Texture**

Synthetic two-dimensional (2D) materials with nanometer textured surfaces have been fabricated by sophisticated technologies, like dip-pen printing [36] or e-beam lithography [37], to elucidate the interactions of cells with defined surfaces. Cell–nanostructure interactions were studied from the gene expression level (cell metabolism) up to the level of microscopic cell behavior. Understanding of the influences of nanostructure on cell adhesion, orientation, motility, proliferation, migration, or differentiation is accessible [38]. In terms of adhesion, proliferation

and migration, nanogratings seem to regulate cell behavior more effectively than do nanoposts and pillars (the latter has not been studied much) [39]. However, despite the intense investigations, no widely accepted hypothesis for proliferation is currently available. In cell differentiation and formation of cell superstructures, nanotopography seems to have a profound effect and hence a high potential to direct cells [40, 41]. Within 5–500 nm to 7–10  $\mu\text{m}$ , topography can alter cell behavior independently of the underlying material chemistry [42, 43]. Cells effectively respond to chemistry if the topography is below their minimum size scale for sensing [44]. In addition, certain cell types show higher interaction with nanometer-scaled patterns than do other cell types. For example, osteoblasts seemed to win the adhesion race against chondrocytes, fibroblasts, and smooth muscle cells on carbon nanofiber [45]. This is now being exploited for the design of implant surfaces. For instance, implants are treated by sand-blasting to generate rough surfaces onto which osteoblasts desire to attach [46].

### 1.1.2 Porosity

Proceeding further, to design synthetic 3D structured scaffolds a variety of top-down and bottom-up approaches have been established, which we will discuss using selected examples. While building up 3D materials, the aspects of internal surfaces, porosity, and interconnectivity come into play. Cells need to effectively penetrate such architectures, and colonization of 3D scaffolds requires bridging of the pores to eventually fully fill the scaffold. In addition, nutrient and waste transport are necessary. To realize this, a hierarchical pore system might be of advantage (Fig. 1). Depending on the fabrication method, different pore sizes, geometries, distributions, and other porosity characteristics are obtained (Fig. 2). For example, scaffolds made



**Fig. 2** Scaffold architecture affects cell binding and spreading. The examples were obtained by (a) phase separation/leaching combination and (b–d) electrospinning. Porosity data was roughly estimated; note that classic nanofiber structure is <100 nm, but here is <1000 nm, as found commonly in biomedicine. *Scale bars:* (a) 500  $\mu\text{m}$ , (b–d) 10  $\mu\text{m}$ . *Top row:* adapted from [12]; *bottom row:* reprinted, with permission, from [47] copyright (2004) Elsevier; [48] copyright (2010) Wiley-VCH

from fibers have mostly an interconnected pore system and inherently an anisotropic nature. This anisotropy can be tuned by fiber alignment, as will be illustrated by electrospun scaffolds that direct neurite outgrowth (see Sect. 2.2.2). As the meshes are composed of submicrometer thin fibers, the pore size is directly correlated to the fiber diameter [49]. Conventional textile technologies like braiding, carding, or knitting are not easily applicable to control of the fiber assembly. The difficulties arise mainly from the handling of submicrometer to nanosized fibers.

### 1.1.3 Mechanical Properties

The porosity of nano- or microstructures might not only be biofunctional in terms of geometry and inner surface topography. Structure also modulates the mechanics of the corresponding scaffold, as shown in natural hierarchical systems (e.g., collagen-fiber-based tissues) [16]. The mechanical properties (e.g., stiffness) also affect cellular behavior. Discher and coworkers showed in their pioneering work that the elasticity of poly(acrylamide) gels with different crosslink densities can direct stem cell lineage specification due to mechanical differences [8]. The cells seem to sense mechanically and geometrically the matrix environment and translate this to a cellular response (mechanosensing → mechanotransduction → mechanoreponse) [12, 13]. The translation might occur due to unfolding of proteins, triggered by externally sensed forces, thereby exposing cryptic binding sites [12].

## 1.2 *Biological Activity of 3D Surfaces*

In cellular infiltration of artificial or natural 3D scaffolds, the cells have to overcome the biophysical resistance given by the surrounding microenvironment. How to evenly distribute cells into such scaffolds while still maintaining or controlling the cell phenotype turns out to be a challenging task.

In nature there are two strategies available, one involving proteolytic and the other nonproteolytic cell migration [50]. In the proteolytic strategy, the cells clear their path through secreting and activating proteases, which locally and specifically degrade components of the pericellular matrix. The nonproteolytic pathway is conducted through amoeboid forward migration, where cells adapt their shape or deform the microenvironment [1]. For artificial 3D scaffolds, cell-adhesive ligands for traction are required, and cell infiltration via the nonproteolytic pathway is enhanced by providing adequate pore sizes and scaffold elasticity for cell migration. The degradation of a scaffold is the first step towards an active remodeling of an artificial matrix. Degradation is often based on hydrolytic ester cleavage, which proceeds with a tunable rate depending on the surface area, hydrophilicity, crystallinity, and ester type. Recently, there have been different bioinspired approaches described, which include the introduction of degradation sites for proteolytic (enzyme catalyzed) cleavage [51, 52]. Healing processes, in which ECM remodeling takes place



via matrix metalloproteinases (MMP), have inspired a scaffold that can be selectively degraded by proteases. In this biomimetic strategy, the cell itself produces the required enzymes to pave the way for infiltration [52].

In both the proteolytic and nonproteolytic pathways, the question remains as to how to facilitate cell penetration into a preformed scaffold. In addition to the above-mentioned factors, seeding strategies are highly relevant. Whereas static seeding relies on active cell migration into the pore system, dynamic seeding in bioreactors can actively assist the cell transport by a directed flow field. Applying flow perturbation additionally increases the transport of nutrient and waste [53, 54]. However, a flow field applies stress on the cell culture. This could influence the cellular behavior and thus limits the application of dynamic seeding. An elegant approach is the direct implantation of scaffold into a patient's body to detour the artificial bioreactor [55].

More frequently, an approach is used in which a scaffold precursor is homogeneously mixed with cells. Subsequently, a scaffold is formed in response to temperature, pH, or crosslinking molecules. The in situ encapsulation strategy often provides systems with homogeneously integrated cells [4]. A similarly promising strategy includes the fabrication of a structured 3D scaffold directly into a dispersion of cells in an appropriate medium (cf. Sect. 2.2.2 on electrospinning and plotting).

The 3D environment alters the mechanosensing and cell adhesion provided in 2D. The cell-adhesion sites (i.e., integrins), integrin ligation, cell contraction, and associated intercellular signaling are substantially different in 3D [11, 56, 57]. In addition, solute diffusion and the binding of proteins (e.g., growth factors, enzymes) are affected by the 3D structure, thus creating gradients. 3D scaffolds might be essential to direct morphogenetic and remodeling events. There is an interplay between cell-generated forces, adhesion-ligand density, and matrix stiffness. The mechanics of the scaffold as the cells migrate into the structure displays certain cell functions, depending on the contraction-response. In mammary epithelia, for example, the increase in gel stiffness across a range disrupts morphogenesis and promotes proliferation [10]. Furthermore, scaffold geometry dictates cell adhesion and migration. For example, the minimum fiber diameter needed for fibroblast to adhere and migrate on a single fiber, was shown to be approximately 10  $\mu\text{m}$ , and an interfiber distance of up to 200  $\mu\text{m}$  was the maximum gap that could be used to bridge two fibers [58].

Combinatorial 3D polymer scaffold libraries for screening might be promising for evaluation of the issues discussed so far. However, in the reported case only 3D scaffolds by salt leaching were constructed [59]. The geometry was not as defined and reproducible as in designer scaffolds (see solid freeform fabrication in Sect. 2.2.1). However, this methodology might be translatable to those techniques.

In order to functionalize scaffolds to mimic the native cell environment, different strategies are available. Recombinant DNA technology can be used to design artificial ECM proteins to avoid the aforementioned complications that can arise with naturally derived materials [60]. However, there is little known about the long-term

in vivo performance of such synthetic biomaterials. Other approaches are directed to compose hybrid structures out of biocompatible synthetic polymers like poly(lactic-co-glycolic acid) (PLGA) or poly(ethylene oxide) (PEO).

Cell adhesion on a nonfunctional scaffold is mediated dominantly by nonspecific, entropically favored adsorption of a layer of cell adhesion proteins, excreted by the cell itself [61]. In order to obtain and retain the native function of these proteins, attempts are being made to tune the hydrophilicity or hydrophobicity of the scaffold surfaces [62]. Different methods of surface activation are commonly applied, e.g., blending, copolymerization, plasma treatment, etching, radiation, chemical surface modification, coatings, and combinations of those.

On such modified surfaces, some of the attached proteins are recognized by cytoskeletally associated receptors in the cell membrane. So, in the end, the extracellular substrate is mechanically connected with the intracellular cytoskeleton, which may secrete its own adhesion proteins. Integrins, as an important class of cell receptors [63], bind to small domains on their adhesion proteins, e.g., the oligopeptide sequence arginine–glycine–aspartic acid (RGD) that is common in fibronectin [64].

In order to facilitate cell adhesion, the aforementioned oligopeptides or adhesion proteins are chemically or physically attached to scaffolds in advance (i.e., cells adhere specifically). The strategy of attaching peptide sequences instead of proteins to surfaces has the advantage of avoiding antigenicity as well as loss of functionality through protein denaturation or degradation. The so-created adhesion sites show a biphasic cellular response, i.e., ligand densities that are too low or too high have an adverse effect on cell spreading and migration [27, 65]. Additionally (e.g., for RGD-containing peptide sequences), different factors like the peptide sequences (i.e., flanking residues), forms (linear, cyclic), immobilization strategies (substrate material, linker), and nanopatterning [26, 66] will be important for cellular behavior.

However, RGD-containing scaffolds seem to only partially exhibit the functions of native fibronectin, as mentioned by Vogel and coworkers. Additionally, the importance of the preservation of native protein structure, especially fibronectin, as it occurs in the extracellular fibrils was highlighted [57]. Cell biologists commonly enhance cell adhesion onto, e.g., polymer surfaces by the adsorption of fibronectin. In a ground-breaking essay [57], Vogel hypothesized that the preservation of the native fibronectin structure would not enhance cell adhesion, but was critical for vascularization of a scaffold. The latter is certainly one of the most important demands for in vivo scaffolds, where additional blood vessels must grow into the scaffold and supply the cells with nutrients. How to functionalize scaffolds with fibronectin while preserving the native protein structure remains an unsolved problem on the track to engineering artificial tissues.

Other functionalization strategies deal with binding and release of signaling molecules triggered by cellular events. Heparin binds with high affinity to various morphogens, i.e., growth factors. Therefore heparin is used to functionalize scaffolds, for example, through electrostatically bound growth factors [67]. The release of these factors can be triggered by specific heparin-degrading enzymes that are ac-

tivated during cellular events, e.g., ECM remodeling. This bioactive route is clearly of advantage compared to common approaches in which physical triggers like pH, or temperature are exploited to release bioactive factors [3]. The advantages of such approaches rely on the fact that growth factors are well controlled with regards to their 3D position, concentration, and timing of cellular events. Additionally, the growth factors might be more functional by immobilization than by being dissolved in cell media, as shown in the case of vascular endothelial growth factor [68].

The concepts and effects of 3D architectures and functionalization mentioned above will be addressed in the following section by presenting selected bottom-up and top-down fabrication approaches.

## 2 Generation of 3D Structured Surfaces

### 2.1 *Bottom-Up Approaches*

#### 2.1.1 Templated Synthesis

Porous polymer materials with a continuous polymer phase consisting of, e.g., a homo- or a statistical copolymer, can be accessed via template strategies. These involve the dispersion of a porogen (gas, liquid or solid) into a fluid phase of a polymer. The removal of the porogen leads to macroporous materials with pore sizes  $\gg 50$  nm [69–73]. For bioapplications, salt crystals are often used, which can be leached easily with water to generate systems with  $<90\%$  porosity and pore sizes in the range of 5–600  $\mu\text{m}$  [47, 74]. These simple and convenient processes are suitable for a range of biomaterials. However, templated strategies do not offer optimal control over pore structure and connectivity. Miscibility gaps and density differences make homogeneous dispersion difficult and result in inhomogeneous materials with imperfect interconnectivity. Advanced control enabling production of hierarchical pore systems via templating processes is only possible in some special cases. Often, physicochemical demixing hampers the templating of mixtures of particles with strongly different sizes [75].

#### 2.1.2 Organization of Polymers

Microcellular foams can be produced by thermally induced phase separation (TIPS) [47, 74, 76]. The induced spinodal decomposition can be optimized to generate, e.g., polylactide scaffolds with the porous morphology and physicochemical characteristics of a foam. Interesting materials can be constructed in a simple process. These materials exhibited bundles of channels with a diameter of  $\sim 100$   $\mu\text{m}$ . The internal walls of the tubular macropores have a porous substructure with pore diameters of  $\sim 10$   $\mu\text{m}$ . It appears to be remarkable that the channels have a preferential

orientation that meets the cooling direction. TIPS is easily implemented by using freeze-drying methods. The porosity of the resulting materials is <90%, average pore sizes are in the range of 5–600  $\mu\text{m}$ , and large interconnectivity can be achieved [77–79].

Materials that are generated by the template or the organization method can be functionalized. The introduction of signaling entities to decorate the pore walls with biologically active molecules is feasible but rather limited. Often, biopolymers such as gelatin (degraded collagen) are blended into the polymer matrix to be statistically exposed on the pore surface. Moreover, physicochemical adsorption of, e.g., fibronectin, can be performed in a post-treatment step. The simplicity of both functionalization methods strongly limits the precise spatial control of bioactive entities.

### 2.1.3 Self-Assembly of Polymers

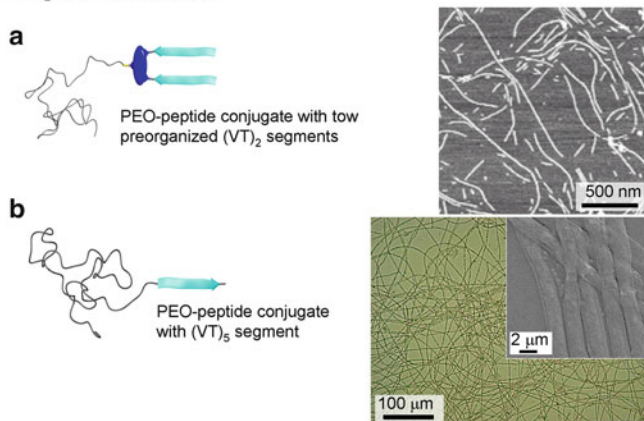
Block copolymers, which combine polymer segments with different properties, are presumably the most widely examined system for the study of self-assembly to large-scale structures that have controlled structural and functional features on the nanometer length scale [80, 81]. Phase segregation of block copolymers, followed by selective degradation of one polymer block, leads to highly ordered porous 3D structures [82]. The pore dimensions obtainable are in the micro- and mesoporous range (<50 nm), which do not meet the requirements for cellular infiltration.

However, the controlled self-assembly of macromolecular building blocks is probably the closest strategy to the concepts found in biology for generation of, e.g., collagen fibers, which structure the ECM. New strategies have emerged in the field of soft-matter structure formation that have paved the way to precisely generate fibrillar or fiber-like nanostructures [83–87]. These nanostructures can exhibit appropriate mechanical properties that fall within the regime of biological matrix fibers, and even provide the possibility to present the required biological signal entities at their surfaces [86, 88, 89].

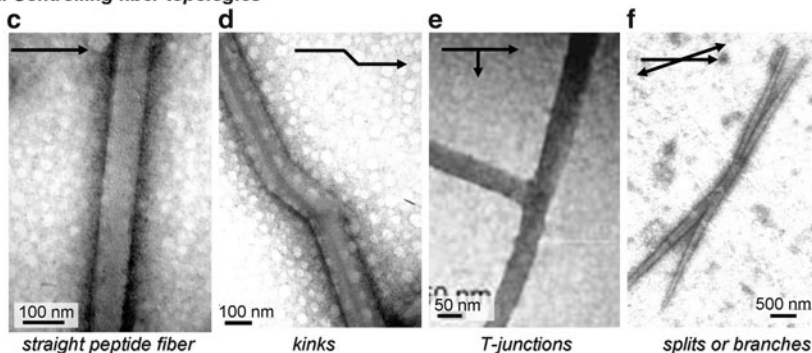
De novo designed peptides, in particular, proved to be a versatile tool for the bottom-up assembly of fibrillar structures [90–96]. A broad set of different biomimetic filaments are described. These can be accessed via the controlled self-assembly of peptides, peptide–amphiphiles, peptide–polymer conjugates, and proteins (Fig. 4) [88, 90, 97–101]. Nowadays, there is a general understanding of the rules determining the relationship of peptide amino acid sequence and secondary structure motifs. For materials and biomedical science applications, mostly the  $\beta$ -sheet, but also the  $\alpha$ -helical coiled-coil motif have been intensively explored as organizational motifs to generate nanofibers [86, 102–105]. The peptide building block together with the assembly motif determines the inner nanostructure, the dimensions, and the mechanical properties of the resulting filaments [106, 107].

Börner and coworkers demonstrated that peptide–polymer conjugates can assemble to nanotapes with persistence lengths close to those of actin filaments (actin composes one part of the intercellular skeleton) [108, 109]. The generated nanostructures are flat ribbons (1.2 nm  $\times$  17 nm  $\times$  2  $\mu\text{m}$ ; height  $\times$  width  $\times$  length) with

### 1. Controlling fiber dimensions



### 2. Controlling fiber topologies



**Fig. 3** Controlling dimensions and topology of self-assembled fibrils. Controlled self-assembly of peptide–polymer conjugates allows tuning of fiber sizes and shapes from nanotapes with  $1.2 \times 17$  nm cross-section (a) to microtapes with  $50 \text{ nm} \times 2 \text{ }\mu\text{m}$  cross-section (b). Self-assembling coiled-coil peptides leads to straight nanofibers (c), fibers with kinks (d), fibers with T-junctions (e), or branched fibers (f). Reprinted, with permission, from [108] copyright (2005) The Royal Society of Chemistry; [110] copyright (2006) American Chemical Society; [111] copyright (2003) Wiley-VCH; [107] copyright (2003) Nature Publishing Group

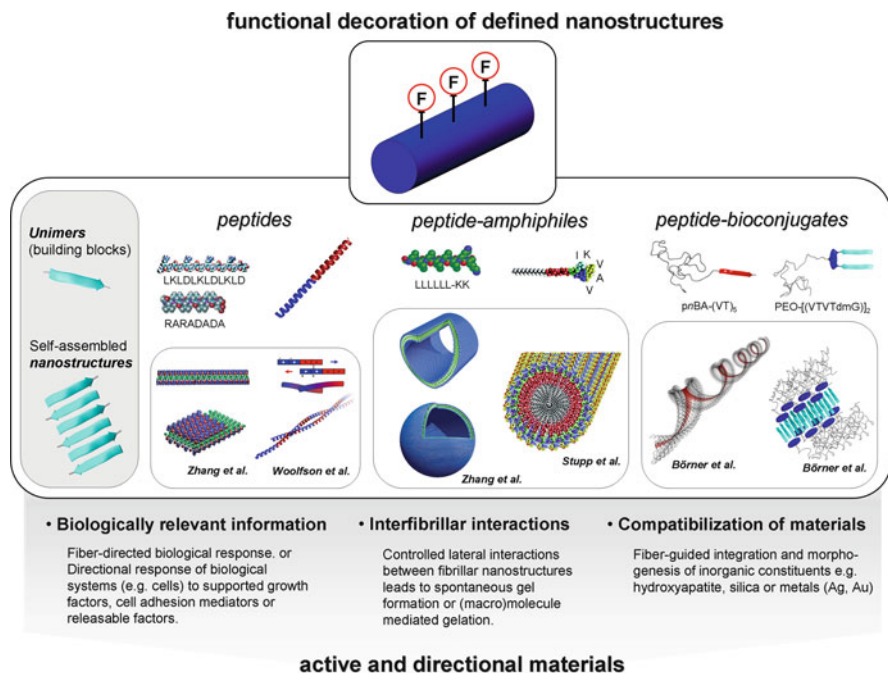
a peptide  $\beta$ -sheet core and a polymer shell (Fig. 3). Similarly to the basic structural element of collagen (rod-like tripel helix), the strong anisotropic nature of the synthetic core–shell ribbon is reflected in a high tendency to pack into bundles with nematic substructure [109]. The vast structural variability of the present concept has been indicated by the fact that a slight variation in the peptide part of the peptide–polymer conjugate led to macroscopic tapes with a cross-section of  $2 \text{ }\mu\text{m} \times 50 \text{ nm}$  and lengths of several millimeters (Fig. 3) [110].

Woolfson and coworkers described impressively the design of peptide fibers based on  $\alpha$ -helical coiled-coil building blocks [107]. By programming at the amino acid sequence level, the fibers could be fine-tuned from thick rigid rods to thinner,

more flexible fibrils [106]. Advanced control could be achieved, including tailoring of the fiber topology. The amino acid sequence could be used to rationally equip peptide nanofibers with kinks, branches, or crosslinks (Fig. 3) [111, 112].

Despite the fact that peptide- or bioconjugate-based filaments are not covalently assembled and the building blocks hold together via soft interactions (e.g., hydrogen bonding, hydrophobic, or ionic interactions), excellent mechanical properties might be achievable. Smith et al. have shown that insulin, for instance, creates fibrils with strengths of up to 0.6 GPa, comparable to that of steel, and with a Young's modulus of 3.3 GPa, corresponding to that of silk [113]. Moreover, the latter is perhaps the most prominent example of a protein-based, high-performance fiber. Silk escape threads combine high-modulus fiber elasticity with enormous toughness, which is still unmatched by synthetic fiber materials [114].

The utilization of peptide self-assembly additionally allows control of structural parameters and the rational control of functionalities, which are displayed at the nanofiber surface. This makes the presentation of biological signals and thus the introduction of bioactivity feasible. Stupp and coworkers investigated the self-assembly of peptide–amphiphiles (Fig. 4) [87, 115]. The resulting worm-like, cylindrical nanostructures consist of a hydrophobic core that is formed by the alkyl



**Fig. 4** Functional decoration (F) of self-assembled nanofibers to mimic fibrillar structures of the ECM. The monodisperse nature of the building blocks and the precise assembly motifs lead to nanostructures with well-defined functional surfaces. Adjusting of these faces enables the generation of bioactivity by presenting biorelevant epitopes [88, 92, 105, 108, 116, 128]



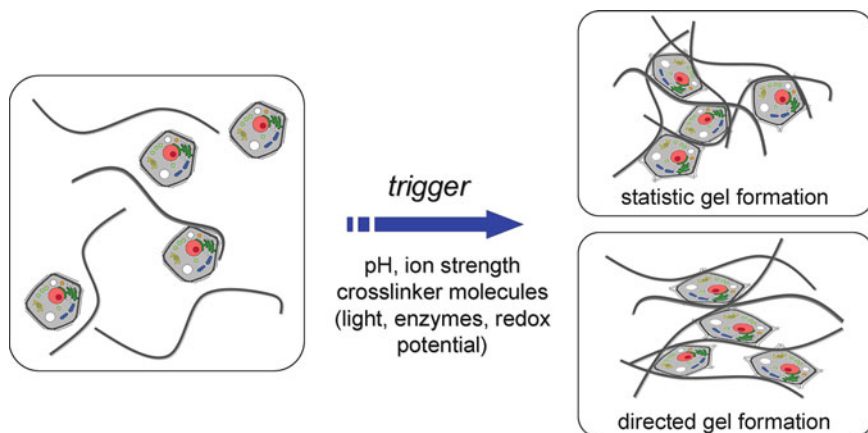
chains of the amphiphiles. The polar peptide segments, instead, are exposed to the water phase on the fiber surface [116]. For instance, the self-assembly of a peptide–amphiphile with a RGD domain leads to nanostructures with RGD surface functionalities [115]. A similar system has been equipped with an epitope of laminin. Laminin is an ECM protein that signals complex information, influencing and regulating neurite outgrowth. The resulting nanofibers presented the bioactive epitope and are apparently capable of stimulating differentiation as well as growth of neural cells in a directional manner [116].

Moreover, self-assembled nanofibers with distinct functional surfaces might enable more than the design of cell–fiber systems. Since peptides and nanofibers direct the growth of inorganic matter in biological systems, the controlled integration of composites into the field of tissue engineering might be feasible [117–119]. For example, functional faces of nanotapes composed of peptide–PEO conjugates could be adjusted to mimic fibrillar proteins such as silicines [94, 120, 121]. The functionality programs the nanofibers to have a high affinity for inorganic precursors and ultimately controls the rapid formation of a complex composite material with six hierarchy levels. This might be useful for biomedical applications, e.g., plotted dental inlays [122]. Hartgering et al. presented different self-assembled nanofibers that could control the crystallization of hydroxyapatite [123]. Because silica and hydroxyapatite are important inorganic components in biological composite materials, interesting biocomposites can be envisioned. In the future, defined cellular integration could be potentially combined with hierarchically structured inorganic–bioorganic composites, which might lead to interesting biointegrated composite materials.

Programming functionalities on the nanofiber surface makes the adjustment of interfibrillar interactions possible. Biology probably controls the hydrophobicity of the fibers in the ECM by using different types of collagen with different degrees of glycosylation. Even if the entire function of the collagen family is not clear, it is possible that a variable glycosylation is one tool for regulation of the hydrophobicity of the collagen fibers, which adjust lateral fiber interactions. Furthermore, biological ECM fibers show soft and reversible multipoint interactions that can be mediated by ligands for specific crosslinking. For example, peptide–amphiphile nanofibers mimic this by presenting heparin-binding peptide sequences on their fiber surfaces. The effective crosslinking of the nanofibers could be mediated by the addition of heparin to a dilute fiber solution [124].

Ultimately, self-assembled nanofibers can possess a fluid–gel transition and thus generate 3D fibrous structured materials (cf. Fig. 5). Preferably, resulting gels should have a high porosity, preserved structural dynamics, and low solid content [125]. Several different systems based on peptides, amphiphiles, and bioconjugates have been described that lead to the formation of hydrogels or organogels [90, 126, 127]. Although the latter are more relevant for materials science applications [128], aqueous media are required for biomaterial scaffolds, e.g., for tissue engineering [89, 127, 129, 130]. A common form of scaffold is a fibrous structured gel in which cells can be encapsulated (cf. Fig. 5) [131–133]. The above-mentioned nanofibers based on peptide–amphiphiles spontaneously form hydrogels at a concentration of about 0.5%. Due to the high persistent length (stiffness) of the fibers in





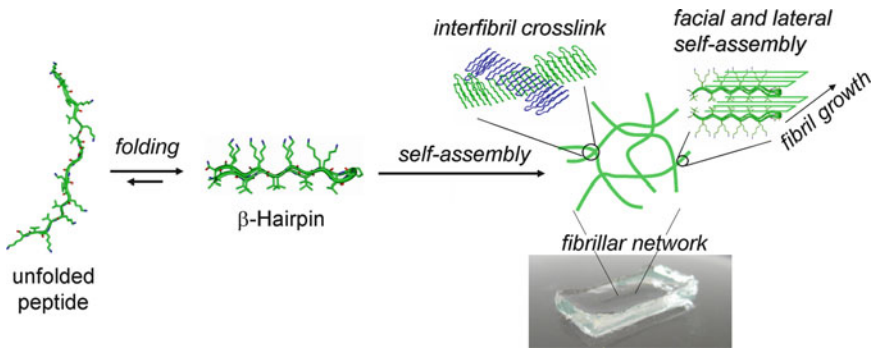
**Fig. 5** Formation of isotropic (*top right*) or anisotropic (*bottom right*) hydrogels. Gel formation can be triggered by inducing lateral interactions between fibrillar nano-objects

contrast to soft fibers they span pores of about 200–800  $\mu\text{m}$  in size, leaving enough space for cellular penetration but still preserving tight cell–fiber contact to influence the included cells. In situ gelation in the presence of different cell lines has been demonstrated, making the gels interesting for tissue engineering [116]. The artificial nanofiber scaffolds have a distinct effect on cell differentiation due to the bioactive epitopes presented on the fiber surface.

Zhang and coworkers investigated a variety of peptides with alternating hydrophobic and hydrophilic amino acid sequences [88, 105]. The polarity sequence meets the requirements for  $\beta$ -sheet formation, leading to fibrils that show a reversible crosslinking to hydrogels. Charged residues, present in the sequence of the peptide, were used to control the self-assembly process via pH or ionic strength. It is noteworthy that cells entrapped into this type of gel are rapidly stimulated to enhance the production of ECM [134]. The rapid reconstitution of the native biological environment makes the nontoxic peptides good candidates for use in strategies for repair of cartilage tissue.

Schneider and coworkers described a highly interesting peptide having a  $\beta$ -hairpin structure (cf. Fig. 6) [135, 136]. The amino acid sequence determines the folding of the peptide into a  $\beta$ -sheet-turn- $\beta$ -sheet tertiary structure. This can self-assemble in a pH-controlled manner into branched nanofibers, which form hydrogels [137]. The self-assembly kinetics is strongly dependent on temperature. Under physiological conditions, aggregation of the peptide proceeds slowly at 10  $^{\circ}\text{C}$  but very rapidly at 20  $^{\circ}\text{C}$ . This is indeed interesting for injection tissue engineering, where rapid gelation is required at body temperature, but fluid flow should be preserved before injection [138].

The examples described above reveal the versatility and potential of bottom-up approaches for generating structures with controlled substructures and, moreover, positioned functionalities to modulate the material–biology interfaces. Certainly,



**Fig. 6** Triggered self-assembly of a peptide  $\beta$ -hairpin that forms fibrillar structures, which show facial and lateral self-assembly to hydrogel networks. Reprinted, with permission, from [96] copyright (2004) Elsevier

this toolbox will be further explored and exploited to program nanostructures for interfacing to biology. However, the control of self-assembly processes over several length scales from nanostructures to macrostructures is still highly challenging. Therefore, an interesting technological interface has been brought into focus, where existing polymer-processing technologies are being evaluated for production of structured materials for biomedical applications. The available processes and the resulting possibilities are discussed in the next section.

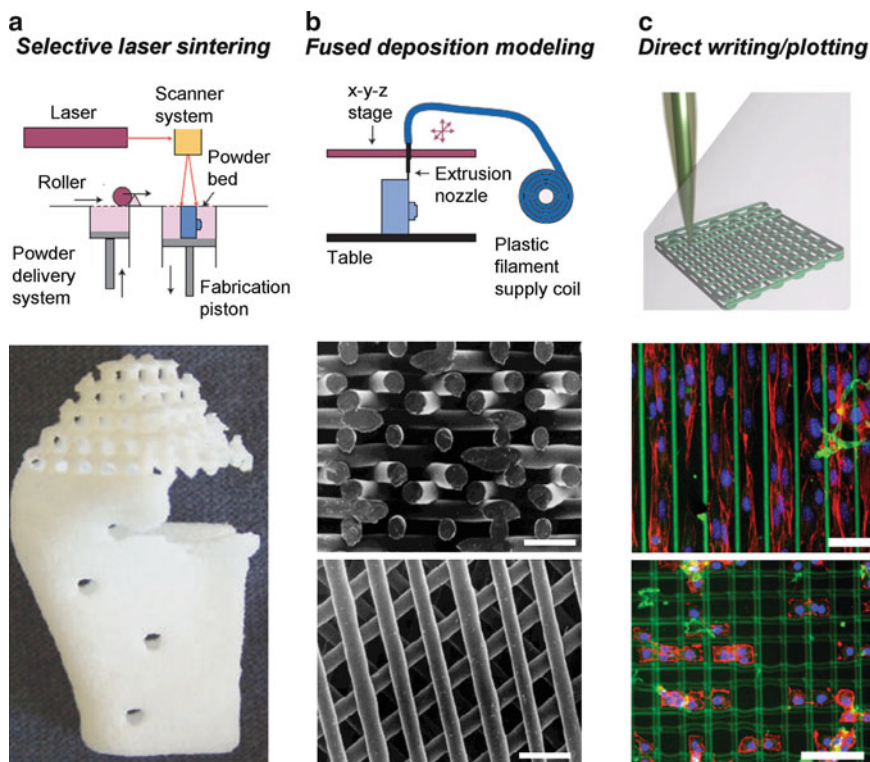
## 2.2 Top-Down Processing

### 2.2.1 Solid Freeform Fabrication

For an adequate scaffold for tissue engineering, the mechanics and porosity have to be optimized preferably by the design of hierarchical porous structures. Because the introduction of holes determines the mechanical properties of a structure, it also will affect the mass-transport required for cell nutrition and cell migration. Computational topology design (CTD) enables the construction of such structures by creation of libraries of particular unit cells at different physical scales; the overall structure is then composed of these unit cells [139]. From these microstructures, stiffness and permeability can be calculated. Using topology optimization, a tailored microstructure can be created in which cell migration and the mechanical properties of the addressed tissue (e.g., bone) are considered [140]. Custom-made implants can be fabricated. The exact shape of a specific anatomic defect in a patient can nowadays be diagnostically determined with computed tomography or magnetic resonance imaging. This data can then be directly intersected with the microstructure database to design an optimized scaffold [141].

The scaffolds for implants can be manufactured by mean of solid freeform fabrication (SFF), which relies on a layer-by-layer (LbL) composition of 3D materials.

The step-by-step assembly proceeds in a highly precise manner that enables accurate definition of pore size, interconnectivity, and the scaffold form of, e.g., an anatomically shaped structure. SFF requires expensive equipment, is limited in resolution, and does not allow the fabrication of all complex geometries generated by CTD. However, different materials like polymers, ceramics, and metal biomaterials can be processed into scaffolds. Due to an accurate inner geometry and shape, SFF scaffolds have typically better mechanical properties than those produced via other methods, e.g., porogen leaching or gas foaming. Therefore, SFF is attractive for mechanical supports of hard tissue with elastic moduli of 10–1500 MPa [142]. There is a large variety of established SFF systems, which have in common the use of a triangular facet structure to replicate a representation of the optimal scaffold. Technology platforms can be divided into three groups according to the way the material is deposited: laser-, printing- and nozzle-based systems. Three examples are schematically shown in Fig. 7.



**Fig. 7** Three examples of SFF: (a) SLS, (b) fused deposition modeling, and (c) DW/plotting. Their corresponding scaffolds can be seen in the pictures beneath. In the lower image for (c), fibroblasts are incorporated and adapt to the 3D environment. Scale bars: (b) 1 mm, (c) 100  $\mu$ m. Reprinted, with permission, from [141] copyright (2005) Nature Publishing Group; [143] copyright (2009) Wiley-VCH; [144] copyright (2001) Wiley, Worldwide Guide to Rapid Prototyping website © Copyright Castle Island Co., All rights reserved <http://www.additive3d.com>

The laser-based systems are stereo lithography (SL) and selective laser sintering (SLS). In SL, a liquid monomer is photo-polymerized, which restricts the range of materials to polymers that are compatible to UV curing. SL provides scaffolds with porosities of <90% and a pore size of 20–1000  $\mu\text{m}$  [145]. SLS uses powders, preferably with narrow size distribution. These are sintered to geometries with <40% porosity and 30–2500  $\mu\text{m}$  pore sizes [146]. In the second group, either a chemical binder is printed onto powder (3D printing) or wax is directly deposited. The powder needs to have a narrow size distribution to compose scaffolds with porosities <45–60% and pore sizes in the range of 45–1600  $\mu\text{m}$  [147, 148]. The third technology exploits extrusion through a nozzle, either using melts (fused deposition modeling, FDM) or solutions that are structure-forming either directly or in response to, e.g., radiation (plotting/direct writing, DW). FDM applies thermoplastics to form structures with porosity <80% and pore sizes of 100–2000  $\mu\text{m}$  [144]. Malda et al. compared the oxygen gradients in a 3D scaffold fabricated by FDM with those in a scaffold produced by porogen leaching [149]. Both scaffolds were seeded with chondrocytes. Two weeks after *in vivo* implantation, the FDM scaffold showed, compared to the other scaffold, significantly higher cell densities in the center and higher glycosaminoglycan content. This suggests a better cell infiltration, lower oxygen gradients, and better cell colonalization in the FDM scaffold and highlights the importance of rationally designed scaffolds for tissue-engineering applications [149]. To achieve smaller feature sizes below the resolution of the FDM process, simple surface roughening by NaOH etching can be applied. This improves early matrix deposition in FDM scaffolds and facilitated bone formation in a rabbit model [150]. DW scaffolds have porosities of <90% and pore sizes of 5–100  $\mu\text{m}$ . Therefore, this method shows the best resolution. However, the long manufacturing time is a clear disadvantage of the method. DW is especially interesting for using DW of cells [151], biomaterials like hydrogels (Fig. 7) [143, 152], or self-assembling systems [153]. The latter shows the possibility of combining bottom-up with top-down approaches. This provides the means to macroscopic nanostructured scaffolds, where the inherent nanostructure is aligned to the macroscopic drawing direction.

In order to functionalize the scaffolds, blending seems to be a feasible approach, as shown in the FDM of polycaprolactone/calcium phosphate composites [144]. These scaffolds exhibit favorable degradation and resorption kinetics, combined with excellent mechanical properties and an optimal hydrophilicity [154]. The biochemical advantages of such structures are shown by the improved cell seeding. Moreover, an enhanced control of the position of supported growth factors, e.g., bone morphogenetic proteins (BMPs), has been shown both *in vitro* and *in vivo* [155]. The functional biomolecules are mostly added after scaffold fabrication because the non-mild conditions used in the fabrication method might affect the functionality. Incorporation of tricalcium phosphate provides a high binding affinity for BMP proteins. The functionality of growth factors is expected to increase by presenting them together with specific cofactors, such as heparin sulfate (HS), within an osteoconductive scaffold. HS is a robust biomacromolecule that tolerates harsh processing conditions, and thus the direct incorporation of HS during scaffold

processing is feasible [154]. In contrast to FDM, the DW method is compatible with several functionalization strategies. Even the direct incorporation of cells or proteins has been demonstrated, as solutions or dispersions can be easily processed. Detailed approaches for in situ and post-functionalization will be discussed in the following section.

### 2.2.2 Electrospinning

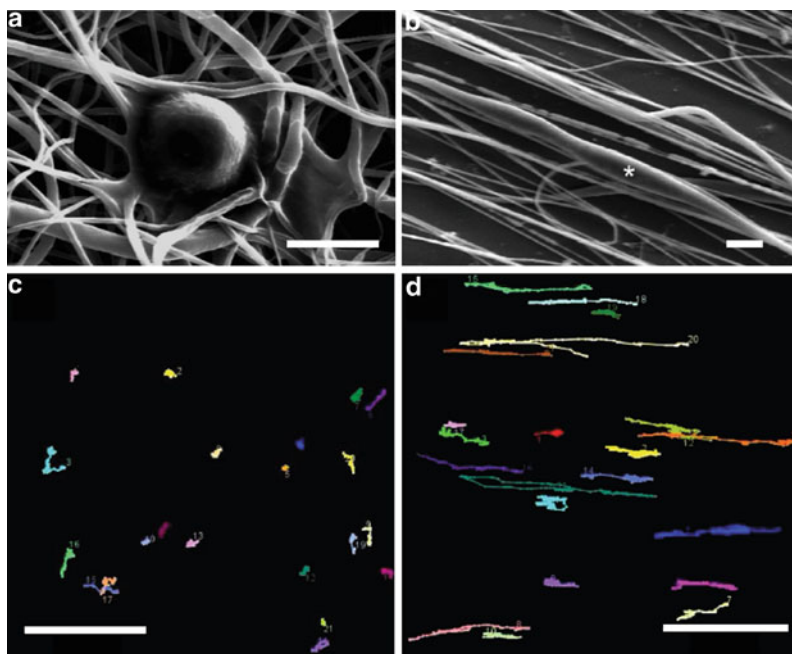
Although the principle of this technique is quite old, electrospinning (ES) has been developed as a powerful tool for the design of fiber meshes with fiber diameters ranging from  $\sim 10\ \mu\text{m}$  down to a few nanometers, mesh porosities of  $<90\%$ , and pore sizes of  $<1$  to  $100\ \mu\text{m}$  [156, 157].

Typically, viscous solutions or melts (not further discussed here) composed of polymers (synthetic or natural), precursors (ceramics, metals), or composite materials are able to be processed. During ES, the viscous solution is extruded through a needle, which is charged at the tip with high voltage. Deposition of the meshes takes place on a grounded collector. Given its simplicity regarding the equipment needed and its versatility (in terms of materials and structures), the ES process is becoming highly popular across different disciplines. Applications range from mesh production for wound dressings and tissue engineering to drug delivery systems. The fact that the fiber dimensions can reach the order of magnitude of fibrillar structures of the ECM makes it a feasible approach to structures that mimic the natural environment of cells. In addition, features like high interconnectivity of pores, high porosity, and high surface area make the resulting nonwoven meshes attractive, for example, for infiltration with cells.

It should be noted that the mechanisms involved in ES are complex and some details are still under heavy discussion. The ionized drop at the tip is first deformed to a Taylor cone (or more precisely a hyperboloidal shape) and then, after overcoming surface tension and viscosity, a so-called liquid jet is ejected and accelerated, undergoing different instabilities before deposition [158, 159]. An interplay of solution properties (surface tension, viscosity, molecular weight, conductivity, solvent volatility, solvent–solute interaction, dielectric constant), apparatus constraints (voltage, tip-to-collector distance, feeding rate, collector geometry, assembly), and environmental conditions (humidity, temperature, atmosphere) influence the process and can be used to control the outcome. For example, by using different concentrations and molecular weights, beads (i.e., from electrospraying), beaded fibers, and fibers with different diameters can be constructed. This depends on the interaction between the surface tension, polymer entanglement/interaction, and pulling force [160]. The latter depends on feed rate, voltage applied, gap distance, dielectric constant, and conductivity of the used solution. Depending on the solution/solute system and the applied “sophisticated” setup (e.g., a coaxial setup [161]), meshes with special features can be obtained consisting of porous [162], hollow [163], wrinkled [164], branched [160], flat [165], coiled [166], and barbed [167] fibers. A variety of factors influence the assembly mechanism of the nonwoven meshes and hence

determine essential parameters such as final fiber-to-fiber distance, porosity, and mechanical properties of the resulting meshes. The amount of remaining solvent, the humidity, the collector material, and the elasticity of the polymer might play dominant roles in screening or grounding of charges, fiber bonding, and buckling of fibers. However, further investigations must be performed to clarify these aspects, which are tightly coupled with each other. By using rotating drums, patterned electrodes, or post-drawing at elevated temperature, an aligned fiber mat or bundle can be obtained [168–170]. Interestingly, reducing the gap distance enables the technology of DW (near-field ES) [171]. In order to increase the productivity of the ES process, multi-nozzle setups or porous tube spinnerets are used to produce various jets in parallel, making industrial scale fabrication feasible [172, 173].

Cell studies on scaffolds of nano- and submicrometer-scaled fibers have shown that these dimensions promote not only cell adhesion, but also have beneficial effects on proliferation and differentiation of cells [174–177]. These effects are more prominent with decreasing fiber diameters. It seems relevant that the cells can be guided and bridged by the artificial fibers. Meshes with aligned fibers are particularly promising, e.g., for guiding the growth of nerve cells (Fig. 8) [178].



**Fig. 8** Nerve cells adjust their adhesion and migration to the corresponding structure, as seen here on random (a, c) and aligned (b, d) cells. (a, b) SEM pictures of PCL nanofibers where glioma cells adhered and followed the fiber alignment (see asterisk in b). (c, d) Motion cell-tracking: 20 individual trajectories were traced manually after a total tracking period of 36 h. Scale bars: (a, b) 10  $\mu\text{m}$ . Reprinted, with permission, from [178] copyright (2009) Mary Ann Liebert



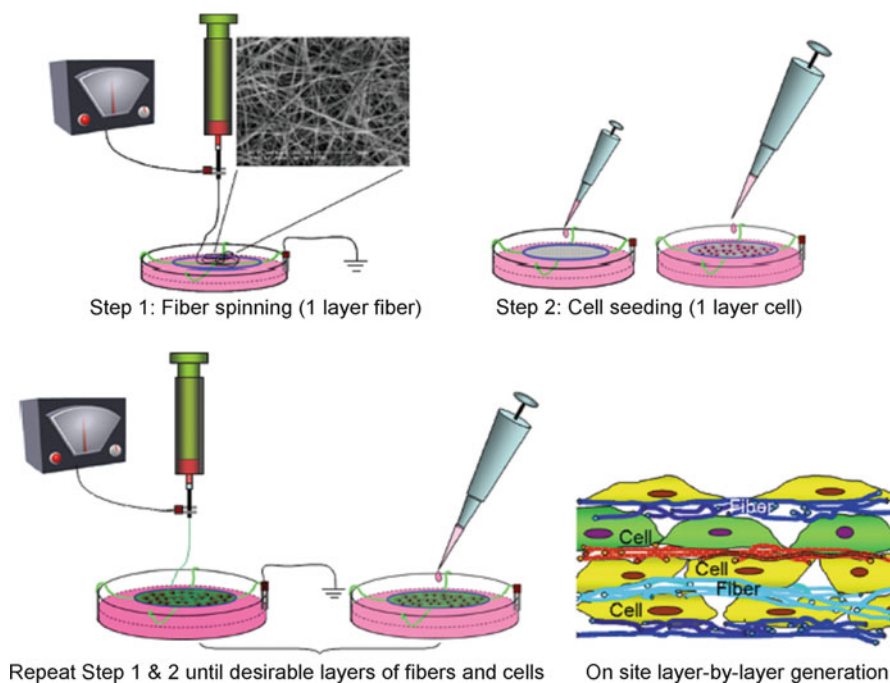
It is noteworthy that aligned fibers, as compared to randomly oriented ones, seem to stimulate fibroblasts to increase the production of ECM proteins. This was rationalized by the more controlled microenvironment, which provides an adequate topology and stimulates mechanotransduction [179]. However, quantitative evaluation is not straightforward because appropriate 2D reference surfaces are not often available. Furthermore, the cellular behavior depends on the cell line, e.g., endothelial cells seem to prefer flat surfaces to nanofibers [180]. Explanation could be complex, but also rather trivial because the projected area of fibers is smaller than that of flat surfaces [181]. In addition, it was found that cells proliferated faster on scaffolds with peak pore diameters greater than 6  $\mu\text{m}$ . In the case of a further increase of the peak pore diameter to 12 or even 23  $\mu\text{m}$ , cells began to align along single fibers instead of attaching to multiple fibers via multiple attachment points [182].

Early reports on electrospun scaffolds described poor cellular infiltration [175]. Frequently, cells adhered at the surface and thus coated the nano- or submicrometer-scaled electrospun meshes due to the small pore size. In order to overcome this limitation, pore sizes were increased by combining ES with other methods. These approaches included the coating of microfibers with nanofibers [183]. Other strategies combine ES with leaching [184, 185], freeze-drying [186], blowing agents [187], or ice templates [188].

ES produces fibers with a wide distribution of diameters. Normally, the intent is to keep the range as narrow as possible. However, for cellular infiltration the other extreme might be of advantage. Recently, a single-step process was realized using a standard ES setup. This enables the fabrication of bimodal fiber meshes with diameters differing by one order of magnitude (Fig. 2c). It was demonstrated that such a hierarchical mesh design is highly suitable for facilitating cellular infiltration. Mixed meshes (e.g., nano- and microfiber meshes) combine the advantage of microfibers that span an open pore structure with the properties of nanofibers, which are known to enable cell adhesion and proliferation. The advantages of mixed scaffolds were demonstrated by initial cell penetration experiments, monitoring the infiltration of epithelial cells into such networks [48]. Another attempt used bioreactors to encourage cell penetration into the fiber meshes [182]. Other approaches include direct spinning of cells by encapsulation into poly(dimethyl siloxane) (PDMS) by coaxial ES [189]. However, the strong electric field might induce some long term effects on cells. It seems to be safer in that regard to spin into the cell culture and then sequentially seed the cells (unpublished results from this group). This interesting procedure and the resulting sandwich scaffolds are schematically outlined in Fig. 9 [190].

To improve and control cell–fiber interactions, the fiber meshes can be either composed of biomacromolecules or postfunctionalized with appropriate biomolecules. The question arises as to which materials can be electrospun. In principle, all polymers can be spun if they provide enough entanglements in solution and adequate interactions between the solvent and solute. Biopolymers, in particular, show dominant H-bonding and/or polyelectrolyte effects, which lead to a strong viscosity increase or poor solvent evaporation. In order to prevent such





**Fig. 9** Cell-fiber sandwiches can be constructed by LbL cell/fiber assembly. The cells are sandwiched between layers of electrospun fiber meshes. The mesh thickness and cell loading can be controlled within this process. Reprinted, with permission, from [190] copyright (2009) Mary Ann Liebert

effects, H-bond breaking or charge-screening agents are added into the solution to facilitate spinning. Changing the interaction between the molecules might, however, change the conformation of biopolymers such as proteins [191]. The most popular strategy is blending with easily spinnable polymers such as high molecular weight PEO [192]. Another interesting approach is to use a coaxial-ES setup. A polymer that is difficult to spin is placed in the core and an easily spinnable polymer will assist fiber production by forming the shell. Subsequently, shell leaching provides fibers from the “difficult” polymer [193].

Furthermore, meshes have been composed of multilayers consisting of different polymers. Matsuda and coworkers produced bilayer meshes of a thick polyurethane microfiber mesh and a thin nanofiber mesh composed of type I collagen. The material decouples mechanical properties from the biochemical functionality of collagen to form a prototype scaffold for artificial grafts [194].

In principle, the functionalization strategies can be subdivided into methods allowing (1) direct incorporation of the functionality during spinning and (2) post-functionalization of the fibers after mesh production.

Coaxial-ES is a straightforward technology for producing meshes with functional fibers. These individual fibers can consist of a synthetic, nonfunctional core and a biofunctionalized shell. However, the production process is not trivial because control over multiple feeding rates is complicated and compatibility issues can occur.

Spinning of homogeneous blends of two polymers usually imposes compatibility problems. However, these can be overcome by use of common solvents, solvent mixtures, or surfactants. The control of the position and distribution of the functionality within the fiber is a complex task, but essential for this form of functionalization. Several studies describe the ES of solution blends of PEO and PCL [185, 192, 195]. Both polymers have a wide range of common solvents, but PEO is water-soluble, which means that a crosslinking step is required to preserve the meshes.

A systematic strategy to enrich a functional compound at the surface during ES is difficult. A particular problem is that bioactive compounds (e.g., proteins or peptides) are frequently expensive substances and hence not available in large quantity. In addition, the biomolecules that are at the surfaces of fibers might quickly undergo dissolution. In that respect, the use of block copolymers with a biofunctional part and a part compatible with a synthetic fiber-forming polymer is an attractive approach. In a model study, a small amount of a PEO-peptide conjugate was field-enriched on a PEO fiber, leading to meshes with a PEO core and a functional peptide shell [195]. According to recent findings, the strategy can be transferred to a biorelevant system. A poly(L-lactic acid) (PLLA)-peptide conjugate containing a bioactive RGD sequence was blended with PLGA. ES of this blend enriches the peptides at the surface of PLGA fibers. The surface segregation was driven by the adequate choice of solvents (our unpublished results). In another approach, block copolymers were spun to provide, after annealing, fibers with concentric lamellar-like substructures. Such compartments might be useful for incorporating functional systems, i.e., nanoparticles, drugs, or biomolecules [196, 197]. In addition, emulsion ES seems to be a feasible method for encapsulating and spinning diverse biomolecules or drugs [198, 199]. Further evaluation has to show whether the surfactants might impose a risk to sensitive biological systems.

Postfunctionalization strategies are very well documented in the literature [200, 201]. Only a few selected examples will be discussed here. Generally, postfunctionalization strategies are frequently applied. They often involve multistep procedures such as fiber surface activation, linker attachment, and introduction of a functional entity. After processing a blend composed of PLGA and PLGA-*b*-PEG-NH<sub>2</sub> the peptide GRGDY could be immobilized at the fiber surfaces through a coupling procedure [202]. In another study, the surface of PCL fibers was first activated by plasma treatment and the generated carboxylates used for the coupling of gelatin by carbodiimide chemistry [203]. In a RGD- and gelatin-functionalized mesh, the cell proliferation and growth was superior to that in unfunctionalized meshes. However, bioactivity was still lower than in established tissue culture

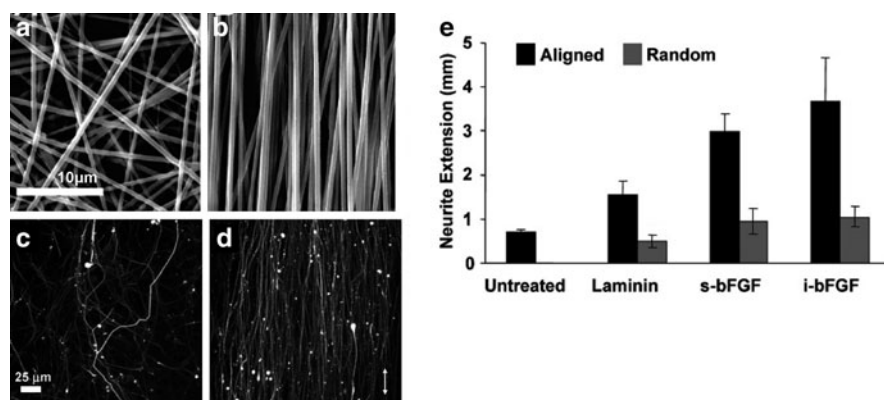
plates. The layer-by-layer method, which has been mainly used for planar surfaces, can also be applied to charged electrospun fiber in order to introduce functional entities [204].

In general, despite the difficulties in understanding the intricate mechanisms involved, ES provides a wide range of tools for structuring a fiber surface or composing a mesh at different length scales.

### 3 Biological Aspects

Synthetic nanofiber matrices can provide physically and chemically stable 3D surfaces for ex vivo growth of cells. Meiners and coworkers showed that fibroblasts or rat kidney cells that have been grown on electrospun polyamide nanofiber meshes displayed all the characteristics of their counterparts in vivo [205]. In addition, breast epithelial cells underwent morphogenesis to form multicellular spheroids containing lumens.

Synergistic effects of nanotopography and chemical signaling in synthetic scaffolds can certainly mimic the physical and biochemical properties of native matrix fibrils to guide cells. Patel et al. functionalized aligned PLLA fibers with heparin, basic fibroblast growth factor (bFGF), and laminin as an ECM protein [170]. When the aligned nanofibers were compared to randomly oriented meshes, a significant induction of neurite outgrowth (cf. Fig. 10) and the enhancement of skin cell



**Fig. 10** Synergistic effects of nanostructure and chemical signaling on cell guidance. The SEM micrographs of random (a) and aligned (b) PLLA nanofibers show a strong effect on neurite morphology. High-magnification confocal microscopy images indicate an isotropic growth on random (c) and directed growth on aligned (d) PLLA nanofibers. Quantitative evaluation of neurite outgrowth on nanofibers suggests benefits from aligned, functionalized nanofibers (e). *s-bFGF* immobilized with laminin, soluble(s) bFGF (fibroblast growth factor); *i-bFGF* immobilized (i) laminin and bFGF. Scale bars: (a, b) 10 μm, (c, d) 25 μm. Reprinted, with permission, from [170] copyright (2007) American Chemical Society

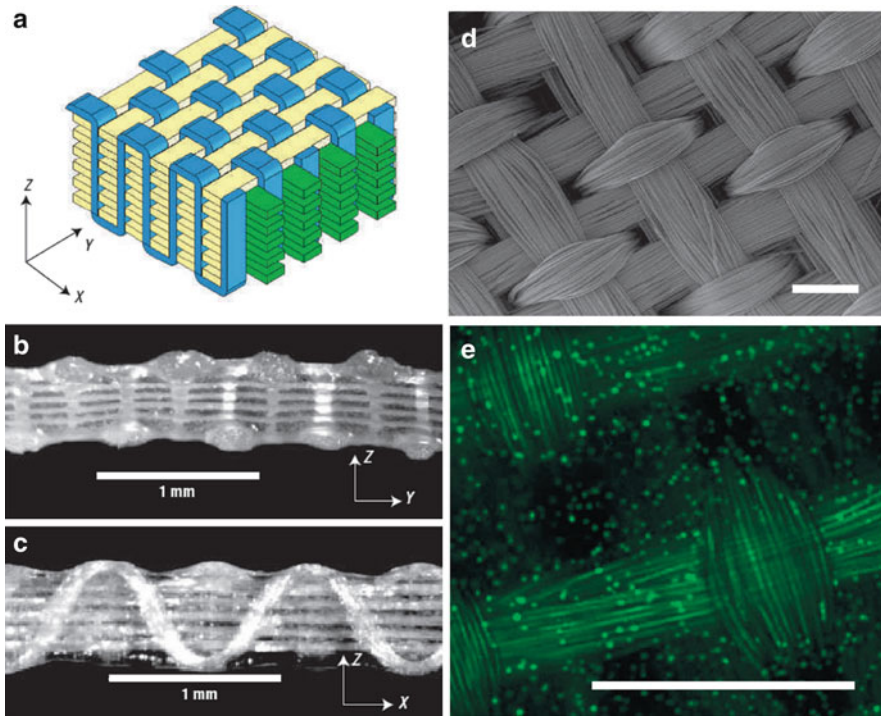
migration during wound healing could be observed with the same treatment. In addition, the immobilized biochemical factors synergized with the aligned nanofibers to promote highly efficient neurite outgrowth and, to a lesser extent, improved skin cell migration (similar to soluble bFGF) compared to untreated aligned PLLA fibers.

Another interesting approach is to use nanofiber scaffolds as a crystallization matrix to mimic biological composites. Xia and coworkers were able to produce meshes with a gradient of calcium phosphate content to mimic the tendon-to-bone insertion site [206]. The variation in composition led to an interesting spatial gradient in stiffness of the scaffold. This was also reflected in an activity gradient of seeded mouse preosteoblast cells.

A promising material seems to be injectable self-assembling peptide nanofibers because they can create, for example, an in situ intramyocardial microenvironment for endothelial cells [207]. Davis et al. injected self-assembling peptides into male C57BL/6 mice. The resulting nanofibrillar microenvironment recruited progenitor cells that expressed endothelial markers to a larger extent than a reference matrigel. After 14 days, vascular smooth muscle cells were additionally recruited to form functional, vascular structures and potential myocyte progenitors. When exogenous donor neonatal cardiomyocytes were coinjected with self-assembling peptides, the transplanted cells survived in the artificial microenvironment and recruited further augmented endogenous cells [207].

In order to create systems with larger dimensions, fibers can be processed into yarns with improved mechanical properties and enhanced cellular infiltration capabilities. For example, electrospun PLLA nanofibers with uniaxial alignment were fabricated into braided wires. These yarns were applied as tissue sutures after coating with chitosan. The handling problem of nanofibers was overcome by processing entire bundles of electrospun fibers via hot-stretch and twisting before braiding. The braided PLLA yarns exhibited comparable tensile and knot strengths to commercially available suture. This enables tying wounded tissue for a complete healing period. The yarns showed no cytotoxicity and promoted cell in-growth in vivo [208]. The results suggested an improved histological compatibility compared to silk suture. Another strategy to form yarn is to use oppositely charged electrospun nanofibers by coupled spinnerets [209].

An even more feasible approach seems to be that of Moutos et al., who used 104- $\mu\text{m}$  sized, commercially available PGA multifilaments to weave into 3D structures [210]. As shown in Fig. 11, interlocking of multiple layers led to porous scaffolds with  $\sim 70\text{--}75\%$  porosity. For cell growth, a composite structure was fabricated by vacuum-assisted infusion of a hydrogel. The resulting scaffolds had mechanical properties similar to those of articular cartilage [210].



**Fig. 11** Fiber architecture of a 3D orthogonally woven structure for cartilage tissue engineering. (a) Interlocking multiple layers of two sets of in-plane fibers ( $x$ - and  $y$ -direction). (b, c) Third set of fibers in the  $z$ -direction; cross-sectional views are of the  $Y$ - $Z$  plane (b) and  $X$ - $Z$  plane (c). (d) SEM view of the  $X$ - $Y$  plane shows the 104  $\mu\text{m}$  thick bundles composed of 8  $\mu\text{m}$  PGA fibers. (e) Fluorescent image of a freshly seeded construct shows the uniform initial distribution of porcine articular chondrocytes (fluorescent label was calcein-AM). Scale bars: (b, c) 1 mm, (d, e) 300  $\mu\text{m}$ . Reprinted, with permission, from [210] copyright (2007) Nature Publishing Group

## 4 Summary and Outlook

An overview of the most promising approaches for fabrication of biomimetic scaffolds for biomedical applications is provided. Self-assembly techniques might be the closest strategy to produce an appropriate bioactive environment for tissue re-growth. This method is, however, still limited when it comes to the production of large quantities or of mechanically loaded parts. In this respect, higher-throughput methods like ES can fabricate fiber scaffolds composed of fibers within the size range of fibrils in the ECM. Ultimately, rapid prototyping methods enable the fastest means of designing large structures, particularly useful for load-bearing tissue replica like bone. Still, a better control of nanoscaled features and more complex geometries is required. In addition, positioning of several functionalities within different structure levels has to be developed. In this direction, further efforts have

to be addressed towards designing scaffolds with proper signaling of biochemical and physical cues. It appears to be predictable that hybrid technologies will provide access to macroscopic nanostructured scaffolds and increase the structural space available for biomedical materials. Additionally, the positioning of precise bioactive entities within such materials by means of printing technologies will pave the way to the ability to guide cellular response, and to recruit both appropriate soluble factors and desired cell lines. Ultimately, artificial materials might mimic the informational background of hierarchical biomaterials, which provide synergistic effects on the mechanical, topological, chemical, and biochemical levels.

## References

1. Lutolf MP, Hubbell JA (2005) *Nat Biotechnol* 23:47
2. Branco MC, Schneider JP (2009) *Acta Biomater* 5:817
3. Place ES, George JH, Williams CK, Stevens MM (2009) *Chem Soc Rev* 38:1139
4. Langer R, Tirrell DA (2004) *Nature* 428:487
5. Levental I, Georges PC, Janmey PA (2007) *Soft Matter* 3:299
6. Vogel V, Baneyx G (2003) *Annu Rev Biomed Eng* 5:441
7. Spatz JP, Geiger B (2007) Molecular engineering of cellular environments: cell adhesion to nano-digital surfaces. In: *Cell mechanics*, vol 83. Elsevier, San Diego, p 89
8. Engler AJ, Sen S, Sweeney HL, Discher DE (2006) *Cell* 126:677
9. Girard PP, Cavalcanti-Adam EA, Kemkemer R, Spatz JP (2007) *Soft Matter* 3:307
10. Griffith LG, Swartz MA (2006) *Nat Rev Mol Cell Biol* 7:211
11. Cukierman E, Pankov R, Stevens DR, Yamada KM (2001) *Science* 294:1708
12. Stevens MM, George JH (2005) *Science* 310:1135
13. Vogel V, Sheetz M (2006) *Nat Rev Mol Cell Biol* 7:265
14. Vanderrest M, Garrone R (1991) *FASEB J* 5:2814
15. Hulmes DJS (1992) The collagen superfamily – diverse structures and assemblies. In: *Essays in biochemistry*, vol 27. Portland, London, p 49
16. Fratzl P (2008) *Collagen: structure and mechanics*. Springer, New York, p 506
17. Hardingham TE, Fosang AJ (1992) *FASEB J* 6:861
18. Ruoslahti E (1988) *Annu Rev Biochem* 57:375
19. Engel J (1992) *Biochemistry* 31:10643
20. Taipale J, Keski-Oja J (1997) *FASEB J* 11:51
21. Roskelley CD, Srebrow A, Bissell MJ (1995) *Curr Opin Cell Biol* 7:736
22. Sanes JR (1989) *Annu Rev Neurosci* 12:491
23. Adams JC, Watt FM (1993) *Development* 117:1183
24. Adams JC (2001) *Cell Mol Life Sci* 58:371
25. Burridge K, Chrzanowska-Wodnicka M (1996) *Annu Rev Cell Dev Biol* 12:463
26. Maheshwari G, Brown G, Lauffenburger DA, Wells A, Griffith LG (2000) *J Cell Sci* 113:1677
27. Palecek SP, Loftus JC, Ginsberg MH, Lauffenburger DA, Horwitz AF (1997) *Nature* 385:537
28. Gumbiner BM (1996) *Cell* 84:345
29. Behonick DJ, Werb Z (2003) *Mech Dev* 120:1327
30. Discher DE, Janmey P, Wang YL (2005) *Science* 310:1139
31. Schena M, Shalon D, Davis RW, Brown PO (1995) *Science* 270:467
32. Kane RS, Takayama S, Ostuni E, Ingber DE, Whitesides GM (1999) *Biomaterials* 20:2363
33. de Paz JL, Seeberger PH (2006) *QSAR Comb Sci* 25:1027
34. Lehnert D, Wehrle-Haller B, David C, Weiland U, Ballestrem C, Imhof BA, Bastmeyer M (2004) *J Cell Sci* 117:41
35. Anderson DG, Levenberg S, Langer R (2004) *Nat Biotechnol* 22:863



36. Ginger DS, Zhang H, Mirkin CA (2004) *Angew Chem Int Ed* 43:30
37. Wei C, Haroon A (1993) *Appl Phys Lett* 62:1499
38. von der Mark K, Park J, Bauer S, Schmuki P (2010) *Cell Tissue Res* 339:131
39. Bettinger CJ, Langer R, Borenstein JT (2009) *Angew Chem Int Ed* 48:5406
40. Dalby MJ, Gadegaard N, Tare R, Andar A, Riehle MO, Herzyk P, Wilkinson CDW, Oreffo ROC (2007) *Nat Mater* 6:997
41. Bettinger CJ, Zhang Z, Gerecht S, Borenstein JT, Langer R (2008) *Adv Mater* 20:99
42. Curtis A, Wilkinson C, Curtis A, Wilkinson C (2001) *Mater Today* 4:22
43. Chen CS, Mrksich M, Huang S, Whitesides GM, Ingber DE (1997) *Science* 276:1425
44. Curtis A, Wilkinson C (1997) *Biomaterials* 18:1573
45. Price RL, Ellison K, Haberstroh KM, Webster TJ (2004) *J Biomed Mater Res A* 70A:129
46. Zinger O, Zhao G, Schwartz Z, Simpson J, Wieland M, Landolt D, Boyan B (2005) *Biomaterials* 26:1837
47. Lickorish D, Guan L, Davies JE (2007) *Biomaterials* 28:1495
48. Gentsch R, Boysen B, Lankenau A, Börner HG (2010) *Macromol Rapid Commun* 31:59
49. Eichhorn SJ, Sampson WW (2005) *J R Soc Interface* 2:309
50. Friedl P (2004) *Curr Opin Cell Biol* 16:14
51. West JL, Hubbell JA (1998) *Macromolecules* 32:241
52. Lutolf MP, Lauer-Fields JL, Schmoekel HG, Metters AT, Weber FE, Fields GB, Hubbell JA (2003) *Proc Natl Acad Sci USA* 100:5413
53. Li Y, Ma T, Kniss DA, Lasky LC, Yang S-T (2001) *Biotechnol Prog* 17:935
54. Hutmacher DW, Singh H (2008) *Trends Biotechnol* 26:166
55. Lutolf MP, Lauer-Fields JL, Schmoekel HG, Metters AT, Weber FE, Fields GB, Hubbell JA (2003) *Proc Natl Acad Sci USA* 100:5413
56. Roskelley CD, Desprez PY, Bissell MJ (1994) *Proc Natl Acad Sci USA* 91:12378
57. Vogel V, Baneyx G (2003) *Annu Rev Biomed Eng* 5:441
58. Sun T, Norton D, McKean RJ, Haycock JW, Ryan AJ, MacNeil S (2007) *Biotechnol Bioeng* 97:1318
59. Yang Y, Bolikal D, Becker ML, Kohn J, Zeiger DN, Simon CG (2008) *Adv Mater* 20:2037
60. van Hest JCM, Tirrell DA (2001) *Chem Commun*:1897
61. Hubbell JA (1995) *Biotechnology* 13:565
62. Kikuchi A, Okano T (2005) *J Control Release* 101:69
63. Hynes RO (1992) *Cell* 69:11
64. Ruoslahti E, Pierschbacher MD (1987) *Science* 238:491
65. Massia SP, Hubbell JA (1991) *J Cell Biol* 114:1089
66. Comisar WA, Kazmers NH, Mooney DJ, Linderman JJ (2007) *Biomaterials* 28:4409
67. Pratt AB, Weber FE, Schmoekel HG, Muller R, Hubbell JA (2004) *Biotechnol Bioeng* 86:27
68. Ehrbar M, Zeisberger SM, Raeber GP, Hubbell JA, Schnell C, Zisch AH (2008) *Biomaterials* 29:1720
69. Chen GP, Ushida T, Tateishi T (2001) *Biomaterials* 22:2563
70. Zhou QL, Gong YH, Gao CY (2005) *J Appl Polym Sci* 98:1373
71. Ho MH, Kuo PY, Hsieh HJ, Hsien TY, Hou LT, Lai JY, Wang DM (2004) *Biomaterials* 25:129
72. Hou QP, Grijpma DW, Feijen J (2003) *Biomaterials* 24:1937
73. Yoon JJ, Park TG (2001) *J Biomed Mater Res* 55:401
74. Goldstein AS, Zhu GM, Morris GE, Meszlenyi RK, Mikos AG (1999) *Tissue Eng* 5:421
75. Groenewolt M, Antonietti M, Polarz S (2004) *Langmuir* 20:7811
76. Kim HD, Bae EH, Kwon IC, Pal RR, Nam JD, Lee DS (2004) *Biomaterials* 25:2319
77. Whang K, Thomas CH, Healy KE, Nuber G (1995) *Polymer* 36:837
78. Degroot JH, Nijenhuis AJ, Bruin P, Pennings AJ, Veth RPH, Klompmaker J, Jansen HWB (1990) *Colloid Polym Sci* 268:1073
79. Elema H, Degroot JH, Nijenhuis AJ, Pennings AJ, Veth RPH, Klompmaker J, Jansen HWB (1990) *Colloid Polym Sci* 268:1082
80. Förster S, Antonietti M (1998) *Adv Mater* 10:195
81. Hamley IW (2003) *Nanotechnology* 14:R39
82. Hawker CJ, Russell TP (2005) *MRS Bulletin* 30:952



83. Discher DE, Ahmed F (2006) *Ann Rev Biomed Eng* 8:323
84. Wang XS, Guerin G, Wang H, Wang YS, Manners I, Winnik MA (2007) *Science* 317:644
85. Aggeli A, Nyrkova IA, Bell M, Harding R, Carrick L, McLeish TCB, Semenov AN, Boden N (2001) *Proc Natl Acad Sci USA* 98:11857
86. MacPhee CE, Woolfson DN (2004) *Curr Opin Solid State Mat Sci* 8:141
87. Hartgerink JD, Zubarev ER, Stupp SI (2001) *Curr Opin Solid State Mat Sci* 5:355
88. Zhang SG (2003) *Nat Biotechnol* 21:1171
89. Holmes TC (2002) *Trends Biotechnol* 20:16
90. Fairman R, Akerfeldt KS (2005) *Curr Opin Struct Biol* 15:453
91. Hirst AR, Escuder B, Miravet JF, Smith DK (2008) *Angew Chem Int Ed* 47:8002
92. Woolfson DN, Ryadnov MG (2006) *Curr Opin Chem Biol* 10:559
93. Börner HG, Schlaad H (2007) *Soft Matter* 3:394
94. Börner HG (2009) *Prog Polym Sci* 34:811
95. Webber MJ, Kessler JA, Stupp SI (2010) *J Intern Med* 267:71
96. Rajagopal K, Schneider JP (2004) *Curr Opin Struct Biol* 14:480
97. Muentner A, Hentschel J, Börner HG, Brezesinski G (2008) *Langmuir* 24:3306
98. Börner HG (2007) *Macromol Chem Phys* 208:124
99. ten Cate MGJ, Severin N, Börner HG (2006) *Macromolecules* 39:7831
100. Kühnle H, Börner HG (2009) *Angew Chem Int Ed* 48:6431
101. Smeenk JM, Otten MJB, Thies J, Tirrell DA, Stunnenberg HG, van Hest JCM (2005) *Angew Chem Int Ed* 44:1968
102. Nesloney CL, Kelly JW (1996) *Bioorg Med Chem* 4:739
103. Ulijn RV, Smith AM (2008) *Chem Soc Rev* 37:664
104. Kopecek J, Yang JY (2009) *Acta Biomater* 5:805
105. Zhang SG, Zhao XJ (2004) *J Mater Chem* 14:2082
106. Papapostolou D, Bromley EHC, Bano C, Woolfson DN (2008) *J Am Chem Soc* 130:5124
107. Ryadnov MG, Woolfson DN (2003) *Nat Mater* 2:329
108. Eckhardt D, Groenewolt M, Krause E, Börner HG (2005) *Chem Commun*:2814
109. Börner HG, Smarsly B, Hentschel J, Rank A, Schubert R, Geng Y, Discher DE, Hellweg T, Brandt A (2008) *Macromolecules* 41:1430
110. Hentschel J, Krause E, Börner HG (2006) *J Am Chem Soc* 128:7722
111. Ryadnov MG, Woolfson DN (2003) *Angew Chem Int Ed* 42:3021
112. Papapostolou D, Smith AM, Atkins EDT, Oliver SJ, Ryadnov MG, Serpell LC, Woolfson DN (2007) *Proc Natl Acad Sci USA* 104:10853
113. Smith JF, Knowles TPJ, Dobson CM, MacPhee CE, Welland ME (2006) *Proc Natl Acad Sci USA* 103:15806
114. Altman GH, Diaz F, Jakuba C, Calabro T, Horan RL, Chen JS, Lu H, Richmond J, Kaplan DL (2003) *Biomaterials* 24:401
115. Guler MO, Hsu L, Soukasene S, Harrington DA, Hulvat JF, Stupp SI (2006) *Biomacromolecules* 7:1855
116. Silva GA, Czeisler C, Niece KL, Beniash E, Harrington DA, Kessler JA, Stupp SI (2004) *Science* 303:1352
117. Ma Y, Börner HG, Hartmann J, Cölfen H (2006) *Chem Eur J* 12:7882
118. Page MG, Nassif N, Börner HG, Antonietti M, Cölfen H (2008) *Cryst Growth Des* 8:1792
119. Wang T, Verch A, Börner HG, Cölfen H, Antonietti A (2009) *J Ceram Soc Jpn* 117:221
120. Kessel S, Thomas A, Börner HG (2007) *Angew Chem Int Ed* 46:9023
121. Kessel S, Börner HG (2008) *Macromol Rapid Commun* 29:419
122. Kessel S, Börner HG (2008) *Macromol Rapid Commun* 29:316
123. Hartgerink JD, Beniash E, Stupp SI (2001) *Science* 294:1684
124. Rajangam K, Arnold MS, Rocco MA, Stupp SI (2008) *Biomaterials* 29:3298
125. Tibbitt MW, Anseth KS (2009) *Biotechnol Bioeng* 103:655
126. Hentschel J, Börner HG (2006) *J Am Chem Soc* 128:14142
127. Lee KY, Mooney DJ (2001) *Chem Rev* 101:1869
128. Hentschel J, ten Cate MGJ, Börner HG (2007) *Macromolecules* 40:9224
129. Stevens MM (2008) *Mater Today* 11:18

130. Eyrich D, Brandl F, Appel B, Wiese H, Maier G, Wenzel M, Staudenmaier R, Goepferich A, Blunk T (2007) *Biomaterials* 28:55
131. Rihova B (2000) *Adv Drug Deliv Rev* 42:65
132. Orive G, Hernandez RM, Gascon AR, Dominguez-Gil A, Pedraz JL (2003) *Curr Opin Biotechnol* 14:659
133. Orive G, Hernandez RM, Gascon AR, Calafiore R, Chang TMS, de Vos P, Hortelano G, Hunkeler D, Lacik I, Pedraz JL (2004) *Trends Biotechnol* 22:87
134. Kisiday J, Jin M, Kurz B, Hung H, Semino C, Zhang S, Grodzinsky AJ (2002) *Proc Natl Acad Sci USA* 99:9996
135. Pochan DJ, Schneider JP, Kretsinger J, Ozbas B, Rajagopal K, Haines L (2003) *J Am Chem Soc* 125:11802
136. Schneider JP, Pochan DJ, Ozbas B, Rajagopal K, Pakstis L, Kretsinger J (2002) *J Am Chem Soc* 124:15030
137. Rajagopal K, Lamm MS, Haines-Butterick LA, Pochan DJ, Schneider JP (2009) *Biomacromolecules* 10:2619
138. Hule RA, Nagarkar RP, Hammouda B, Schneider JP, Pochan DJ (2009) *Macromolecules* 42:7137
139. Hollister SJ, Lin CY (2007) *Comput Methods Appl Mech Eng* 196:2991
140. Lin CY, Kikuchi N, Hollister SJ (2004) *J Biomech* 37:623
141. Hollister SJ (2005) *Nat Mater* 4:518
142. Goulet RW, Goldstein SA, Ciarelli MJ, Kuhn JL, Brown MB, Feldkamp LA (1994) *J Biomech* 27:375
143. Barry RA, Shepherd RF, Hanson JN, Nuzzo RG, Wiltzius P, Lewis JA (2009) *Adv Mater* 21:2407
144. Huttmacher DW, Schantz T, Zein I, Ng KW, Teoh SH, Tan KC (2001) *J Biomed Mater Res* 55:203
145. Cooke MN, Fisher JP, Dean D, Rinnac C, Mikos AG (2003) *J Biomed Mater Res B* 64B:65
146. Williams JM, Adewunmi A, Schek RM, Flanagan CL, Krebsbach PH, Feinberg SE, Hollister SJ, Das S (2005) *Biomaterials* 26:4817
147. Kim SS, Utsunomiya H, Koski JA, Wu BM, Cima MJ, Sohn J, Mukai K, Griffith LG, Vacanti JP (1998) *Ann Surg* 228:8
148. Lam CXF, Mo XM, Teoh SH, Huttmacher DW (2002) *Mater Sci Eng C Biomimetic Supramol Syst* 20:49
149. Malda J, Woodfield TBF, van der Vloodt F, Kooy FK, Martens DE, Tramper J, van Blitterswijk CA, Riesle J (2004) *Biomaterials* 25:5773
150. Yeo A, Wong WJ, Khoo HH, Teoh SH (2010) *J Biomed Mater Res A* 92A:311
151. Tao X, Joyce J, Cassie G, J. HJ, Thomas B (2005) *Biomaterials* 26:93
152. Landers R, Hubner U, Schmelzeisen R, Mulhaupt R (2002) *Biomaterials* 23:4437
153. Kessel S, Börner HG (2008) *Macromol Rapid Commun* 29:316
154. Huttmacher DW, Cool S (2007) *J Cell Mol Med* 11:654
155. Rai B, Teoh SH, Huttmacher DW, Cao T, Ho KH (2005) *Biomaterials* 26:3739
156. Greiner A, Wendorff JH (2007) *Angew Chem Int Ed* 46:5670
157. Ramakrishna S, Fujihara K, Teo W-E, Lim T-C, Ma Z (2005) *An introduction to electrospinning and nanofibers*. World Scientific, Singapore, p 275
158. Hohman MM, Shin M, Rutledge G, Brenner MP (2001) *Phys Fluids* 13:2221
159. Yarin AL, Koombhongse S, Reneker DH (2001) *J Appl Phys* 90:4836
160. McKee MG, Wilkes GL, Colby RH, Long TE (2004) *Macromolecules* 37:1760
161. Sun ZC, Zussman E, Yarin AL, Wendorff JH, Greiner A (2003) *Adv Mater* 15:1929
162. Bognitzki M, Czado W, Frese T, Schaper A, Hellwig M, Steinhart M, Greiner A, Wendorff JH (2001) *Adv Mater* 13:70
163. Dror Y, Salalha W, Avrahami R, Zussman E, Yarin AL, Dersch R, Greiner A, Wendorff JH (2007) *Small* 3:1064
164. Pai CL, Boyce MC, Rutledge GC (2009) *Macromolecules* 42:2102
165. Koombhongse S, Liu WX, Reneker DH (2001) *J Polym Sci B Polym Phys* 39:2598

166. Chen SL, Hou HQ, Hu P, Wendorff JH, Greiner A, Agarwal S (2009) *Macromol Mater Eng* 294:265
167. Holzmeister A, Greiner A, Wendorff JH (2009) *Polym Eng Sci* 49:148
168. Teo WE, Ramakrishna S (2006) *Nanotechnology* 17:R89
169. Li D, Wang YL, Xia YN (2003) *Nano Lett* 3:1167
170. Patel S, Kurpinski K, Quigley R, Gao HF, Hsiao BS, Poo MM, Li S (2007) *Nano Lett* 7:2122
171. Hellmann C, Belardi J, Dersch R, Greiner A, Wendorff JH, Bahnmueller S (2009) *Polymer* 50:1197
172. Dosunmu OO, Chase GG, Kataphinan W, Reneker DH (2006) *Nanotechnology* 17:1123
173. Varabhas JS, Chase GG, Reneker DH (2008) *Polymer* 49:4226
174. Boudriot U, Dersch R, Greiner A, Wendorff JH (2006) *Artificial Organs* 30:785
175. Mo XM, Xu CY, Kotaki M, Ramakrishna S (2004) *Biomaterials* 25:1883
176. Kwon IK, Kidoaki S, Matsuda T (2005) *Biomaterials* 26:3929
177. Christopherson GT, Song H, Mao HQ (2009) *Biomaterials* 30:556
178. Johnson J, Nowicki MO, Lee CH, Chioocca EA, Viapiano MS, Lawler SE, Lannutti JJ (2009) *Tissue Eng Part C* 15:531
179. Lee CH, Shin HJ, Cho IH, Kang YM, Kim IA, Park KD, Shin JW (2005) *Biomaterials* 26:1261
180. Xu CY, Yang F, Wang S, Ramakrishna S (2004) *J Biomed Mater Res A* 71A:154
181. Badami AS, Kreke MR, Thompson MS, Riffle JS, Goldstein AS (2006) *Biomaterials* 27:596
182. Lowery JL, Datta N, Rutledge GC (2010) *Biomaterials* 31:491
183. Thorvaldsson A, Stenhamre H, Gatenholm P, Walkenstrom P (2008) *Biomacromolecules* 9:1044
184. Nam J, Huang Y, Agarwal S, Lannutti J (2007) *Tissue Eng* 13:2249
185. Ekaputra AK, Prestwich GD, Cool SM, Hutmacher DW (2008) *Biomacromolecules* 9:2097
186. Jeong SI, Kim SY, Cho SK, Chong MS, Kim KS, Kim H, Lee SB, Lee YM (2007) *Biomaterials* 28:1115
187. Kim G, Kim W (2007) *J Biomed Mater Res A* 81B:104
188. Simonet M, Schneider OD, Neuenschwander P, Stark WJ (2007) *Polym Eng Sci* 47:2020
189. Townsend-Nicholson A, Jayasinghe SN (2006) *Biomacromolecules* 7:3364
190. Yang XC, Shah JD, Wang HJ (2009) *Tissue Eng Part A* 15:945
191. Zeugolis DI, Khew ST, Yew ESY, Ekaputra AK, Tong YW, Yung LYL, Hutmacher DW, Sheppard C, Raghunath M (2008) *Biomaterials* 29:2293
192. Bhattarai N, Edmondson D, Veiseh O, Matsen FA, Zhang MQ (2005) *Biomaterials* 26:6176
193. Reddy CS, Arinstein A, Avrahami R, Zussman E (2009) *J Mater Chem* 19:7198
194. Kidoaki S, Kwon IK, Matsuda T (2005) *Biomaterials* 26:37
195. Sun XY, Shankar R, Börner HG, Ghosh TK, Spontak RJ (2007) *Adv Mater* 19:87
196. Ma ML, Titievsky K, Thomas EL, Rutledge GC (2009) *Nano Lett* 9:1678
197. Kalra V, Lee J, Lee JH, Lee SG, Marquez M, Wiesner U, Joo YL (2008) *Small* 4:2067
198. Xu XL, Yang LX, Xu XY, Wang X, Chen XS, Liang QZ, Zeng J, Jing XB (2005) *J Control Release* 108:33
199. Sy JC, Klemm AS, Shastri VP (2009) *Adv Mater* 21:1814
200. Yoo HS, Kim TG, Park TG (2009) *Adv Drug Deliv Rev* 61:1033
201. Liang D, Hsiao BS, Chu B (2007) *Adv Drug Deliv Rev* 59:1392
202. Kim TG, Park TG (2006) *Tissue Eng* 12:221
203. Ma ZW, He W, Yong T, Ramakrishna S (2005) *Tissue Eng* 11:1149
204. Krogman KC, Lowery JL, Zacharia NS, Rutledge GC, Hammond PT (2009) *Nat Mater* 8:512
205. Schindler M, Ahmed I, Kamal J, Nur-E-Kamal A, Grafe TH, Chung HY, Meiners S (2005) *Biomaterials* 26:5624
206. Li X, Xie J, Lipner J, Yuan X, Thomopoulos S, Xia Y (2009) *Nano Lett* 9:2763
207. Davis ME, Motion JPM, Narmoneva DA, Takahashi T, Hakuno D, Kamm RD, Zhang SG, Lee RT (2005) *Circulation* 111:442
208. Hu W, Huang Z-M (2009) *Polym Int* 59:92
209. Li XS, Yao C, Sun FQ, Song TY, Li YH, Pu YP (2008) *J Appl Polym Sci* 107:3756
210. Moutos FT, Freed LE, Guilak F (2007) *Nat Mater* 6:162

# Antimicrobial Surfaces

Joerg C. Tiller

**Abstract** In this review, the general principles of antimicrobial surfaces will be discussed in detail. Because many common products that keep microbes off surfaces have been banned in the past decade, the search for alternatives is in full run. In recent research, numerous new ways to produce so-called self-sterilizing surfaces have been introduced. These technologies are discussed with respect to their mechanism, particularly focusing on the distinction between biocide-releasing and non-releasing contact-active systems. New developments in the catalytic formation of biocides and their advantages and limitations are also covered. The combination of several mechanisms in one surface modification has considerable benefits, and will be discussed.

**Keywords** Antibacterial · Antimicrobial · Bacteria · Biocide · Contact-active · Light-activated · Photocatalytic · Release · Self-polishing · Surface

## Contents

1	Introduction .....	194
2	Preliminary Considerations .....	195
2.1	Classification of Antimicrobial Surfaces .....	195
2.2	Contact-Active versus Releasing Systems .....	195
3	Microbe-Repelling Surfaces .....	198
4	Contact-Active Surfaces .....	199
5	Biocide-Releasing Surfaces .....	203
5.1	Controlled Release .....	203
5.2	Triggered Release .....	204

---

J.C. Tiller (✉)

Biomaterials and Polymer Science, Department of Bio- and Chemical Engineering,  
TU Dortmund, Emil-Figge-Strasse 66, 44227 Dortmund, Germany  
e-mail: [joerg.tiller@udo.edu](mailto:joerg.tiller@udo.edu)

5.3	Catalytic Formation of Biocides and Their Release .....	205
6	Multiple Antimicrobial Actions.....	207
6.1	Releasing and Repelling .....	207
6.2	Contact-Killing and Repelling .....	209
6.3	Releasing and Contact-Killing.....	209
7	Conclusion .....	210
	References .....	211

## 1 Introduction

It is generally accepted that our planet is ruled by microorganisms, such as bacteria, yeast, fungi, and algae, which dominate us in number and mass. We just happen to roam in their realm for a certain period of time. Even our own body is outnumbered by microbial cells 10:1 with respect to our own cell count. We only survive because we can accommodate that fact and try for coexistence. Nevertheless, modern human society also requires a certain control over the microbial population. This is particularly true for pathogenic microbial strains, which are still the cause of millions of deaths every year. However, the treatment of microbial infections is becoming increasingly difficult because the number of antibiotic-resistant microbial strains and patients is growing a lot faster than the number of useable antibiotics [1, 2]. It was reported that the number of deaths caused by the resistant microbial strain MRSA (methicillin-resistant *Staphylococcus aureus*) exceeds the number of deaths caused by HIV in the USA [3]. For this reason, the application of antimicrobial surface modifications on all sorts of medical devices and implants seems to be a necessary tool for fighting microbial infections, particularly in hospitals, by preventing the spread of microbial cells [4]. Another less life-threatening, but economically important, area that requires the control of microbial populations is the formation of biofilms on manmade materials, which corrode and deteriorate and are rendered dysfunctional by these biofilms [5]. Typical biofilms are depicted in Fig. 1. Although biomedical applications mainly require biocompatibility of the



**Fig. 1** Examples of biofilms. *Left*: typical mold in households. *Center*: typical biofouling on a ship hull, including algae and barnacles. *Right*: microbial *Pseudomonas aeruginosa* biofilm on a catheter

whole system for the targeted application, the fight against biofilms on materials has to consider environmental pollution issues. Besides medical devices and implants, there are numerous other fields of interest for antimicrobial surfaces, including food protection, household hygiene, water towers, air conditioners, and sportswear.

This chapter is dedicated to discussion of the state of the art of antimicrobial surfaces, particularly with respect to their mechanism of action.

## 2 Preliminary Considerations

### 2.1 Classification of Antimicrobial Surfaces

Many microbial infections and toxins are spread by biofilms. Biofilm formation occurs on virtually every surface, starting with the adhesion of planctonic cells or small dispersed biofilm fragments. Proliferation of the cells is accompanied by the expression of an extracellular polysaccharide-based matrix [6]. The cells embedded in this matrix are well protected and up to 1000 times less susceptible to antibiotics [7]. Once a biofilm is formed, it is extremely difficult to remove this contamination. Thus, all antimicrobial surfaces should prevent the primary attack [8]. One class of antimicrobial surfaces prevents the primary attack by creating surfaces that are not sticky to microbial cells, i.e., they do not allow adhesion of these cells. The other major class of antimicrobial surfaces is based on the killing of approaching microbes (see Fig. 2). Interestingly, both approaches can be achieved either by permanent surface modifications or by releasing bioactive compounds.

### 2.2 Contact-Active versus Releasing Systems

It seems obvious that repelling or killing approaching microbes without releasing a chemical compound would be desirable. Numerous recent publications claim to

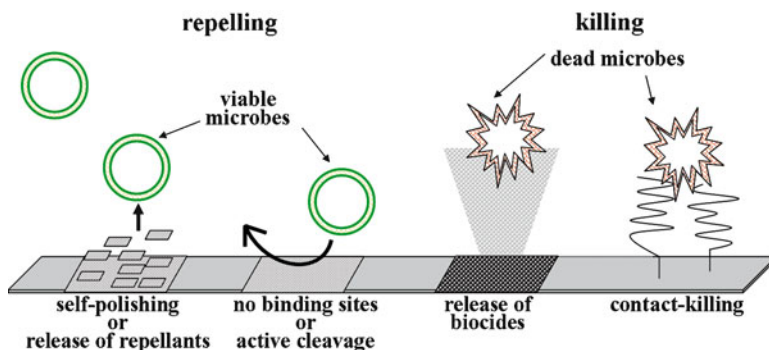
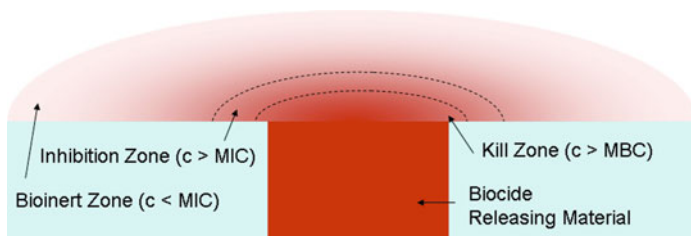


Fig. 2 General classes of antimicrobial surfaces

have developed contact-active surfaces, mostly for killing microbes or delaying their growth [9–11]. A surface that kills on contact must function with a different mechanism compared to one that releases a biocide. Thus, knowledge of the mode of action is very important for the differentiation between those two. However, contact activity is hard to prove because of the very complex analytics of the process of killing a cell.

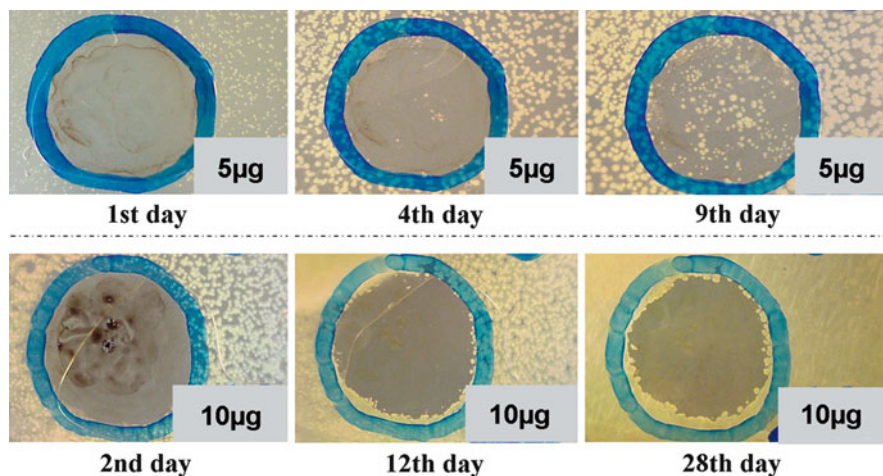
One common way to distinguish between contact-active killing and release of a biocide is to look for an inhibition zone, which occurs if a biocidal compound is released from the treated area and diffuses into the untreated control zone. Unfortunately, the size of such an inhibition zone depends on many parameters, including the release kinetics, and the amount and activity of the released biocide in the test system. The lack of a visible inhibition zone does not automatically prove contact activity [12]. Another test for contact activity is the so-called DOW suspension test, which assumes that the modified surface kills approaching microbes so effectively that the overall number of living cells (colony forming units, CFUs) in the surrounding medium decreases [13]. Studies have shown that some biocidal surfaces kill very slowly in terms of hours and thus they probably do not reduce surrounding bacterial cell numbers. Sometimes, a loss of biocidal activity of the medium after removing the active test sample is interpreted as an indication of contact activity [14]. This claim is rather hard to prove because, in the case of releasing systems, the medium certainly dilutes any released compound and the overall concentration can easily be below the active concentration in most practical setups. Figure 3 depicts a model to illustrate the situation in a release system.

Every compound that leaches from a material has to permeate through the material first and is later distributed into the surroundings. In every case, there will be a diffusion zone on the surface that consists of fairly highly concentrated released compound. The size of this zone depends on diffusion rates through the material, through the interface, and in the surroundings as well as on the surface affinity between released compound and material interface. If this released compound is a biocide, the area where the concentration of the biocide is above the minimal biocidal concentration (MBC, 99.9% of all microbial cells are killed) is called the kill zone. The area with at least the minimal inhibitory concentration (MIC, 99% of all microbial cells are inhibited in growth) is called the inhibition zone. Systems with just an inhibition zone and no kill zone do not damage microbes and are only active



**Fig. 3** Surface-release profile of a biocide loaded into a matrix. *MBC* minimal biocidal concentration, *MIC* minimal inhibitory concentration, *c* concentration of biocide





**Fig. 4** Photographs of coatings containing silver nanoparticles at concentrations of  $5\ \mu\text{g Ag/cm}^2$  (top line) and  $10\ \mu\text{g Ag/cm}^2$  (bottom line) sprayed with *S. aureus* cells from aqueous suspension, air dried, covered with liquefied growth agar (1.5 wt% in cultivation medium), and incubated at  $37^\circ\text{C}$ . The sample in each line was recorded after varying incubation times. Photographs in part reproduced from [12]

in a surface test. An example of such a system was reported previously for silver nanoparticle-loaded surfaces [12]. When using coatings containing  $5\ \mu\text{g Ag/cm}^2$ , the *S. aureus* cells sprayed onto the surface were delayed in growth for up to 9 days and no bacterial cells were killed, due to the lack of a kill zone (Fig. 4, top row). Increasing the concentration to  $10\ \mu\text{g/cm}^2$  completely killed the cells (Fig. 4, bottom row). In the case of the existence of a kill zone, living microbial cells in the surrounding can be decimated by diffusion through the kill zone. This is effective if fast-killing biocides are used.

It has been shown that a material that releases the biocidal compound cetyltrimethylammonium chloride seemingly kills microbes on contact, while the number of the surrounding bacterial cells does not decrease [15]. In this case, the biocidal compound kills slowly in terms of hours and therefore a free-moving bacterial cell will not stay long enough in the kill zone to be damaged. In the early 1980s, surface modifications with tributyltin (TBT) were believed to be contact-active antimicrobial [16]. In such coatings, TBT is released very slowly. Because of its very high activity and its low solubility, TBT kills microbes in the small kill zone quickly, but not in the diluted test medium. According to the proposed mechanism, the same might be true for *N*-halamine-based coatings that release the very active biocide hypochloride [17].

Another way to measure the efficiency of a biocidal surface is by detection of the ATP bioluminescence of the adhering microbial cells [18]. With this elaborate method, the killing rate of a surface can be measured and it is possible to distinguish between growth inhibition and killing. However, the method does not distinguish between release and contact activity. In general, there is no test that can clearly tell the difference between a contact-active and a release system.

### 3 Microbe-Repelling Surfaces

The repelling of microbes can generally be achieved by surfaces that do not allow protein adhesion. Such surfaces can be obtained in various ways, including the modification of surfaces using polyethylene glycol (PEG). The first example was found when Brash and Uniyal investigated the antithrombic potential of polyurethanes and found a very low adhesion of albumin and fibrinogen on polyurethanes containing PEG soft segments [19]. In contrast to protein adhesion, the reduction of cell adhesion is never complete. This is due to the different size and the complex patch-like chemical composition of the microbial cell surfaces, as well as to the fact that microbes actively adhere to surfaces [20]. Thus, it is not possible to fully describe bacterial adhesion using DLVO theory (Derjaguin, Landau, Verwey, and Overbeek theory describing the interaction of colloidal particles) [21]. Nevertheless, the great hydrophilicity of PEG and the fact that it is only a hydrogen acceptor might be reasons why PEG repels microbes better than any other surface modification.

The first example of a bacteria-repelling surface was described by Humphries et al., who examined surface modifications using PEG-containing block copolymers and found that PEGylation afforded an anti-adhesive effect of over 99% against *Pseudomonas* sp., *Serratia marcescens*, and *Streptococcus mutans* [22]. Additionally, it was found that a negatively charged surface repels microbial cells because of their negative surface net charge [23]. However, due to the patch-like surface structure every microbial cell has also positively charged areas on the surface, which will eventually allow adhesion of the cell to a negatively charged surface. Nevertheless, Park et al. could demonstrate that the combination of PEGylation and a negatively charged surface is more effective against *Staphylococcus epidermidis* and *Escherichia coli* than each modification alone [24]. Interestingly, control of charge and PEGylation of collagen can be used to control adhesion of the Gram-positive bacterium *S. aureus* and of mouse fibroblast cells in order to obtain biomaterials with full mammalian cell adhesion and fivefold reduction in bacterial adhesion [25]. Also, surface-grafted zwitterionic polymers, e.g., phosphorylcholine-containing polymers and poly(sulfobetaine methacrylate), have been found to repel microbes effectively [26, 27]. Such surfaces can reduce the adhesion of *S. epidermidis* and *Pseudomonas aeruginosa* by up to 96% compared with the control [28]. More recently, the use of thermosensitive polymers, such as poly(*N*-isopropylamide), has been discussed as a controlled repel mechanism that allows the temperature-sensitive switching between adhesive state and repelling state for biofilms [29].

Besides the numerous synthetic and natural polymers that are suited for repelling microbes from surfaces (summarized in [8]), the negatively charged protein albumin can also reduce bacterial adhesion [30]. Further, the nature of the surface-attached repelling polymer and its mechanical properties both seem to play a role in the attraction of microbes. This was demonstrated by Lichter et al., who investigated poly(allylammonium hydrochloride) (PAH) and poly(acrylic acid) (PAA) multilayers and found that the stiffness of the coating positively correlated with the adhesion of *E. coli*. [31].

Another way to keep microbial cells off surfaces is to create materials that constantly renew their surface, e.g., by being degraded. This so-called self-polishing does not keep microbes away effectively because the degradation process and the formation of a biofilm have different time scales. The latter takes merely hours, whereas the first should be in the range of days to months to provide a useful protection. In practice, such self-polishing systems only work in combination with released biocides and are discussed in Sect. 6.1 in greater detail.

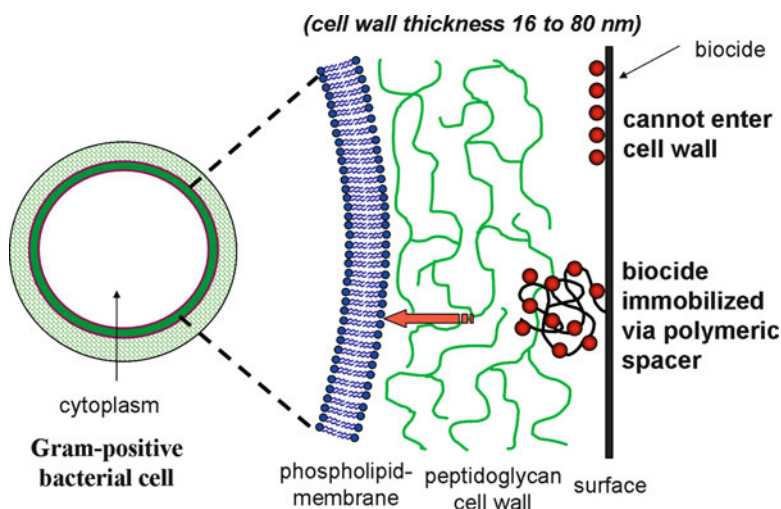
A more recent approach is the release of substances that keep microbial cells from actively adhering to a surface. This effect is discussed for silver ions released from a solid silver surface [32] as well as for nitric-oxide-releasing hydrogels [33].

Alternatively, if the binding sites (adhesion proteins, polysaccharides) of the approaching microbes are actively cut, they cannot adhere either. This can be achieved using hydrolytic enzymes. The recently reviewed use of hydrolytic enzymes in antifouling coatings classifies the action of the enzymes by the breakdown of adhesive components such as proteins and polysaccharides, and by the catalytic production of repellent compounds [34]. In general, hydrolases such as proteases, glycosidases, and lipases are considered to show microbe-repelling properties when tethered to surfaces [35]. For example, immobilized subtilisin is very effective in preventing adhesion of marine microorganisms such as *Ulva linza* and the diatom *Navicula perminuta* [35, 36]. In another successful approach, a coating based on chymotrypsin immobilized in silicate effectively lowered microbial adhesion over months [37]. Serine proteases are also effective repellents [38]. So far, only price and limited operational stability hinders these approaches from appearing on the market.

## 4 Contact-Active Surfaces

The first contact-killing surface was described by Isquith et al., who modified glass substrates with the silane 3-(trimethoxysilyl)-propyldimethyloctadecylammonium chloride, often referred to as DOW5700 [39]. However, the claim was made on the basis of the DOW suspension test (see Sect. 2.2), which cannot distinguish between biocide release and contact activity. In subsequent work, neither the original authors nor followers proposed a working model for a mechanisms that was able to explain the contact activity of this surface modification. The first model for contact activity was proposed in 2001 (see Fig. 5) [40].

The model was based on the idea that a surface-grafted membrane-active biocide on a polymeric spacer might be capable of penetrating the bacterial cell wall of an adhered Gram-positive bacterium, thus reaching its cell membrane and killing the microorganism. This was demonstrated by surface grafting of the antimicrobial polymer poly (4-vinyl-*N*-hexylpyridinium bromide) to glass and later to several plastics [40, 41]. It could be shown that Gram-positive *Staphylococci* as well as Gram-negative *P. aeruginosa* cells do not grow on such a surface. The latter microbial strain is not susceptible to quarternary ammonium ions. This indicates a different mechanism of action of such surfaces compared to the respective polymers



**Fig. 5** Concept of contact-killing membrane-active biocides surface-coupled via a polymeric spacer

in solution. It could also be shown that the surface kills MRSA in the same way as it kills non-resistant *S. aureus* [42]. Another highly potent polymer for this application was found to be poly(ethyleneimine), which effectively kills microbes [43] and even deactivates certain influenza viruses [44] when grafted to surfaces and quarternized with dodecyl and methyl groups. It could also be demonstrated that these surfaces did not develop resistant *S. aureus* or *E. coli* strains [45]. Lee et al. confirmed this concept to be general by using atom transfer radical polymerization (ATRP) grafting of tertiary amine 2-(dimethylamino) ethyl methacrylate followed by quarternization of the amines with methyl iodide [46].

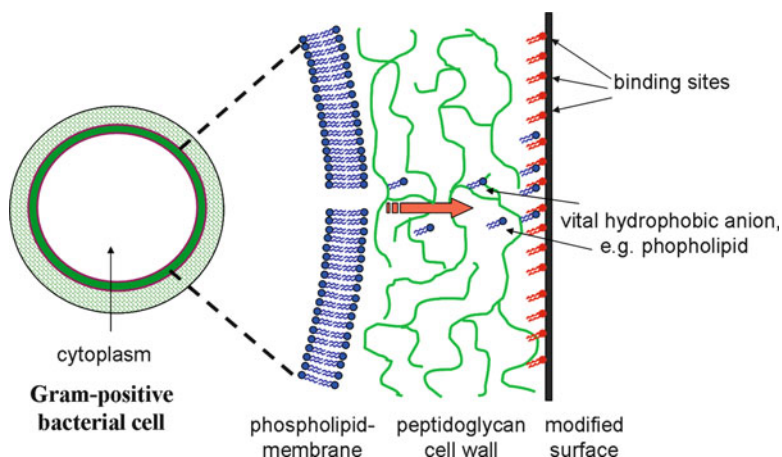
The elaborate surface modification of all coatings so far was overcome by using block copolymers containing a hydrophobic and a hydrophilic antimicrobial block as the emulsifiers for the emulsion polymerization of styrene and acrylates in water. The resulting paint was useful for obtaining contact-active antimicrobial coatings from aqueous suspensions. In parallel, polymeric additives for polyurethane [47] and acrylate [48] coatings were developed that migrate to the surface of the coating during the preparation process. This way, antimicrobial contact-active materials can be obtained without a finishing procedure. Whereas the first approach uses 1,3-propylene oxide blocks with alkylammonium groups as crosslinked segments, the second approach applies macromonomers based on polyoxazolines with biocidal quarternary ammonium end groups [49–51], which are copolymerized with the acrylate monomers and crosslinkers. Recently, coatings based on single-walled carbon nanotubes were also claimed to be antimicrobially active because, according to the authors, the nanotubes might poke through the cell walls of approaching microbial cells [52].

The concept of polymeric spacers was controversially discussed at a very early stage of these developments, because the proposed mechanism is difficult to imagine and the active lengths of most grafted polymers require high stretching of the macromolecules to reach the inner cell membrane of attached microbes. This is usually discussed as a distribution problem, i.e., there are always chains that are longer than the average that can cross the distance more easily. Furthermore, an increasing number of contact-active antimicrobial surfaces containing quarternary ammonium groups are described that do not contain a polymeric spacer [53–55].

In order to gain better insights into the mechanism, Kugler et al. directly grafted poly(4-vinylpyridine) to glass surfaces and investigated the influence of the degree of quarternization on the antimicrobial action [56]. He found a very sharp transition between active and inactive at a certain partial alkylation level. Instead of interpreting this as a degree of required hydrophilicity, as done by others [57], Kugler proposed a new mechanism that somehow involved the exchange of divalent ions from the cell wall of the attached microbe by the surface. These arguments were pursued in subsequent publications [58, 59]. Other authors used the argument that microbes have a hydrophobic surface and a negative surface net charge. This might lead to the attraction of microbes and somehow to the destruction of their cell envelope [60]. Because hydrophilic surfaces such as chitosan coatings attract microbial cells in the same way without killing them, the first argument seems insufficient. Furthermore, there is no reasonable explanation of how the surface might actually destroy the cell envelope.

In recent research, a series of cellulose derivatives with varying quarternary ammonium groups and additional hydrophobic groups have been investigated regarding their potential as antimicrobial coatings [61]. It could be shown that the main factor contributing to the antimicrobial activity of coatings made of these derivatives is indeed their cationic/hydrophobic balance, i.e., a sufficient charge density is not all that is required. We propose that the antimicrobial action of these coatings originates from their ability to adhere hydrophobic anionic molecules. In order to explore this, SDS was allowed to adhere to the surface of the investigated surfaces. The antimicrobial action of the coatings was completely quenched after this treatment. When doing the same experiment using surfaces modified by the attachment of long-chain antimicrobial polymers (as shown in Fig. 5), SDS did not affect the antimicrobial activity. It seems obvious to us that the two kinds of investigated coatings work according to different mechanisms. Whereas the long-chain antimicrobial polymers seem to show the polymeric spacer effect, the directly surface-attached molecules seem to attract hydrophobic anionic molecules from the attached cells (see Fig. 6). If these molecules were negatively charged phospholipids, then the attached microbial cells would indeed die.

Another kind of contact-active antimicrobial surface was achieved by tethering antimicrobial peptides to surfaces [62]. If such peptides were exclusively membrane-active they could not work like in solution but would be immobilized via a polymeric spacer that could potentially cross the cell wall. The latter was demonstrated by the group of Dathe, who immobilized cationic antimicrobial peptides on PentaGels [63]. Also, the well-known antimicrobial peptide magainin I



**Fig. 6** Concept of contact-killing by the surface-induced removal of a vital hydrophobic anion from the envelope of an attached microbial cell

was successfully immobilized on a polymeric spacer grafted from the surface using ATRP [64]. In contrast, the immobilization of magainin I without a polymeric spacer as a self-assembled monolayer (SAM) on gold did not prove to be sufficiently effective against various bacterial strains [65]. However, it was found in recent research that some of these peptides have more than one working mechanism. For instance, they are membrane-active and also inhibit enzymes involved in cell wall synthesis [66]. Such a peptide would be effective in an immobilized form, at least for inhibiting the enzymes.

One very intriguing way for creating a contact-active surface is to form a hydrogel on a surface using a cationic hair-pin-like antimicrobial peptide that is also a hydrogelator [67]. So far, the experiments of the Schneider group have shown that the gel is not toxic to mammalian cells and effectively kills various pathogenic Gram-positive and Gram-negative bacterial strains. However, if not released, the peptide should be more than membrane-active. The other possibilities would be that it works similarly to surface-attached cations or that it leaches to form a very small kill zone. This is also true for other directly surface-tethered antimicrobial peptides [68–71]. The approach of using hydrogelation as way to create antimicrobial surfaces has also been applied for a hydrogelling vancomycin derivative [72], and by Das and coworkers for cationic amino-acid-based antimicrobial hydrogelators [73, 74].

Besides peptides, antimicrobial enzymes can also be used to create contact-active antimicrobial surfaces. The first discovered cell lytic enzyme was the mureinase lysozyme, first described by Fleming in 1922 [75]. During the search for new antibiotics, numerous other even more effective lytic enzymes have been found. These include the endopeptidase lysostaphin [76], enzymes with mureinase and endopeptidase activity [77], lysins [78], and the fast-killing pneumococcal bacteriophage lytic enzyme (Pal) [79]. Although these enzymes have a great potential as antibiotic



alternatives, they have not been used for contact-active antimicrobial coatings so far. One reason for this might be that it seems unlikely for surface-immobilized enzymes to digest the cell wall of an attached microbe enough to kill it; this probably requires a long polymeric spacer. Only a few examples have been published that describe surface-attached lysozyme as contact-killer of *Micrococcus lysodeikticus* and *Bacillus subtilis*, and as growth-inhibitor of *S. aureus* [80–83].

In order to avoid chemical compounds at all, it is also possible to apply a high voltage to kill microbes on surfaces. It was found that a direct current kills *E. coli* cells, probably by heat or by hydrogen peroxide formation [84]. Microbial cells can be effectively killed by using pulsed electric fields (PEF), probably by frequently disturbing the cell membrane potential [85]. PEF that was found to lower microbial cell numbers in food and drinks was also shown to effectively kill *E. coli* and *Listeria innocua* cells attached to polystyrene beads [86]. This demonstrates the potential of applying this purely physical method to surfaces as well.

## 5 Biocide-Releasing Surfaces

Repelling microbes or killing them on contact are obviously the optimal ways for an antimicrobial surface to function. However, most moist and biologically contaminated areas contain large amounts of material that nonspecifically attach to a surface and deactivate it fully. Furthermore, high concentrations of microbes will eventually cover any surface with dead cells, which also deactivate the surface. In the latter case, only surfaces that release biocides will retain their activity.

### 5.1 Controlled Release

The controlled release of biocides is the oldest approach for keeping surfaces free of biofilms. The released biocides usually form an outer inhibition zone and an inner kill zone that destroys microbes in the proximity of the surface. Because dead microbial cells cannot actively adhere, they usually do not cover the releasing material at high densities. Nevertheless, all of these systems eventually exhaust and become ineffective. Furthermore, in all cases a considerable reservoir in the form of a matrix must be involved.

The oldest and still intensely used biocidal materials release silver ions. Variations in the design of such materials is still the subject of the majority of publications on antimicrobial coatings. The designs cover sparingly soluble silver salts [87], silver nanoparticles [88], silver nanocomposites [89], and elemental silver coatings [32]. The release of the silver ions and of other biocides is controlled by the encapsulating matrix, the solubility of the compound, and the material/medium equilibrium constant.

The most common way to create an antimicrobial coating is still by impregnation with biocides such as silver compounds [90], furanones [91], iodine [92], triclosan



[93], quarternary ammonium compounds [15], nitric oxide [94], hypochloride [95], and octenidine [96] that are simply released and kill microorganisms in the surroundings [97]. Antibiotics are also still used in medical applications [98]. The simultaneous release of different biocides (e.g., silver ions and lysozyme) from one coating has proven to be more efficient than that of one alone [99].

A more recent approach to the control of the release rate of a biocide is to use the layer-by-layer (LbL) technique. This method allows nearly perfect distribution of the drug in the matrix and can be used for designing the leaching characteristics of any biocide, including antimicrobial enzymes [100–103].

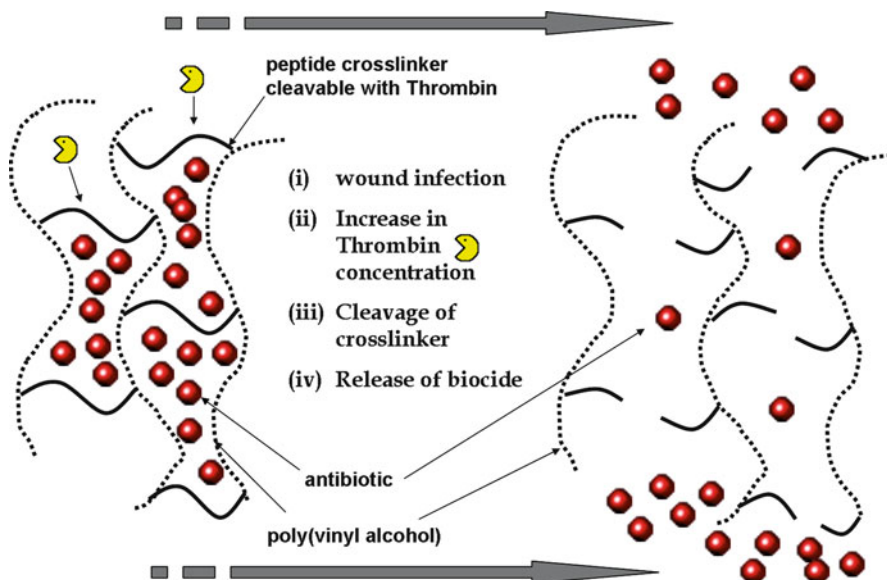
Another way to control the release of biocides is to entrap them into a matrix that is slowly hydrolyzed, e.g., into polylactic acid or other polyesters [104, 105] or degradable polyelectrolyte multilayers [106]. By choosing a matrix that is degradable by a specific enzyme, the location of release in the body can be controlled. An example of this approach, which is very common for drug release but rarely used for biocides, is fluoroquinolone-modified biodegradable polyurethane that releases the antibiotic ciprofloxacin upon degradation catalyzed by the enzyme cholesterol esterase [107].

## 5.2 Triggered Release

All release systems that liberate an immobilized biocide into the surroundings will exhaust rather quickly. Furthermore, the constant release is an environmental issue and supports the building of biocide-resistance in microbial strains. If a release system is the only possible option, then it would be desirable to release the biocide on demand, e.g., in cases of infection or the start of biofilm formation. This can be achieved by either degrading or swelling the matrix with an infection-specific enzyme or metabolite, or by cleaving the linker between biocide and surface with a biochemical factor.

One of the first examples is a polymer network that consists of polyvinylalcohol crosslinked by a thrombin-degradable peptide-linker [108] and the encapsulated antibiotic Gentamycin. In the case of a wound infection, the thrombin content increases dramatically. This enzyme degrades the co-network, and releases the Gentamycin, which then fights a possible bacterial infection (see Fig. 7). Suzuki and Tanihara have shown that the antibiotic is only released in the presence of thrombin and only then effectively kills *S. aureus* and *P. aeruginosa* cells [109, 110].

Another way to trigger the release of a biocide is to entrap the bioactive compound into a polymer network that changes its swelling characteristics with pH, temperature, or ionic strength. This could be of importance because biofilm formation causes changes in pH and ionic strength, an infected tissue becomes hotter, and biofouling is more critical in warmer water. Surprisingly, this approach is rarely followed for biocide release. In one example, Yancheva et al. prepared polyelectrolyte complexes from *N*-carboxyethylchitosan and subsequently quarternized poly[2-(dimethylamino)ethyl methacrylate]. The complex had no antimicrobial



**Fig. 7** Concept of the wound infection-induced thrombin-triggered release of Gentamycin from a surface-grafted network containing thrombin-cleavable linkers. Adapted from the idea in [109, 110]

effect in neutral medium but showed strong biocidal activity in an acidic medium that was capable of disintegrating the polyelectrolyte complexes [111]. Similar results were found for LbL-deposited antimicrobial poly(allylamine hydrochloride) and poly(sodium 4-styrene sulfonate) [112].

### 5.3 Catalytic Formation of Biocides and Their Release

A potential way to obtain a release system that does not exhaust is to continuously produce the leaching biocide by a catalyzed reaction. This approach is one of the most promising recent developments in biocide release materials. The downsides of this seemingly perfect system are that the produced biocides are highly reactive and therefore potentially toxic, and that energy must be constantly feed into the system. The needed energy is often UV or visible light, but electric current or chemical energy sources can also be used. The catalysts for the biocide formation are inorganic nanocompounds, organic photosensitizers, or even enzymes.

One of the most successful light-activated, biocidal materials is photocatalytic  $\text{TiO}_2$  [113]. The photocatalytic behavior originates from surface defects of the nano-sized  $\text{TiO}_2$  crystals [114]. Both  $\text{TiO}_2$  crystal modifications (anatase and rutile) were found to form photocatalytic material [115]. In the presence of water, oxygen and UV light, the surface of such nanocrystals constantly produces hydroxyl radicals,

superoxide radical anions, hydrogen peroxide, and other highly reactive oxygen species (ROS) by converting water and oxygen at the light-activated catalytic sites [116]. The half-life of these compounds is merely milliseconds and thus they can only diffuse distances in the submicrometer range. If the released ROS convert other molecules within this distance, they can form secondary reactive and longer-living species that greatly increase the reactive range of the released ROS. It has been shown that microbes, such as *E. coli*, attached to a reactive TiO<sub>2</sub> surface in the presence of UV light become completely degraded with time [117]. Although seemingly perfect, TiO<sub>2</sub> has three major problems that make it difficult to use the material universally:

1. It degrades every organic material with time
2. Requirement of water
3. Requirement of UV light

Thus, photocatalytic TiO<sub>2</sub> can only be used successfully in an inorganic environment (e.g., on glass, calcium carbonate, or silica) in the presence of water and UV light. The first two problems can be addressed by the design of porous, inorganic coatings containing TiO<sub>2</sub> nanoparticles. The commonly unavailable and also unwelcome presence of UV light is circumvented by doping of the TiO<sub>2</sub> with organic compounds such as 8-hydroxyquinoline, organometal complexes, platinum salts, silver ions, and other heavy metal ions [118–120]. The resulting shift in the absorbance of the photocatalytic nanocomposites renders them antimicrobial in visible light. So far, the catalytic activity of the composites in the presence of visible light is still orders of magnitude less than in the UV region. Alternative metal oxides that adsorb visible light, such as NiO/SrBi<sub>2</sub>O<sub>4</sub>, have also been found to kill pathogenic bacteria effectively [121].

Organic molecules can also be used to produce ROS in the presence of visible light. More than 100 years ago, Oscar Raab published the first example of a photodynamic effect on the antimicrobial activity of a chemical compound, acridine hydrochloride [122]. Since then, many so-called photosensitizers or light-activated agents have been found. In the presence of visible light and oxygen and/or water these agents either release radical species similar to that formed by TiO<sub>2</sub> or they react directly with oxygen to form the extremely reactive singlet oxygen (<sup>1</sup>O<sub>2</sub>), which has a high potential to oxidize the cell walls, lipid membranes, enzymes, or nucleic acids of attaching microbes [123, 124]. Modern design of such photosensitizers, the so-called XF drugs, which are based on protoporphyrins, are currently being discussed as a potent tool for fighting MRSA [2].

Numerous materials have been loaded with such organic light-activated agents [60, 125]. One of the early examples was realized by treating cellulose acetate with toluidine blue and rose bengal [126]. Various Gram-positive and Gram-negative bacteria, as well as the yeast *Candida albicans*, could be killed effectively by shining light onto the material. In another example, protoporphyrins were immobilized on nylon and the material showed excellent activity against *S. aureus* but no activity against *E. coli* in the presence of room light [127]. This was expected, because the outer cell membrane of *E. coli* will greatly delay the penetration of the released

ROS into more vital regions of the bacterial cells (note that *S. aureus* has no outer cell membrane). In recent research, it was demonstrated by Wilson that the photosensitizer methylene blue is more active on gold particles and kills even MRSA (with 2 log reductions after 10 min irradiation with green light) without degrading a polysiloxane or a polyurethane matrix and with only 10% photobleaching after 6 months [128].

The use of enzymes as catalysts for producing biocides began with oxidase enzymes (e.g., glucose oxidase), which produce the biocide hydrogen peroxide by oxidizing their substrate (e.g., glucose) with oxygen. Garcia-Garibay et al. immobilized lactase and glucose oxidase on nylon pellets and showed that these pellets effectively kill various bacteria in milk [129]. It could also be shown that a polypropylene film with immobilized glucose oxidase does not allow the growth of any *E. coli* cells on its surface and substantially inhibits the growth of *B. subtilis* [130]. The main problem of the function of oxidases is their need for a substrate as energy source. This problem was successfully addressed by Kristensen et al., who created a coating that contained starch, glucoamylase, and hexose oxidase [131]. The starch was the source for glucose, which was constantly liberated by the starch-degrading enzyme glucoamylase. The H<sub>2</sub>O<sub>2</sub> released from these coatings inhibited bacterial biofilm formation by eight out of nine marine Proteobacteria in the laboratory. Another downside of the use of oxidases is the relatively low biocidal activity of hydrogen peroxide. Even Nature transforms hydrogen peroxide into the 50-fold more active hypochloride by the enzyme myeloperoxidase in leukocytes. The group of Russell was successful in mimicking such a mechanism on a materials surface by co-immobilizing glucose oxidase and horse radish peroxidase upon co-electrospinning with polyurethane. The enzymes converted glucose and NaI in a tandem reaction to free iodine, which effectively killed *E. coli* and MRSA [132].

The use of electric current as hydrogen-peroxide-releasing antimicrobial surface has been discussed in Sect. 4 [84].

## 6 Multiple Antimicrobial Actions

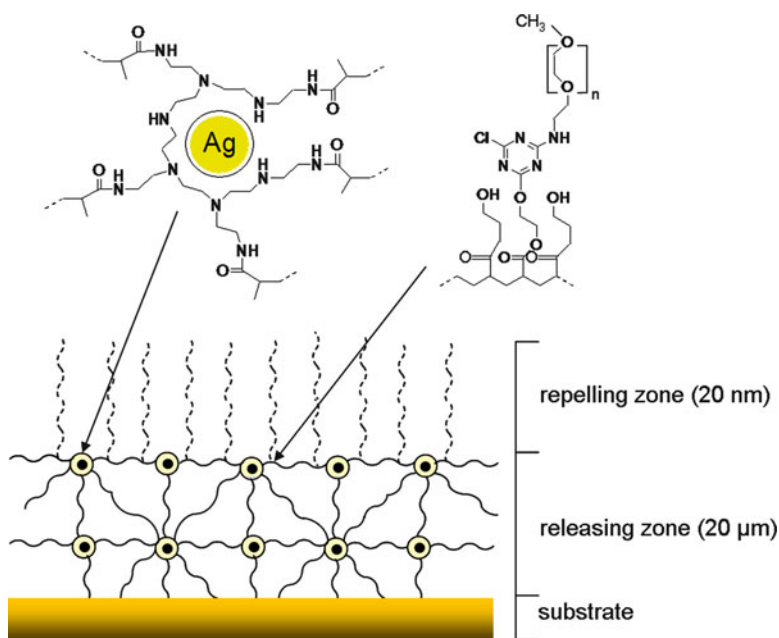
### 6.1 Releasing and Repelling

Although the release of biocides prevents microbes from active adhesion, surfaces still become clogged in heavily contaminated areas; in marine environments, higher organisms such as mussels and barnacles additionally attach to the surface.

The most successful way to prevent such clogging is to combine the release of a biocide with frequent renewal of the surface (self-polishing), which will wash away all attached microbes and other creatures dead or alive. The major problem of combined self-polishing and biocide release is the time frame, because the killing must effectively prevent strong irremovable biofilm formation until the slower self-polishing becomes effective. Modern antifouling paints on ship hulls work according to this principle. They consist of hydrophobic organo-copper esters

of PAA copolymers filled with so-called booster biocides, usually pesticides [133]. The extremely hydrophobic coating takes up water in the upper 10–100 nm, is then hydrolyzed in the swollen layers, and releases copper ions, pesticides, and water-soluble polymers. The hydrolyzed layer of the coating is removed by shear stress caused by the ship's movement and thus constantly presents a new, clean and hydrophobic surface. This highly effective coating, although only 80–90% as effective as the already banned TBT-based coatings [134], still releases large amounts of biocides and is therefore a great environmental problem. The implementation of the International Maritime Organization Treaty on biocides in 2008 requests environmentally benign but effective antifouling coatings. Although much has been done since then, including the partial exchange of the synthetic booster biocides with natural products [135], there are no competitive alternatives on the market, so far.

In applications where self-polishing is not possible, the combination of a microbe-repelling surface and a release system seems to be desirable. One example of a design for such a surface is shown in Fig. 8. The depicted coating is based on a hydrophilic polymer network that contains polyethyleneimine crosslinkers, which are capable of selectively taking up silver ions and acting as a template for silver nanoparticles [90]. This reloadable co-network was surface-modified with PEG,



**Fig. 8** Concept of simultaneous microbe repulsion and biocide release of a specifically designed network. The network is composed of poly(2-hydroxyethylacrylate) crosslinked with polyethyleneimine and surface-grafted with polyethylene glycol. The polyethyleneimine junctions take up silver ions, which then form nanoparticles due to the template character of these nanocontainers. Reproduced and adapted from [90]

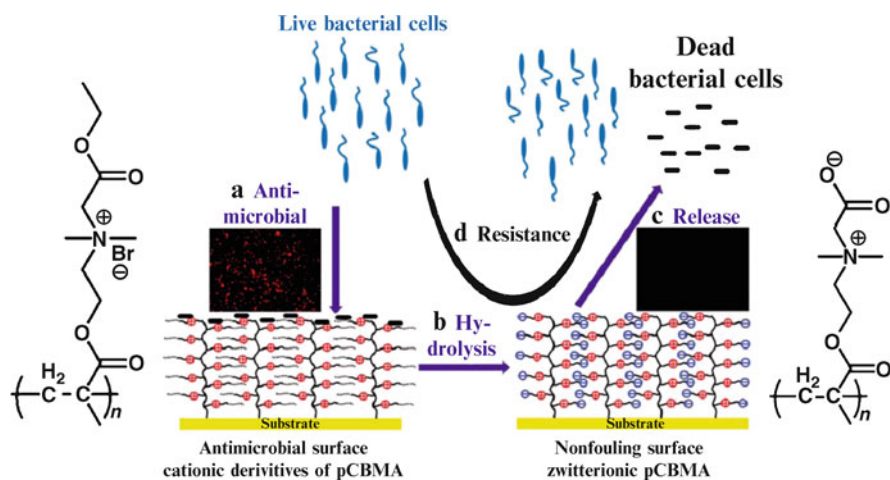
which does not hinder diffusion of the silver ions but repels microbes efficiently. It could be shown that the co-network efficiently kills *S. aureus* cells and still repels them after the exhaustion of the silver.

## 6.2 Contact-Killing and Repelling

More recently, Chen et al. described a surface modification whereby the polymer poly(*N,N*-dimethyl-*N*-(ethoxycarbonylmethyl)-*N*-[2'-(methacryloyloxy)ethyl]-ammonium bromide) was grafted from a surface via ATRP [136]. The cationic polymer effectively kills *E. coli* and is subsequently converted into a zwitterionic polymer by hydrolysis of the head group (Fig. 9). It then repels all attached cells dead or alive. This is the first example of a surface that can kill microbes on contact and repels them after that. The only downside of this elegant system is that it will eventually exhaust and turn into a more or less effective repelling surface.

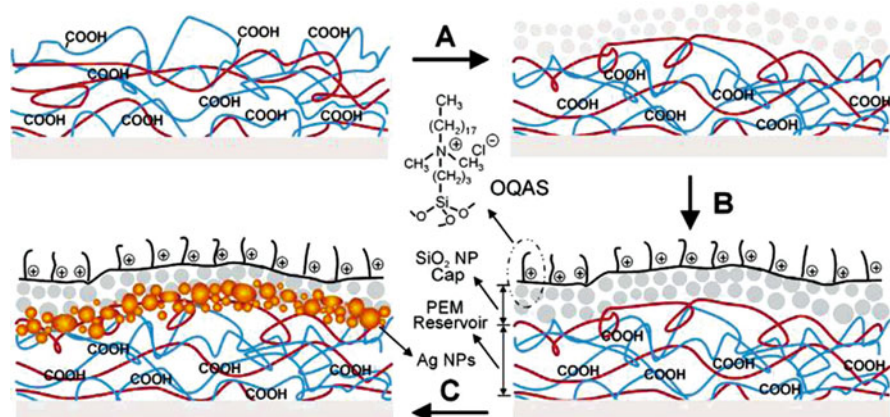
## 6.3 Releasing and Contact-Killing

A coating described by Worley and coworkers was shown to efficiently kill both on contact and by release [137]. The polyurethane-based material contains quarternary ammonium groups for contact-killing and *N*-halamine groups for releasing chlorine



**Fig. 9** Example of a contact-killing and microbe-repelling surface. (a) Antimicrobial cationic poly(*N,N*-dimethyl-*N*-(ethoxycarbonylmethyl)-*N*-[2'-(methacryloyloxy)ethyl]-ammonium bromide) (left structure) effectively kills bacteria. (b) The polymer is converted into the corresponding nonfouling zwitterionic derivative (right structure) upon hydrolysis. (c) Dead bacteria remaining on the surface are repelled from the nonfouling surface. (d) The zwitterionic surface itself is highly resistant to bacterial adhesion. Reproduced and adapted from [136]





**Fig. 10** Example of a contact-killing and microbe-releasing surface. The scheme shows the design of a two-level dual-functional antibacterial coating containing both quarternary ammonium salts and silver. The coating process begins with LbL deposition of a reservoir made of bilayers of PAH and PAA. (A) Cap region made of bilayers of PAH and SiO<sub>2</sub> nanoparticles (NP) is added to the top. (B) The SiO<sub>2</sub> nanoparticle cap is modified with a quarternary ammonium silane (QAS); PEM polyelectrolyte multilayer. (C) Ag<sup>+</sup> is loaded into the coating using the available unreacted carboxylic acid groups in the LbL multilayers. Scheme was reproduced from [138]

or hypochloride. As illustrated in Fig. 10, the incorporation of silver nanoparticles into an LbL coating and finishing it with quarternary ammonium groups resulted in the same effect [138]. This repeatedly reloadable coating described by the group of Rubner releases silver ions and kills on contact with the surface-attached quarternary ammonium groups [138].

Shamby et al. described a surface finish that consists of a water-insoluble composite of silver bromide nanoparticles and poly(4-vinylpyridinium) salts. Again, silver is released and the quarternary ammonium groups kill on contact [139]. Gyomard et al. incorporated the natural antimicrobial peptide gramicidin A into a LbL matrix and were able to show, that the peptide kills *Enterococcus faecalis* in the surroundings when released and on the surface in immobilized form [140]. It is also possible that the antimicrobial  $\alpha$ -poly-L-lysine in the LbL layer helped a little.

## 7 Conclusion

The design of antimicrobial surfaces by means of modern polymer and material science technologies, such as surface grafting by living polymerization, LbL techniques, nanotechnology, and others, allows the realization of nearly every surface design on a large scale. Modern biotechnology provides techniques that make biologically benign antifoulants available and affordable. This is particularly important because of the increasing restrictions on the use of biocides due to environmental



reasons and because of the increasing number of biocide-resistant microbial strains. Although many new solutions for antimicrobial surfaces have been presented recently, there is still no fully satisfying concept realized for any application.

Modern antifouling coatings, which must replace the existing toxin-releasing products, tend towards microbe-repelling solutions. These make use of ultrahydrophilic and ultrahydrophobic modifications as well as surface-active hydrolases that actively repel microbes and other marine organisms. An alternative is an extensive search for natural, or at least environmentally benign, biocides that can use the ubiquitous and highly successful approach of self-polishing materials.

In household applications, self-cleaning materials are popular and promising. These use surface-attached inorganic (UV-activated photocatalytic TiO<sub>2</sub> and visible-light-absorbing derivatives) or organic (protoporphyrins and diverse aromatic dyes) light-activated agents that release ROS. The latter are non-specific and kill the surrounding microbes, even antibiotic-resistant forms. Although, ROS can be toxic to mammalian cells, they are now even being considered for medical applications.

A novel approach is the development of multifunctional antimicrobial surfaces that work synergistically and are therefore very promising for the future.

Antimicrobial surfaces are still in the focus of academic and industrial research. One important issue for new developments is to find the true mechanism of existing and new antimicrobial surfaces, because only that knowledge allows useful predictions for their optimization in terms of reactivity and long-term activity.

## References

1. Lode HM (2009) Clinical impact of antibiotic-resistant Gram-positive pathogens. *Clin Microbiol Infect* 15:212–217
2. Gonzales FP, Maisch T (2010) XF drugs: a new family of antibacterials. *Drug News Perspect* 23:167–174
3. Klevens RM, Morrison MA, Nadle J et al. (2007) Invasive methicillin-resistant *Staphylococcus aureus* infections in the United States. *JAMA* 298:1763–1771
4. Zilberman M, Elsner JJ (2008) Antibiotic-eluting medical devices for various applications. *J Control Release* 130:202–215
5. Meyer B (2003) Approaches to prevention, removal and killing of biofilms. *Int Biodeterior Biodegradation* 51:249–253
6. Landini P, Antoniani D, Burgess JG et al. Molecular mechanisms of compounds affecting bacterial biofilm formation and dispersal. *Appl Microbiol Biotechnol* 86:813–823
7. Mah T-F, Pitts B, Pellock B et al. (2003) A genetic basis for *Pseudomonas aeruginosa* biofilm antibiotic resistance. *Nature* 426:306–310
8. Tiller JC (2008) Coatings for prevention or deactivation of biological contamination. In: Kohli R, Mittal KL (eds) *Developments in surface contamination and cleaning*. William Andrew, Norwich, NY, pp 1013–1065
9. Lichter JA, Van Vliet KJ, Rubner MF (2009) Design of antibacterial surfaces and interfaces: polyelectrolyte multilayers as a multifunctional platform. *Macromolecules* 42:8573–8586
10. Kenawy E-R, Worley SD, Broughton R (2007) The chemistry and applications of antimicrobial polymers: a state-of-the-art review. *Biomacromolecules* 8:1359–1384
11. Tew GN, Scott RW, Klein ML et al. (2010) De novo design of antimicrobial polymers, foldamers, and small molecules: from discovery to practical applications. *Acc Chem Res* 43:30–39

12. Tiller JC (2006) Silver-based antimicrobial coatings. *ACS Symp Ser* 924:215–231
13. Gettings RL, White WC (1987) Formation of polymeric antimicrobial surfaces from organofunctional silanes. *Polym Mater Sci Eng* 57:181–185
14. Kanazawa A, Ikeda T, Endo T (1993) Polymeric phosphonium salts as a novel class of cationic biocides. III. Immobilization of phosphonium salts by surface photografting and antibacterial activity of the surface-treated polymer films. *J Poly Sci A Poly Chem* 31: 1467–1472
15. Tiller JC, Sprich C, Hartmann L (2005) Amphiphilic conetworks as regenerative controlled releasing antimicrobial coatings. *J Control Release* 103:355–367
16. Huttinger KJ, Muller H, Bomar MT (1982) Synthesis and effect of carrier-bound disinfectants. *J Colloid Interface Sci* 88:274–285
17. Eknoian MW, Worley SD, Bickert J et al. (1998) Novel antimicrobial *N*-halamine polymer coatings generated by emulsion polymerization. *Polymer* 40:1367–1371
18. Fallgren C, Utt M, Petersson AC et al. (1998) In vitro anti-staphylococcal activity of heparinized biomaterials bonded with combinations of rifampicin. *Zentralbl Bakteriol* 287:19–31
19. Brash JL, Uniyal S (1979) Dependence of albumin-fibrinogen simple and competitive adsorption on surface-properties of biomaterials. *J Poly Sci C Poly Symp* (66):377–389
20. An YH, Friedman RJ (1998) Concise review of mechanisms of bacterial adhesion to biomaterial surfaces. *J Biomed Mater Res* 43:338–348
21. Hermansson M (1999) The DLVO theory in microbial adhesion. *Colloids Surf B Biointerfaces* 14:105–119
22. Humphries M, Nemcek J, Cantwell JB et al. (1987) The use of graft-copolymers to inhibit the adhesion of bacteria to solid-surfaces. *FEMS Microbiol Ecol* 45:297–304
23. Jansen B, Kohnen W (1995) Prevention of biofilm formation by polymer modification. *J Ind Microbiol* 15:391–396
24. Park KD, Kim YS, Han DK et al. (1998) Bacterial adhesion on PEG modified polyurethane surfaces. *Biomaterials* 19:851–859
25. Tiller JC, Bonner G, Pan L-C et al. (2001) Improving biomaterial properties of collagen films by chemical modification. *Biotechnol Bioeng* 73:246–252
26. Lewis AL (2000) Phosphorylcholine-based polymers and their use in the prevention of biofouling. *Colloids Surf B Biointerfaces* 18:261–275
27. Jiang SY, Cao ZQ (2010) Ultralow-fouling, functionalizable, and hydrolyzable zwitterionic materials and their derivatives for biological applications. *Adv Mater* 22:920–932
28. Cheng G, Zhang Z, Chen SF et al. (2007) Inhibition of bacterial adhesion and biofilm formation on zwitterionic surfaces. *Biomaterials* 28:4192–4199
29. Ista LK, Perez-Luna VH, Lopez GP (1999) Surface-grafted, environmentally sensitive polymers for biofilm release. *Appl Environ Microbiol* 65:1603–1609
30. Pratt-Terpstra IH, Weerkamp AH, Busscher HJ (1987) Adhesion of oral Streptococci from a flowing suspension to uncoated and albumin-coated surfaces. *J Gen Microbiol* 133: 3199–3206
31. Lichter JA, Thompson MT, Delgadillo M et al. (2008) Substrata mechanical stiffness can regulate adhesion of viable bacteria. *Biomacromolecules* 9:1571–1578
32. Dowling DP, Donnelly K, McConnell ML et al. (2001) Deposition of anti-bacterial silver coatings on polymeric substrates. *Thin Solid Films* 398–399:602–606
33. Charville GW, Hetrick EM, Geer CB et al. (2008) Reduced bacterial adhesion to fibrinogen-coated substrates via nitric oxide release. *Biomaterials* 29:4039–4044
34. Kristensen JB, Meyer RL, Laursen BS et al. (2008) Antifouling enzymes and the biochemistry of marine settlement. *Biotechnol Adv* 26:471–481
35. Leroy C, Delbarre-Ladrat C, Ghillebaert F et al. (2008) Effects of commercial enzymes on the adhesion of a marine biofilm-forming bacterium. *Biofouling* 24:11–22
36. Tasso M, Pettitt ME, Cordeiro AL et al. (2009) Antifouling potential of Subtilisin A immobilized onto maleic anhydride copolymer thin films. *Biofouling* 25:505–516
37. Kim J, Delio R, Dordick JS (2002) Protease-containing silicates as active antifouling materials. *Biotechnol Prog* 18:551–555

38. Aldred N, Phang IY, Conlan SL et al. (2008) The effects of a serine protease, Alcalase (R), on the adhesives of barnacle cyprids (*Balanus amphitrite*). *Biofouling* 24:97–107
39. Isquith AJ, Abbott EA, Walters PA (1972) Surface-bonded antimicrobial activity of an organosilicon quaternary ammonium chloride. *Appl Microbiol* 24:859–863
40. Tiller JC, Liao C-J, Lewis K et al. (2001) Designing surfaces that kill bacteria on contact. *Proc Natl Acad Sci USA* 98:5981–5985
41. Tiller JC, Lee SB, Lewis K et al. (2002) Polymer surfaces derivatized with poly(vinyl-*N*-hexylpyridinium) kill airborne and waterborne bacteria. *Biotechnol Bioeng* 79:465–471
42. Lin J, Tiller JC, Lee SB et al. (2002) Insights into bactericidal action of surface-attached poly(vinyl-*N*-hexylpyridinium) chains. *Biotechnol Lett* 24:801–805
43. Lin J, Qiu SY, Lewis K et al. (2002) Bactericidal properties of flat surfaces and nanoparticles derivatized with alkylated polyethylenimines. *Biotechnol Prog* 18:1082–1086
44. Haldar J, An DQ, de Cienfuegos LA et al. (2006) Polymeric coatings that inactivate both influenza virus and pathogenic bacteria. *Proc Natl Acad Sci USA* 103:17667–17671
45. Milovic NM, Wang J, Lewis K et al. (2005) Immobilized *N*-alkylated polyethylenimine avidly kills bacteria by rupturing cell membranes with no resistance developed. *Biotechnol Bioeng* 90:715–722
46. Lee SB, Koepsel RR, Morley SW et al. (2004) Permanent, nonleaching antibacterial surfaces. I. Synthesis by atom transfer radical polymerization. *Biomacromolecules* 5:877–882
47. Kurt P, Wood L, Ohman DE et al. (2007) Highly effective contact antimicrobial surfaces via polymer surface modifiers. *Langmuir* 23:4719–4723
48. Waschinski CJ, Zimmermann J, Salz U et al. (2008) Design of contact-active antimicrobial acrylate-based materials using biocidal macromers. *Adv Mater* 20:104–108
49. Waschinski CJ, Barnert S, Theobald A et al. (2008) Insights in the antibacterial action of poly(methyloxazoline)s with a biocidal end group and varying satellite groups. *Biomacromolecules* 9:1764–1771
50. Waschinski CJ, Herdes V, Schueler F et al. (2005) Influence of satellite groups on telechelic antimicrobial functions of polyoxazolines. *Macromol Biosci* 5:149–156
51. Waschinski CJ, Tiller JC (2005) Poly(oxazoline)s with telechelic antimicrobial functions. *Biomacromolecules* 6:235–243
52. Kang S, Pinault M, Pfefferle LD et al. (2007) Single-walled carbon nanotubes exhibit strong antimicrobial activity. *Langmuir* 23:8670–8673
53. Gottenbos B, van der Mei HC, Klatter F et al. (2002) In vitro and in vivo antimicrobial activity of covalently coupled quaternary ammonium silane coatings on silicone rubber. *Biomaterials* 23:1417–1423
54. Madkour AE, Dabkowski JM, Nusslein K et al. (2009) Fast disinfecting antimicrobial surfaces. *Langmuir* 25:1060–1067
55. Bouloussa O, Rondelez F, Semetey V (2008) A new, simple approach to confer permanent antimicrobial properties to hydroxylated surfaces by surface functionalization. *Chem Commun*:951–953
56. Kugler R, Bouloussa O, Rondelez F (2005) Evidence of a charge-density threshold for optimum efficiency of biocidal cationic surfaces. *Microbiology* 151:1341–1348
57. Tiller JC, Liao CJ, Lewis K et al. (2001) Designing surfaces that kill bacteria on contact. *Proc Natl Acad Sci USA* 98:5981–5985
58. Murata H, Koepsel RR, Matyjaszewski K et al. (2007) Permanent, non-leaching antibacterial surfaces - 2: How high density cationic surfaces kill bacterial cells. *Biomaterials* 28:4870–4879
59. Huang JY, Koepsel RR, Murata H et al. (2008) Nonleaching antibacterial glass surfaces via “Grafting Onto”: the effect of the number of quaternary ammonium groups on biocidal activity. *Langmuir* 24:6785–6795
60. Page K, Wilson M, Parkin IP (2009) Antimicrobial surfaces and their potential in reducing the role of the inanimate environment in the incidence of hospital-acquired infections. *J Mater Chem* 19:3819–3831
61. Bieser A (2008) Surface modifications by hydrogelation and by coating with antimicrobial cellulose derivatives Dissertation, University of Freiburg

62. Hancock REW, Chapple DS (1999) Peptide antibiotics. *Antimicrob Agents Chemother* 43:1317–1323
63. Bagheri M, Beyermann M, Dathe M (2009) Immobilization reduces the activity of surface-bound cationic antimicrobial peptides with no influence upon the activity spectrum. *Antimicrob Agents Chemother* 53:1132–1141
64. Glinel K, Jonas AM, Jouenne T et al. (2009) Antibacterial and antifouling polymer brushes incorporating antimicrobial peptide. *Bioconjug Chem* 20:71–77
65. Humblot V, Yala JF, Thebault P et al. (2009) The antibacterial activity of Magainin I immobilized onto mixed thiols self-assembled monolayers. *Biomaterials* 30:3503–3512
66. Brogden KA (2005) Antimicrobial peptides: pore formers or metabolic inhibitors in bacteria? *Nat Rev Microbiol* 3:238–250
67. Salick DA, Kretsinger JK, Pochan DJ et al. (2007) Inherent antibacterial activity of a peptide-based beta-hairpin hydrogel. *J Am Chem Soc* 129:14793–14799
68. Chen R, Cole N, Willcox Mark DP et al. (2009) Synthesis, characterization and in vitro activity of a surface-attached antimicrobial cationic peptide. *Biofouling* 25:517–524
69. Hilpert K, Elliott M, Jenssen H et al. (2009) Screening and characterization of surface-tethered cationic peptides for antimicrobial activity. *Chem Biol* 16:58–69
70. Statz Andrea R, Park Jong P, Chongsiriwatana Nathaniel P et al. (2008) Surface-immobilised antimicrobial peptides. *Biofouling* 24:439–448
71. Willcox MDP, Hume EBH, Aliwarga Y et al. (2008) A novel cationic-peptide coating for the prevention of microbial colonization on contact lenses. *J Appl Microbiol* 105:1817–1825
72. Xing BG, Yu CW, Chow KH et al. (2002) Hydrophobic interaction and hydrogen bonding cooperatively confer a vancomycin hydrogel: a potential candidate for biomaterials. *J Am Chem Soc* 124:14846–14847
73. Roy S, Das PK (2008) Antibacterial hydrogels of amino acid-based cationic amphiphiles. *Biotechnol Bioeng* 100:756–764
74. Debnath S, Shome A, Das D et al. Hydrogelation through self-assembly of Fmoc-peptide functionalized cationic amphiphiles: potent antibacterial agent. *J Phys Chem B* 114:4407–4415
75. Fleming A (1922) Containing papers of a biological character. *Proc R Soc Lond B* 93:306–317
76. Schindler CA, Schuhardt VT (1964) Lysostaphin – new bacteriolytic agent for *Staphylococcus*. *Proc Natl Acad Sci USA* 51:414–421
77. Navarre WW, Ton-That H, Faull KF et al. (1999) Multiple enzymatic activities of the murein hydrolase from staphylococcal phage phi 11 – identification of a D-alanyl-glycine endopeptidase activity. *J Biol Chem* 274:15847–15856
78. Schuch R, Nelson D, Fischetti VA (2002) A bacteriolytic agent that detects and kills *Bacillus anthracis*. *Nature* 418:884–889
79. Loeffler JM, Nelson D, Fischetti VA (2001) Rapid killing of *Streptococcus pneumoniae* with a bacteriophage cell wall hydrolase. *Science* 294:2170–2172
80. Edwards JV, Sethumadhavan K, Ullah AHJ (2000) Conjugation and modeled structure/function analysis of lysozyme on glycine esterified cotton cellulose-fibers. *Bioconjug Chem* 11:469–473
81. Luckarift HR, Dickerson MB, Sandhage KH et al. (2006) Rapid, room-temperature synthesis of antibacterial bionanocomposites of lysozyme with amorphous silica or titania. *Small* 2:640–643
82. Wang Q, Fan XR, Hu YJ et al. (2009) Antibacterial functionalization of wool fabric via immobilizing lysozymes. *Bioprocess Biosyst Eng* 32:633–639
83. Watanabe S, Kato H, Shimizu Y et al. (1981) Antibacterial biomaterials by immobilization of hen egg-white lysozyme onto collagen-synthetic polymer composites – histological-findings of immobilized lysozyme in the tissue of a different species. *Artif Organs* 5:309–309
84. Liu WK, Brown MRW, Elliott TSJ (1997) Mechanisms of the bactericidal activity of low amperage electric current (DC). *J Antimicrob Chemother* 39:687–695
85. Grahl T, Maerkl H (1996) Killing of microorganisms by pulsed electric fields. *Appl Microbiol Biotechnol* 45:148–157

86. Dutreux N, Notermans S, Wijtzes T et al. (2000) Pulsed electric fields inactivation of attached and free-living *Escherichia coli* and *Listeria innocua* under several conditions. *Int J Food Microbiol* 54:91–98
87. Conner CJ, Harper RJ Jr. (1979) Biocidal rating system for outdoor weathered cotton fabric. *Textile Chemist Colorist* 11:62–65
88. Aymonier C, Schlotterbeck U, Antonietti L et al. (2002) Hybrids of silver nanoparticles with amphiphilic hyperbranched macromolecules exhibiting antimicrobial properties. *Chem Commun*:3018–3019
89. Brunt KD (1995) A silver lining for paints and coatings - a revolutionary preservative system. *Spec Publ R Soc Chem* 165:243–251
90. Ho CH, Tobis J, Sprich C et al. (2004) Nanoseparated polymeric networks with multiple antimicrobial properties. *Adv Mater* 16:957–961
91. de Nys R, Givskov M, Kumar N et al. (2006) Furanones. *Prog Mol Subcell Biol* 42:55–86
92. Kristinsson KG, Jansen B, Treitz U et al. (1991) Antimicrobial activity of polymers coated with iodine-complexed polyvinylpyrrolidone. *J Biomater Appl* 5:173–184
93. Kugel AJ, Jarabek LE, Daniels JW et al. (2009) Combinatorial materials research applied to the development of new surface coatings XII: novel, environmentally friendly antimicrobial coatings derived from biocide-functional acrylic polyols and isocyanates. *J Coat Technol Res* 6:107–121
94. Nablo BJ, Schoenfisch MH (2003) Antibacterial properties of nitric oxide-releasing sol-gels. *J Biomed Mater Res A* 67A:1276–1283
95. Li Y, Worley SD (2001) Biocidal copolymers of *N*-haloacryloxymethylhydantoin. *J Bioact Compat Polym* 16:493–506
96. Matl FD, Zlotnyk J, Obermeier A et al. (2009) New anti-infective coatings of surgical sutures based on a combination of antiseptics and fatty acids. *J Biomater Sci Polym Ed* 20:1439–1449
97. Hetrick EM, Schoenfisch MH (2006) Reducing implant-related infections: active release strategies. *Chem Soc Rev* 35:780–789
98. Norowski PA Jr, Bumgardner Joel D (2009) Biomaterial and antibiotic strategies for peri-implantitis: a review. *J Biomed Mater Res B Appl Biomater* 88:530–543
99. Eby DM, Luckarift HR, Johnson GR (2009) Hybrid antimicrobial enzyme and silver nanoparticle coatings for medical instruments. *ACS Appl Mater Interfaces* 1:1553–1560
100. Rudra JS, Dave K, Haynie DT (2006) Antimicrobial polypeptide multilayer nanocoatings. *J Biomater Sci Polym Ed* 17:1301–1315
101. Chuang HF, Smith RC, Hammond PT (2008) Polyelectrolyte multilayers for tunable release of antibiotics. *Biomacromolecules* 9:1660–1668
102. Dai JH, Bruening ML (2002) Catalytic nanoparticles formed by reduction of metal ions in multilayered polyelectrolyte films. *Nano Lett* 2:497–501
103. Lichter JA, Van Vliet KJ, Rubner MF (2009) Design of antibacterial surfaces and interfaces: polyelectrolyte multilayers as a multifunctional platform. *Macromolecules* 42:8573–8586
104. Gollwitzer H, Ibrahim K, Meyer H et al. (2003) Antibacterial poly(D,L-lactic acid) coating of medical implants using a biodegradable drug delivery technology. *J Antimicrob Chemother* 51:585–591
105. Tamilvanan S, Venkateshan N, Ludwig A (2008) The potential of lipid- and polymer-based drug delivery carriers for eradicating biofilm consortia on device-related nosocomial infections. *J Control Release* 128:2–22
106. Shukla A, Fleming Kathleen E, Chuang Helen F et al. (2010) Controlling the release of peptide antimicrobial agents from surfaces. *Biomaterials* 31:2348–2357
107. Woo GLY, Yang ML, Yin HQ et al. (2002) Biological characterization of a novel biodegradable antimicrobial polymer synthesized with fluoroquinolones. *J Biomed Mater Res* 59:35–45
108. Tanihara M, Suzuki Y, Nishimura Y et al. (1998) Thrombin-sensitive peptide linkers for biological signal-responsive drug release systems. *Peptides* 19:421–425
109. Suzuki Y, Tanihara M, Nishimura Y et al. (1998) A new drug delivery system with controlled release of antibiotic only in the presence of infection. *J Biomed Mater Res* 42:112–116
110. Tanihara M, Suzuki Y, Nishimura Y et al. (1999) A novel microbial infection-responsive drug release system. *J Pharm Sci* 88:510–514

111. Yancheva E, Paneva D, Maximova V et al. (2007) Polyelectrolyte complexes between (cross-linked) *N*-carboxyethylchitosan and (quaternized) poly[2-(dimethylamino)ethyl methacrylate]: preparation, characterization, and antibacterial properties. *Biomacromolecules* 8:976–984
112. Lichter JA, Rubner MF (2009) Polyelectrolyte multilayers with intrinsic antimicrobial functionality: the importance of mobile polycations. *Langmuir* 25:7686–7694
113. Fujishima A, Zhang XT, Tryk DA (2008) TiO<sub>2</sub> photocatalysis and related surface phenomena. *Surf Sci Rep* 63:515–582
114. Zeiger HJ, Henrich VE, Dresselhaus G (1977) Interaction of O<sub>2</sub> and H<sub>2</sub>O with surface defects on TiO<sub>2</sub> and SrTiO<sub>3</sub>. *Bull Am Phys Soc* 22:419–419
115. Watanabe T, Nakajima A, Wang R et al. (1999) Photocatalytic activity and photoinduced hydrophilicity of titanium dioxide coated glass. *Thin Solid Films* 351:260–263
116. Jaeger CD, Bard AJ (1979) Spin trapping and electron-spin resonance detection of radical intermediates in the photo-decomposition of water at TiO<sub>2</sub> particulate systems. *J Phys Chem* 83:3146–3152
117. Nadochenko V, Denisov N, Sarkisov O et al. (2006) Laser kinetic spectroscopy of the interfacial charge transfer between membrane cell walls of *E. coli* and TiO<sub>2</sub>. *J Photochem Photobiol A Chem* 181:401–407
118. Dung DH, Serpone N, Gratzel M (1984) Integrated systems for water cleavage by visible-light – sensitization of TiO<sub>2</sub> particles by surface derivatization with ruthenium complexes. *Helv Chim Acta* 67:1012–1018
119. Houlding VH, Gratzel M (1983) Photochemical H<sub>2</sub> generation by visible-light – sensitization of TiO<sub>2</sub> particles by surface complexation with 8-hydroxyquinoline. *J Am Chem Soc* 105:5695–5696
120. Sung-Suh HM, Choi JR, Hah HJ et al. (2004) Comparison of Ag deposition effects on the photocatalytic activity of nanoparticulate TiO<sub>2</sub> under visible and UV light irradiation. *J Photochem Photobiol A Chem* 163:37–44
121. Hu C, Hu XX, Guo J et al. (2006) Efficient destruction of pathogenic bacteria with NiO/SrBi<sub>2</sub>O<sub>4</sub> under visible light irradiation. *Environ Sci Technol* 40:5508–5513
122. Raab O (1900) Effect of fluorescent substances on Infusoria. *Z Biol* 39:524
123. Foote CS (1991) Definition of type-I and type-II photosensitized oxidation. *Photochem Photobiol* 54:659–659
124. Halliwell B, Gutteridge JMC (1984) Lipid-peroxidation, oxygen radicals, cell-damage, and antioxidant therapy. *Lancet* 1:1396–1397
125. Noimark S, Dunnill CW, Wilson M et al. (2009) The role of surfaces in catheter-associated infections. *Chem Soc Rev* 38:3435–3448
126. Wilson M (2003) Light-activated antimicrobial coating for the continuous disinfection of surfaces. *Infect Control Hosp Epidemiol* 24:782–784
127. Bozja J, Sherrill J, Michielsen S et al. (2003) Porphyrin-based, light-activated antimicrobial materials. *J Polym Sci A Polym Chem* 41:2297–2303
128. Perni S, Piccirillo C, Pratten J et al. (2009) The antimicrobial properties of light-activated polymers containing methylene blue and gold nanoparticles. *Biomaterials* 30:89–93
129. Garcia-Garibay M, Luna-Salazar A, Casas LT (1995) Antimicrobial effect of the lactoperoxidase system in milk activated by immobilized enzymes. *Food Biotechnol* 9:157–166
130. Vartiainen J, Ratto M, Paulussen S (2005) Antimicrobial activity of glucose oxidase-immobilized plasma-activated polypropylene films. *Packag Technol Sci* 18:243–251
131. Kristensen JB, Olsen SM, Laursen BS et al. (2010) Enzymatic generation of hydrogen peroxide shows promising antifouling effect. *Biofouling* 26:141–153
132. Amitai G, Andersen J, Wargo S et al. (2009) Polyurethane-based leukocyte-inspired biocidal materials. *Biomaterials* 30:6522–6529
133. Kuo PL, Chuang TF, Wang HL (1999) Surface-fragmenting, self-polishing, tin-free antifouling coatings. *J Coat Technol* 71:77–83
134. Ibbitson D, Johnson AF, Morley NJ et al. (1986) Structure property relationships in TIN-based antifouling paints. *ACS Symp Ser* 322:326–340

135. Qian PY, Xu Y, Fusetani N (2010) Natural products as antifouling compounds: recent progress and future perspectives. *Biofouling* 26:223–234
136. Cheng G, Xue H, Zhang Z et al. (2008) A switchable biocompatible polymer surface with self-sterilizing and nonfouling capabilities. *Angew Chem Int Ed* 47:8831–8834
137. Liang J, Chen Y, Barnes K et al. (2006) *N*-halamine/quat siloxane copolymers for use in biocidal coatings. *Biomaterials* 27:2495–2501
138. Li Z, Lee D, Sheng XX et al. (2006) Two-level antibacterial coating with both release-killing and contact-killing capabilities. *Langmuir* 22:9820–9823
139. Sambhy V, MacBride MM, Peterson BR et al. (2006) Silver bromide nanoparticle/polymer composites: dual action tunable antimicrobial materials. *J Am Chem Soc* 128:9798–9808
140. Guyomard A, De E, Jouenne T et al. (2008) Incorporation of a hydrophobic antibacterial peptide into amphiphilic polyelectrolyte multilayers: a bioinspired approach to prepare biocidal thin coatings. *Adv Funct Mater* 18:758–765



# Index

## A

Actin 82, 118  
Albumin/heparin 153  
Alginate/chitosan films 142  
Alkanethiolates, gold 105  
Antibacterial surfaces 193, 153, 208  
Antifouling surfaces 1, 19, 199, 206  
Antimicrobial surfaces 193, 195  
Asialotransferrin 25  
Atom transfer radical polymerization (ATRP)  
3, 12, 115, 200, 209  
Azo dyes 7

## B

*Bacillus subtilis* 202  
Bacteria 193  
Bacteriorhodopsin 8  
Barnacles 207  
Basic fibroblast growth factor (bFGF) 185  
Benzoxadiazole 7  
Bioactive molecules 135, 163  
Bioactive surfaces 1, 35  
Bioassays 26  
Biocide-releasing surfaces 203  
Biocides 193  
Biocompatible polymers 1  
Biofunctionalisation 79  
Biological interface 103  
Biomaterials 163  
Biomimetics 163  
Bioresponsive polymers 8  
Bioseparation 1, 24  
Biotin/streptavidin 22  
Block copolymers, adsorption 16  
Bone morphogenetic proteins (BMPs) 179  
Booster biocides 208  
BSA 48, 65, 115, 124, 147

## C

CaCO<sub>3</sub> core 146  
Cadherins 38  
Capsules 137  
*N*-Carboxyethylchitosan 204  
Carboxy-methyl-dextran (CMD) 61  
Cell adhesion 35, 79, 103  
control 22  
guided 39, 46  
Cell adhesion molecules (CAMs) 38  
Cell chip 35  
Cell culture 82  
Cell engineering 1  
Cell migration 95, 103, 126  
Cell polarization 95, 119, 126  
Cell surface receptors 90  
Cell-membrane-ECM interface 38  
Cellular infiltration 163  
Cetyltrimethylammonium chloride 197  
Chemoresponsive polymers 8  
Chitosan/hyaluronic acid (CHI/HA) 138  
Chlorine 209  
Chondrocytes 167, 179, 187  
Chymotrypsin 147, 199  
Collagen 39, 47, 59, 165, 172, 175, 198  
Computational topology design  
(CTD) 177  
Concanavalin A 20  
Contact activation 193  
Contact killing 209  
membrane-active biocides 200  
Critical micellar concentration  
(CMC) 88  
Cucurbit[6]uril 5  
[2+2]Cycloaddition 5  
Cyclodextrin 7  
Cytochrome c 7  
Cytokines 85

**D**

Delivery, light-triggered, intracellular 150  
 Diblock copolymer micellar nanolithography (dBCML) 88  
 2-(Diethylamino)ethyl methacrylate (DEA) 16  
 1,2-Dipalmitoyl-*sn*-glycero-3-phosphocholine (DPPC) 139  
 Dip-pen nanolithography (DPN) 106, 126, 166  
 DLVO theory 198  
 DMAEMA 19  
 DNA, LbL films 138  
 DNA aptamer 111  
 DNA/spermidine capsules 148  
 DNA-chips 36  
 DOW suspension test 196, 199  
 Doxorubicin 17  
 Drug delivery 5, 17  
 Dynamic substrates 103  
 Dynamic surfaces 116, 120

**E**

Elastin-like polypeptides (ELP) 3  
 Electron-beam lithography (EBL) 51, 87  
 Electrospinning (ES) 163, 180  
*Enterococcus faecalis* 210  
 Enzymes, antimicrobial 204  
 Epidermal growth factor (EGF) 85  
 Extracellular matrix (ECM) 38, 79, 80, 163, 165

**F**

Fibronectin (FN) 48, 165  
 FITC-labeled bovine serum albumin (FITC-BSA) 21  
 Fluorescence microscopy 120  
 Fluorescence resonance energy transfer (FRET) 7  
 Focal adhesions (FAs) 81  
 Furanones 203

**G**

Gentamycin 204  
 Glucoamylase 207  
 Glucose oxidase 12, 207  
   photoswitchable 114  
 Glucose sensing 9  
 Gold nanoparticles 87  
 Gold nanopatterns 79  
   biofunctionalised 90  
 Gold thin film, SAM 83  
 Grafting from/to 13, 44

Gramicidin A 210  
 Growth factor receptor (GFR) 82

**H**

HA/PLL film 144  
 Haptotaxis 95, 126  
 Heparin 170  
 Heparin sulfate (HS) 179  
 Horse radish peroxidase 207  
 Human serum albumin 21  
 Hydrogels 35, 163  
   surface-bounded 17  
 2-Hydroxymethylmethacrylate 5  
 Hypochloride 204

**I**

Immobilization 103, 106  
 Immunoglobulins 38  
 Insulin 85  
 Integrins 38, 60, 79, 80, 117, 169, 170  
   adhesion ligands 58  
   nanoclustering 91  
   receptor 59, 127  
 Interpolyelectrolyte interactions 139  
 Iodine 203

**L**

Lactase 207  
 Laminin 39, 48, 53, 68, 118, 127, 165, 175, 185  
 Layer-by-layer (LbL) films 135, 177, 204  
   cellular response 152  
 Leukemia inhibitory factor (LIF) 85  
 Light-activation 193  
 Light-responsive hydrogels 17  
 Light-triggered delivery, intracellular 150  
 Lipid-polyelectrolyte interactions 139  
 Liposomes 137  
*Listeria innocua* 202  
 Lysins 202  
 Lysostaphin 202  
 Lysozyme 147  
   adsorption 5

**M**

Magainin I 201  
 Matrix metalloproteinases 169  
 MEO<sub>2</sub>MA 3  
 Mesoporous silica nanoparticles (MNPs),  
   pH-responsive 5

- Micellar nanolithography 88  
Microbe repulsion, biocide release 208  
Microbe-repelling surfaces 198  
Microcapsules 135, 145  
*Micrococcus lysodeikticus* 202  
Microcontact printing ( $\mu$ CP) 85, 106, 108, 124  
Microengineering 35  
Microfluidic lithography ( $\mu$ FL) 109, 128  
Microfluidic patterning ( $\mu$ FP) 55  
Micropatterning 35, 50, 85  
Microtubule-organizing center (MTOC) 119, 126, 128  
Molecular surface gradients 126  
Molecularly imprinted polymers (MIPs) 7  
MRSA (methicillin-resistant *Staphylococcus aureus*) 194  
Multilayered films 135  
Mureinase 202  
Mussels 207  
Myeloperoxidase 207
- N**  
Nanofibers 163  
Nanogold 86  
Nanometer texture 166  
Nanopatterning biocues 90  
*Navicula perminuta* 199  
Nerve cells 181  
NIPAM 12  
Nitric oxide 204  
Nitroxide-mediated polymerization (NMP) 14  
Nucleotides 13
- O**  
Octenidine 204  
Oligo(ethylene glycol) methacrylate (OEGMA) 3  
Oligo(ethylene glycol)-alkanethiols 106  
Osteoblasts 167
- P**  
P(MEO<sub>2</sub>MA-*co*-OEGMA) 18  
P(OEGMA-*co*-MEO<sub>2</sub>MA) 25  
Patterning, proteins 48  
Peptide fibers 173  
Peptide self-assembly 174  
Peptide-decorated surfaces 56  
Peptides 35  
pH control 110  
Photocatalysis 193  
Photochemical control 113  
Photodeprotection 124  
Photolithography 50, 85, 93, 106  
Photoresponsive polymer surfaces 5  
Photoswitching 9  
pH-responsive polymers 4  
Pneumococcal bacteriophage lytic enzyme (Pal) 202  
Poly(acrylic acid) (PAA) 198  
Poly(allylamine hydrochloride), antimicrobial 205  
Poly(allylammonium hydrochloride) (PAH) 198  
Poly[*N,N*-bis(hydroxyethyl)acrylamide] 18  
Poly(dimethylacrylamide) (PDMAA) 43  
Poly(*N,N*-dimethylaminoethyl methacrylate) (PDMAEMA) 4, 204  
Poly(dimethylallylammonium chloride) (PDAD) 138  
Poly(*N,N*-dimethyl-*N*-(ethoxycarbonylmethyl)-*N*-[2'-(methacryloyloxy)ethyl]-ammonium bromide) 209  
Poly(dimethylsiloxane) (PDMS) 48, 108, 182  
Poly(ethylene glycol) (PEG) 84  
Poly(ethylene oxide) (PEO) 170  
Poly(ethyleneimine) 200  
Poly(*N*-ethyl-4-vinylpyridinium bromide) 139  
Poly(L-glutamic acid) (PGA) 138  
Poly(2-hydroxyethyl methacrylate) 11  
Poly(*N*-2-hydroxypropylmethacrylamide) 18  
Poly(*N*-isopropylacrylamide) (PNIPAM) 3, 7, 17, 98, 115  
Poly(lactic-*co*-glycolic acid) (PLGA) 170  
Poly(L-lysine) (PLL) 138  
Poly(methacrylic acid) (PMAA) 4  
Poly(2-methacryloyl phosphorylcholine) (MPC) 16  
Poly(methyl methacrylate) (PMMA) 16  
Poly(MMA-*co*-MAA) 4  
Poly(NIPAM-*co*-MAA) 5  
Poly(OEGMA) 19  
Poly(sodium 4-styrene sulfonate), antimicrobial 205  
Poly(styrene sulfonate)/poly(allylamine hydrochloride) (PSS/PAH) 136  
Poly(*tert*-butylstyrene)-*block*-sodium poly(styrenesulfonate) 16  
Poly[*N*-[tris(hydroxymethyl)-methyl]acrylamide] 18  
Poly(4-vinyl-*N*-hexylpyridinium bromide) 199  
Poly(2-vinylpyridine) 21  
Poly(4-vinylpyridine) 201  
Poly(4-vinylpyridinium) 210  
Polyelectrolyte LbL membrane 149

- Polyelectrolyte self-assembly 135  
 Polyethylene glycol (PEG) 198  
 Polyethyleneimine (PEI) 138  
 Poly-L-lysine (PLL) 53  
 Polymer brushes 35, 44  
 Polymer scaffolds 163  
 Polymer-modified surfaces 1  
 Polymerase chain reaction (PCR) 98  
 Polynucleotide-sensitive copolymers 13  
 Polypeptide (PLL) coating 139  
 Polystyrene-*block*-poly(methyl methacrylate) (PS-*b*-PMMA) 16  
 Polystyrene-*block*-poly(2-vinylpyridine) (PS-*b*-P2VP) 89  
 Polyurethane, fluoroquinolone-modified biodegradable 204  
 Polyvinylalcohol 204  
 Porosity 167  
 Protein adhesion 20  
 Protein adsorption/immobilisation 28, 35, 83  
 Protein-resistant surface coatings 43  
 Proteoglycans (PG) 127  
 Proteolytic cleavage 168  
 Protoporphyrins 206  
 PS-*b*-PMEO<sub>3</sub>MA 17  
*Pseudomonas aeruginosa* 198  
     biofilm 194
- Q**
- Quarternary ammonium compounds 204
- R**
- Release 141, 148, 193, 195  
     remote 135  
     triggered 204  
 RGD 39, 81, 91, 170  
 RhoA 120  
*Ricinus communis* agglutinin (RCA120) 25  
 ROS 211
- S**
- Scaffolds 164  
 Selective laser sintering (SLS) 178  
 Self-assembled fibrils 173  
 Self-assembled monolayers (SAMs) 43, 83, 103
- Self-polishing 193  
*Serratia marcescens* 198  
 Silver coatings 203  
 Smart polymers 1  
 Solid freeform fabrication (SFF) 177  
*Staphylococcus epidermidis* 198  
 Stereo lithography (SL) 178  
 Stimuli-controlled dynamic surfaces 110  
 Stimuli-responsive polymers 1  
 Streptavidin 22  
*Streptococcus mutans* 115, 198  
 Stress fibers 39  
 Surface plasmon resonance (SPR) 87  
 Surfaces, bioresponsive 12  
     grafting onto/from 13  
     pH-switchable 4
- T**
- Tetra(ethylene glycol) alkanethiol 119  
 Tetraoxacyclododecane (12-crown-4) 52  
 Thermal control 115  
 Thermally induced phase separation (TIPS) 171  
 Thermoplasmonic nanoarray 98  
 Thermoresponsive polymers 3  
 Tissue culture 82  
 Tissue engineering 83, 163  
 Total internal reflection fluorescence microscopy (TIRFM) 120  
 Tributyltin (TBT) 197  
 Triclosan 203  
 Trx-ELP 3
- U**
- Ulva linza* 199
- V**
- Vancomycin 202  
 Vinculin 92  
*N*-(4-Vinyl)-benzyl iminodiacetic acid 22  
 Vitronectin 59
- Z**
- Zyxin 92